Percutaneous Interventions for Structural Heart Disease
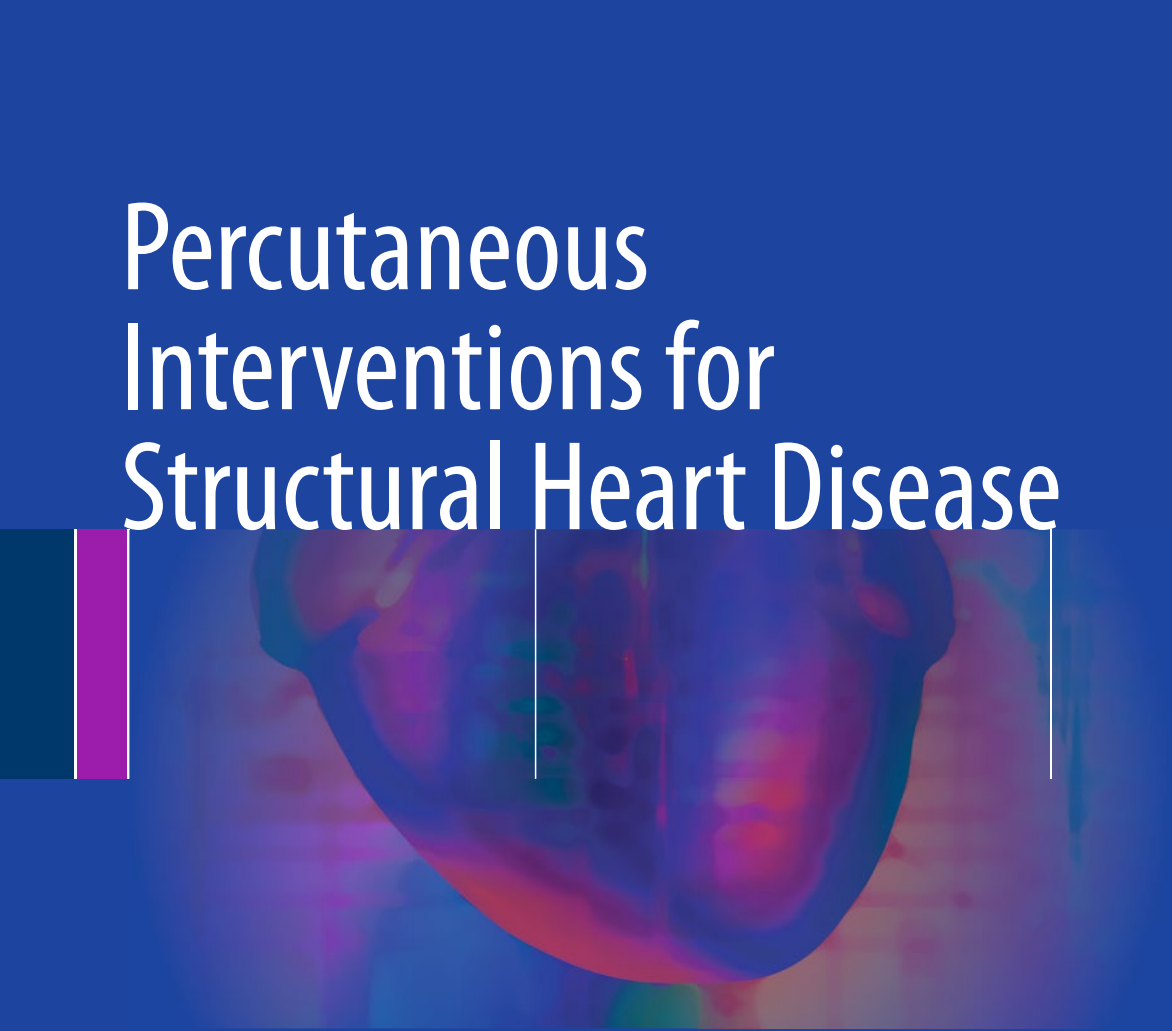
An Illustrated Guide

Bernhard Reimers
Issam Moussa
Andrea Pacchioni

Editors

🐎 Springer

Percutaneous Interventions for Structural Heart Disease

Bernhard Reimers
Issam Moussa • Andrea Pacchioni
Editors

Percutaneous Interventions for Structural Heart Disease

An Illustrated Guide

Springer

Editors
Bernhard Reimers
Cardiovascular Department
Humanitas University
Rozzano – Milano
Italy

Rutgers Robert Wood Johnson Medical School
Robert Wood Johnson University Hospital
RWJBarnabas Health
New Brunswick
New Jersey
USA

Issam Moussa
Cardiac and Endovascular Interventions
First Coast Cardiovascular Institute
Jacksonville
Florida
USA

Andrea Pacchioni
Department of Cardiology
Mirano Hospital
Mirano
Italy

Foreword

Structural interventions bring a new set of information that every interventional cardiologist needs to master. This field is such in a rapid evolution that anybody is likely to assume that a book will become obsolete quite fast. This consideration is valid only at a certain extent, because there is always an amount of basic knowledge that will not change significantly. This fact represents a valid reason to put together a book.

As far as I am concerned, I am very happy to have had the opportunity to write the introduction to *Percutaneous Interventions for Structural Heart Disease: An Illustrated Guide* edited by Bernhard Reimers, Issam Moussa, and Andrea Pacchioni. This task gave me the opportunity to read most of the chapters: a rewarding experience because I learned a lot. The topics are very well organized with a large amount of practical suggestions not easy to be found in other publications.

The first section about the aortic valve is really complete. The step-by-step guide to use OSIRIS to read and evaluate the multislice CT scan is unique and tremendously useful.

The suggestions regarding procedural planning, valve selection, and dealing with problems are very clear and up to date.

The chapters regarding mitral valve are a serious attempt to cover this enormous field in rapid expansion and may appear incomplete. We cannot dismiss that such a fast-moving target will always be difficult to be fully captured in a book. Nevertheless, the content represents a ground knowledge that cannot be dismissed.

I liked reading about left appendix closure with many practical suggestions such as the need to deploy the Watchman device as a quick solution to close a traumatic appendix rupture.

Closure of paravalvular leaks represents such an evolving field and the reader needs to perform additional homework to learn about new techniques and additional vascular plugs.

Patent foramen ovale is fully covered, and even the issue of nickel allergy is presented with a controversial case description. I wish a preventive approach to this problem and a more in-depth discussion would have been included.

The last chapters deal with transcatheter closure of postmyocardial infarction ventricular septal defect. The authors are very clear to direct the reader into a detailed description of the procedure: very useful and practical. The case on this

topic illustrates the utilization of a transeptal approach to enter the left ventricle from the left atrium to gain access into the right ventricle from the septal defect.

Throughout this book, there are a lot of figures with clear commentaries. I would state that most of the chapters satisfy this need, while in others, a more extensive endeavor to document the writing with more pictures and schemes would have been appropriate.

Very important are the case presentations following each major topic giving a lively atmosphere necessary to keep the interest alive and to bring the reader into real-life scenarios.

Without question, this book represents a must to have and more importantly to read for every interventional cardiologist who desires entering the field of structural transcatheter procedures.

The editors and all the contributors need to be commended for this remarkable production.

Milan, Italy   Antonio Colombo

Preface

Structural interventions should be considered a true revolution in many cath labs, which, before the exponential increase in structural procedures, mostly treated coronary and sometimes peripheral artery disease.

We should thank the pioneering work of doctors such as Alain Cribier and Philipp Bonhoeffer, who believed in a mission, thought by many to be impossible, to insert a valve prosthesis percutaneously. Other colleagues, such as Horst Sievert, for many years a "structural interventionalist," and Antonio Colombo, fortunately both among the authors of this volume, improved the techniques of structural interventions with numerous practical tips and tricks followed by pivotal clinical trials.

The present book seeks to put together the experience, mostly practical, of real experts of the field, to be transmitted to the rapidly increasing community of interventionalists performing structural heart therapies. We wanted to create a practical guide, starting with the correct preparation of the intervention, by evaluating cardiac images obtained with CT and transesophageal echography, new but basic knowledge, and absolutely essential to the success of a procedure. In the following section, procedural techniques and available devices are presented. Finally, a description of complications and how to manage and avoid them are a core part of the book. We considered this particularly important in honoring those patients who suffered a complication and helped to make our procedures safer.

Of course, this book does not claim to be complete, but we hope that it will become a small but precious part of the learning process toward becoming a structural interventionalist. We acknowledge the work, diligence, and willingness of our distinguished authors, colleagues, and friends who wrote the various chapters. We thank them for sharing with us and the readers their vast experience to the advantage of our patients.

Last but not least, we are particularly grateful to our wives Antonella, Corinna, and Mireille.

Mirano, Italy	Bernhard Reimers
Mirano, Italy	Andrea Pacchioni
FL, USA	Issam Moussa

Contents

Part I

Aortic Valve Intervention

Severe Aortic Stenosis Treatment: Percutaneous Options, Patient Selection, and Preoperative Evaluation

1

Renato Razzolini and Elisa Covolo

1.1 Introduction

The implantation procedure of transcatheter aortic valve prosthesis (TAVI) was introduced in 2002 by Prof. Alain Cribier [1]. This interventional strategy has emerged as an attractive treatment superior to medical therapy alone and as the only treatment option for patients with severe symptomatic aortic valve stenosis judged inoperable with conventional surgery [2]. Furthermore, it has proven to be a viable alternative therapy for patients considered at high and intermediate surgical risk [3–5]. Conventional aortic valve replacement (AVR) however still remains the approach of choice in symptomatic patients with low-intermediate operative risk.

Although several multicenter registries and randomized trials have demonstrated the safety and efficacy of TAVI in improving the survival as well as functional capacity, some patients may not benefit from TAVI procedure. In fact, most of the elderly patients with severe aortic stenosis (AS) present multiple noncardiac comorbidities, which might limit survival and improvement in functional capacity afforded by TAVI.

It is essential firstly to identify for each patient the operative risk with a multifaceted approach to accurately evaluate the best risk/benefit ratio of therapeutic options. Therefore, optimal patient selection based on precise risk assessment represents the cornerstone of evaluation of patients for TAVI [6]. The judgment on the operative risk of the patient and consequently the choice of the candidate for transcatheter approach should be established through collegial discussion of each case by a multidisciplinary team (defined Heart Team).

R. Razzolini (✉) • E. Covolo
Department of Cardiological, Thoracic and Vascular Sciences, Clinical Cardiology,
University of Padova, Padova, Italy
e-mail: renato.razzolini@unipd.it

1.2   Guidelines

According to current guidelines, treatment options depend on risk assessment [7]:

- Surgical AVR is recommended in patients who meet an indication for AVR with low or intermediate surgical risk (class I; level of evidence, A).
- TAVI is recommended in patients who meet an indication for AVR and have a prohibitive risk for surgical AVR and a predicted post-TAVI survival greater than 12 months (class I; level of evidence, B).
- TAVI is a reasonable alternative to surgical AVR in patients who meet an indication for AVR and have high surgical risk for surgical AVR (class IIa; level of evidence, B).
- Percutaneous aortic balloon dilation may be considered as a bridge to surgical AVR or TAVI in patients with severe symptomatic AS (class IIb; level of evidence, C).
- TAVI is not recommended in patients in whom existing comorbidities would preclude the expected benefit from correction of AS (class III; level of evidence, B) [8].

1.3   Heart Team

Evolving options in therapeutic strategies have identified the central role of the Heart Team in optimizing patient selection. The Heart Team consists of an integrated, multidisciplinary group of healthcare professionals with expertise in valvular heart disease, cardiac imaging, interventional cardiology, cardiac anesthesia, and cardiac surgery. Physicians should collaborate to provide optimal strategy decision for patients in whom TAVI or high-risk surgical AVR is being considered (class I; level of evidence, C) [7].

In fact, most of patients are old with multiple comorbidities, increasing complexity, and risks of any approach; in addition, evaluation of candidates for TAVI includes peripheral arterial access, underlying coronary artery disease, and left ventricular function. Individualized life expectancy assumptions should be incorporated by the Heart Team in the clinical decision-making process.

This collaborative approach allows accurate evaluation of the risk/benefit ratio of either surgical AVR, TAVI, or medical therapy (Fig. 1.1). The Heart Team members should agree on an estimated 30-day mortality risk for each patient based upon integrating a careful clinical assessment and using appropriate risk prediction scoring systems. Moreover, case screening; optimal treatment strategy; procedural detail planning, including valve type choice, access routes, and methods; and detailed postprocedural management including postdischarge care are all part of the Heart Team decisional process [9].

The Heart Team discussion includes:

- Confirmation of the severity of aortic valve stenosis
- Evaluation of patient's symptoms
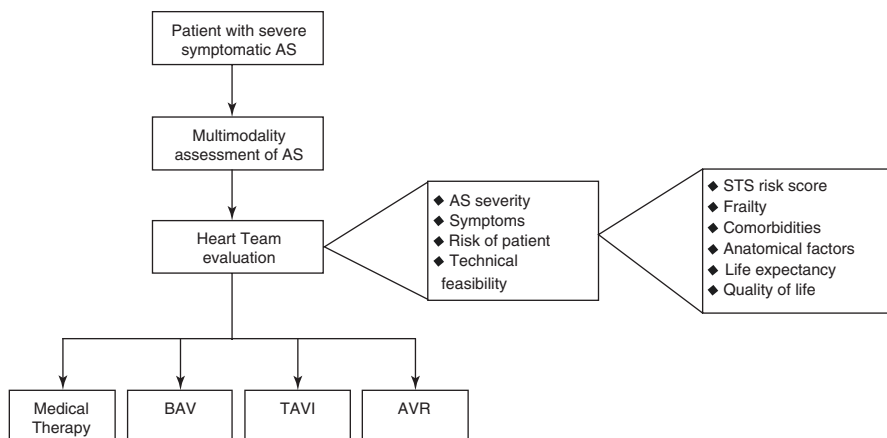
Fig. 1.1 The collaborative approach of the Heart Team allows accurate evaluation of the risk/benefit ratio of either surgical AVR, TAVI, BAV, or medical therapy. *AS* aortic stenosis, *AVR* aortic valve replacement, *BAV* balloon aortic valvuloplasy, *TAVI* transcatheter aortic valve implantation

- Assessment of cardiac risk, life expectancy, and quality of life of the patient
- Feasibility and contraindications of transcatheter approach

1.4   Patient Selection

Optimal patient selection by the Heart Team is essential for a successful TAVI program.

First of all, patient's operative risk should be assessed according not only to age and severity of heart disease but also to systemic comorbidities (e.g., respiratory failure, kidney and liver disease, prior cerebrovascular accident, neurological deficit, peripheral vascular disease, previous or current cancer, connective tissue and autoimmune diseases, etc.).

Risk assessment depends on the combination of multiple evaluations:

- Conventional surgical risk scores
- Frailty
- Major organ system dysfunction
- Procedure-specific problems

The guidelines state that selected patients should be expected to gain improvement in their quality of life and to have a life expectancy of 1 year after consideration of their comorbidities. It should be noted that some patients' risk is even too high also for TAVI and that significant comorbidities (e.g., severe chronic

obstructive pulmonary disease) may lead to persistent impaired quality of life and high mortality despite TAVI.

1.5   Conventional Surgical Risk Scores

Different algorithms are described in literature to estimate the risk of mortality and perioperative morbidity, which were built on the basis of large cardiac surgery series. The scores most widely used in clinical practice to predict operative mortality in cardiac surgery are:

- The Society of Thoracic Surgery Predicted Risk of Mortality (STS-PROM) [10]
- Additional or logistic European System for Cardiac Operative Risk Evaluation II (EuroSCORE II) [11]

Although many other risk scores are available (Ambler, Initial Parsonnet, Cleveland Clinic, French, Pons, and Ontario Province Risk score among the others), most of them take into account a limited number of variables with poor predictive value. In the current practice, a patient is considered to be at high surgical risk when the estimated 30-day mortality is >10 % with STS score and >20 % with EuroSCORE II. However, if used for TAVI risk stratification, they showed a weak predictive power [12], since they were developed from and for unselected surgical patients and they do not take into account clinical and anatomical variables (radiation heart disease, heavily calcified or porcelain ascending aorta, the intrinsic fragility of the patient ("frailty"), and liver disease) that could have a role in TAVI prognosis. However, a TAVI-oriented risk stratification score is still missing.

1.6   Frailty

The frailty is defined by slowness, weakness, exhaustion, wasting and malnutrition, poor endurance and inactivity, and loss of independence which reflect the poor physical and cognitive performance of the patient. The frailty is often estimated subjectively on the basis of a so-called eyeball test but can be objectified with some simple tests such as analysis of physical performance by measuring gait speed and grip strength. These continuous measures are reproducible and can be reassessed at various time points; in addition, they don't require language translation. Evaluation of physical performance should always be accompanied by assessment of mental abilities, underweight (BMI <20 kg/m^2 and/or weight loss 5 kg/year), activity level, and independence in activities of daily living. The most utilized is the Katz Activities of Daily Living Index, which evaluates independence in feeding, bathing, dressing, transferring, toileting, and urinary continence and independence in ambulation (no walking aid or assist required or 5 m walk in <6 s) [13, 14].

Laboratory findings (e.g., serum albumin <3.5 g/dL, elevated inflammatory markers, anemia) may further reflect the health state and physiological reserve of the frail patient.

One essential part of the initial risk stratification is represented by the evaluation of the presence of preprocedural cognitive dysfunction with degrees varying from mild cognitive impairment to dementia, particularly in populations of elderly patients, in order to weigh carefully the risk, the benefit, and the cost-effectiveness of invasive procedures. Furthermore, preexisting cognitive impairment can worsen during hospitalization, and careful differential diagnosis with new cerebrovascular complications could be challenging.

Different neurocognitive tests are available (e.g., Mini-Mental State Examination, Clinical Dementia Rating Scale), and a cognitive assessment should be considered systematically in Heart Team evaluations, eventually carried out by neuropsychological experts.

Table 1.1 Comorbidities associated with increased risk

Major organ system compromised	
Heart	Severely reduced left ventricular function
	Low transvalvular gradient (mean gradient <20 mm Hg)
	Low flow (low stroke volume index $\leq$35 ml/m^2)
	Severe myocardial fibrosis
	Severe concomitant mitral and/or tricuspid valve disease
	Severe right ventricular dysfunction (TAPSE <15 mm, RV end-systolic area >20 cm^2)
	Primary or secondary severe pulmonary hypertension (pulmonary systolic pressures greater than two-thirds of systemic pressure)
Lung	Severe lung disease, particularly oxygen dependent
	FEV$_1$ <50 % or DLCO <50 % of predicted
CNS	Dementia, Alzheimer's disease, Parkinson's disease
	CVA with persistent physical limitation
GI	Crohn's disease, ulcerative colitis
	Nutritional impairment
	CKD stage 3 or worse
Liver	Severe liver disease/cirrhosis
	Variceal bleeding
	Child-Pugh class C
	Portacaval, splenorenal, or transjugular intrahepatic portal shunt
Cancer	Active malignancy

CKD chronic renal disease, *CNS* central nervous system, *CVA* cerebrovascular accident, *DLCO* diffusing capacity of carbon monoxide, *FEV1* forced expiratory volume in 1 s, *GI* gastrointestinal, *RV* right ventricle

1.7 Major Organ System Dysfunction

Numerous comorbidities are not included in the commonly used risk score, but they should be considered in risk stratification for TAVI (Table 1.1).

First of all, heart function at transthoracic echocardiography must be taken into account: patients with low ejection fraction (<40 %) could present as low-flow, low-gradient severe AS that should be distinguished by pseudostenosis by means of low-dose dobutamine stress echo: in true severe AS with recovery of function, the ejection fraction increases with parallel increase of mean aortic gradient, whereas in pseudostenosis the mean aortic gradient does not increase at the increase of ejection fraction. Patients with low-flow, low-gradient severe AS have been associated with high mortality after AVR, up to 35 % in those without contractile reserve [15] and with a resting mean gradient <20 mmHg [16]. TAVI is a feasible approach in this subset of patients [17]: despite a high short-term mortality, the surviving patients showed symptomatic benefit and significant improvement of myocardial function and exercise capacity along with significant improvement in quality of life. Patients with paradoxically low-flow, low-gradient severe AS (i.e., with preserved ejection fraction and low stroke volume index (<35 ml/m^2)) have increased mortality after TAVI, independently of ejection fraction [18]. Nevertheless, feasibility and safety of TAVI have been demonstrated in low-flow, low-gradient, severe AS and preserved ejection fraction [19].

Risk assessment should include coronary artery disease evaluation. Appropriate revascularization strategies in the setting of AS should be considered in the Heart Team and should be individualized based on comorbidities and bleeding risk factors. When needed, percutaneous coronary intervention can be safely performed in patients eligible to TAVI, without an increased risk of short-term adverse outcomes [20].

The presence of severe of pulmonary hypertension is an independent predictor for mortality after surgical AVR, as may reflect more advanced state of disease [21]. Advanced disease of other organs, including severe obstructive lung disease, is independently associated with increased mortality in patients undergoing TAVI [22].

Many major organ systems may be compromised in elderly population affected by severe AS, thus increasing surgical risk beyond common used risk scores. Therefore, a systematic approach should be used to analyze multiple comorbidities. In Table 1.2 a schematic method of evaluation of patient eligible to TAVI is reported, utilized in Padua University for Heart Team discussion.

Finally, evaluation includes multidetector CT and coronary angiography to assess aortic annulus size, aorta and peripheral vessel anatomy, and coronary disease. This allows accurate TAVI procedure planning.

1.8 Procedure-Specific Problems

The traditional surgical risk score also does not take into account important conditions that may pose prohibitive surgical risk from the technical standpoint such as radiation heart disease and heavily calcified or porcelain ascending aorta (defined as

Table 1.2 Schematic checklist for Heart Team evaluation

Name ____	Surname____	Address___	Telephone ___
Gender___	Age___	Height___	Weigh___
Clinical history			
☐ Smoke	☐ Hypertension	☐ Dyslipidemia	☐ Atrial fibrillation
☐ ACS	☐ CHF	☐ Previous surgery	☐ previous PCI
☐ COPD:			
Creatinine: ___	eGFR: ___	CKD: ___	☐ Dialysis
Logistic Euroscore __	Standard Eurscore ___	Euroscore II ___	STS score ___
Frailty index ___	Other comorbidities	_____	☐ Allergies: ___
Symptoms			
NYHA ___	CCS ___	☐ Syncope	
EKG ___	___		
Echocardiogram	EF ___	Max/mean gradient __	AVA ___
AR ___	MR ___	TR ___	Ascending aorta ___
Carotid echo	___		
Spirometry	FEV$_1$ ___		
Angio CT	Annulus ___	Ascending aorta	___
Aoto-iliac-femoral axis _____			
Cardiac catheterization	EF ___	Gradient ___	AVA ___
AR ___	MR ___		
Aortography	___		
Coronarography	___		
Therapy	___		

ACS acute coronary syndrome, *AR* aortic regurgitation, *AVA* aortic valve area, *CHF* chronic heart failure, *CKD* chronic kidney disease, *COPD* chronic obstructive pulmonary disease, *eGFR* estimated glomerular filtration rate, *EF* ejection fraction, *MR* mitral regurgitation, *TR* tricuspid regurgitation

heavy circumferential calcification or severe atheromatous plaques of the entire ascending aorta extending to the arch such that aortic cross-clamping is not feasible). The presence of "hostile chest" makes the surgical intervention prohibitively hazardous, such as in case of prior chest surgeries with adhesions, history of multiple recurrent pleural effusions causing internal adhesions, tracheostomy, evidence of severe radiation damage (e.g., skin burns, bone destruction, muscle loss, lung fibrosis, or esophageal stricture), and abnormal chest wall anatomy due to severe kyphoscoliosis or other skeletal abnormalities (including thoracoplasty, Pott's disease).

Moreover, redo operation through sternotomy or right anterior thoracotomy may be dangerous in case of bypass graft anatomy such as left internal mammary graft adherent to the inner chest wall.

1.9   Futility

The benefits of TAVI in old, high-risk patients incorporate not only the reduced mortality but also the early recovery and quality-of-life improvement. However, considering the advanced age of patients, important comorbidities and life expectancy must be assessed as a corner point in Heart Team evaluation. TAVI should not be offered to patients who have noncardiac illnesses that are the predominant cause of the limiting symptoms or to those who have an estimated life expectancy <12 months from noncardiac illnesses. The "poor outcome" in some patient after TAVI reflects a failure to achieve the goals of intervention, both in terms of mortality and of quality of life [23]. A "poor outcome," defined as death at 6-month follow-up or Kansas City Cardiomyopathy Questionnaire-Overall Summary (KCCQ-OS) score <45 or ≥10-point decrease compared to the baseline [24], may be predicted by poor functional capacity (as measured by the 6-minute walking test) and low mean aortic valve gradients. Other important predictors included oxygen-dependent lung disease, renal dysfunction, and poorer baseline cognitive function.

Accordingly so, a critical point faced by the Heart Team is to reliably identify patients who are unlikely to benefit in terms of survival or functional capacity following TAVI. Therapeutic futility is the lack of intended benefits from a medical treatment, and it includes both survival and improvement in functional capacity. Therapeutic futility could be defined from different points of view: (1) the lack of efficacy of a medical procedure, in particular when the interventional therapy has little chance of obtaining the desired effect, as the clinical state is driven by noncardiac illness (point of view of the doctor), (2) the lack of improvement of life expectancy or clinical conditions and functional capacity (point of view of the patient), and (3) the lack of an acceptable benefit despite an important consumption of resources in terms of cost-effectiveness (drug, economic point of view). It is essential to understand when the benefit offered by TAVI is actually proportionate to care needs related to the procedure and the subsequent hospitalization, in particular in patients who present high risk of mortality still regardless of the outcome of the procedure (Fig. 1.2). In fact, beyond traditional clinical comorbidities, several age-related conditions may predispose an old patient to adverse outcomes following TAVI [25]. These include frailty, disability in daily activities, malnutrition, mobility impairment, low muscle mass (sarcopenia), cognitive impairment, mood disorders, and social isolation. Frailty assessment has improved risk stratification prior to TAVI [26].

1.10   TAVI Contraindication

There are clinical criteria that contraindicate in absolute terms or relative to the procedure of TAVI, among these:

- Life expectancy <1 year or unlikely improvement in quality of life by TAVI because of comorbidities
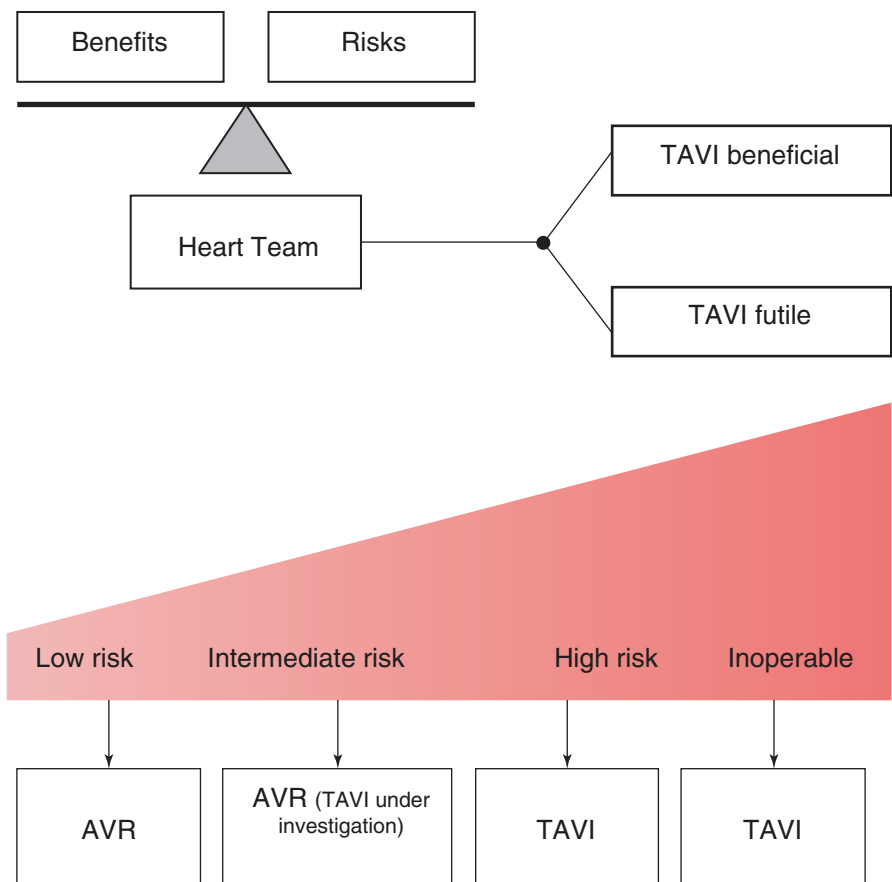
Fig. 1.2 The multidisciplinary Heart Team considers and weighs the anticipated benefits and risks of TAVI and makes a decision regarding whether TAVI will likely be beneficial or futile. In some cases, uncertainty requires clinical judgment. *AVR* aortic valve replacement, *TAVI* transcatheter aortic valve implantation

- Presence of sepsis or active endocarditis
- Bleeding diathesis or coagulopathy
- Presence of other relevant concomitant valvular diseases (in particular massive organic mitral regurgitation)
- Recent stroke (<1 month)
- Recent myocardial infarction (<1 month)
- Allergy to iodinated contrast
- Excessively small or large aortic annulus
- Intracardiac mass, thrombus, or vegetation
- Location of the left main coronary ostium within 10 mm of the annulus with large bulky aortic valve leaflets

References

1. Cribier A, Eltchaninoff H, Bash A, Borenstein N, Tron C, Bauer F, Derumeaux G, Anselme F, Laborde F, Leon MB. Percutaneous transcatheter implantation of an aortic valve prosthesis for calcific aortic stenosis: first human case description. Circulation. 2002;106(24):3006–8.
2. Leon MB, Smith CR, Mack M, et al. Transcatheter aortic valve implantation for aortic stenosis in patients who cannot undergo surgery. N Engl J Med. 2010;363:1597–607.
3. Smith CR, Leon MB, Mack MJ, et al. Transcatheter versus surgical aortic valve replacement in high-risk patients. N Engl J Med. 2011;364:2187–98.
4. Leon MB, Smith CR, Mack MJ, et al. Transcatheter or surgical aortic-valve replacement in intermediate-risk patients. N Engl J Med. 2016;374:1609–20.
5. Thorani VH, Kodali S, Makkar RR, et al. Transcatheter aortic valve replacement versus surgical valve replacement in intermediate-risk patients: a propensity score analysis. Lancet. 2016. doi:10.1016/S0140-6736(16)30073-3.
6. Agarwal S, Tuzcu EM, Krishnaswamy A, et al. Transcatheter aortic valve replacement: current perspectives and future implications. Heart. 2015;101:169–77.
7. Nishimura RA, Otto CM, Bonow RO, Carabello BA, Erwin 3rd JP, Guyton RA, O'Gara PT, Ruiz CE, Skubas NJ, Sorajja P, Sundt 3rd TM, Thomas JD, ACC/AHA Task Force Members. 2014 AHA/ACC guideline for the management of patients with valvular heart disease: executive summary: a report of the american college of cardiology/american heart association task force on practice guidelines. Circulation. 2014;129(23):2440–92.
8. Leon MB, Smith CR, Mack M, et al. Transcatheter aortic-valve implantation for aortic stenosis in patients who cannot undergo surgery. N Engl J Med. 2010;363:1597–607.
9. Holmes Jr DR, Rich JB, Zoghbi WA, Mack MJ. The heart team of cardiovascular care. J Am Coll Cardiol. 2013;61(9):903–7.
10. Shroyer AL, Coombs LP, Peterson ED, Eiken MC, DeLong ER, Chen A, Ferguson Jr TB, Grover FL, Edwards FH. The society of thoracic surgeons: 30-day operative mortality and morbidity risk models. Ann Thorac Surg. 2003;75(6):1856–64; discussion 1864–5.
11. Nashef SA, Roques F, Michel P, et al. European system for cardiac operative risk evaluation (EuroSCORE). Eur J Cardiothorac Surg. 1999;16:9–13.
12. Johansson M, Nozohoor S, Zindovic I, Nilsson J, Kimblad PO, Sjögren J. Prediction of 30-day mortality after transcatheter aortic valve implantation: a comparison of logistic EuroSCORE, STS score, and EuroSCORE II. J Heart Valve Dis. 2014;23(5):567–74.
13. Green P, Woglom AE, Genereux P, Daneault B, Paradis JM, Schnell S, Hawkey M, Maurer MS, Kirtane AJ, Kodali S, Moses JW, Leon MB, Smith CR, Williams M. The impact of frailty status on survival after transcatheter aortic valve replacement in older adults with severe aortic stenosis: a single-center experience. JACC Cardiovasc Interv. 2012;5(9):974–81.
14. Stortecky S, Schoenenberger AW, Moser A, Kalesan B, Jüni P, Carrel T, Bischoff S, Schoenenberger CM, Stuck AE, Windecker S, Wenaweser P. Evaluation of multidimensional geriatric assessment as a predictor of mortality and cardiovascular events after transcatheter aortic valve implantation. JACC Cardiovasc Interv. 2012;5(5):489–96.
15. Carabello BA. Low-gradient, low-ejection fraction aortic stenosis: what we know and what we do not know. JACC Cardiovasc Interv. 2012;5:560–2.
16. Tribouilloy C, Lévy F, Rusinaru D, et al. Outcome after aortic valve replacement for low-flow/low-gradient aortic stenosis without contractile reserve on dobutamine stress echocardiography. J Am Coll Cardiol. 2009;53:1865–73.
17. Gotzmann M, Lindstaedt M, Bojara W, et al. Clinical outcome of transcatheter aortic valve implantation in patients with low-flow, low gradient aortic stenosis. Catheter Cardiovasc Interv. 2012;79:693–701.
18. Le Ven F, Freeman M, Webb J, et al. Impact of low flow on the outcome of high-risk patients undergoing transcatheter aortic valve replacement. J Am Coll Cardiol. 2013;62:782–8.
19. Covolo E, Saia F, Napodano M, et al. Comparison of balloon-expandable versus self-expandable valves for transcatheter aortic valve implantation in patients with low-gradient

severe aortic stenosis and preserved left ventricular ejection fraction. Am J Cardiol. 2015;115(6):810–5.

20. Gasparetto V, Fraccaro C, Tarantini G, Buja P, D'Onofrio A, Yzeiraj E, Pittarello D, Isabella G, Gerosa G, Iliceto S, Napodano M. Safety and effectiveness of a selective strategy for coronary artery revascularization before transcatheter aortic valve implantation. Catheter Cardiovasc Interv. 2013;81(2):376–83.

21. Melby SJ, Moon MR, Lindman BR, Bailey MS, Hill LL, Damiano Jr RJ. Impact of pulmonary hypertension on outcomes after aortic valve replacement for aortic valve stenosis. J Thorac Cardiovasc Surg. 2011;141:1424–30.

22. Dvir D, Waksman R, Barbash IM, et al. Outcomes of patients with chronic lung disease and severe aortic stenosis treated with transcatheter versus surgical aortic valve replacement or standard therapy: insights from the PARTNER trial (Placement of Aortic Transcatheter Valve). J Am Coll Cardiol. 2014;63:269–79.

23. Arnold SV, Reynolds MR, Lei Y, et al. Predictors of poor outcomes after transcatheter aortic valve replacement: results from the PARTNER (Placement of Aortic Transcatheter Valve) trial. Circulation. 2014;129:2682–90.

24. Arnold SV, Spertus JA, Lei Y, et al. How to define a poor outcome after transcatheter aortic valve replacement: conceptual framework and empirical observations from the placement of aortic transcatheter valve (PARTNER) trial. Circ Cardiovasc Qual Outcomes. 2013;6:591–7.

25. Lindman BR, Alexander KP, O' Gara PT, et al. Futility, benefit, and transcatheter aortic valve replacement. JACC Cardiovasc Interv. 2014;7:707–16.

26. Stortecky S, Schoenenberger AW, Moser A, et al. Evaluation of multidimensional geriatric assessment as a predictor of mortality and cardiovascular events after transcatheter aortic valve implantation. JACC Cardiovasc Interv. 2012;5:489–96.

How to Size Aortic Bioprosthesis

2

M. Rinaldi and A. Pacchioni

2.1 Introduction

Correct measurements of the structures of the aortic root and annulus are crucial to correctly size the prosthesis and evaluate potential challenges during TAVI implantation. Sole measurement of the aortic annulus may not always be enough to correctly size the prosthesis, so it is very important to consider also:

- Width and height of the sinuses of Valsalva
- Coronaries ostium height
- Calcium amount and distribution on the aortic valve
- Diameters and distribution of calcifications on sinotubular junction (STJ)
- As needed, ascending aorta diameters and LVOT width

Currently, the choice of valve size depends on annulus diameters, perimeters, and area, varying according to valve type (see appendix). Being independent and proficient in valve sizing requires experience, but it is a mandatory skill for interventionists. We hope this tutorial could help everyone interested in TAVI in this difficult task.

OsiriX software is a GNU-free software (download at www.osirix.org) running on Mac OS, powerful and easy to use, which allows elaboration of DICOM images.

M. Rinaldi (✉)
Heart Valve Therapies, Medtronic, Mounds View, MN, USA
e-mail: michele.rinaldi@medtronic.com

A. Pacchioni
Department of Cardiology, Mirano Hospital, Mirano, Italy
e-mail: andreapacchioni@gmail.com

First of all, a systolic- or diastolic-triggered cardiac and angio-CT scan (heart, aorta, iliac, and femoral arteries) is needed.

Measurements of all these structures are performed using the 3D MPR module of the OsiriX software (*3D Viewer -> 3D MPR*).

Tip: customize the module toolbar by right-clicking on it and selecting Customize Toolbar, and then choose the needed tools.

Trick: learn to use keyboard shortcuts to speed up your work; a list can be found under *OsiriX Preferences -> Hot Keys*.

Note: the OsiriX version used to write this paper is OsiriX MD 1.4 (a pretty old one), but the methods described should work for OsiriX-free versions and later versions (newer version may actually ease some of the described methods).

2.2   Annulus Plane Identification and Measurements

Tip: set the Thick Slab parameter at the lowest possible to minimize slice thickness and thus measurements mistakes.

Aortic annulus plane is defined as the plane on which the nadir of each of the three cusps lay; there are various algorithms to identify this plane, and they all produce the same results. Basically, aortic annulus plane is the plane on which the three cusps disappear at the same time when scrolling images from STJ to LVOT. Measurements of the annulus can be performed either in a systolic-triggered series or in a diastolic-triggered series; anyway note that measurements could slightly differ among the series (mid-systole-triggered series are generally considered the best series to measure the aortic annulus).

One of the simplest algorithms that can be used to identify annular basal plane is the following: the goal is to have the annulus plane depicted in the axial plane (purple plane in the default color setting of the software); starting from aortic bulb, orient the axes so that the three cusps are more or less equal in size (see Fig. below).
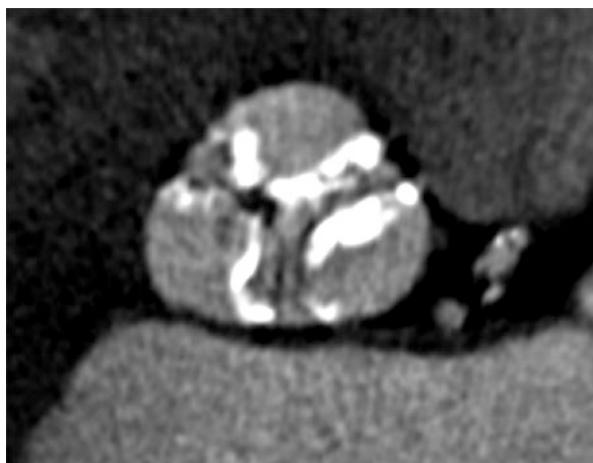
Suppose that the nadir of each cusp is in the middle of the cusp itself and remember the orientation of each nadir (e.g., nadir of RCC at 12 o'clock, nadir of LCC at 4 o'clock, nadir of NCC at 8 o'clock in the Fig. above).

In axial plane, drag the axes toward the middle of the RCC (Fig. 2.1) and then scroll images toward LVOT until RCC disappears (Fig. 2.2).

In axial plane, rotate the blue axis toward the nadir of the LCC (at 4:00, Fig. 2.3) and check in the corresponding plane (coronal) if the purple axis touches the nadir of the LCC; if not, rotate the axis itself in the coronal plane until it touches the nadir of the LCC, so you should see the LCC disappearing in the axial plane (Fig. 2.4).
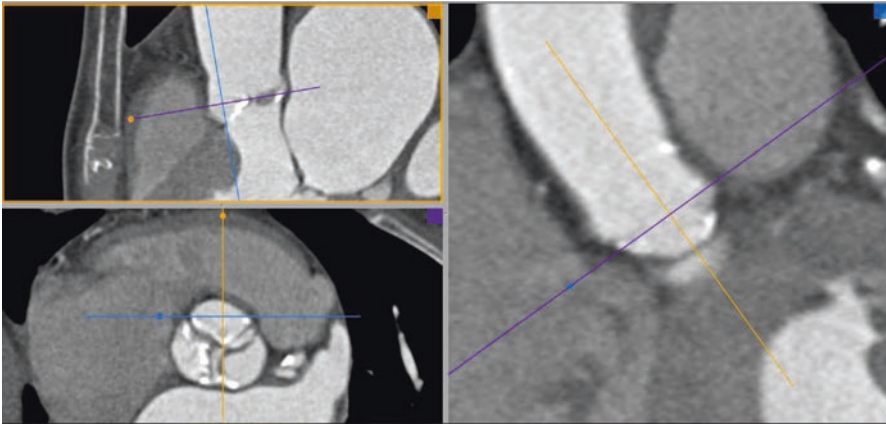
Fig. 2.1 Drag the axes toward the middle of the RCC
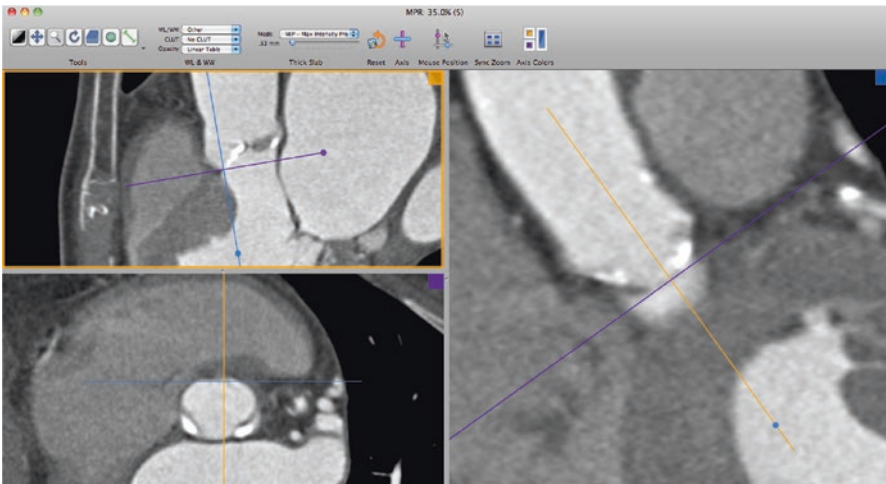
Fig. 2.2 Scroll images toward LVOT until RCC disappears
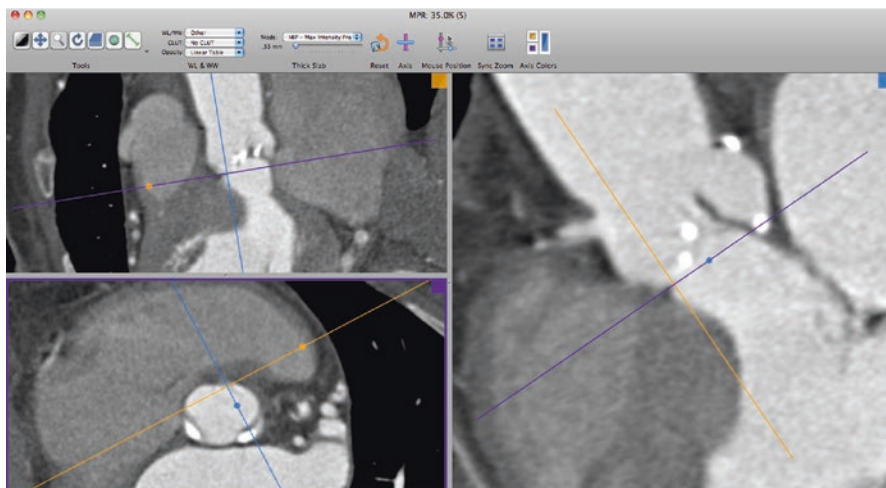
Fig. 2.3 Rotate the blue axis toward the nadir of the LCC
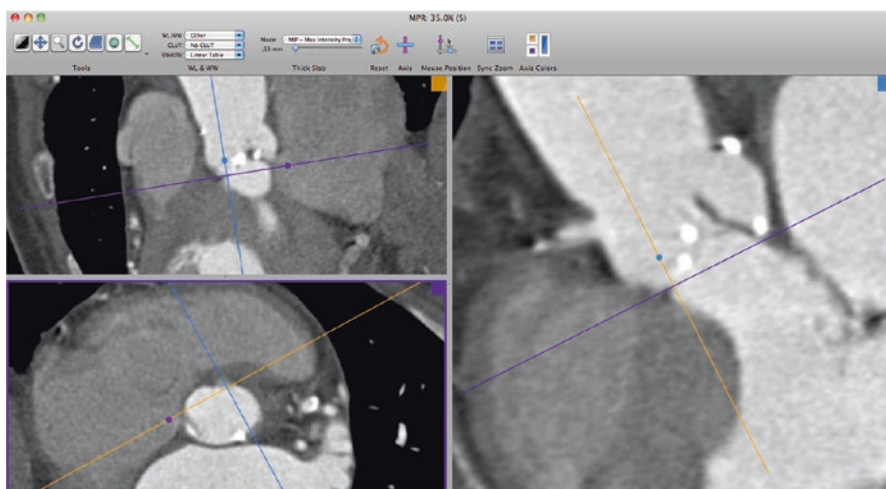
Fig. 2.4 Rotate the purple axis in the coronal plane until it touches the nadir of the LCC

Back to the axial plane, rotate the orange axis toward the nadir of the NCC (at 8:00, Fig. 2.5) and check in the corresponding plane (sagittal) if the purple axis touches the nadir of the NCC; if not, rotate the purple axis itself in the sagittal plane until it touches the nadir of the NCC, so you should see the NCC disappearing in the axial plane (Fig. 2.6).
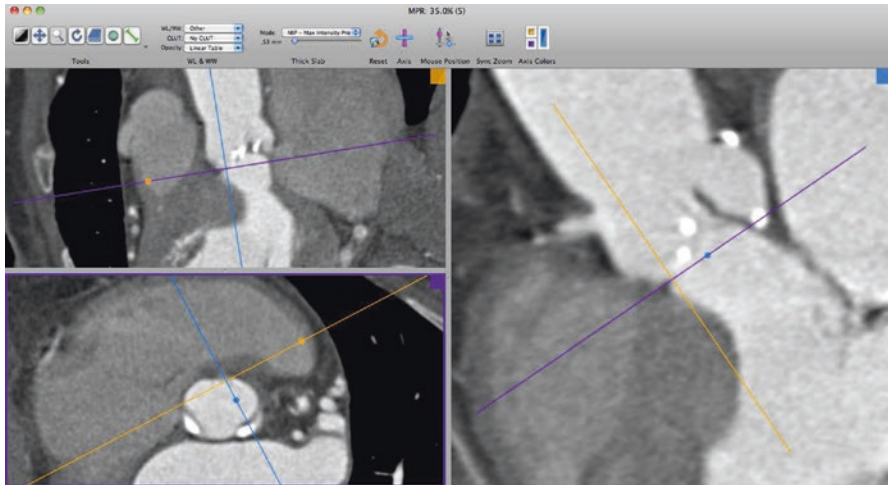
Fig. 2.5 Rotate the orange axis toward the nadir of the NCC
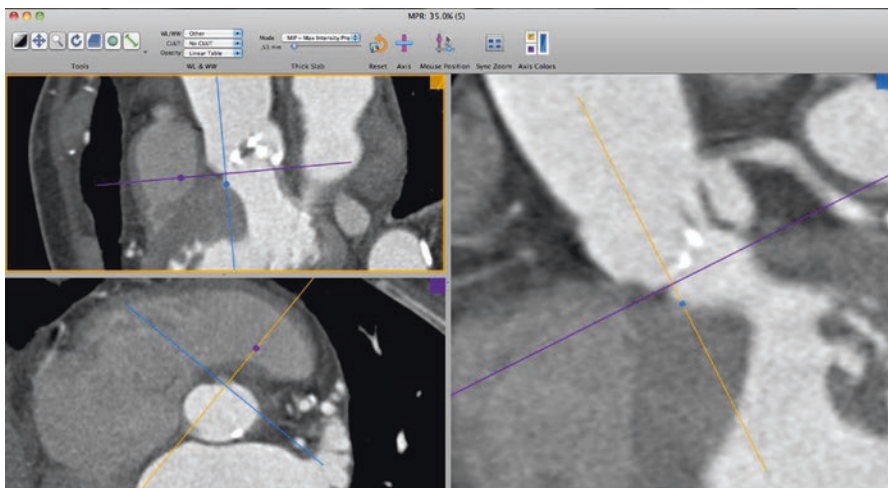
Fig. 2.6 Rotate the purple axis in the sagittal plane until it touches the nadir of the NCC

Back to the axial plane, double check the result repeating the above steps for the other two cusps:

For example, LCC first:

– Drag the axes from RCC to LCC (Fig. 2.7).
– Rotate the orange axis toward the RCC and check in the corresponding plane if the purple axis touches the nadir, and, if needed, correct the orientation of the purple axis accordingly (Fig. 2.8).
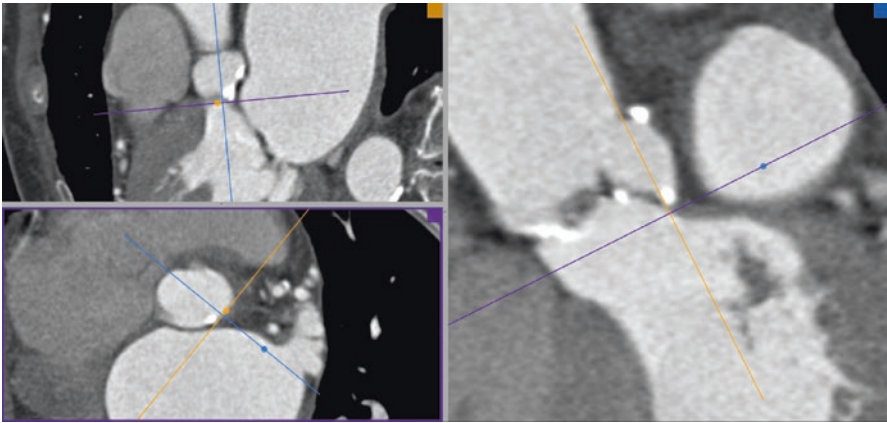
Fig. 2.7 Drag the axes from RCC to LCC
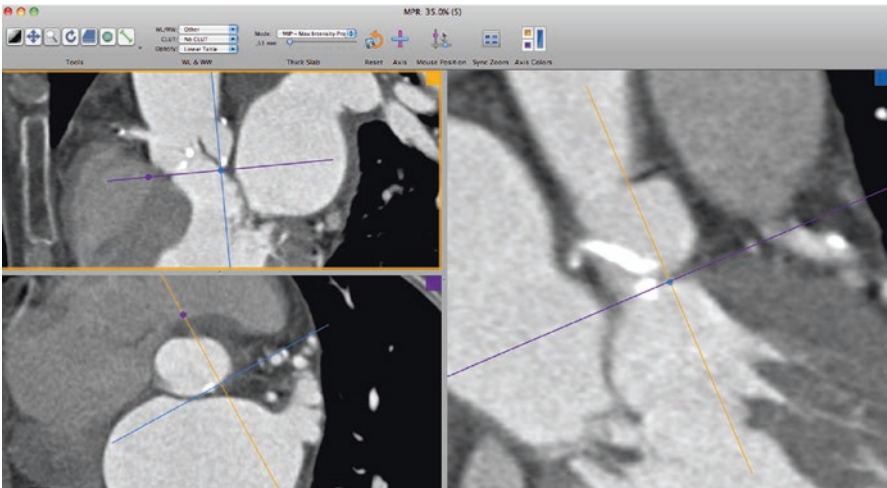
Fig. 2.8 Rotate the orange axis toward the RCC and check in the corresponding plane if the purple axis touches the nadir, and correct the orientation of the purple axis accordingly

– Rotate the blue axis toward the NCC and check in the corresponding plane if the purple axis touches the nadir, and, if needed, correct the orientation of the purple axis accordingly (Fig. 2.9).

Then repeat for the NCC:

– In axial plane, drag the axes from LCC to NCC (Fig. 2.10).
– Rotate the blue axis toward the RCC and check in the corresponding plane if the purple axis touches the nadir, and correct the orientation of the purple axis accordingly (Fig. 2.11).
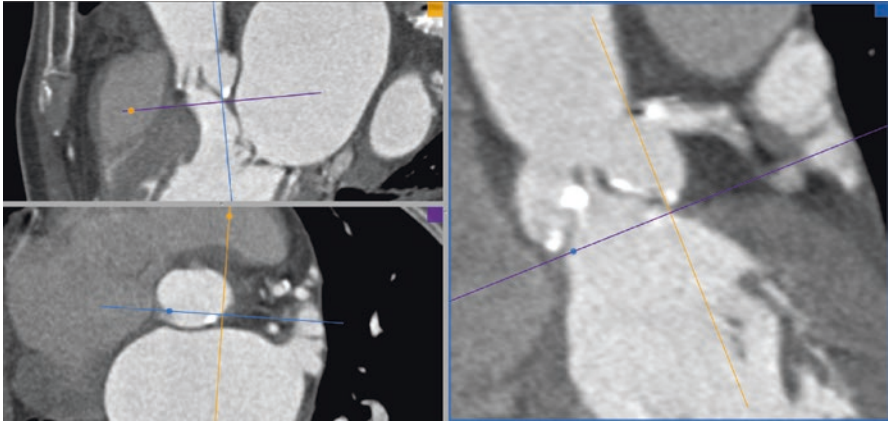
Fig. 2.9 Rotate the blue axis toward the NCC and check in the corresponding plane if the purple axis touches the nadir, and correct the orientation of the purple axis accordingly
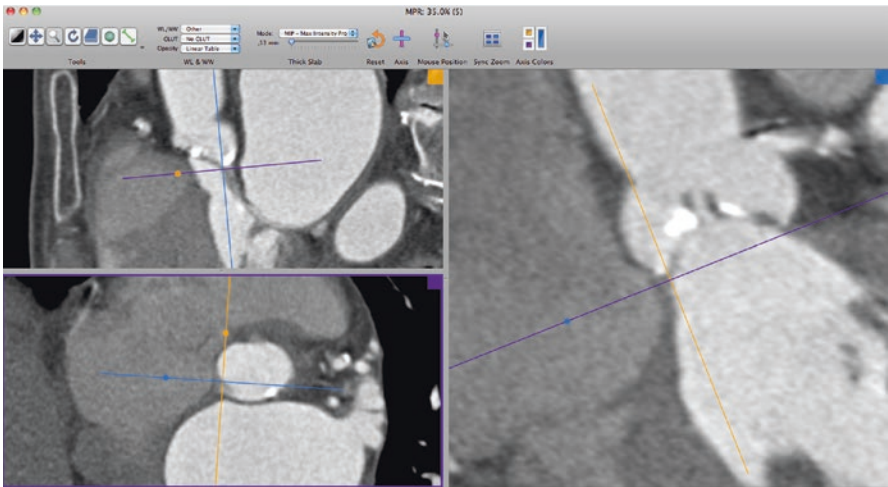
Fig. 2.10 Drag the axes from LCC to NCC

– Rotate the orange axis toward the LCC and check in the corresponding plane if the purple axis touches the nadir, and correct the orientation of the purple axis accordingly (Fig. 2.12).

At the end of this process, the annulus plane should be identified on the axial plane (purple plane). To double check the findings, scroll images in the axial plane from annulus to STJ, and check if the cusps of the aortic valve appear at the same time (or inversely, scroll from the STJ to the LVOT and check if the cusps of the aortic valve disappear at the same time).
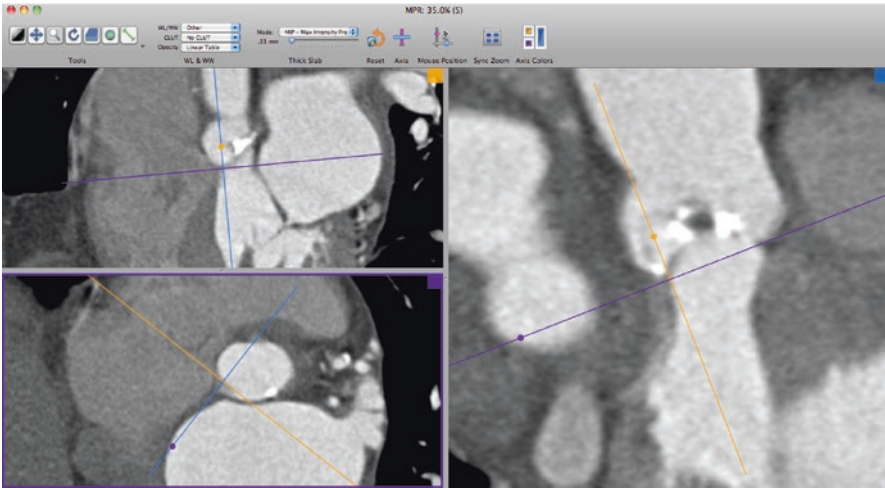
Fig. 2.11 Rotate the blue axis toward the RCC and check in the corresponding plane if the purple axis touches the nadir, and correct the orientation of the purple axis accordingly
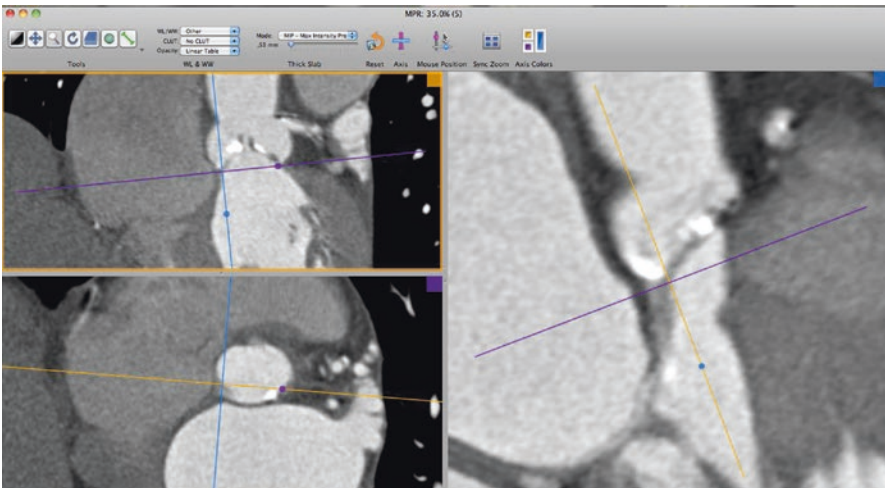
Fig. 2.12 Rotate the orange axis toward the LCC and check in the corresponding plane if the purple axis touches the nadir, and correct the orientation of the purple axis accordingly

Once confident with the plane, start measuring diameters (with the length tool) and perimeter (with either the closed polygon tool or the pencil tool); the latter will give also measure of the area of the annulus (Fig. 2.13).
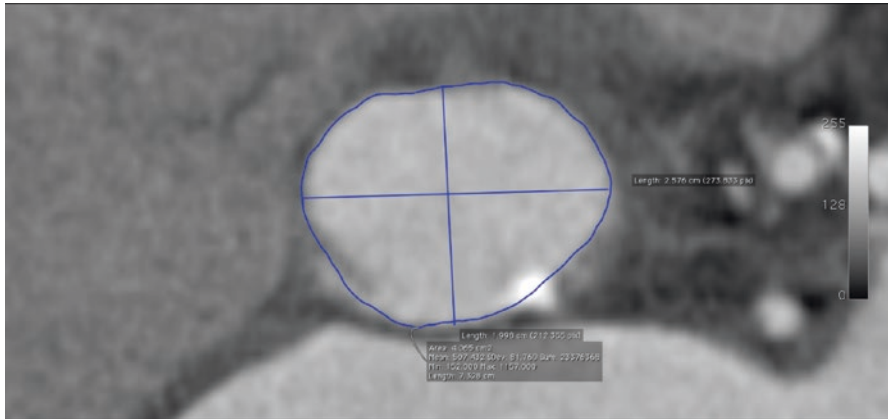
Fig. 2.13 Measurements of annulus diameters and perimeter
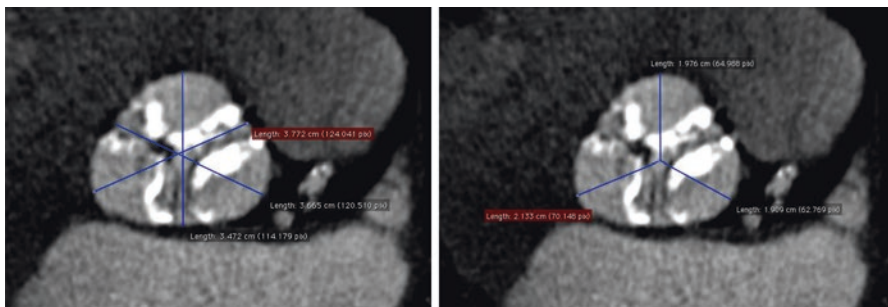
Image A   **Image B**

2.3   Measurement of Aortic Bulb Structures

(a) Sinuses of Valsalva width (best measured in diastolic phase): after identifying annulus plane, in the axial plane scroll images toward the middle of the aortic bulb and determine sinus width for each cusp measuring the length from one commissure to the edge of the opposite cusp (*image A*); alternatively, measure the length of each leaflet in axial plane (*image B*).

(b) Sinuses of Valsalva height: length from annulus plane to STJ, measured for each cusp (measured either in the coronal or sagittal plane).

(c) Coronary ostium height: on axial plane, rotate axes so that the left main ostium appears in the coronal plane, and measure the distance from the lower edge to annulus; repeat the same method for the right coronary ostium.

Tip: if coronary ostia are low, measure the length of the leaflets too to try to understand the risk of occlusion (Fig. 2.14).

(d) Aortic valve calcifications: on axial plane, scroll back and forth over the aortic valve to verify symmetry and distribution of calcifications on the leaflets.

Tip: check for bulky calcifications on the edge of the leaflets that may cause coronary ostia occlusion; if in doubt, measure calcification thickness on coronal or sagittal planes (Fig. 2.15).
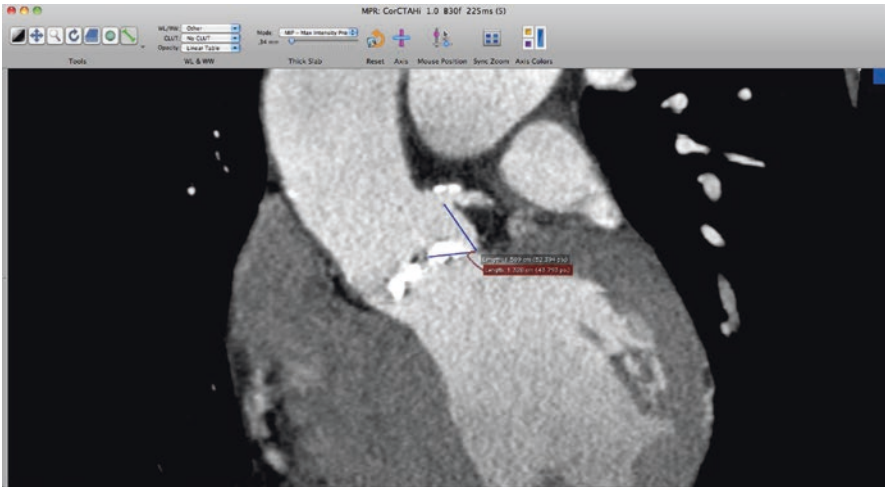
Fig. 2.14 Measurements of coronary ostium height and leaflet approximate length
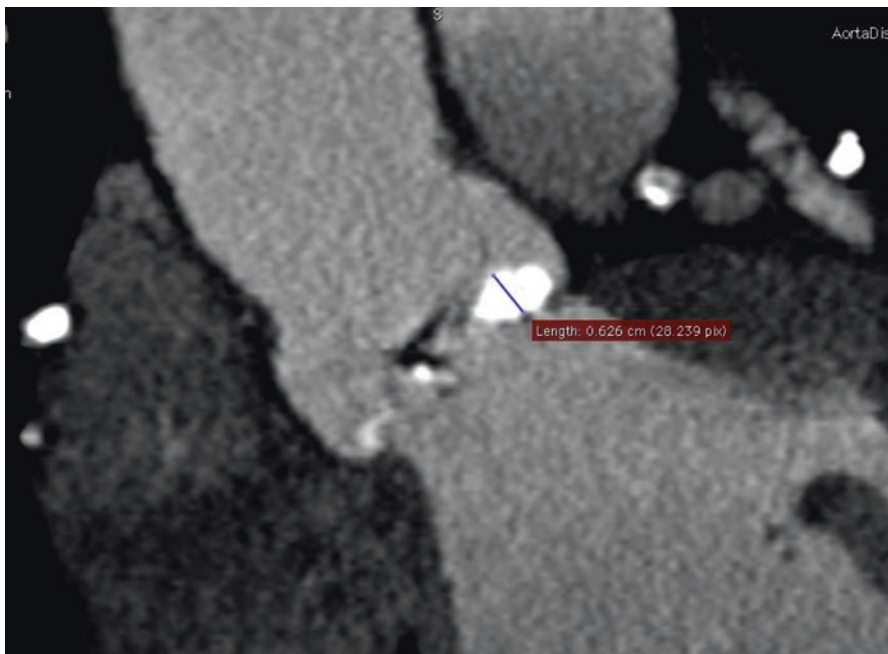
Fig. 2.15 Measurement of bulky calcification on the leaflet

Tip: when measuring sinotubular junction diameters, take a special look about circumferential calcifications to size BAV balloons (Fig. 2.16).

Tip: after measuring annulus plane, take a look at the LVOT diameters a few millimeters (3–4 mm) under the annulus plane to check if there's a narrowing or widening of the LVOT.

Tip: check the aorta/annulus angle to identify horizontal aorta; to do it, simply align the aortic cusps on the same line and then take an angle measurement between the valve and the horizontal plane (Fig. 2.17).

Fig. 2.16
Circumferential calcification of the STJ
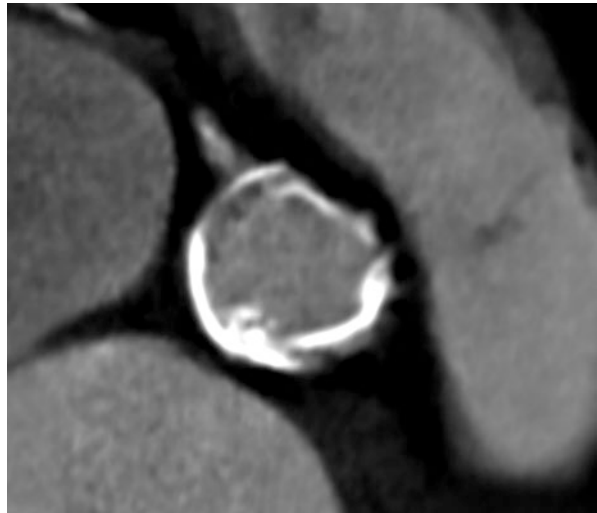
Fig. 2.17 Measurement of annulus angulation

2.4   Optimal Implant Projection

There are some different methods to identify optimal implant projection for the TAVI procedure.

In older versions of OsiriX, one of the quickest requires to identify the annulus plane in the 3D MPR module and then to place a point on the nadir of every cusp (Fig. 2.18). Then, using 3D volume rendering module and adjusting contrast in order to see the three points, it is possible to rotate the projection with the "Rotate around a focal point" tool until the three points lay on the same line. The angulation of C-arm is then reported on the bottom right corner (L-R stands for LAO-RAO, S-I stands for cranial-caudal) (Fig. 2.19).
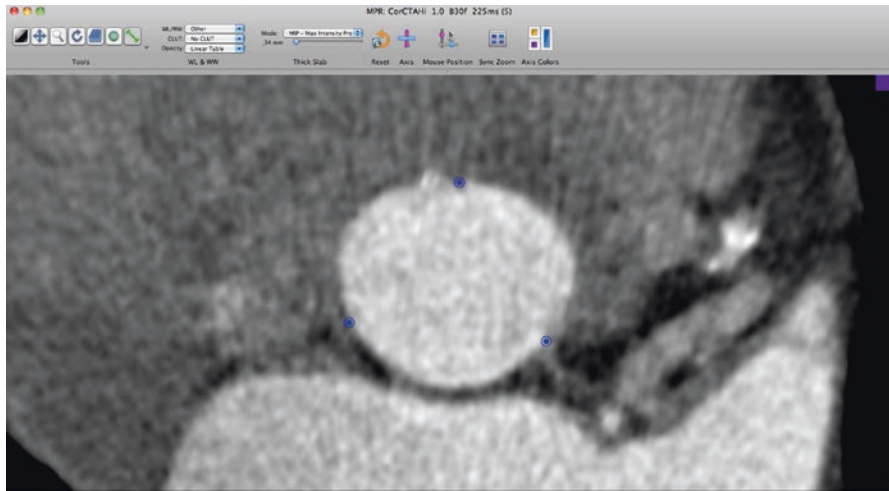
Fig. 2.18 Placement of points on the nadirs
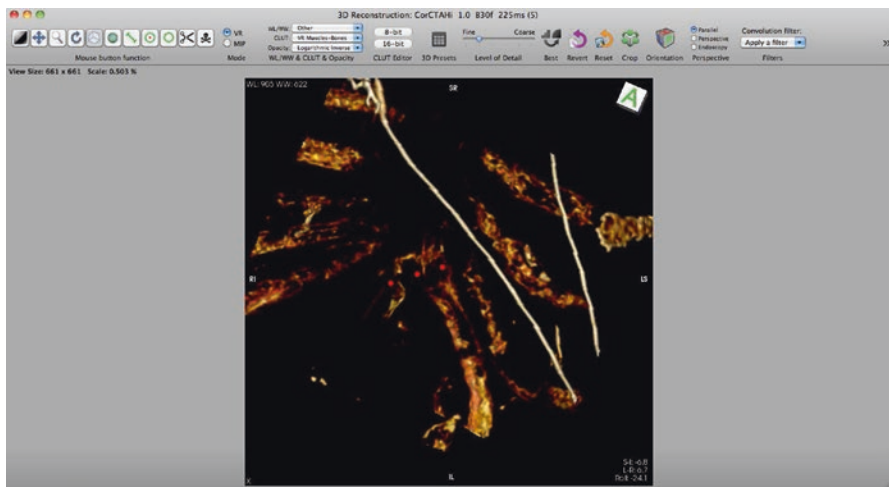
Fig. 2.19 Implanters projection, see C-arm angulation on the bottom right corner

Tip: if the patient has not laid straight on the CT table, this may lead to mistakes in identifying the optimal projection; to correct this, measure the angle between the sternum and the vertical line (Fig. 2.20), and subtract this angle from the LAO-RAO angle obtained from the above method.

2.5   Evaluation of the Access Site

Tip: adjust contrast and scroll through the aorta to check for dissection, thrombus, and aneurysms before evaluating the access site (Fig. 2.21).

Tip: when evaluating femoral arteries for percutaneous or surgical access, check distance from the skin to the anterior wall of the artery around the potential puncture site to help the decision.

2.6   3D Reconstruction of the Aorta

This is a multistep algorithm that has to be performed on an angio-CT series.

First of all, we need to identify the starting point of the algorithm, so scroll to the descending aorta and open *ROI -> Grow Region*; a good starting parameter for the

Fig. 2.20 Measurement of the angle correction for patient misalignment on the table
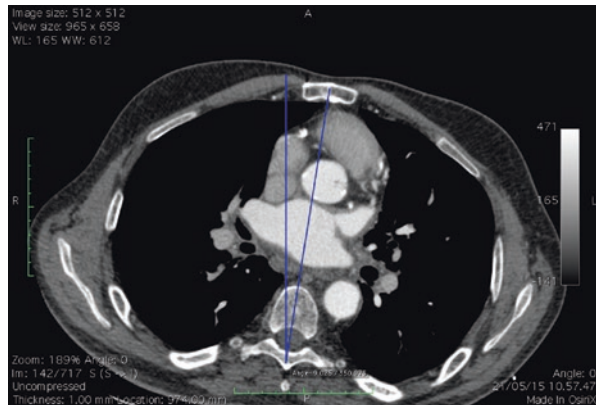
Fig. 2.21 Mobile atheroma in thoracic descending aorta
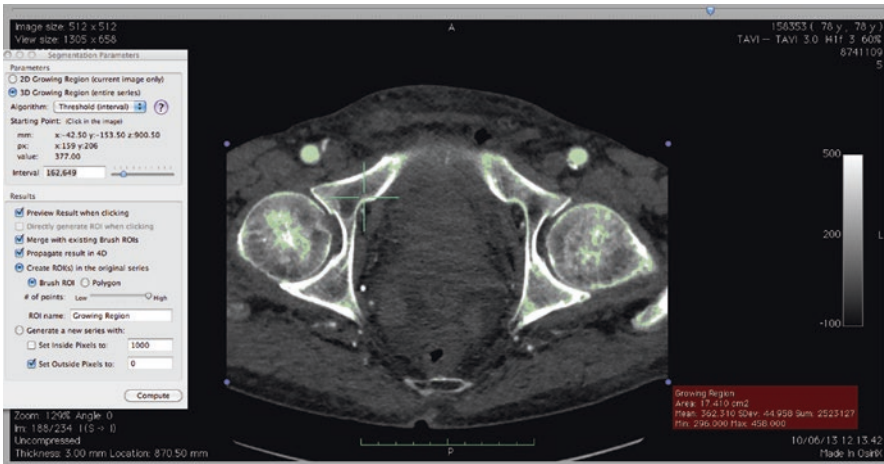
Fig. 2.22 *Segmentation Parameters* box and ROI identification

threshold interval algorithm is 120 (it can be however changed accordingly to extend or diminish the ROI), and then click inside the descending aorta, and then click on *Compute* to run the algorithm (Fig. 2.22).

Tip: to check if the algorithm succeeded to recognize the aorta and the iliofemoral arteries, just scroll the images after the algorithm finished the elaboration, so a failure in detecting a vessel is immediately noticed.

If the algorithm did not identify all vessels correctly, just click on the missing part of the vessel and then click *Compute* to run the algorithm again; a second run should be enough to identify the needed anatomy. Close the Segmentation Parameters box.

The second step is to dilate the current region to include the entire vessel and calcifications, so click on *ROI -> Brush ROI ->Dilatation* and set the structuring element radius to 5 and check "Apply to all ROIs with the same name" and then click OK.

As the last step, you need to remove the anatomy outside the region of interest that has just been identified. Open *ROI -> Set Pixel Values* and set the pixels outside the ROIs to -1024 in order to blacken all the anatomy outside the ROI (Fig. 2.23).

After this step, the ROI is ready to be reconstructed in 3D; to do so, click on *3D -> 3D volume rendering*.

Tip: if the previous algorithm included part of the bones, one can remove this exceeding anatomy from the 3D reconstruction just by using the forceps tool in the toolbox, pay attention that you need to select the part of the anatomy you want to remove with this tool, and press backspace to actually delete it (Fig. 2.24).
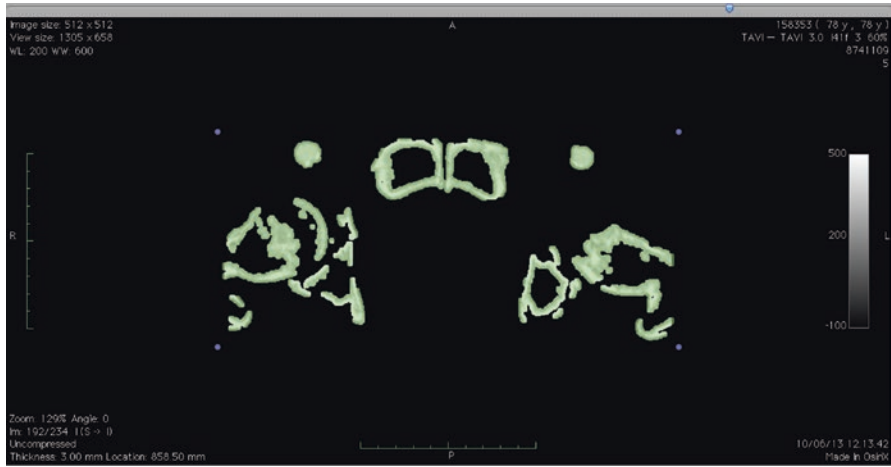
Fig. 2.23   Polished ROI

Fig. 2.24   Use of *Forceps* tool to remove unnecessary detail

2.7   Vessels Analysis with 3D Curved MPR

With the 3D Curved MPR module, reconstruction of iliofemoral and subclavian vessels is pretty straightforward. Once assured that the thick slab parameter is at its minimum (as done in the 3D MPR module), semiautomatic reconstruction of the vessel is performed using the dedicated tool by placing consecutive dots in the middle of the vessel that needs to be reconstructed, starting from descending aorta to the

common femoral artery just prior to the bifurcation. The software starts reconstruct-ing the vessel after the placement of the third consecutive point. Double click on the reconstruction to enlarge the view and perform measurements.

Tip: it is possible to reconstruct the vessel even starting from the common femo-ral artery toward the descending aorta.

Tip: it is useful to save the curved path file that leads to the reconstruction of the vessel; go to *3D Viewer -> Save Curved path*; to retrieve a previously saved path, open the same series used for reconstruction and open 3D Curved MPR module and then *3D Viewer -> Load Curved Path*.

Here is an example of a reconstruction of a right iliofemoral vessel (for subcla-vian vessel, start from the arch toward axillary artery) (Fig. 2.25).

It is possible to switch between the straightened and stretched version of the same reconstruction; decide the best one upon tortuosity of the vessel.

Measurements can be taken on the reconstructed vessel itself or on the axial sec-tions corresponding to vertical lines A, B, and C (right end of the screen). Lines A and C can be dragged toward the end of the reconstructed vessel; line B can drag the whole system together.

Trick: to quickly analyze the vessel to understand if the anatomy is suitable for the intended device, simply draw a circle (by selecting the *Oval* tool in the measure-ments toolbox) with diameter as the minimum vessel diameter you can treat with the device, and place it on the B axial section. Then drag the B vertical line through-out the vessel to see if the drawn circle is always inside the artery; this gives imme-diate quantification of the feasibility of the reconstructed vessel (Fig. 2.26).

Note that in older OsiriX versions, the circle measurement tool does not include the diameter of the circle itself (like the newest versions); in this case use area instead; e.g., if the minimum vessel diameter for the device is 5 mm, draw a circle with 19.63 squared mm area ($5\times5\times\pi$).
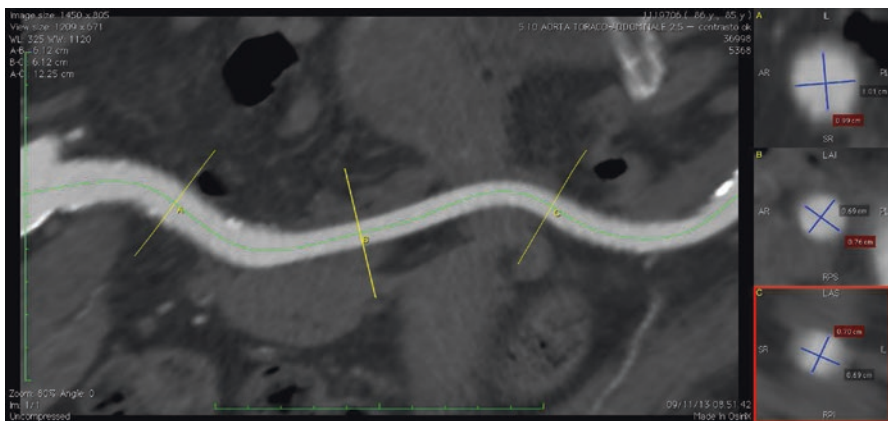
Fig. 2.25 Example of a reconstructed iliofemoral vessel
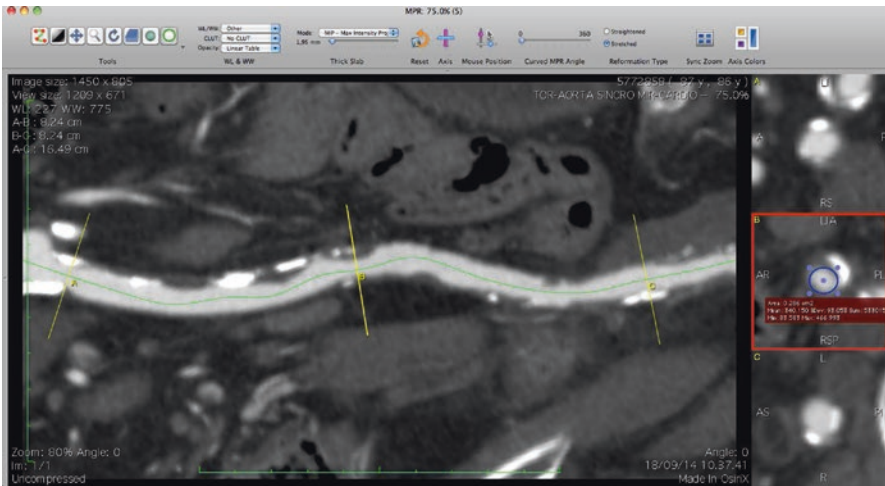
Fig. 2.26 Circle placed on slice B, the drag B axis to assess viability of the access

2.7.1   Direct Aortic Access

If a direct aortic access has to be evaluated, after the identification of the annuls plane in the 3D MPR module, draw a straight line from the annulus plane to the ascending aorta with the minimum required distance, and then evaluate the ascending aorta section at the desired height (check for calcifications on the anterior wall especially).

Tip: place a point on the anterior wall of the ascending aorta that will represent the lowest access point for the direct aortic access (Fig. 2.27).
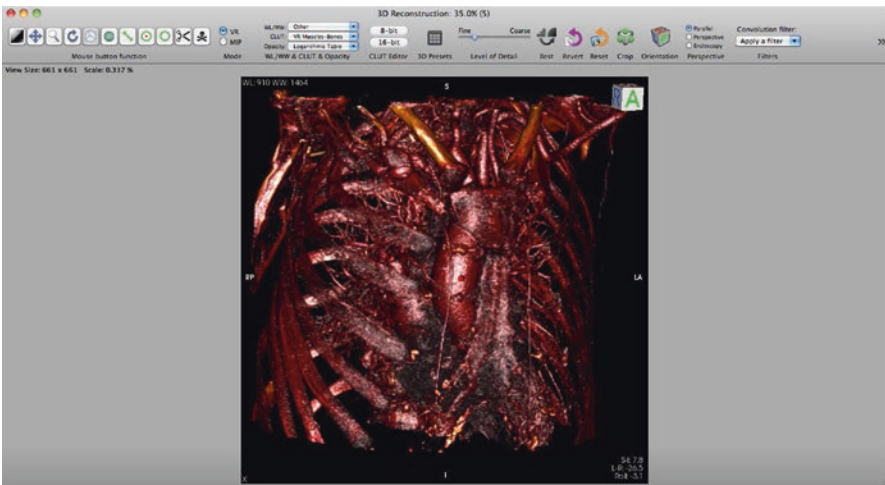
Fig. 2.27 Point (in red) placed in the ascending aorta

Trick: to evaluate if a mini-sternotomy approach or a mini-thoracotomy approach is needed, just check in the axial view how much of the ascending aorta is behind the sternum: if more than 50 % of the ascending aorta is on the right of the sternum and the distance from the skin to the anterior wall of the ascending aorta is less than 6 cm, mini-thoracotomy should be chosen; otherwise, mini-sternotomy should be easier.

Use 3D volume rendering to take a quick look to potential bypass grafts (RIMA grafts or SVGs); adjust contrast to see the ribs and the aorta as well. This is helpful also to identify which intercostal space is easier to access in case of mini-thoracotomy approach.

2.7.2   Transapical Access

Use 3D volume rendering adjusting contrast to identify in which intercostal space the apex is easier to access.

Tip: using the *Crop* tool is beneficial to reduce the 3D volume to only the interesting part that needs to be analyzed (e.g., only to the torso in Fig. 2.28).
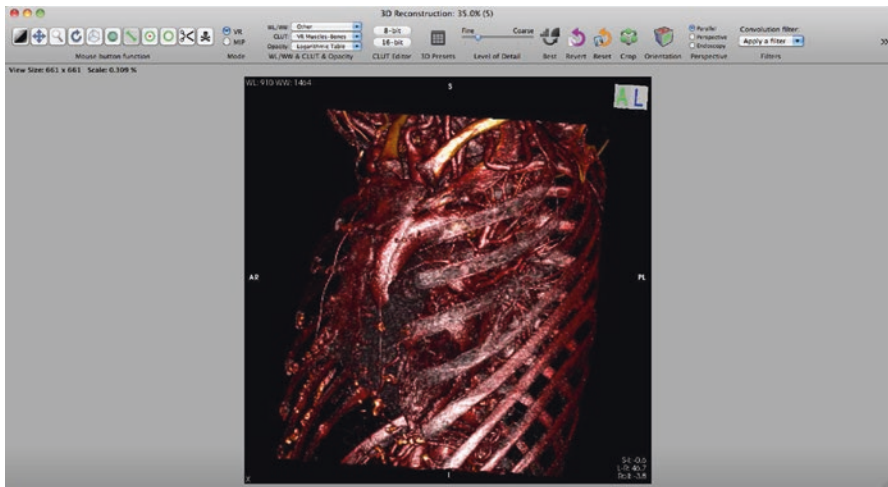
Fig. 2.28 Lateral view of the torso to assess LV apex position

Techniques and Devices

3

Francesco Bedogni, Mauro Agnifili, and Luca Testa

3.1 Introduction

The first transcatheter aortic valve replacement (TAVR) was performed by Cribier and colleagues in 2002 in a compassionate case of inoperable patient admitted for cardiogenic shock as a consequence of severe symptomatic aortic valve stenosis [1]. Thereafter, after a long period of technical development and animal studies, a large amount of literature reported promising results that confirmed the feasibility of TAVR [2–9]. Since commencing of its clinical application, about 100,000 transcatheter valves have been implanted worldwide, and the rate of implants is sharply increasing. The results of several large multicenter registries [10–18], and the prospective randomized trials [19–22], consistently showed that this treatment can be reasonably considered the standard of care for high or prohibitive surgical risk patients with severe symptomatic aortic stenosis. The recently published randomized CoreValve US High-Risk Pivotal Trial [22] was the first to demonstrate a significantly higher rate of survival at 1 year with TAVR compared with SAVR in high-risk patients. More recent publications [23–25] have shown by means of propensity score matching no difference in terms of mortality even in lower-risk patients. These groundbreaking results achieved in the last decade are a consequence of the progressive technological improvement of the devices and of operator's experience. The size of the valves and delivery systems decreased from very large size, 24–25 Fr of the initial devices to the current 14–18 Fr, thus increasing the deliverability through the femoral route and reducing the access complication rate. The accurate sizing and procedure planning obtained with the routine use of CT scan allowed the physicians to choose the optimal approach and to minimize the paravalvular leaks that still remains the major Achilles heel of this procedure.

F. Bedogni (✉) • M. Agnifili • L. Testa
IRCCS Policlinico San Donato, San Donato, Milan, Italy
e-mail: francesco.bedogni@grupposandonato.it

The objective of this chapter is to provide a comprehensive review on technical and procedural aspects of TAVR, to discuss acute and late outcomes, and to highlight the current expectations and potential future development of this rapidly evolving technology.

3.1.1 Preprocedural Assessment

The preprocedural work-up using contemporary prostheses is summarized in Fig. 3.1. Evaluation of the size, tortuosity, and degree of calcification of iliofemoral arteries using multidetector computed tomography (MDCT) or iliofemoral angiography is mandatory to determine the feasibility of the transfemoral approach (Fig. 3.2).

The size of the aortic annulus is usually measured by transesophageal echocardiography (TEE), aortic root angiography (during coronary angiography), MDCT, or a combination of these imaging techniques. Accurate measurement of the aortic annulus is crucial to determine the appropriate transcatheter valve size, and although sizing the aortic annulus with 2DTEE has been associated with good clinical results
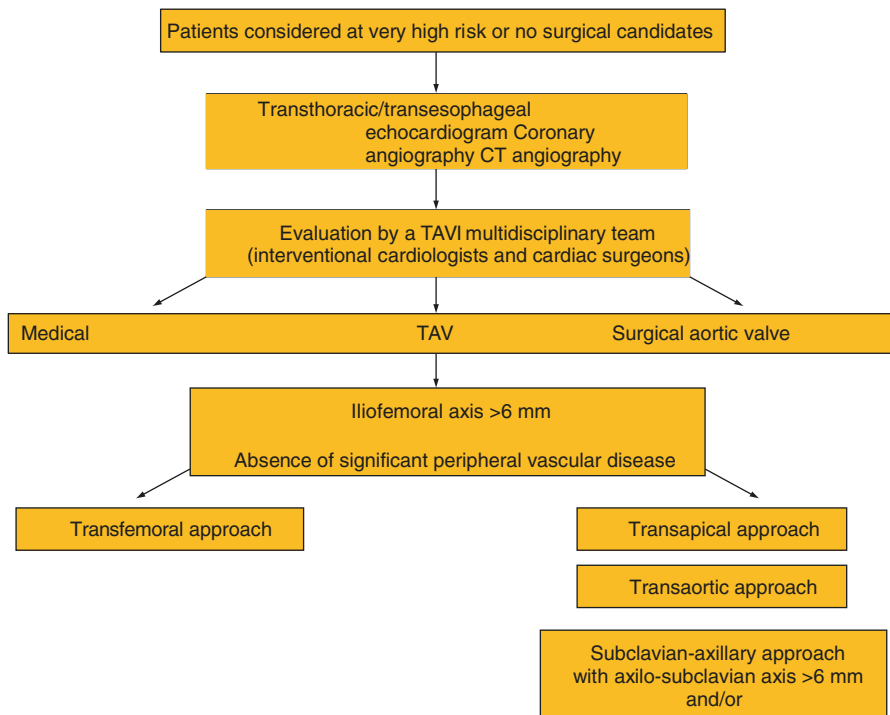
Fig. 3.1 Pre-TAVR work-up. Preprocedural work-up in patients with severe aortic stenosis who are candidates for a TAVI procedure. *CT* computed tomography, *LIMA* left internal mammary artery, *TAVR* transcatheter aortic valve replacement
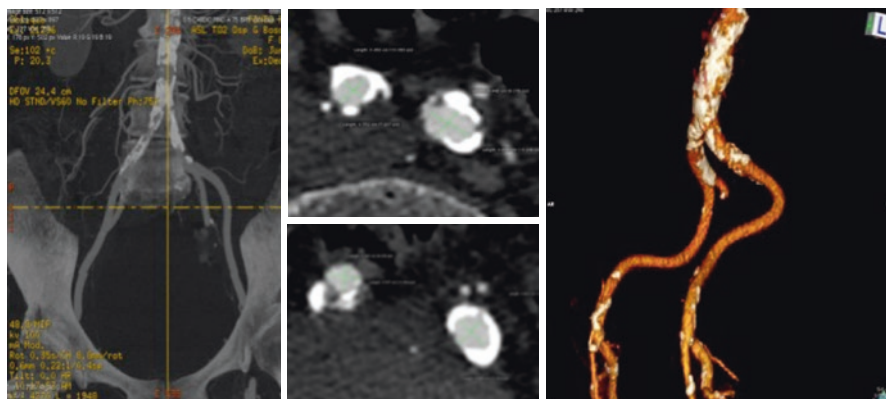
Fig. 3.2 MSCT: femoral accesses. Iliofemoral axes measurement with MSCT scan (Osiris software); Iliofemoral axes 3D reconstruction
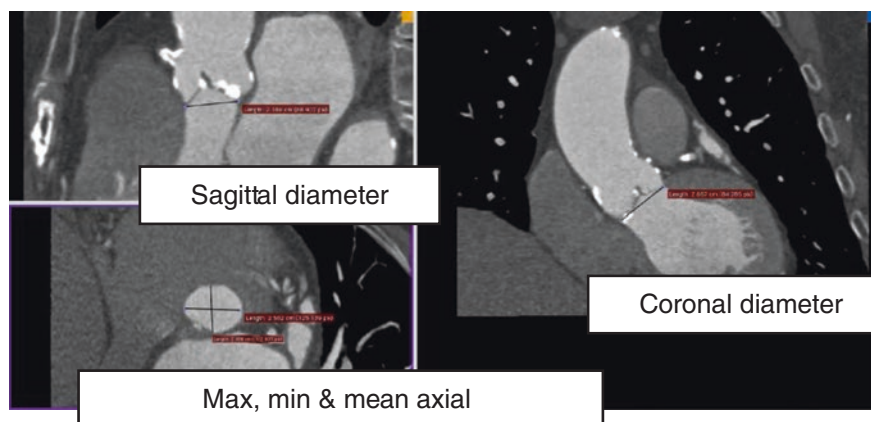
Fig. 3.3 MSCT: annulus measurement. Annulus measurement with MSCT scan (Osiris software)

in most cases, many studies have suggested a tendency toward an underestimation of the aortic annulus by echocardiography as compared with MDCT [26–31]. MDCT studies have clearly shown the oval shape of the aortic annulus in most patients, and nowadays this is the gold standard method for accurate aortic annulus measurement, to assess the most appropriate degree of valve oversizing, as extreme oversizing may increase the risk of aortic annulus rupture and coronary occlusion, while undersizing increases the risk for paravalvular leak and valve embolization (Fig. 3.3). Only in case of severe renal failure TEE might be an alternative to avoid the use of contrast media.

Coronary angiography is performed before the procedure to evaluate the presence and severity of coronary artery disease (CAD). Many concerns arise when undergoing TAVR in the presence of significant yet untreated coronary

atherosclerosis, such as possible coronary access limitations because of the presence of the prosthesis, and worsening of myocardial ischemia during implant. But on the other hand, percutaneous coronary intervention (PCI) in a patient with severe aortic stenosis may be problematic, and PCI prior to TAVR may increase complications because of the necessity of dual antiplatelet therapy and could potentially increase the risk of contrast-related kidney injury in such elderly patients. In cases of severe stenoses in the main coronary vessels, complete or partial coronary revascularization is often performed before TAVR. Data about both safety and feasibility of this strategy are limited but encouraging [32, 33].

Apart from this specific TAVI work-up to determine the feasibility and planning of the procedure, a complete risk stratification including assessment of concomitant diseases, comorbid conditions, and frailty is needed to adequately assess and determine the risk of the procedure.

3.2   General Anesthesia vs. Sedation

TAVR implantation can be done in general anesthesia or in local anesthesia and conscious sedation. In any case, the presence of the anesthesiologist during the procedure is strongly recommended. Subsequently in the progressive ease of the procedure over the years, many centers opted for an anesthesiologist "on call." General anesthesia is mandatory for transapical, transaortic, and transcarotid access and is preferable for trans-subclavian and surgical femoral access and when transesophageal echo is used. For the percutaneous femoral procedure that represents the large majority of interventions, a local anesthesia with Xylocaine and Chirocaine, and if necessary a mild conscious sedation, is the best option. This approach is well tolerated by the patient and allows a lower complication rates, a quicker mobilization, and early discharge [33, 34]. This option is moreover mandatory in patients with severe obstructive respiratory disease where the intubation may lead to difficult weaning from the ventilator. In general, all the team has to be ready in case of severe and life-threatening complications to immediately convert into general anesthesia.

3.3   Percutaneous Femoral Access: Technique of Puncture, Prevention and Treatment of Complications of the Sheath Positioning

The transfemoral route (Fig. 3.4) is the first choice in the vast majority of centers performing TAVR procedures. Most centers are now using a fully percutaneous technique using vascular closure devices instead of the surgical cutdown [35]. Bleeding complications are strongly related to mortality. In the early phase of TAVR experience, the complication rate related to the femoral vascular access, as reported in all the registries and randomized trials, was dramatically high and was the major cause of immediate [13, 20] and late mortality [36]. The progressive reduction of the devices' size; the accurate planning by means of CT scan to detect
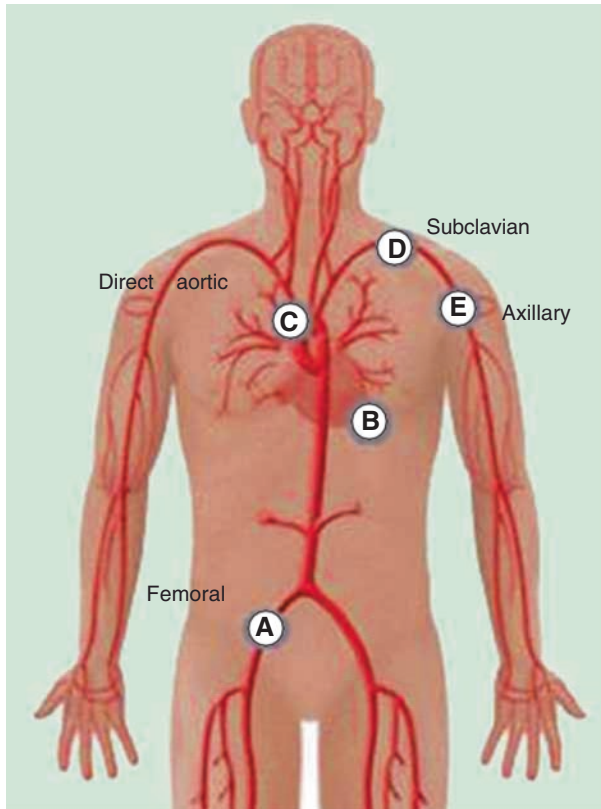
Fig. 3.4 Multiple accesses. Approaches used for transcatheter aortic valve implantation. *A* the transfemoral approach. *B* the transapical approach. *C* the transaortic approach. *D* the subclavian approach. *E* the transaxillary approach (usually the left vessel)

size, calcifications, tortuosity, and atherosclerotic disease; the correct puncture of the artery; and the contralateral protection led to a dramatic reduction of vascular complications [37–40]. The technique of femoral puncture for TAVR significantly differs from the conventional femoral artery puncture. The first step consists of the puncture of the secondary access leading to the crossover of the abdominal aorta with a catheter (pigtail, JR, LIMa catheter) and to the selective injection of few mls of contrast to visualize the correct puncture at the main access (Fig. 3.5). The latter should ideally be far above the bifurcation of the common femoral artery and below the inguinal ligamentum. After the injection, a 0.018-in. extra-stiff wire is positioned distal segment of the superficial femoral artery (Fig. 3.6). If crossover is impossible, the wire protection may be done from the radial artery. The puncture is then performed under fluoroscopy with a quite vertical angle (Fig. 3.7). For the transfemoral access, vascular pre-closure can be done with one ProStar or two ProGlide systems (Abbott Laboratories, IL, USA) (Fig. 3.8). After the insertion of an 0.35 extra-stiff wire, an 18-Fr sheath is advanced up to the abdominal aorta. In

Fig. 3.5 Crossover angiography. The aortic crossover is performed with a 5-Fr catheter; after that a selective injection is performed in the iliofemoral axes with few mls of contrast to visualize the correct puncture at the main access
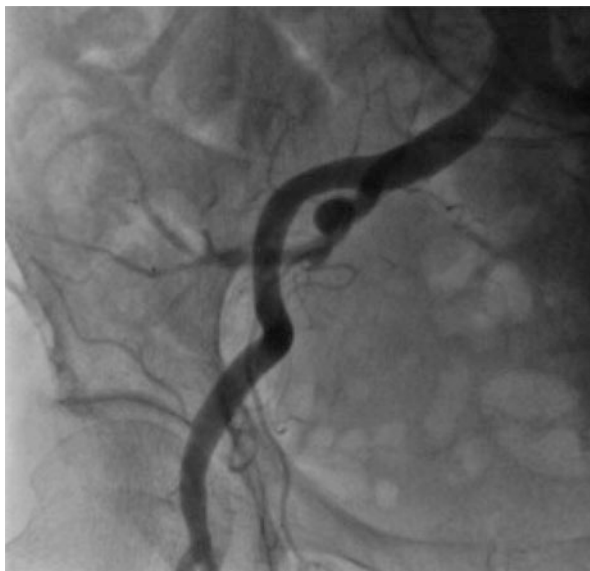
Fig. 3.6 Crossover wire. Using the 5-Fr. crossover catheter, a 0.018-in. extra-stiff wire is positioned in the distal segment of the superficial femoral artery
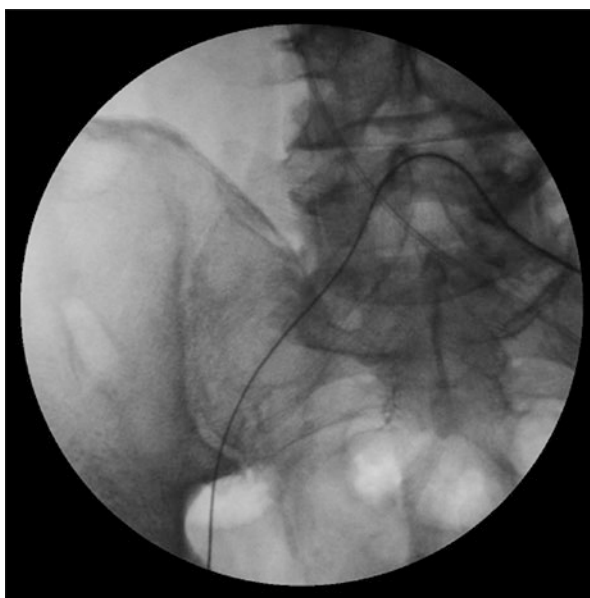
case of severely tortuous femoral artery, the use of even stiffer wires as Lunderquist or Backup Meier wires is useful or sometimes necessary. The new Edwards Sapien 3 and Medtronic Evolut R require smaller-caliber introducers. All maneuvers with the introducer sheath should be done gently and under fluoroscopic guidance. In case of excessive resistance to the sheath advancement, peripheral balloon dilation

Fig. 3.7 Main vessel: femoral puncture. The puncture is performed under fluoroscopy with a quite vertical angle of the needle

a   **b**
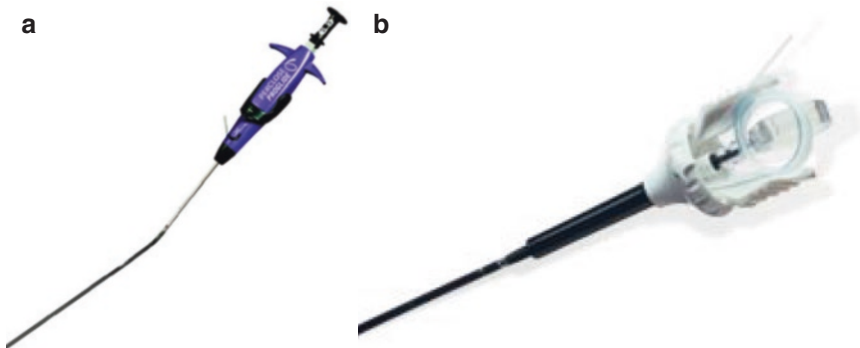
Fig. 3.8 Femoral pre-closure: ProStar and ProGlide. For the transfemoral access, vascular pre-closure can be done with two ProGlide (**a**) or one ProStar system (**b**)

may be considered. At the end of the procedure, sheath retrieval is one of crucial points for complete TAVR success. Best practice suggests to gently remove the introducer with pressure monitoring at the tip just above the puncture site. If sheath retrieval is difficult, we suggest to reinsert the mandrel to avoid the "sucking effect" possibly leading to the avulsion of the iliac artery. Then using a crossover balloon over the 0.018 crossover wire to completely occlude the common femoral artery and reduce bleeding during the suture is safe (Fig. 3.9). After that a selective angiography has to be performed to assess the final result (Fig. 3.10). In case of visualization of bleeding, the balloon has to be inflated at the puncture site for some minutes to achieve the vessel closure and avoid major bleedings [38]. In case of
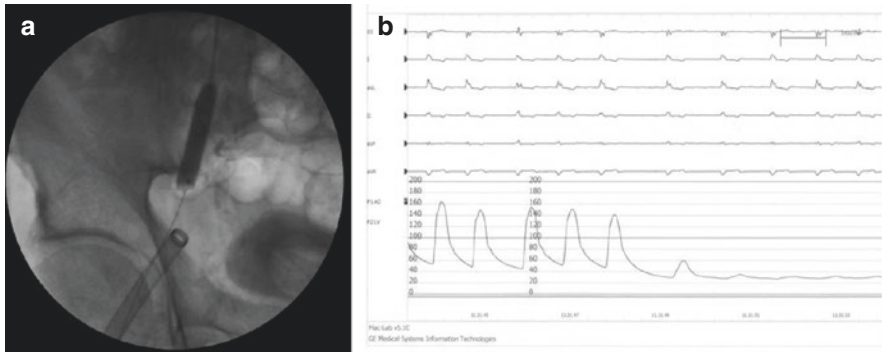
Fig. 3.9 Crossover balloon inflation. It's strongly recommended to use a crossover balloon over the 0.018 crossover wire to completely occlude the common femoral artery and reduce bleeding during the suture (**a**); the pressure drop recorded on the tip of the balloon assesses the vessel occlusion (**b**)
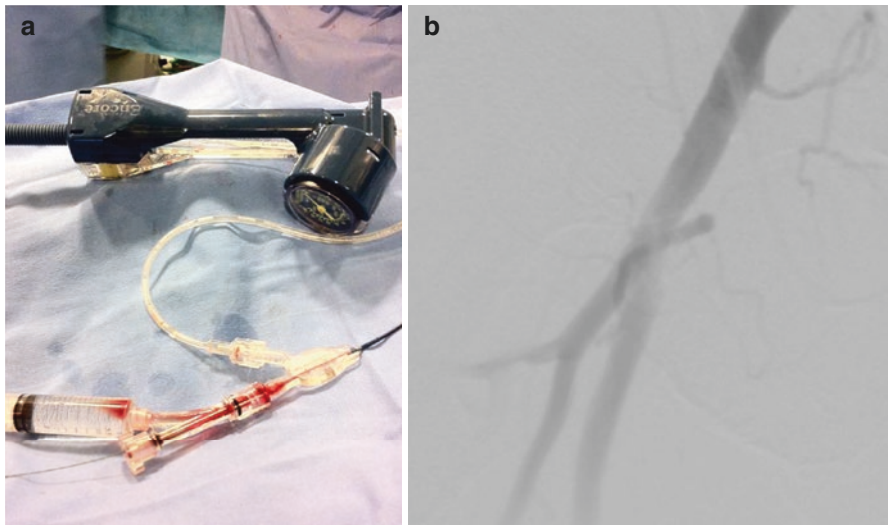
Fig. 3.10 Final selective angiography. "Y" connector with a 10 cc Luer-Lok syringe allows manually dye injection, keeping the protection wire in place (**a**); a selective angiography has to be performed to assess the final result (**b**)

failure, the sealing may be easily obtained using a covered stent from the contralateral access through the crossover wire (Fig. 3.11). Different 18-French femoral introducers are now available on the market. The Cook sheath was suggested from the beginning for CoreValve implantation for its stiffness allowing the device retrieval (Fig. 3.12). Medtronic Sentrant, Saint Jude, Jo-tech, Boston Scientific, and GORE are good alternatives. There are two other introducers, such as the "eSheath" and the "Solopath," which share a common feature such as the modifiable profile, i.e., they implement a dynamic expansion mechanism aiming at reducing the vascular injury (Fig. 3.13).
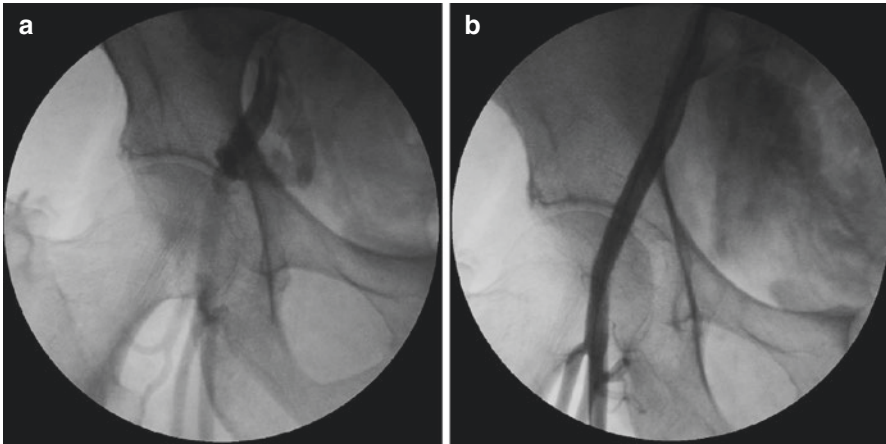
Fig. 3.11 Covered stent. In case of vessel closure failure with bleeding, (**a**) the sealing may be easily obtained using a covered stent from the contralateral access through the crossover wire. A selective angiography has to be performed to assess the final result and the artery sealing (**b**)
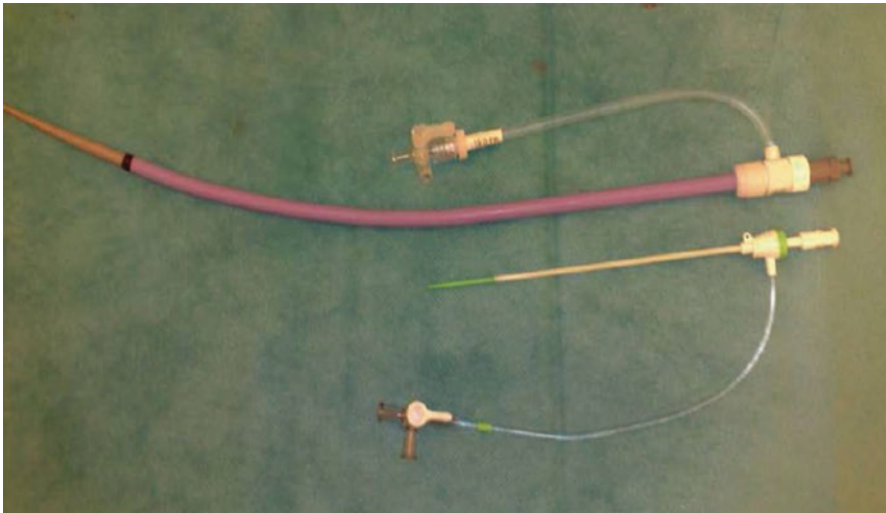
Fig. 3.12 Cook sheath. The Cook sheath was suggested from the beginning for CoreValve implantation for its stiffness allowing the device retrieval

3.3.1   Alternative accesses: Subclavian, Transaortic, Transapical, Transcarotid

3.3.1.1 Transapical Approach

Lichtenstein and colleagues [4] in 2006 implanted a Cribier-Edwards via the transapical approach for the first time. Potential advantages of the transapical approach include the avoidance of large catheters through the iliofemoral system, aortic arch,
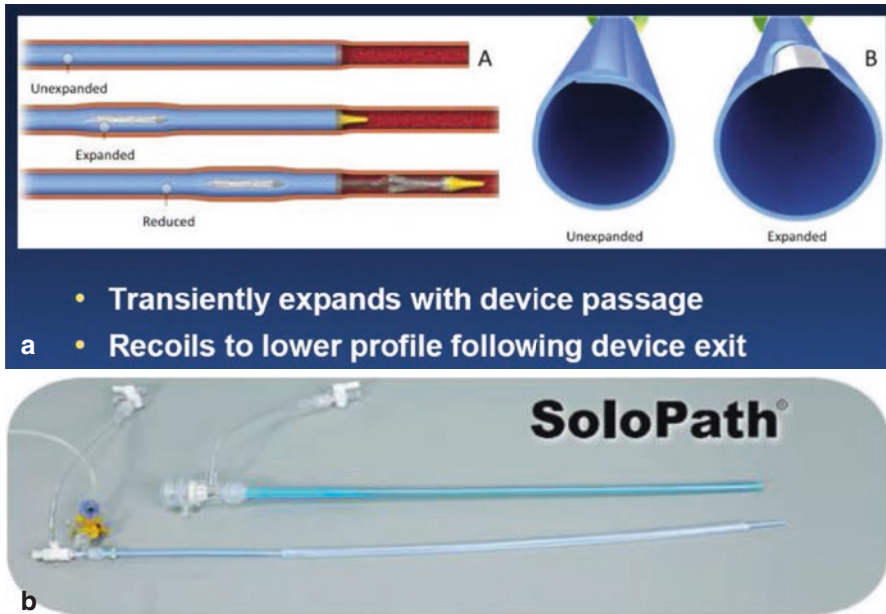
Fig. 3.13 eSheath and Solopath. The "eSheath" (**a**) and the "Solopath" (**b**) share a common feature. With a modifiable profile, they implement a Dynamic Expansion Mechanism aiming to reduce the vascular injury

ascending aorta, and aortic valve and an improved coaxiality of the delivery system with the aortic annulus. The main disadvantages are the need for general anesthesia; a thoracotomy; a greater degree of myocardial injury, owing to the apical perforation of the left ventricle [41]; and the potential bleeding complications associated with the surgical repair of the apex. Transapical approach is associated in literature with worse outcomes compared to transfemoral approach [20, 25, 42].

3.3.1.2 Transaortic Approach

In 2009 and 2010, the use of the transaortic approach through a hemisternotomy (mini-J sternotomy) or a right thoracotomy was proposed as an alternative approach with the MCV and ESV systems [43]. Possible advantages are avoidance of large catheters through the iliofemoral system and aortic arch and avoidance of puncture of the ventricular apex. Possible disadvantages are the surgical local complications including those to the chest wall and pleurae.

3.3.1.3 Subclavian Approach

The subclavian approach has emerged as an alternative to the transfemoral approach with the MCV system [44, 45]. A surgical cutdown is needed to isolate the subclavian artery (both left and right). Possible advantages rely on the very short distance between the vascular access and the aortic valve leading to a better control of the MCV prosthesis during positioning and deployment. However, any injury of the

subclavian artery will translate into a major intrathoracic bleeding that might be difficult to control. Minor injury of the subclavian artery such as dissection or stenosis due to the surgical sutures is easily managed percutaneously. Recently, a direct percutaneous approach has been developed by Schafer and his colleagues using a vascular closure device or a graft stent when this fails [46].

3.3.1.4 Transaxillary and Transcarotid Approach

De Robertis and colleagues described the first-in-human MCV implantation by the surgically isolated transaxillary artery [47]. The potential advantage of this approach versus the subclavian approach is that any injury to the axillary artery can be easily repaired with no major clinical consequences. Indeed, and unlike in iliofemoral vessels, occlusion of the axillary artery would be compensated by the collateral circulation between the thyrocervical trunk of the subclavian artery and the subscapular artery. Some case reports and small series described successful implant via the common carotid artery [48].

3.4   How to Find Good Projection: Crossing Aortic Valve

3.4.1   Aortography

After introduction of the appropriate sheath, a pigtail catheter is placed in the bottom of the noncoronary cusp, and aortic root injection is performed using 10–15 mL of contrast at a rate of 15–20 mL/s. This aortogram should be obtained in 15° left anterior oblique (LAO) projection to align the three aortic cusps (Fig. 3.14). Usually,

Fig. 3.14 Angio with three cusps' visualization. A pigtail catheter is placed in the bottom of the noncoronary cusp, and aortic root injection is performed using 10–15 mL of contrast at a rate of 15–20 mL/s. This aortogram should be obtained in, e.g., a 15° left anterior oblique (LAO) projection aligning the three aortic cusps
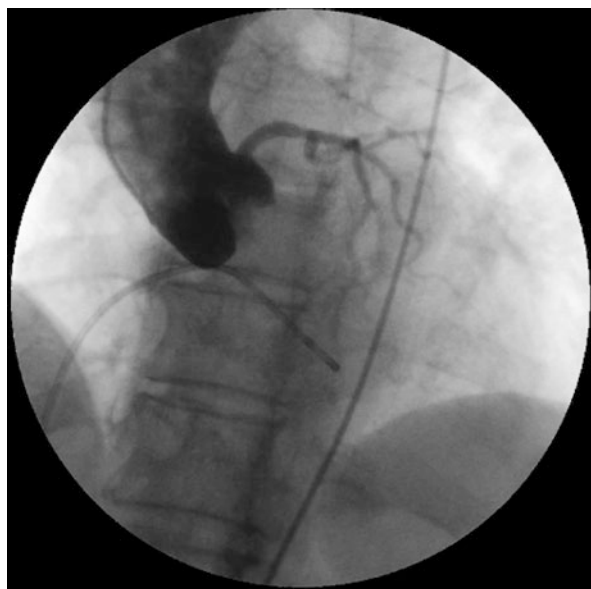
this will visualize the valve opening to guide the crossing of the aortic valve. If the valve opening is not well visualized, a 15° right anterior oblique (RAO) projection may be useful.

In case of impaired renal function, cinematography without contrast will often visualize leaflet calcification and valve orifice. The baseline aortogram should be stored and used as a reference point to avoid multiple contrast injections during valve implantation.

3.4.2 Crossing the Aortic Valve

The way of crossing the aortic valve is according to operator's discretion. This may be done using an AL1 or AL2 catheter and a straight standard or soft guidewire.

When the aortic valve is crossed, the AL catheter may be replaced over a standard J-tip exchange guidewire to a pigtail catheter. This allows better hemodynamic assessment and also reduces the risk of left ventricle perforation when the stiff guidewire is introduced.

3.4.3 Stiff Wire in the Left Ventricle

An either manually shaped or dedicated pre-shaped super stiff wire with a minimum length of 260 can be used. If manually shaped, the curved part should include both the soft and stiff distal part of the wire. The size of the wire curvature may be based on the left ventricular dimensions.

The stiff guidewire is introduced through the pigtail catheter in, e.g., RAO 15° projection to ensure placement at the left ventricular apex. The pigtail shape of the guidewire is used to prevent left ventricular perforation when advancing the valve system and if pushing on the guidewire is used during valve deployment. An example of a non-pre-shaped guidewire is the Amplatz Super Stiff wire (Boston Scientific, MN, US). Dedicated pre-shaped guidewires include Confida (Medtronic, MN, US) and the even stiffer Safari (Boston Scientific, MN, US) guidewire (Fig. 3.15).

3.5 Predilation

3.5.1 Balloon Aortic Valvuloplasty

Balloon aortic valvuloplasty (BAV) with rapid ventricular pacing (e.g., 160–180 bpm) is suggested before valve implantation. The size of the balloon should be slightly smaller than the annulus diameter to minimize the risk of annulus rupture. Both straight and dog bone-shaped and compliant and noncompliant balloons can be used.

In case of severe calcification of the aortic valve, an even smaller balloon may be used.

a

0.035" / 0.89mm
Outer diameter

Small curve 16 cm distal grind
Large curve 18 cm distal grind

Small curve 1.7"/4.2 cm
Large curve 1.9"/4.9 cm

Small curve
1.7"/4.25 cm

Large curve
2.0"/5.05 cm

b
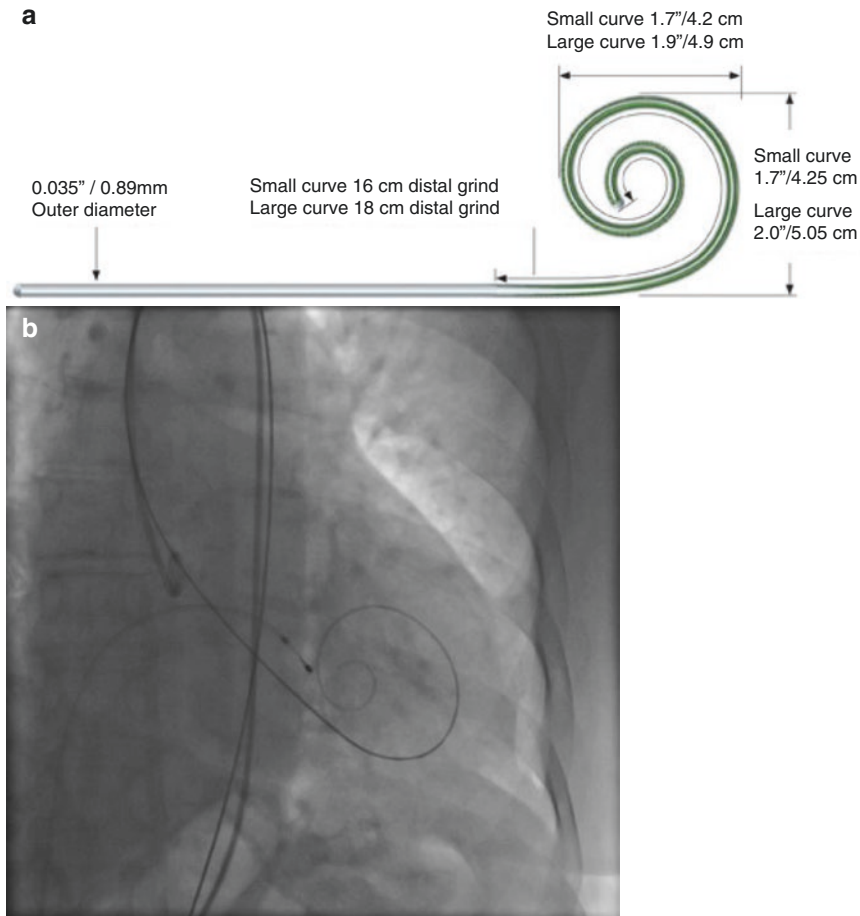
Fig. 3.15 Safari wire and Safari in the ventricle. Dedicated pre-shaped guidewires: technical features of Safari (Boston Scientific, MN, US) wire (**a**); Safari wire placed in the left ventricle (**b**)

There are many cases where direct valve implantation may easily be done avoiding predilation, especially with self-expandable valves as CoreValve, Portico, or Boston Lotus, but is feasible even with Sapien 3 balloon-expandable valve [49, 50]. In our experience, we perform direct implant in case of minimal valve calcification, large size annulus, and presence of aortic regurgitation, low flow-low gradient aortic stenosis to avoid rapid pacing in reduced left ventricular function, and in valve-in-valve procedures to reduce the risk of debris embolization.

Simultaneous contrast injection with a pigtail during BAV may be helpful in ensuring the correct size of the valve prosthesis in case of doubt (Fig. 3.16). Appropriate annulus sealing by the use of balloon diameter may help in estimating the required device diameter to achieve optimal sealing. This technique may also reveal the motion of the native valve leaflets toward the sinuses of Valsalva and potential coronary occlusion by calcified nodules.
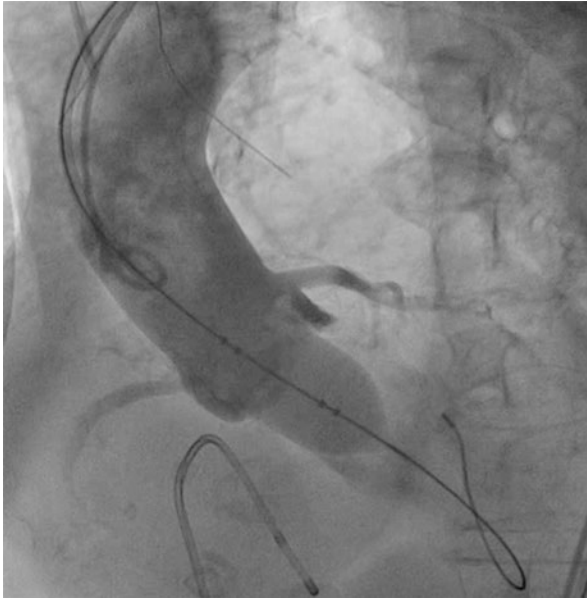
Fig. 3.16 Valvuloplasty and aortic root injection. Simultaneous contrast injection with a pigtail during BAV may be helpful in ensuring the correct size of the valve prosthesis in doubtful cases

The procedure described above is the same for all the transcatheter aortic valves implanted through the femoral route, but valve implantation significantly differs depending on the type of device used.

3.6   Technique of Valve Release (Balloon Expandable vs. Self-Expandable): Tips and Tricks

3.6.1   Medtronic CoreValve and Edwards Valves

Two transcatheter heart valve (THV) designs have been largely used in Europe for many years and are now both approved in the United States (Fig. 3.17) and described in Table 3.1: the Edwards Sapien THV (ESV; Edwards Lifesciences, Irvine, CA, USA), in bovine pericardium which utilizes a balloon-expandable tubular frame, implanted at the intra-annular position and the Medtronic CoreValve prosthesis (MCV; Medtronic Inc, Minneapolis, MN, USA), in porcine pericardium which utilizes a self-expanding multistage frame. A unique feature of the MCV is that this device is anchored not only within the aortic annulus but also extends superiorly to anchor in the supracoronary aorta and works in supra-annular position. Early versions of both the ESV (prototypic Cribier-Edwards and the more widely used Sapien THV) and MCV devices required large 22–25-Fr delivery systems. The subsequent evolution of the devices (Sapien XT and last generation of CoreValve) led to the use
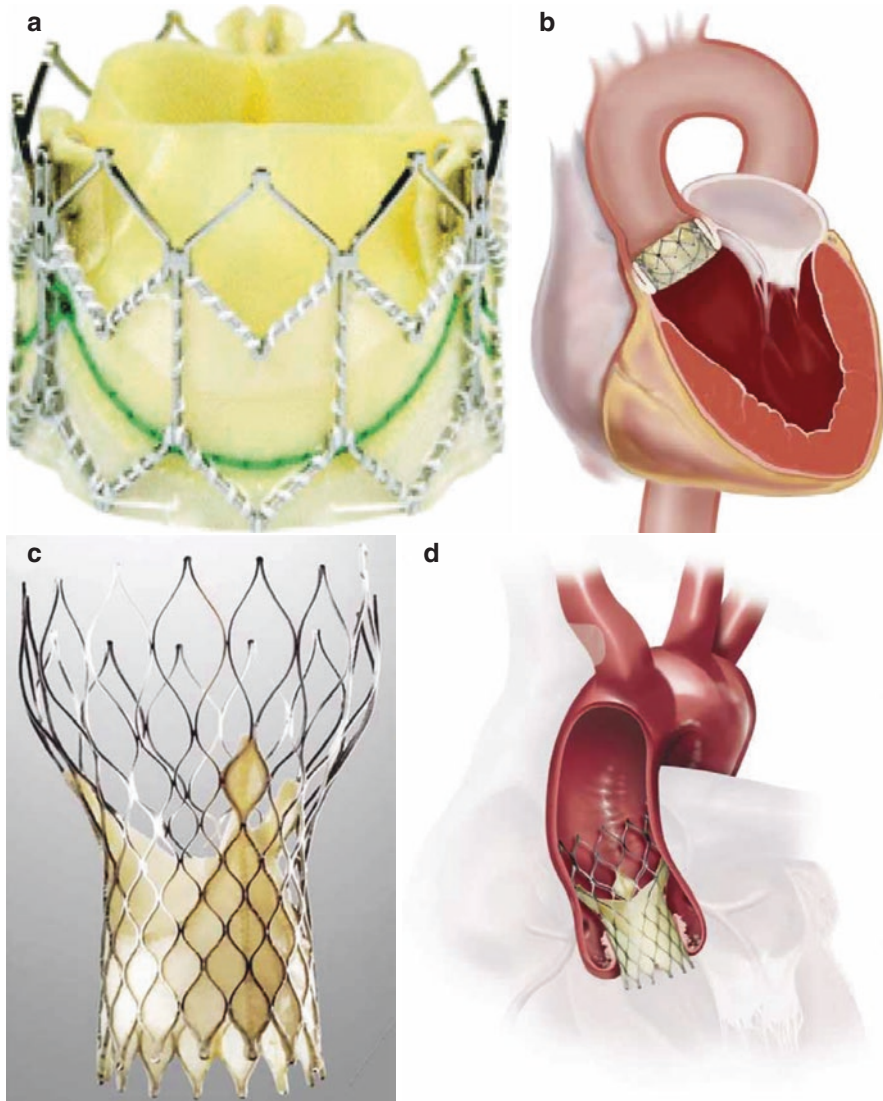
Fig. 3.17 THV. Transcatheter heart valves currently used for transcatheter aortic valve implanta-
tion. (**a**, **b**) The Edwards Sapien XT (Edwards Lifesciences, Irvine, CA, USA) valve. (**c**, **d**) The
third-generation of the CoreValve prosthesis (Medtronic Inc, Minneapolis, MN, USA)

of low-profile delivery systems, and until 2014 both were available with comparable
18-Fr delivery systems, allowing transfemoral application in the majority of patients
with aortic stenosis. The MCV device is a long device allowing for a wide range of
implant depths and is associated with less hemodynamic instability during deploy-
ment as it can be implanted without rapid ventricular pacing. It could also be
implanted without balloon predilation entirely eliminating the need for rapid

Table 3.1 Comparison of the Edwards Sapien XT and the Medtronic CoreValve prosthesis

	Edwards Sapien XT	Medtronic CoreValve
Frame	Cobalt chromium	Nitinol
Leaflets	Bovine pericardial	Porcine pericardial
Expansion	Balloon expandable	Self-expandable
Retrievable	No	Prior to release (difficult)
Annular/valvular fixation	Yes	Yes
Ascending aorta stabilization	No	Yes
Manufacturer diameters and delivery system	20 and 23 mm (16-Fr expandable sheath)	26, 29, and 31 mm
		(18-Fr sheath and delivery system)
	26 mm (18-Fr, expandable sheath)	(23-mm CoreValve Evolut device)
Annulus diameter (mm)	18–27	18–29
Minimum arterial diameter	6	6
Suitability	AS	AS
	Combined AS and AR	Combined AS and AR
	Pulmonary position	Valve in valve (aortic position only)
	Valve in valve (all four positions)	
Transapical access	Yes	No
Pacemaker incidence	4–8 %	15–40 %
Randomized trials	PARTNER trial (completed)	CoreValve US trial (completed)
AR: aortic regurgitation; AS: aortic stenosis		

pacing [49]. It is potentially retrievable if positioned incorrectly, although this is technically demanding. The risk of acute coronary obstruction by a displaced native valve leaflet may be lower [50]. Both valves are supported by a larger body of publications. Two randomized trials one with ESV [19] and one with MCV [21] have shown the great benefit of TAVR in terms of mortality over medical management in non-operable patients. PARTNER A trial [20] in 2011 with ESV and CoreValve US trial [22] in 2014 demonstrated clearly that TAVR is the best option even for operable but at high surgical risk patients with comparable or superior immediate- and long-term results. The efficacy of TAVR compared to surgery in intermediate- and low-risk patients has to be demonstrated in ongoing randomized trials with both valves (PARTNER 2 and SURTAVI), but propensity matched registries [22–24] have already confirmed this hypothesis. Balloon-expandable valves and self-expandable valves have different pros and cons in different clinical and anatomic subsets, and it is difficult compare their results in randomized trial. The only published Comparison of Transcatheter Heart Valves in High-Risk Patients with Severe Aortic Stenosis: Medtronic CoreValve versus Edwards Sapien XT is the CHOICE trial that compared for the first time the two different THV technologies. The primary end point of the trial was device success and showed a lower frequency of residual more than mild aortic regurgitation and less need for implanting more than

one valve for ESV but without difference in clinical outcomes at 30 days [52]. Comparisons with regard to durability are largely speculative; nevertheless, the available long-term follow-up of MCV and ESV patients documents no major structural valve deteriorations up to 3 and 5 years, respectively, after valve implantation [36, 53, 54].

3.6.2 CoreValve Implantation

The technique of CoreValve implantation is similar to other self-expandable valves.

The delivery system is advanced over the stiff guidewire in the left ventricle until the distal part of the valve frame has crossed the aortic valve. There are two options for the C-arm projection during valve deployment, having either the three aortic cusps aligned or the delivery system aligned. For the first option, this projection can be determined from computed tomography (CT) scanning used for work-up or by aortic root injections until the correct projection is found (Fig. 3.14). Often a LAO/cranial projection is used. For the second option, the projection is determined reducing the "parallax effect" by "closing" the distal marker band of the protective sheath (Fig. 3.18). The marker band should appear as a line, often requiring a LAO/caudal projection. Usually, the C-arm orientation will remain unchanged during the entire deployment but may also be adjusted several times in order to have the inflow part of the valve frame in-plane. Crossing the aortic valve is usually easy due to the low profile of the protective sheath and the atraumatic tip. However, in case of difficult crossing, combination of pushing the system and pulling the guidewire can facilitate advancement to the intended position. Alternatively, a stiffer guidewire can be used
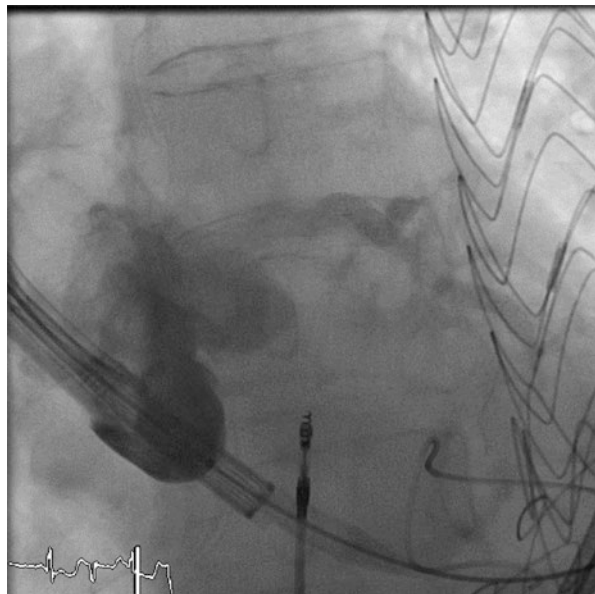
Fig. 3.18 Prosthesis alignment in the native valve. The prosthesis is advanced over the stiff guidewire until the distal part of the valve frame has crossed the aortic valve. Optimal alignment is crucial

(i.e., Lunderquist, Cook Medical, IN, USA). All maneuvers should be done gently, especially when a very stiff guidewire is used, in order to avoid left ventricular perforation. Deployment of the valve begins with clockwise rotation of the deployment wheel on the handle. Usually two operators are involved when deploying the valve: one operator controls the depth of implantation by pulling or pushing on the delivery system, while the second operator rotates the wheel. Any adjustment of the guidewire will affect the control of the deployment and thus the depth and angulation of implantation. The ideal depth of implantation is represented by the frame's inflow edge placed 2–6 mm below the aortic annulus (range 0–12 mm). Low implants are associated with higher rate of PVL and AV block [64]. The pigtail in the noncoronary cusp serves as a landmark, and small aortic root injections (e.g., 10 ml at 20 ml/s) may be used to evaluate the implantation depth (Fig. 3.19). When the protective sheath is withdrawn and the valve prosthesis is exposed, the system tends to dive into
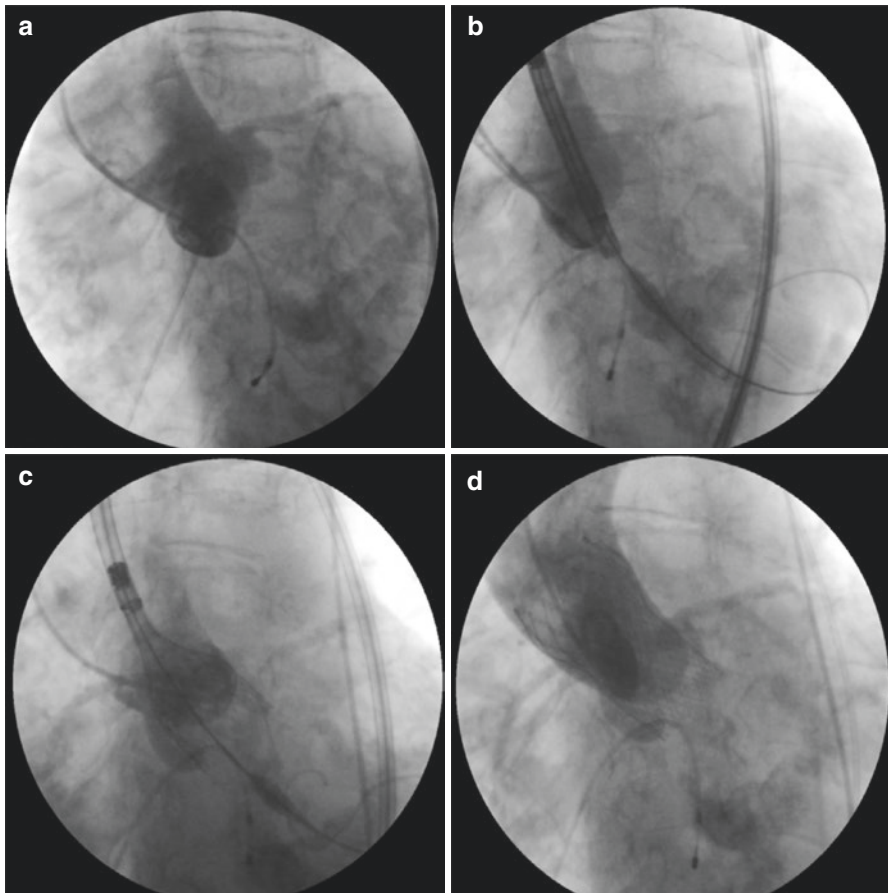
Fig. 3.19 CoreValve implantation. (**a**) Baseline aortic angiography. (**b**) Initial stage of prosthesis deployment. (**c**) Prosthesis almost released. (**d**) Prosthesis fully deployed with trivial paravalvular leak

the left ventricular outflow tract (LVOT). This movement can be minimized by slow rotation of the wheel and by adjusting the position of the valve frame by pulling the delivery system or pushing on the guidewire. Furthermore, some tension should be applied to the delivery system should in order to prevent such diving motion. Further rotation of the wheel allows more exposure and flaring of the frame that is slowly apposed on the left coronary cusp wall, fixing the distal part of the device to the virtual basal ring (Fig. 3.19). At this point, due to the supra-annular position, the Corevalve bioprosthesis might be still closed thus determining a drop of systemic pressure. A quick rotation of the wheel until two-thirds of the frame allows the increase of the pressure. At that point, it is possible to control the position before the release, and small adjustments may be done pulling the catheter. For the valve release, any tension or compression should be released by ensuring that the delivery system is central within the ascending aorta and that there is no remaining tension or compression on the guidewire. Fluoroscopic visualization of retention tabs being detached from the delivery system confirms complete valve release. Withdrawal of the delivery system is attempted only when valve release is confirmed. The stiff guidewire is slightly pulled back in order to lift the nose cone up as it crosses the inflow part of the valve. Once pulled back in the descending aorta, the delivery system is closed pushing forward the sledge of the protective sheath.

A deep implantation may be associated with moderate to severe paravalvular leakage because the sealing cuff is located below the annulus. Whereas indicated, a second valve should be implanted in a higher position (valve in valve). Snaring the implanted valve and pulling it to a higher position may cause vascular complications in the ascending aorta and is only recommended if the valve impedes on cardiac structures in the left ventricle or obstructs the coronary ostia.

3.6.3   Edwards Valve Implantation

The technique of implantation of ESV is unique and completely different from self-expandable valve implantation. It is probably more predictable, but being a "one-shot implant," you have less possibility to correct wrong positions. Edwards XT and the new Sapien 3 valve is loaded over the balloon in a straight segment of descending aorta pulling back the catheter until the distal part of the valve matches exactly with the central marker band of the balloon. Then, in an angiographic projection perpendicular to the valve, counterclockwise rotate the fine alignment wheel for exactly centering the valve between the balloon's markers. Once loaded the valve aortic arch is crossed clockwise rotating the flexion wheel to deflect the catheter avoiding to scrape the aortic arch. Then, the native aortic valve is slowly crossed avoiding abrupt movements. Before the release, it is possible to adjust the angiographic position and the centering of the valve by rotating the flexion wheel. Valve expansion is achieved by balloon inflation under rapid pacing (180–220 bpm) to minimize cardiac output and avoid valve embolization during valve implantation. Balloon inflation has to be maintained for at least 3 s. During the valve release, an angiography with few mls of contrast may be done to assess the position and the
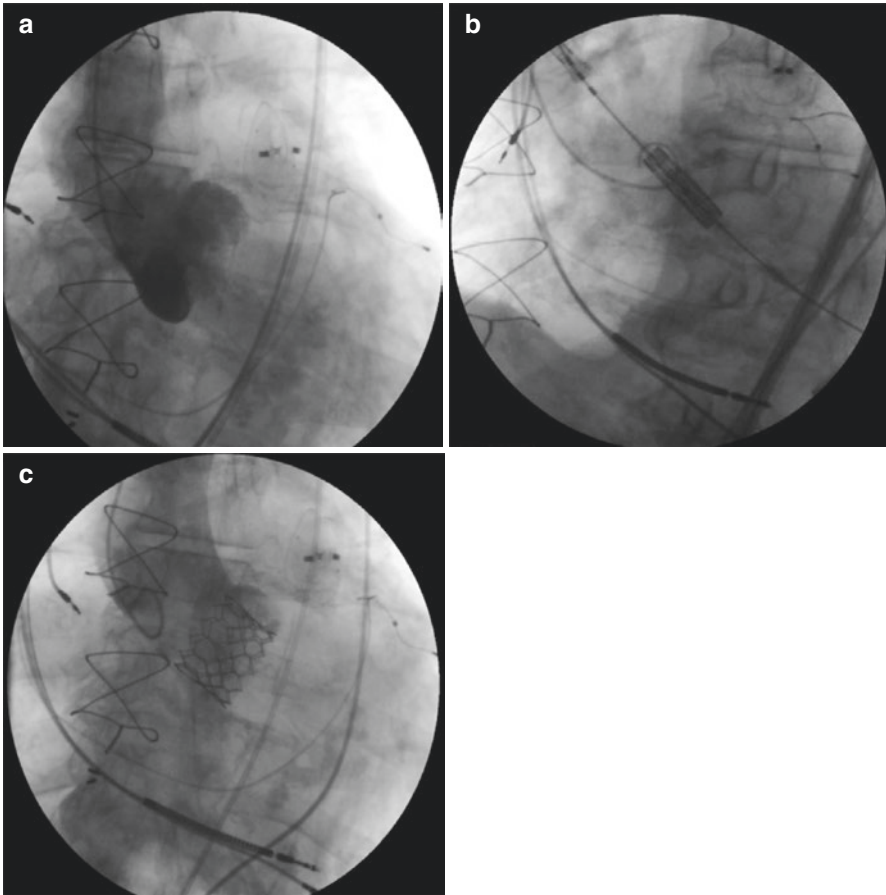
Fig. 3.20 Edwards XT implantation. (**a**) Baseline aortic angiography, (**b**) image showing the deployment of the valve, (**c**) the fully deployed Edwards Sapien transcatheter heart valve; at final aortic angiography, no paravalvular leak was observed

complete expansion. The rapid pacing has to be stopped after the complete deflection. Then the delivery system is retracting in the descending aorta and the result is evaluated (Fig. 3.20).

3.7   Assessment of the Result

The assessment of the result is the same for all the devices. Trivial or mild PVL is commonly observed after TAVI. More than mild PVL is reported in 15–40 % of cases, in early experience series, which is considerably higher than after SAVR [55–62]. Moderate to severe PVL can have important consequences on patient safety and outcome, leading to hemodynamic deterioration, left ventricular (LV) remodeling, and aortic valve reintervention, and is one of the major predictors of long-term

mortality [13, 18, 56, 57]. Aortic root angiography and echocardiography, in addition to hemodynamic assessment, are currently used to estimate the degree of PVL during the procedure and indicate whether further interventions are necessary. Simultaneous aortic and left ventricular pressure measurements at the end of the procedure are important to calculate the aortic regurgitation (AR) index, which is the ratio of the transvalvular gradient between diastolic blood pressure in the aorta and left ventricular end-diastolic pressure to systolic blood pressure in the aorta: ([diastolic blood pressure – left ventricular end-diastolic pressure]/systolic blood pressure) ×100 [57]. The AR index showed an inverse proportion to the severity of PAR differentiating between patients suffering from mild, moderate, or severe PAR and independently predicting the associated 1-year mortality risk. The AR index is a helpful tool to identify cases in which corrective measures to decrease the severity of PAR must be applied; however, it still has to be validated in a larger and controlled study population. Semiquantitative evaluation by means of angiography and echocardiography is obviously very important to obtain a final multiparametric evaluation of the acute result. Angiography is limited in adjudicating the PVL as the classification proposed by Sellers [63] relates to the regurgitation of the native valve, not of a transcatheter bioprosthesis valves that is completely different because the regurgitant jet paints the ventricular wall and might be overestimated thus suffering of a interobserver variability. It depends also to the pigtail position and to the timing of angiography that usually is not standardized. Echocardiography maintains therefore a great importance to judge acute results in case of doubt and to assess the result at discharge and during follow-up. In all recent studies, it is considered the gold standard to judge residual aortic regurgitation. Significant PVL most commonly results from incomplete prosthesis apposition to the native annulus due to pattern/extent of calcification [64–68] or annular eccentricity [69, 70], undersizing of the device [71, 72], and/or malpositioning of the valve [73].

3.8 Postdilation

Valve under-expansion or mal-apposition should be corrected with balloon postdilation. Reviewing the baseline balloon sizing aortogram can facilitate the selection of the appropriate balloon size. To avoid annulus rupture, the postdilation balloon size should not exceed the mean annulus diameter. Occasionally, the use of a smaller balloon may result in equally good result and is preferable in case of a heavily calcified valve. During postdilation, rapid ventricular pacing (180–220 bpm) is recommended to avoid valve embolization into the aorta. These observations seem to be true for both balloon-expandable and self-expandable valves [74].

3.9 Complications

The first phase of TAVR was characterized by a high rate of periprocedural complications that deeply affect the survival [13–19]. With a sharp increase of the learning curve and the improvement of the devices, the complication rate of this procedure is

now largely acceptable, even if a small rate of events is still described even in the last series with the new devices [69–79]. The main issues are vascular complications, conduction disturbances, paravalvular leaks, stroke, coronary occlusion, and annular rupture. We discussed before how to prevent and treat vascular access complications and bleeding. We will describe below the incidence and how we can try to reduce or avoid the other major complications.

3.9.1   Conduction Disturbances

Although generally considered benign, conduction disturbances may portend significant clinical and economic effects, in particular when leading to the implantation of a permanent pacemaker or to the development of permanent atrial fibrillation.

3.9.2   Left Bundle Branch Block

The new left bundle branch block (LBBB) is reported in 29–65 % of patients after the implantation of the self-expanding Medtronic CoreValve and in 4–18 % of patients receiving the balloon-expandable Edwards Sapien ® valve [58]. The main cause of LBBB after TAVI is presumed to be the mechanical compression exerted on the atrioventricular conduction tissue [57]. Indeed, from a technical perspective, avoidance of a low implant is presumed, perhaps generally accepted, as helpful in order to avoid the development of a LBBB, although even the balloon aortic valvuloplasty is capable of determining a new LBBB. A newly developed LBBB is destined to resolve in about 30 % of the cases [76, 77] yet at discharge. A persistent LBBB has been associated with a worse outcome in one study [75], while in two large multicenter registries with Edwards Sapien [76] or CoreValve [77], this association has been denied. However, the persistence of a LBBB has been consistently associated with a higher incidence of advanced AV block requiring a PM implantation [75, 77].

3.9.3   Atrioventricular Block and Permanent Pacemaker Implantation

A high-degree atrioventricular block is reported after CoreValve implantation in 14–44 % of the cases while in up to 12 % after Edwards Sapien implantation [78]. These figures are consistent with the subsequent rate of PM implantation of 18–49 % for CoreValve and 0–12 % after Edwards Sapien implantation [79, 80]. Although generally considered a minor issue, PPM implantation not only implies an additional intervention that is not free from complications by itself, it may also have effects on long-term cardiac function as a consequence of left-to-right ventricular dyssynchrony. The latter will become an issue when TAVR technology will move to younger and lower-risk patients. On the other hand, it is well known that the rate of long-term PM dependency is overtly lower than to the number of the PM implanted

for an acute high-degree AV block [81–83]. From a technical point of view and similarly to the LBBB, the conduction disturbance leading to high-degree AV block is deemed to be a consequence of mechanical compression on the AV node. Indeed, among other predictors of PM implantation (preexisting right bundle branch block, atrial fibrillation, first-degree AV block, and so on), the implantation depth and the mismatch annulus/prosthesis seem to be of outmost importance to predict the possible evolution to advanced AV block [84].

3.10 Paravalvular Leak Causes and Evolution

Multiple studies have reported the frequency and severity of PVL after TAVR [85]. There is, however, significant heterogeneity that is caused by differences in (1) imaging modalities (transthoracic echocardiography, transesophageal echocardiography, angiography), (2) timing of assessment (immediately after implantation, before discharge, at 30 days), (3) transcatheter heart valve (THV) system, (4) grading scale, and (5) adjudication of events. When PVL was evaluated before hospital discharge and without central core laboratory analysis, its absence was reported in 6–59 % of patients, whereas moderate or severe PVL was seen in 0–24 % [85]. PVL tends to be stable over time, and in some cases, it can even improve [85].

Although it was generally believed that only moderate or severe regurgitation would impact long-term outcomes, the 2-year results from the PARTNER trial showed that even mild PVL was associated with significant mortality [62].

See Sect. "3.7" for predictors and corrective measures of PVL.

3.10.1 Stroke and Cerebrovascular Accident

The risk of CVA is inherently related to both patient-based and procedure-related risks. The variability of CVA rates among studies might be due to study design, sample size, methodology, and patient- and site-specific factors, as well as different event ascertainment and definitions [86].

In a recent meta-analysis including randomized clinical trials along with observational studies, Khatri et al. analyzed data from 16,063 patients who underwent TAVR with the commercially available valves in the United States (Edwards Sapien valve and CoreValve). Overall, the early stroke rate (<30 days) was as low as 2.9 %, and CVA rates did not differ significantly according to valve type (Sapien 2.9 % vs. CoreValve 3.6 %, P = not significant) [87]. The time distribution of strokes is inherently correlated to the underlying pathophysiology. Strokes occurring in the acute (<24 h) and subacute early (<30 days) post-TAVR period are strongly related to procedural factors, whereas late events (1–12 months) are mostly connected to patient and disease factors [86]. Indeed, predictive factors for early/subacute stroke/CVA are AF, smaller aortic valve area, balloon postdilation, device embolization, and severe calcification of the aorta. On the other hand, predictors of late stroke/CVA are AF, prior stroke within 12 months, non-transfemoral route, and peripheral arterial disease [86].

Mechanical factors should be targeted for stroke rate improvement. Similarly, to carotid artery stenting, cerebral protection devices have been developed and designed to fit the aortic arch or the anonymous and common carotid arteries: these devices have been developed to avert cerebral embolism either by means of filtration (Claret Montage Device, Claret Medical Inc., Santa Rosa, CA; and EMBOL-X, Edwards Lifesciences) or diversion (Embrella Embolic Deflector, Edwards Lifesciences; and TriGuard Cerebral Protection Device, Keystone Heart, Caesarea, Israel) of debris away from the cerebral circulation while maintaining normal cerebral perfusion. Safety, feasibility, and efficacy are currently being tested in ongoing trials.

Antithrombotic treatment is believed to be a cornerstone for the prevention of ischemic CVAs during and after TAVR. Although TAVR procedures have been performed for more than a decade, little is known about optimal antiplatelet and anticoagulation therapy, and recommendations are based over consensus [88–90]. Thus, there is an unmet need for better antithrombotic therapies given the fact that major stroke rate has not declined significantly over time [88–90].

3.10.2 Coronary Occlusion

Coronary occlusion is a very rare although ominous complication of TAVR with a mortality rate as high as 50 % [19, 20, 22]. It is a consequence of the obstruction of coronary ostia by the frame of the prosthesis, and immediate countermeasures (snaring of the valve or PCI of the coronary ostium) must be performed to restore adequate coronary flow. This complication is far more common during the "valve-in-valve" procedure, as described in the appropriate section.

3.10.3 Annular Rupture/Left Ventricular Outflow Tract Rupture/ Periaortic Hematoma

According to recent data, this complication happens in a cumulative 1.1 % of the cases [85].

Possible predictors are the presence of moderate/severe LVOT calcification and the significant oversize of the prosthesis [91]. This mechanical complication is obviously able to acutely worsen the hemodynamic conditions with a very high mortality rate, in particular when the rupture is uncontained [91]. Conversion to surgery is almost always required as only a lifesaving option [91].

3.11 Special Indications

TAVR was born to treat degenerative aortic stenosis in elderly patients, but there are several different anatomical and clinical situations where this innovative treatment has already been applied, at the beginning as off-label indications but nowadays as good opportunity in cases of high or prohibitive surgical risk.

3.11.1 The "Valve-in-Valve" Procedure

The VIV approach is safe and effective in most cases [92, 93], and it is a great opportunity avoiding sometimes complex redo for surgery. Nevertheless, there are two major safety concerns when performing VIV procedures: device malposition (15.3 %) and ostial coronary obstruction (3.5 %) [92]. The elevated risk for malposition during VIV cases is secondary to the relatively lack of valve calcification and difficulty in defining the optimal target for implantation during the procedure, especially in some of the stentless bioprostheses where no anatomical markers are available. Ostial left-main obstruction, which is only rarely reported during native valve TAVR, seems to be more common during VIV procedures. This complication has a dreadful prognosis. The predisposition for this ominous complication is related to the spatial geometry of the surgical valve leaflets inside the aortic sinuses, i.e., it is a composite not only of the type of valve but of the "virtual ring" of the post of the valve in relationship with the side of tubular junction, the sinuses, and the coronary orifices. Information regarding the height of the leaflet, the height of the coronary ostia, and the inner and outer dimensions of the prosthesis must be clearly addressed, and, for those information that cannot be retrieved by the manufacturer's instruction for use, a computed tomography is mandatory to complete the preprocedural work-up. Nonetheless, even with a complete collection of available information, including the mode of degeneration, echocardiographic and CT scan parameters, bioprosthesis sizes, valve position with respect to the aortic annulus, and valve type (stented vs. stentless), the VIV procedure remains technically demanding. Of note, there are some key points that should always be considered. The use of transesophageal echocardiography (TEE), particularly when dealing with a stentless valves, can be of great value. However, the majority of the cases is nowadays done in mild sedation rather than in general anesthesia; thus, the implementation of TEE could be limited in favor of a less invasive approach, considering that a rapid conversion to open heart surgery is actually anecdotic [92, 93]. The predilation should be avoided in cases of severe regurgitation and considered only when crossing a severely stenotic bioprosthesis is impossible. On the other hand, in some cases, a postdilation is needed. The issue of advanced atrioventricular block and subsequent pacemaker implantation is less relevant as compared to the setting of native aortic valve stenosis as well as the incidence of permanent left bundle branch block [92, 93].

3.11.2 Aortic Regurgitation

Transcatheter aortic valve implantation (TAVR) has not been validated for the treatment of severe aortic regurgitation (AR), and limited data have been reported for severely regurgitant native aortic valves [94, 95]. Surgery is the gold standard treatment for these patients; however, in some cases they are deemed inoperable for the prohibitive risk of mortality/morbidity after surgery and thus considered for TAVR as compassionate therapy. From a technical point of view, the preprocedural workup is the same as that for patients with aortic stenosis. However, patients undergoing

TAVR for aortic regurgitation are usually younger and sicker for the presence of multiple comorbidities and often show a dilated left ventricle, outflow tract, and aortic annulus [94, 95]. These features explain the observed high rate of large-sized transcatheter prostheses implanted. Moreover, notwithstanding a 10–20 % oversizing, such large annuli often predispose to device malposition and need for a second valve. Differently from the procedure for aortic stenosis, the predilation is not needed, perhaps significant calcifications are usually lacking; on the other hand, as the anchoring of the prosthesis may be suboptimal, yet for the lack of calcium, the chance of having a significant paravalvular leak is higher as compared to patients with aortic stenosis.

A simple hint to optimize the device positioning is to perform the deployment under rapid pacing. Provided that a real alternative to surgery is still lacking, while waiting for data, it is conceivable that retrievable and repositionable devices could be able to optimize the results.

3.12   The "Tailored Approach"

These second-generation valves associated with the increasing experience of operators are leading to a dramatic improvement of results and a simplification of the procedure that is now safe and more predictable even compared to few years ago. In Table 3.2, an overview of a 30-day published results between some previous studies using the first-generation valves and the second-generation valves studies is reported. There is evidence of reduction in terms of death rate, PVL, and bleeding complications. The major advantage in terms of efficacy was reached by the new devices in reducing the degree of aortic regurgitation due to the paravalvular leak (Fig. 3.21). The large availability of devices with different mechanism of action and different construction features gives to expert operators the possibility to select the appropriate device for patient's clinical and anatomical characteristics, i.e., "one does not fit all." Any further improvement of the results largely relies on the possibility to individualize the treatment. For example, in case of difficult femoral approach, Medtronic Evolut R or Sapien 3 could be the choice due to the lower profile. In horizontal aorta Sapien 3, Direct Flow or Symetis are the best options. In case of highly calcified or bicuspid valves or with calcifications in the outflow tract, the Boston Lotus, thanks to the adaptive seal surrounding the valve, could give a better apposition to the irregularity of the native valve. In valve-in-valve procedure, especially in small-sized valves, Evolut R or Portico is preferable because they give a lower gradient compared to Edwards valves and because they are repositionable in case of the risk of coronary occlusion. In aortic regurgitation, there is a problem of anchoring and fixation; therefore, ESV is not indicated. These situations may be faced with Lotus valve or with Medtronic CoreValve or Evolut R. In the presence of heavy tortuous or calcified descending aorta or aortic arch, Boston Lotus is contraindicated, while the use of more trackable valves as Evolut R, Portico, or Symetis is certainly more appropriate. For trans-subclavian approach, Medtronic valves or Portico could be the preferred choice, while for transaortic you can choose different kinds of valve except Direct Flow. The only used for transapical are the Edwards balloon-expandable valves.

Table 3.2 An overview of published clinical results at 30 days. A comparison between first- and second-generation transcatheter valves

	CoreValve (US Pivotal extreme risk)	Sapien (PARTNER)	Sapien XT (PARTNER II)	Sapien 3	Direct flow	Lotus valve	Portico
Death	7.5%	5.0%	3.5%	2.1%	1.9%	4.2%	2.9%
Stroke (bleeding)	2.4%	5.0%	5.2%	0.0%	4.0%	1.7%	2.0%
New pacemaker	22.2%	3.4%	0.4%	12.5%	17.0%	28.5%	0.8%
MI	1.3%	0.0%	1.8%	2.1%	1.5%	3.3%	2.0%
Major vascular complications	8.5%	16.2%	9.6%	5.2%	2.7%	2.5%	5.0%
Disabling bleeding	11.7%	16.8%[a]	7.8%	2.1%	2.7%	5.0%	3.9%
Mean gradient	8.5 mmHg	11 mmHg	10 mmHg	10.7 mmHg	12.5 mmHg	11.5 mmHg	8.7 mmHg
PVL (mod/severe)	11.5%	11.4%	24.2%	2.0%	2.0%	1.0%	5.0%

[a] As per trial definition
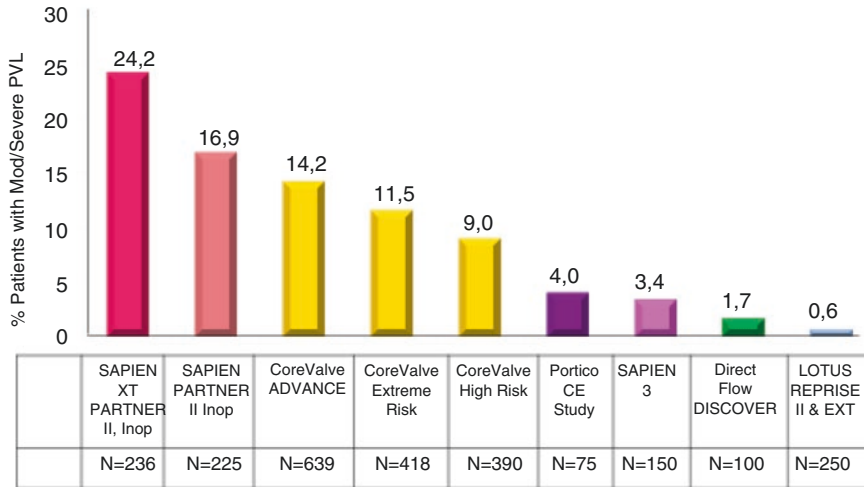
Fig. 3.21 One month moderate and severe PVL in TAVR clinical trials

---

Conclusions

Over the years, operators gradually developed the necessary experience to safely perform the procedure and rapidly manage possible complications. Meticulous risk stratification and accurate procedural planning with the necessary imaging modalities should always be performed as they were pivotal for the observed groundbreaking results of TAVR. In the upcoming 5 years, the results from randomized trials and large registries with the new devices, the awaited long-term durability data, and the expected downsizing of the vascular access sheaths will definitely lead to an even safer and more predictable procedure. This is an essential requirement with the aim of extending the current indication to a low-risk population in which TAVR still has to prove that it can be a valid alternative to surgical aortic valve replacement.

References

1. Cribier A, Eltchaninoff H, Bash A, et al. Percutaneous transcatheter implantation of an aortic valve prosthesis for calcific aortic stenosis: first human case description. Circulation. 2002;106:3006–8.
2. Cribier A, Eltchaninoff H, Tron C, et al. Early experience with percutaneous transcatheter implantation of heart valve prosthesis for the treatment of end-stage inoperable patients with calcific aortic stenosis. J Am Coll Cardiol. 2004;43:698–703.
3. Webb JG, Pasupati S, Humphries K, et al. Percutaneous transarterial aortic valve replacement in selected high-risk patients with aortic stenosis. Circulation. 2007;116:755–63.
4. Lichtenstein SV, Cheung A, Ye J, et al. Transapical transcatheter aortic valve implantation in humans: initial clinical experience. Circulation. 2006;114:591–6.

5. Simon P, Dewey T, Wimmer-Greinecker G, et al. Transapical minimally invasive aortic valve implantation: multicenter experience. Circulation. 2007;116(11 Suppl):I240–5.

6. Walther T, Kasimir MT, Doss M, et al. One-year interim follow-up results of the TRAVERCE trial: the initial feasibility study for trans-apical aortic-valve implantation. Eur J Cardiothorac Surg. 2011;39:532–7.

7. Rode's-Cabau J, Dumont E, De LaRochellie`re R, et al. Feasibility and initial results of percutaneous aortic valve implantation including selection of the transfemoral or transapical approach in patients with severe aortic stenosis. Am J Cardiol. 2008;102:1240–6.

8. Kodali SK, O'Neill WW, Moses JW, et al. Early and late (one year) outcomes following transcatheter aortic valve implantation in patients with severe aortic stenosis (from the United States REVIVAL trial). Am J Cardiol. 2011;107:1058–64.

9. Grube E, Schuler G, Buellesfeld L, et al. Percutaneous aortic valve replacement for severe aortic stenosis in high-risk patients using the second- and current third-generation self-expanding core valve prosthesis: device success and 30-day clinical outcome. J Am Coll Cardiol. 2007;50:69–76.

10. Rode's-Cabau J, Webb JG, Cheung A, et al. Transcatheter aortic valve implantation for the treatment of severe symptomatic aortic stenosis in patients at very high or prohibitive surgical risk: acute and late outcomes of the multicenter Canadian experience. J Am Coll Cardiol. 2010;55:1080–90.

11. Thomas M, Schymik G, Walther T, et al. One-year outcomes of cohort 1 in the Edwards SAPIEN aortic bioprosthesis European outcome (SOURCE) registry: the European registry of transcatheter aortic valve implantation using the Edwards SAPIEN valve. Circulation. 2011;124:425–33.

12. Piazza N, Grube E, Gerckens U, et al. Procedural and 30-day outcomes following transcatheter aortic valve implantation using the third generation (18 Fr) corevalve revalving system: results from the multicentre, expanded evaluation registry 1-year following CE mark approval. EuroIntervention. 2008;4:242–9.

13. Tamburino C, Capodanno D, Ramondo A, et al. Incidence and predictors of early and late mortality after transcatheter aortic valve implantation in 663 patients with severe aortic stenosis. Circulation. 2011;123:299–308.

14. Eltchaninoff H, Prat A, Gilard M, FRANCE Registry Investigators, et al. Transcatheter aortic valve implantation: early results of the FRANCE (FRench Aortic National CoreValve and Edwards) registry. Eur Heart J. 2011;32:191–7.

15. Zahn R, Gerckens U, Grube E, et al. German transcatheter aortic valve interventions-registry investigators. Transcatheter aortic valve implantation: first results from a multi-centre real-world registry. Eur Heart J. 2011;32:198–204.

16. Bosmans JM, Kefer J, De Bruyne B, Belgian TAVI Registry Participants, et al. Procedural, 30-day and one year outcome following core valve or Edwards transcatheter aortic valve implantation: result of the Belgian national Registry. Interact Cardiovasc Thorac Surgery. 2011;12:762–7.

17. Moat NE, Ludman P, de Belder MA, et al. Long-term outcomes after transcatheter aortic valve implantation in high-risk patients with severe aortic stenosis: the U.K. TAVI (United Kingdom transcatheter aortic valve implantation) registry. J Am Coll Cardiol. 2011;58:2130.

18. Linke A, Wenaweser P, Gerckens U, Tamburino C, Bosmans J, Bleiziffer S, Blackman D, Schäfer U, Müller R, Sievert H, Søndergaard L, Klugmann S, Hoffmann R, Tchétché D, Colombo A, Legrand VM, Bedogni F, LePrince P, Schuler G, Mazzitelli D, Eftychiou C, Frerker C, Boekstegers P, Windecker S, Mohr FW, Woitek F, Lange R, Bauernschmitt R, Brecker S, ADVANCE study Investigators. Treatment of aortic stenosis with a self-expanding transcatheter valve: the international multi-centre ADVANCE study. Eur Heart J. 2014;35(38):2672–84.

19. Leon MB, Smith CR, Mack M, PARTNER Trial Investigators, et al. Transcatheter aortic-valve implantation for aortic stenosis in patients who cannot undergo surgery. N Engl J Med. 2010;363:1597–607.

20. Smith CR, Leon MB, Mack MJ, et al. Transcatheter versus surgical aortic-valve replacement in high-risk patients. N Engl J Med. 2011;364:2187–98.

21. Popma JJ, et al. Transcatheter aortic valve replacement using a self expanding bioprosthe-sis in patients with severe aortic stenosis in extreme risk for surgery. J Am Coll Cardiol. 2014;63(19):1972–81.
22. Adams DH, Popma JJ, Reardon MJ, et al. The U.S. corevalve clinical investigators. transcathe-ter aortic-valve replacement with a self-expanding prosthesis. N Engl J Med. 2014;370:1790–8.
23. Latib A, Maisano F, Bertoldi L, et al. Transcatheter vs surgical aortic valve replacement in intermediate surgical risk patients with aortic valve stenosis: a propensity score matched case-control study. Am Heart J. 2012;164:910–7.
24. Piazza N, Kalesan B, van Mieghen N. A 3 center comparison of 1 year mortality outcomes between transcatheter aortic valve implantation and surgical aortic valve replacement on the basis of propensity score matching among intermediate risk patients. J Am Coll Cardiol Intv. 2013;6(5):443–51.
25. D'Errigo P, Barbanti M, Santini F, et al. Risultati dello studio OBSERVANT. Caratteristiche cliniche e risultati a breve termine nella popolazione arruolata sottoposta a sostituzione val-volare aortica (Transcatetere vs Chirurgica). G Ital Cardiol. 2014;15(3):177–84.
26. AC, Delgado V, van der Kley F, et al. Comparison of aortic root dimensions and geometries before and after transcatheter aortic valve implantation by 2- and 3-dimensional transesoph-ageal echocardiography and multislice computed tomography. Circ Cardiovasc Imaging. 2010;3:94–102.
27. Kahlert P, Al-Rashid F, Plicht B, et al. Suture-mediated arterial access site closure after trans-femoral aortic valve implantation. Catheter Cardiovasc Interv. 2013;8:E139–50.
28. Messika-Zeitoun D, Serfaty JM, Brochet E, et al. Multimodal assessment of the aortic annu-lus diameter: implications for transcatheter aortic valve implantation. J Am Coll Cardiol. 2010;55:186–94.
29. Koos R, Altiok E, Mahnken AH, et al. Evaluation of aortic root for definition of prosthesis size by magnetic resonance imaging and cardiac computed tomography: implications for transcath-eter aortic valve implantation. Int J Cardiol. 2012;158:353–8.
30. Tzikas A, Schultz CJ, Piazza N, et al. Assessment of the aortic annulus by multislice computed tomography, contrast aortography, and trans-thoracic echocardiography in patients referred for transcatheter aortic valve implantation. Catheter Cardiovasc Interv. 2011;77:868–75.
31. Schultz CJ, Moelker A, Piazza N, et al. Three dimensional evaluation of the aortic annulus using multislice computer tomography: are manufacturer's guidelines for sizing for percutane-ous aortic valve replacement helpful? Eur Heart J. 2010;31:849–56.
32. Gasparetto V, Fraccaro C, Tarantini G, et al. Safety and effectiveness of a selective strategy for coronary artery revascularization before transcatheter aortic valve implantation. Catheter Cardiovasc Interv. 2013;81:376–83.
33. Abdel-Wahab M, Mostafa AE, Geist V, et al. Comparison of outcomes in patients having iso-lated transcatheter aortic valve implantation versus combined with preprocedural percutaneous coronary intervention. Am J Cardiol. 2012;109:581–6.
34. Dvir D, Jhaveri R, Pichard AD. The minimalist approach for transcatheter aortic valve replacement in high-risk patients. J Am Coll Cardiol Intv. 2012;5(5):468–9. doi:10.1016/j.jcin.2012.01.019.
35. Toggweiler S, et al. Percutaneous aortic valve replacement. Vascular outcomes with a fully percutaneous procedure. Jam Coll Cardiol. 2012;59:113–8.
36. Ussia GP, Barbanti M, Petronio AS, CoreValve Italian Registry Investigators, et al. 3-year outcomes of self-expanding corevalve prosthesis. Eur Heart J. 2012;33:969–76.
37. Hayashida K, et al. True percutaneous approach for transfemoral aortic valve implantation using the prostar XL device. Impact of learning curve on vascular complications. J Am Coll Cardiol Intv. 2012;5:207–2014.
38. Alli O, et al. Transcatheter aortic valve implantation. Assessing the learning curve. J Am Coll Cardiol Intv. 2012;5:72–9.
39. Genereux P, Kodaly S, Leon MB, et al. Clinical outcomes using a new crossover balloon occlu-sion technique for percutaneous closure after transfemoral aortic valve implantation. JACC Cardiovasc Interv. 2011;4:861–7.
40. Gurvitch, et al. Transcatheter aortic valve implantation: lesson from the learning curve of the first 270 high-risk patients. Catheter Cardiovasc Inter. 2011;78:977–84.

41. Rode's-Cabau J, Gutie'rrez M, Bagur R, et al. Incidence, predictive factors, and prognostic value of myocardial injury following uncomplicated transcatheter aortic valve implantation. J Am Coll Cardiol. 2011;57:1988–99.

42. Schymik G, Würth A, Bramlage P, et al. Long-term results of transapical versus transfemoral TAVI in a real world population of 1000 patients with severe symptomatic aortic stenosis. Circ Cardiovasc Interv. 2015;8:e000761.

43. Latsios G, Gerckens U, Grube E. Transaortic transcatheter aortic valve implantation: a novel approach for the truly "no-access option" patients. Catheter Cardiovasc Interv. 2010;75:1129–36.

44. Petronio AS, De Carlo M, Bedogni F, et al. Safety and efficacy of the subclavian approach for transcatheter aortic valve implantation with the CoreValve revalving system. Circ Cardiovasc Interv. 2010;3:359–66.

45. Testa L, Brambilla N, Laudisa ML, et al. Right subclavian approach as a feasible alternative for transcatheter aortic valve implantation with the CoreValve ReValving system. EuroIntervention. 2012;8(6):685–90.

46. Scha¨fer U, Ho Y, Frerker C, et al. Direct percutaneous access technique for transaxillary transcatheter aortic valve implantation: "the Hamburg Sankt Georg approach". JACC Cardiovasc Interv. 2012;5:477–86.

47. DeRobertis F, Asgar A, Davies S, et al. The left axillary artery – a new approach for transcatheter aortic valve implantation. Eur J Cardiothorac Surg. 2009;36:807–1.

48. Guyton RA, Block PC, Thourani VH, Lerakis S, Babaliaros V. Carotid artery access for transcatheter aortic valve replacement. Catheter Cardiovasc Interv. 2013;82(4):E583–6. doi:10.1002/ccd.24596. Epub 2013 Mar 28.

49. Grube E, Naber C, Abizaid A, et al. Feasibility of transcatheter aortic valve implantation without balloon pre-dilation: a pilot study. JACC Cardiovasc Interv. 2011;4:751–7.

50. Garcia E, Almer'ıa C, Unzue' L, et al. Transfemoral implantation of Edwards Sapien XT aortic valve without previous valvuloplasty: role of 2D/3D transesophageal echocardiography. Catheter Cardiovasc Interv. 2014;84:868–76. Epub ahead of print.

51. Webb J, Cribier A. Percutaneous transarterial aortic valve implantation: what do we know? Eur Heart J. 2011;32:140–7.

52. Abdel-Wahab M, Mehilli J, Frerker C, CHOICE investigators, et al. Comparison of balloon-expandable vs self-expandable valves in patients undergoing transcatheter aortic valve replacement: the CHOICE randomized clinical trial. JAMA. 2014;311:1503–14.

53. Toggweiler S, Humphries KH, Lee M, et al. 5-year outcome after transcatheter aortic valve implantation. J Am Coll Cardiol. 2013;61:413–9.

54. Barbanti M, Petronio AS, Ettori F, Latib A, Bedogni F, De Marco F, Poli A, Carla Boschetti M, De Carlo M, Fiorina C, Colombo A, Brambilla N, Bruschi G, Martina P, Pandolfi C, Giannini C, Curello S, Sgroi C, Gulino S, Patanè M, Ohno Y, Tamburino C, Attizzani GF, Immè S, Gentili A. 5-year outcomes after transcatheter aortic valve implantation with CoreValve prosthesis. J Am Coll Cardiol Intv. 2015;8:1084–91. E pub Ahead to print.

55. Detaint D, Lepage L, Himbert D, et al. Determinants of significant paravalvular regurgitation after transcatheter aortic valve: implantation impact of device and annulus discongruence. JACC Cardiovasc Interv. 2009;2:821–7.

56. Abdel-Wahab M, Zahn R, Horack M, et al. Aortic regurgitation after transcatheter aortic valve implantation: incidence and early outcome. Results from the German transcatheter aortic valve interventions registry. Heart. 2011;97:899–906.

57. Sinning JM, Hammerstingl C, Vasa-Nicotera M, et al. Aortic regurgitation index defines severity of peri-prosthetic regurgitation and predicts outcome in patients after transcatheter aortic valve implantation. J Am Coll Cardiol. 2012;59:1134–41.

58. Sponga S, Perron J, Dagenais F, et al. Impact of residual regurgitation after aortic valve replacement. Eur J Cardiothorac Surg. 2012;42:486–92.

59. Sherif MA, Abdel-Wahab M, Stocker B, et al. Anatomic and procedural predictors of paravalvular aortic regurgitation after implantation of the medtronic corevalve bioprosthesis. J Am Coll Cardiol. 2010;56:1623–9.

60. Takagi K, Latib A, Al-Lamee R, et al. Predictors of moderate-to-severe paravalvular aortic regurgitation immediately after CoreValve implantation and the impact of postdilatation. Catheter Cardiovasc Interv. 2011;78:432–43.

61. Ussia GP, Barbanti M, Tamburino C. Consequences of underexpansion of a percutaneous aortic valve bioprosthesis. J Invasive Cardiol. 2010;22:E86–9.
62. Kodali SK, Williams MR, Smith CR, et al. Two-year outcomes after transcatheter or surgical aortic-valve replacement. N Engl J Med. 2012;366:1686–95.
63. Sellers RD, Levy MJ, Amplatz K, Lillehei CW. Left retrograde cardioangiography in acquired cardiac disease: technic, indications, and interpretations in 700 cases. Am J Cardiol. 1964;14:437–47.
64. Ewe SH, Ng AC, Schuijf JD, et al. Location and severity of aortic valve calcium and implications for aortic regurgitation after transcatheter aortic valve implantation. Am J Cardiol. 2011;108:1470–7.
65. Colli A, D'Amico R, Kempfert J, et al. Transesophageal echocardiographic scoring for transcatheter aortic valve implantation: impact of aortic cusp calcification on postoperative aortic regurgitation. J Thorac Cardiovasc Surg. 2011;142:1229–35.
66. Haensig M, Lehmkuhl L, Rastan AJ, et al. Aortic valve calcium scoring is a predictor of significant paravalvular aortic insufficiency in transapical-aortic valve implantation. Eur J Cardiothorac Surg. 2012;41:1234–43.
67. Koos R, Mahnken AH, Dohmen G, et al. Association of aortic valve calcification severity with the degree of aortic regurgitation after transcatheter aortic valve implantation. Int J Cardiol. 2011;150:142–5.
68. Yared K, Garcia-Camarero T, Fernandez-Friera L, et al. Impact of aortic regurgitation after transcatheter aortic valve implantation: results from the REVIVAL trial. JACC Cardiovasc Imaging. 2012;5:469–77.
69. Unbehaun A, Pasic M, Dreysse S, et al. Transapical aortic valve implantation: incidence and predictors of paravalvular leakage and transvalvular regurgitation in a series of 358 patients. J Am Coll Cardiol. 2012;59:211–21.
70. Wong DT, Bertaso AG, Liew GY, et al. Relationship of aortic annular eccentricity and paravalvular regurgitation post transcatheter aortic valve implantation with CoreValve. J Invasive Cardiol. 2013;25:190–5.
71. Buzzatti N, Maisano F, Latib A, et al. Computed tomography-based evaluation of aortic annulus, prosthesis size and impact on early residual aortic regurgitation after transcatheter aortic valve implantation. Eur J Cardiothorac Surg. 2013;43:43–51.
72. Schultz CJ, Tzikas A, Moelker A, et al. Correlates on MSCT of paravalvular aortic regurgitation after transcatheter aortic valve implantation using the medtronic CoreValve prosthesis. Catheter Cardiovasc Interv. 2011;78:446–55.
73. Block PC. Leaks and the "great ship" TAVI. Catheter Cardiovasc Interv. 2010;75:873–4.
74. Genereux P, Head SJ, Hahn R, et al. Paravalvular leak after transcatheter aortic valve replacement: the new Achilles' heel? A comprehensive review of the literature. J Am Coll Cardiol. 2013;61:1125.
75. Houthuizen P, Van Garsse LAFM, Poels TT, de Jaegere P, van der Boon RMA, Swinkels BM, et al. Left bundle-branch block induced by trans-catheter aortic valve implantation increases risk of death. Circulation. 2012;126(6):720–8.
76. Urena M, Mok M, Serra V, Dumont E, Nombela-Franco L, DeLarochellière R, et al. Predictive factors and long-term clinical consequences of persistent left bundle branch block following trans-catheter aortic valve implantation with a balloon-expandable valve. J Am Coll Cardiol. 2012;60(18):1743–52.
77. Testa L, Latib A, De Marco F, De Carlo M, Agnifili M, Latini RA, et al. Clinical impact of persistent left bundle-branch block after transcatheter aortic valve implantation with CoreValve revalving system. Circulation. 2013;127(12):1300–7.
78. van der Boon RM, Nuis R-J, Van Mieghem NM, Jordaens L, Rodés-Cabau J, van Domburg RT, et al. New conduction abnormalities after TAVI–frequency and causes. Nat Rev Cardiol. 2012;9(8):454–63.
79. Sinhal A, Altwegg L, Pasupati S, Humphries KH, Allard M, Martin P, et al. Atrioventricular block after transcatheter balloon expandable aortic valve implantation. JACC Cardiovasc Interv. 2008;1(3):305–9.

80. Jilaihawi H, Chin D, Vasa-Nicotera M, Jeilan M, Spyt T, Ng GA, et al. Predictors for permanent pacemaker requirement after trans-catheter aortic valve implantation with the CoreValve bioprosthesis. Am Heart J. 2009;157(5):860–6.

81. Van der Boon RMA, Van Mieghem NM, Theuns DA, Nuis R-J, Nauta ST, Serruys PW, et al. Pacemaker dependency after transcatheter aortic valve implantation with the self-expanding medtronic CoreValve system. Int J Cardiol. 2013;168(2):1269.

82. Simms AD, Hogarth AJ, Hudson EA, Worsnop VL, Blackman DJ, O'Regan DJ, et al. Ongoing requirement for pacing post-transcatheter aortic valve implantation and surgical aortic valve replacement. Interact Cardiovasc Thorac Surg. 2013;17(2):328–33.

83. Pereira E, Ferreira N, Caeiro D, Primo J, Adão L, Oliveira M, et al. Transcatheter aortic valve implantation and requirements of pacing over time. Pacing Clin Electrophysiol. 2013;36(5):559–69.

84. van der Boon RM, Houthuizen P, Nuis RJ, van Mieghem NM, Prinzen F, de Jaegere PP. Clinical implications of conduction abnormalities and arrhythmias after transcatheter aortic valve implantation. Curr Cardiol Rep. 2014;16(1):429.

85. Généreux P, Head SJ, Van Mieghem NM, et al. Clinical outcomes after transcatheter aortic valve replacement using valve academic research consortium definitions: a weighted meta-analysis of 3,519 patients from 16 studies. J Am Coll Cardiol. 2012;59:2317–26.

86. Mastoris I, Schoos MM, Dangas GD, Mehran R. Stroke after transcatheter aortic valve replacement: incidence, risk factors, prognosis, and preventive strategies. Clin Cardiol. 2014;12:756–64.

87. Khatri PJ, Webb JG, Rod'es-Cabau J, et al. Adverse effects associated with transcatheter aortic valve implantation: a meta-analysis of contemporary studies. Ann Intern Med. 2013;158:35–46.

88. Holmes Jr DR, Mack MJ, Kaul S, et al. 2012 ACCF/AATS/SCAI/STS expert consensus document on transcatheter aortic valve replacement. J Am Coll Cardiol. 2012;59:1200–54.

89. Vahanian A, Alfieri O, Andreotti F, et al. Guidelines on the management of valvular heart disease (version 2012): the joint task force on the management of valvular heart disease of the European society of cardiology (ESC) and the European association for cardio-thoracic surgery (EACTS). Eur J Cardiothorac Surg. 2012;42:S1–44.

90. Webb J, Rod'es-Cabau J, Fremes S, et al. Transcatheter aortic valve implantation: a Canadian cardiovascular Society position statement. Can J Cardiol. 2012;28:520–8.

91. Barbanti M, Yang TH, Rodes Cabau J, et al. Anatomical and procedural features associated with aortic root rupture during balloon expandable transcatheter aortic valve replacement. Circulation. 2013;128:244–53.

92. Dvir D, Webb JG, Bleiziffer S, Pasic M, Waksman R, Kodali S, Barbanti M, Latib A, Schaefer U, Rodés-Cabau J, Treede H, Piazza N, Hildick-Smith D, Himbert D, Walther T, Hengstenberg C, Nissen H, Bekeredjian R, Presbitero P, Ferrari E, Segev A, de Weger A, Windecker S, Moat NE, Napodano M, Wilbring M, Cerillo AG, Brecker S, Tchetche D, Lefèvre T, De Marco F, Fiorina C, Petronio AS, Teles RC, Testa L, Laborde JC, Leon MB, Kornowski R. Valve-in-valve international data registry investigators. Transcatheter aortic valve implantation in failed bioprosthetic surgical valves. JAMA. 2014;312(2):162–70.

93. Bedogni F, Laudisa ML, Pizzocri S, Tamburino C, Ussia GP, Petronio AS, Napodano M, Ramondo A, Presbitero P, Ettori F, Santoro G, Klugman S, De Marco F, Brambilla N, Testa L. Transcatheter valve-in-valve implantation using Corevalve Revalving System for failed surgical aortic bioprostheses. JACC Cardiovasc Interv. 2011;11:1228–34.

94. Roy DA, Schaefer U, Guetta V, Hildick-Smith D, Möllmann H, Dumonteil N, Modine T, Bosmans J, Petronio AS, Moat N, Linke A, Moris C, Champagnac D, Parma R, Ochala A, Medvedofsky D, Patterson T, Woitek F, Jahangiri M, Laborde JC, Brecker SJ. Transcatheter aortic valve implantation for pure severe native aortic valve regurgitation. J Am Coll Cardiol. 2013;61(15):1577–84.

95. Testa L, Latib A, Rossi ML, De Marco F, De Carlo M, Fiorina C, Oreglia J, Petronio AS, Ettori F, De Servi S, Klugmann S, Ussia GP, Tamburino C, Panisi P, Brambilla N, Colombo A, Presbitero P, Bedogni F. CoreValve implantation for severe aortic regurgitation: a multicentre registry. EuroIntervention. 2014;10(6):739–45.

Aortic Perivalvular Leakage: Percutaneous Treatment Options

Sameer Gafoor, Predrag Matic, Fawad Kazemi,
Luisa Heuer, Jennifer Franke, Stefan Bertog,
Laura Vaskelyte, Ilona Hofmann, and Horst Sievert

4.1   Introduction

Paravalvular leak (PVL) is known to occur in 5–17 % of mechanical valves [1].

Mitral valve leaks are more common than aortic leaks [2, 3]. Aside from regurgitation, other symptoms of PVL include hemolysis (13–47 %) and heart failure (85 %) [4, 5]. About 1–5 % of leaks have a negative prognosis, with severe regurgitation and/or an increase in mortality [6–8].

Leaks shortly after surgery can be due to an incomplete seal between the sewing ring and annulus (often due to annular calcification). Infection predisposes patients to leak due to weaker durability of infected tissue. In addition, the type and technique of suturing (continuous or small monofilament polypropylene stitches), type of sewing ring, and methods of myocardial preservation used can contribute to development of paraprosthetic leaks.

Surgery is the traditional way of treatment, with options including re-suture and re-replacement. However, mortality rates of 13 %, 15 %, and 35 % for the first, second, and third redo surgeries, respectively, have been reported [9]. Further, freedom

S. Gafoor
Swedish Heart and Vascular, Seattle, WA, USA

Cardiovascular Center Frankfurt CVC, Frankfurt, Germany

P. Matic • F. Kazemi • L. Heuer • L. Vaskelyte • I. Hofmann • H. Sievert (✉)
Cardiovascular Center Frankfurt CVC, Frankfurt, Germany
e-mail: info@cvcfrankfurt.de

J. Franke
Cardiovascular Center Frankfurt CVC, Frankfurt, Germany

University of Heidelberg, Heidelberg, Germany

S. Bertog
Minneapolis Veterans Affairs Hospital, Minneapolis, MN, USA

Cardiovascular Center Frankfurt CVC, Frankfurt, Germany

from recurrence is less likely with each repeat redo operation. There is evidence to show that early intervention may be beneficial [4]. Other techniques, including video-assisted, minimal-access techniques, may also lower mortality risk [10]. However, extremely symptomatic patients exist where surgical risk is still high. These patients are ideal for a percutaneous method.

Important contraindications to PVL closure include presence of active local or systemic infection, mechanical instability of the prosthetic valve, and intracardiac thrombus [7].

4.2   Imaging of Paravalvular Leak

PVL is difficult to quantify. Available noninvasive imaging methods include transthoracic echocardiography (TTE), transesophageal echocardiography (TEE), computerized tomography (CT), and magnetic resonance imaging (MRI). It is important to know the strengths and limitations of each technique in regard to artifacts from mechanical and bioprosthetic valves. The key questions to answer are location, cause of leak, as well as defect size, shape, severity, and number.

Echocardiography allows an easy method to visualize and screen for PVL. Transthoracic and transesophageal echocardiography have different strengths, with the additive value of providing a baseline that can be used to compare with periprocedural imaging. It is important to distinguish normal from pathological regurgitation and rule out prosthetic shadowing [11]. For PVL involving the mitral valve, it is our practice to use both TTE and TEE evaluations; for leak involving the aortic valve, TTE is used as a screen and in case of poor windows TEE is used.

Angiography can be used for aortic leaks by varying the angle of C-arm fluoroscopy to find the optimal projection to visualize the leak. The best technique is to cross the leak with a wire and to place a sheath just above the leak.

CT and MRI provide new insights into PVL. The use of CT and in the future MRI may help show the course of leak and size within the leak at each end. Retrospective ECG-gated reconstruction can be used for both systolic and diastolic evaluations. However, artifacts specific to CT and MRI may be accentuated due to calcification or prosthetic valve itself. There is also a risk of increased radiation and, in the case of CT, contrast dye exposure. Some centers have used this for intraprocedural guidance and to minimize procedural time [12–14].

4.3   Location of Paravalvular Leak

Aortic PVL location is described by a clock face in the short-axis view in TEE. . The commissure between the left and right coronary sinus is seen as 5 o'clock, commissure between the right and noncoronary sinus is 8 o'clock, and the commissure between the noncoronary and left coronary sinus is 11 o'clock. Aortic PVL is most likely found between 7 and 11 o'clock position (46 %) and then between 11 and 3 o'clock position (36 %) [15].

4.4   Sizing of Paravalvular Leak

Sizing of PVL is often difficult. Many leaks take a serpiginous pattern through the valve annulus. In addition, many are crescentic in shape, which adds to the level of complexity. By echocardiogram, the vena contracta immediately adjacent to the leak gives a sense of leak size. A CT or MR evaluation may allow more insight to course of leak and size at each end [16]. Invasive sizing can be done with balloon sizing. It is not our practice to perform balloon sizing because of annular calcium or sharp edges leading to potential balloon entrapment in the leak.

4.5   Access

There are three main access options methods for PVL closure, i.e., transfemoral, transseptal, and transapical access.

Transfemoral retrograde access is often used for aortic or medial mitral paravalvular leaks. For aortic leaks, this is done with a hydrophilic 0.035″ wire (e.g., Glidewire, Terumo Medical Corp., Somerset, New Jersey) with a 5-Fr diagnostic catheter (JR4, MP). For a medial mitral leak, a JR4 or IM catheter is used; an EBU4 guide catheter may also be considered. Once the leak is crossed, the catheter is advanced through the leak. The leak is then measured by echocardiography at both sides of the valve to coordinate the defect location and crossing. A device is chosen based on leak size and shape. The device dictates the size of the delivery sheath or guide catheter. The original hydrophilic wire is exchanged for an Amplatz Extra-Stiff wire (St. Jude Corporation, Minneapolis, MN, USA), which is used to exchange the diagnostic catheter for the delivery sheath/guide catheter. At this point, TEE can be used to evaluate the leak with the guide/sheath in place. The device is then advanced and deployed. If the wire and catheter cross but the sheath does not (often due to friction within the leak), the wire can be snared using transseptal access or ventricular puncture. With any rail, it is important to protect ventricular structures when strong force is used to advance the catheters – this is done by covering the rail with a catheter (often a 5-Fr MP is used).

Transseptal access is performed under both fluoroscopic and transesophageal echocardiographic guidance (using both 30° and 110° views). This can prove helpful for mitral PVL and as support in case of difficult aortic PVL. For difficult aortic PVL, the leak is crossed through a retrograde femoral approach, and a rail is formed by snaring the wire in the left atrium using an available gooseneck snare, e.g., ev3 Snare (ev3, Plymouth, MN, USA).

Transapical access can be the method of choice for mitral leaks that cannot be reached easily via the other two methods or in the case of mechanical heart valves in both aortic and mitral positions. Coronary angiography is performed to visualize position of the coronary arteries (left anterior coronary branch for left ventricular puncture). TTE or fluoroscopic guidance is used to perform ventricular puncture using an apical approach. A 4-Fr sheath is placed, and heparin 100 U/kg is given. After device placement, it is important to have safe closure of the ventricular

puncture site. An occluder device, e.g., an Amplatzer PDA Occluder (St. Jude Corporation, Minneapolis, MN, USA), may be used [17]. Protamine is given to reverse the effects of heparin. It is important to watch for complications such as coronary puncture, tamponade, and hemothorax. Follow-up transthoracic echocardiography and chest x-ray should be performed.

4.6   Device Selection for Paravalvular Leaks

Without dedicated devices for paravalvular leak, devices designed for other indications have to be used. These include Amplatzer VSD Occluder, Amplatzer Duct Occluder, Amplatzer Septal Occluder, and Amplatzer Vascular Plug (all St. Jude Corporation, Minneapolis, MN) or similar devices from other manufactures. Other devices that have been used include coils, Gianturco-Grifka vascular occlusion device [18], CardioSEAL, and Rashkind double-umbrella device [19]. The new Occlutech occluder device is the only CE-marked device for paravalvular leak.

It is important to use a device that can approximate the size and shape of the defect. In addition, it is key to watch out for obstruction of coronary ostia and/or the prosthetic valve leaflets. Sometimes the first device deployed is not correct, and the device must be exchanged. Therefore, the device is not released until fully evaluated.

Devices rarely close the defect entirely, because they do not often match a unique defect size or shape. To pursue total leak closure, often larger or multiple devices are used. This increases infectious risk and also can impinge leaflet motion [20, 21]. However, it is important to note that in a patient with minimal to no surgical options, paravalvular leak closure provides the possibility for symptom relief, relief from hemolysis, and possibility to defer surgery. In addition, this points to the need for more geometrically appropriate devices to treat this condition.

In light of this, we have come with general paradigm as to what device to select for what type of leak. For a small cylindrical leak, we will often use an AVP II. For an oval leak, an AVP III occluder is preferred. For a small leak with significant angulation and small neck, an AVP IV occluder is considered. Sizing of these devices comes most often from echocardiographic measurements, both in 2D or 3D. Angiography can also be useful for aortic PVL, which can be measured in profile using appropriate C-arm angulation. We do not recommend using external catheter size to measure leak size, as a variety of factors, e.g., calcification and tortuosity, can cause difficulty in the catheter's ability to cross the leak. However, once a catheter has successfully crossed the leak, echocardiography can be used to evaluate the regurgitant jet with catheter in place, which occasionally can give an idea of volume within the leak.

4.7   Aortic Paravalvular Leak

For aortic paravalvular leak, the preferred access route is retrograde transfemoral access. It is important to determine not only the leak size but also the location of the leak in relation to the appropriate cusp or clock face using TEE. Appropriate

catheters to cross the leak include a JR4, MP, or Amplatz-1 catheter. A hydrophilic 0.035″ wire (Glidewire, Terumo Medical Corp., Somerset, New Jersey) is also used. Once the leak is crossed with the wire, the catheter is advanced through the leak. Defect size determines device size, which dictates the size of the guide catheter or long sheath used to deliver the device. We often use a Cook Shuttle Sheath (Cook Corporation, Bloomington, IN, USA) for this purpose. An Amplatz Extra-Stiff wire is used to exchange this catheter for a guide catheter or long sheath. Once the sheath/guide is in place, TEE is used to monitor interval change in the regurgitant jet. An appropriate device is delivered, and this is evaluated with TEE prior to release. It is important to note the absence of leaflet obstruction and also coronary ostial obstruction. If these are present, the device should be removed.

There can be issues at various steps in the process due to leak tortuosity or irregular borders of the leak (often due to calcium or fibrous tissue). If the wire crosses the leak but there is difficulty with the guide catheter/sheath, a smaller guide catheter/sheath may be used. If the catheter is determined to be the appropriate size based on the echocardiographic measurements, more support is needed. This can be done by establishing a rail – either with transseptal access and snaring the wire in the left atrium or by transapical access and externalizing the wire out of the left ventricular apex. Figures 4.1 and 4.2 show examples of aortic PVL closure.

Once the device in place, it is important to rule out complications from the device. The prosthetic aortic valve should be evaluated, preferably both by echocardiography and fluoroscopy, to make sure leaflet movement is not compromised (Figs. 4.1 and 4.2). If the device is in the area of the former left and right coronary cusp, coronary patency should be shown, either by selective or root angiography or by TEE. If the device is in the area of the former noncoronary cusp, the anterior mitral valve leaflet should also be evaluated.

Device success consists of a decrease in aortic regurgitation and improvement in symptoms. Regular follow-up with TTE can be performed at 6 months and earlier if symptoms occur. For patients with hemolysis, a hemoglobin/hematocrit level should be checked as well.

4.8   Complications

A variety of complications can occur with paravalvular leak closure [17]. Access-site complications occur between 0.7 and 4 %. Valve interference occurs between 3.5 and 5 %. Other complications include stroke, endocarditis, postprocedural hemolysis, and device erosion. Emergent cardiac surgery may occur 0.7–2 % of the time, and death may occur in 1.4–2 % of cases. One series reported major adverse events with percutaneous PVL closure at 30 days (death, myocardial infarction, stroke, major bleeding, and emergency surgery) at 8.7 % [17].

Devices that embolize from the aortic position may travel anywhere. Larger devices are less likely to go cranially and are often found at the iliac bifurcation. The same holds true for devices that embolize from the mitral position; however, the risk
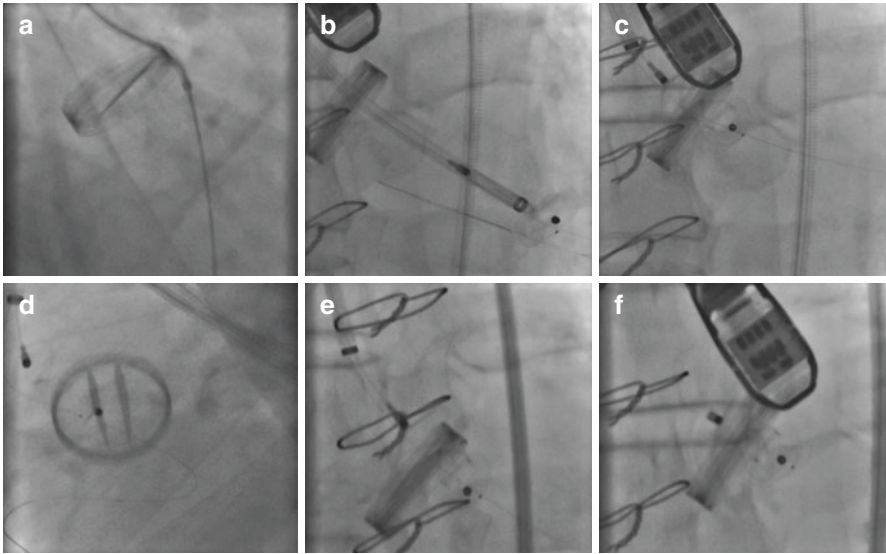
Fig. 4.1 Aortic paravalvular leak, single device. A 74-year-old male with paravalvular leak in relation to mechanical aortic valve. The leak is an eccentric leak in the region of the noncoronary cusp and measured 10- × 3-mm on echocardiogram. Right femoral arterial access was obtained and a 5-Fr sheath was placed. A 5-Fr AL1 guide catheter and Terumo hydrophilic 0.035″ wire were used to cross the leak in a retrograde fashion (**a**). This catheter was exchanged over an Amplatz Extra-Stiff wire for a 7-Fr Cook Shuttle Sheath, which was placed in the left ventricle (**b**). A 0.014″ Ironman wire was placed as access protection through the paravalvular leak into the left ventricle. A 10-mm PDA occluder device was attempted but was unsuccessful in closing the defect (**c**) and was removed. The 0.014″ wire stayed in place (**d**). A 4-Fr 125 cm JR4 catheter was placed coaxial inside the shuttle sheath to traverse the paravalvular leak over the 0.014″ wire and reestablish the shuttle sheath across the leak (not pictured). Then a 12/3-mm AVP III device was placed across the leak (**e**). After fluoroscopic and echocardiographic confirmation of minimal leak and good valve function, the device was released (**f**)

holds that they may get caught in the left ventricular outflow tract. Surgery is often indicated in these cases.

For postprocedural hemolysis, this usually resolves after complete endothelialization. This may take up to 6 months.

4.9 Long-Term Results

Technical success, as defined by Kliger et al. [17], is correct deployment of an occlusive defect without significant residual regurgitation or new prosthetic valve malfunction. Clinical success may be an improvement in NYHA functional class by at least one grade and/or improvement in mechanical hemolysis. There are two large case series with 57 [12] and 141 [22] PVL closures. Technical success ranges from 77 to 86 % and clinical success from 67 to 77 %. Ruiz et al. [12] reported long-term
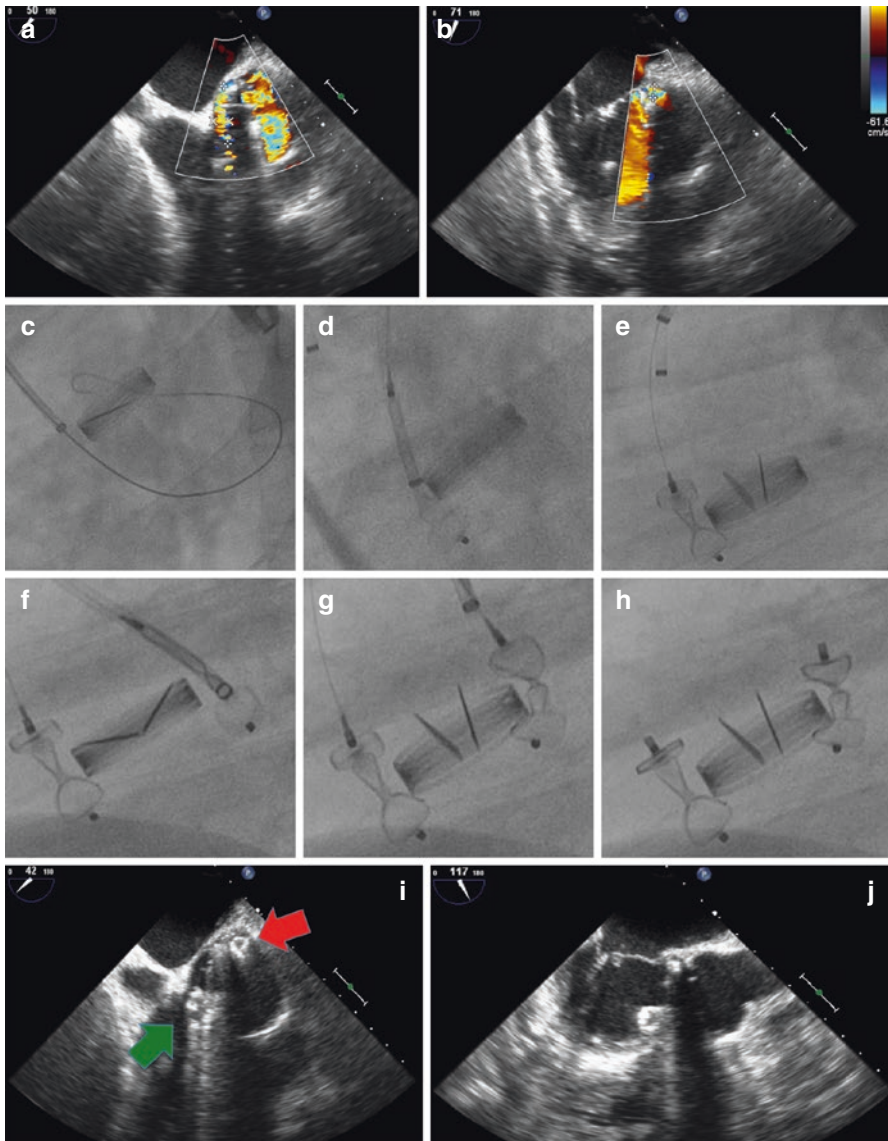
Fig. 4.2 Aortic paravalvular leak, multiple leaks. After having a mechanical aortic valve in 2008, the patient presented 4 years later with symptoms of heart failure and severe regurgitation. A 5-×11-mm PVL was noted near the left coronary cusp and 5-×8-mm PVL in the area of the noncoronary cusp (**a**, **b**). A 5-Fr MP catheter and 0.035″ hydrophilic wire were used to cross the leak near the noncoronary cusp. This was then exchanged over an Amplatz ES 0.035″ wire (**c**) for a 10-Fr Cook Shuttle Sheath. This was then used to advance an AVP III size 5-×14-mm device (**d**), which was then deployed (**e**). Similar access was obtained through the other femoral artery, and a similar technique was used to cross the leak near the left coronary cusp. An AVP III 5-×14-mm device was also implanted (**f**–**h**). Follow-up echocardiographic views at 42 and 117° show the position of the noncoronary cusp (*green arrow*) and left coronary cusp (*red arrow*) devices (**i**, **j**). Both aortic and mitral valve leaflets moved well on TEE

follow-up at 6, 12, and 18 months as 91.9 %, 89.2 %, and 86.5 %, respectively. Sorajja et al. [23] found 1–2-year survival after PVL closure of 70–75 % with an estimated 3-year survival of 64.5 %.

> **Conclusion**
>
> Treatment of paravalvular regurgitation requires careful preprocedural imaging, planning, and patient selection. Through principles of access, technique, and device choice, it is possible to achieve both technical and clinical success. It has become the primary therapy of choice in appropriately selected cases.

References

1. Vongpatanasin W, Hillis LD, Lange RA. Prosthetic heart valves. N Engl J Med. 1996;335:407–16.
2. Hammermeister K, Sethi GK, Henderson WG, Grover FL, Oprian C, Rahimtoola SH. Outcomes 15 years after valve replacement with a mechanical versus a bioprosthetic valve: final report of the Veterans Affairs randomized trial. J Am Coll Cardiol. 2000;36:1152–8.
3. Ionescu A, Fraser AG, Butchart EG. Prevalence and clinical significance of incidental para-prosthetic valvar regurgitation: a prospective study using transoesophageal echocardiography. Heart. 2003;89:1316–21.
4. Genoni M, Franzen D, Vogt P, et al. Paravalvular leakage after mitral valve replacement: improved long-term survival with aggressive surgery? Eur J Cardiothorac Surg. 2000;17:14–9.
5. De Cicco G, Russo C, Moreo A, et al. Mitral valve periprosthetic leakage: anatomical observations in 135 patients from a multicentre study. Eur J Cardiothorac Surg. 2006;30:887–91.
6. Rallidis LS, Moyssakis IE, Ikonomidis I, Nihoyannopoulos P. Natural history of early aortic paraprosthetic regurgitation: a five-year follow-up. Am Heart J. 1999;138:351–7.
7. Pate GE, Al Zubaidi A, Chandavimol M, Thompson CR, Munt BI, Webb JG. Percutaneous closure of prosthetic paravalvular leaks: case series and review. Catheter Cardiovasc Interv. 2006;68:528–33.
8. Davila-Roman VG, Waggoner AD, Kennard ED, et al. Prevalence and severity of paravalvular regurgitation in the artificial valve endocarditis reduction trial (AVERT) echocardiography study. J Am Coll Cardiol. 2004;44:1467–72.
9. Echevarria JR, Bernal JM, Rabasa JM, Morales D, Revilla Y, Revuelta JM. Reoperation for bioprosthetic valve dysfunction. A decade of clinical experience. Eur J Cardiothorac Surg. 1991;5:523–6. discussion 7.
10. Casselman FP, La Meir M, Jeanmart H, et al. Endoscopic mitral and tricuspid valve surgery after previous cardiac surgery. Circulation. 2007;116:I270–5.
11. Zoghbi WA. New recommendations for evaluation of prosthetic valves with echocardiography and doppler ultrasound. Methodist Debakey Cardiovasc J. 2010;6:20–6.
12. Ruiz CE, Jelnin V, Kronzon I, et al. Clinical outcomes in patients undergoing percutaneous closure of periprosthetic paravalvular leaks. J Am Coll Cardiol. 2011;58:2210–7.
13. Jelnin V, Co J, Muneer B, Swaminathan B, Toska S, Ruiz CE. Three dimensional CT angiography for patients with congenital heart disease: scanning protocol for pediatric patients. Catheter Cardiovasc Interv. 2006;67:120–6.
14. Jelnin V, Dudiy Y, Einhorn BN, Kronzon I, Cohen HA, Ruiz CE. Clinical experience with percutaneous left ventricular transapical access for interventions in structural heart defects a safe access and secure exit. JACC Cardiovasc Interv. 2011;4:868–74.
15. Krishnaswamy A, Kapadia SR, Tuzcu EM. Percutaneous paravalvular leak closure – imaging, techniques and outcomes. Circ J. 2013;77:19–27.

16. Ruiz CE, Cohen H, Valle-Fernandez RD, Jelnin V, Perk G, Kronzon I. Closure of prosthetic paravalvular leaks: a long way to go. Eur Heart J Suppl. 2010;12:E52–62.
17. Kliger C, Eiros R, Isasti G, et al. Review of surgical prosthetic paravalvular leaks: diagnosis and catheter-based closure. Eur Heart J. 2013;34:638–49.
18. Eisenhauer AC, Piemonte TC, Watson PS. Closure of prosthetic paravalvular mitral regurgitation with the Gianturco-Grifka vascular occlusion device. Catheter Cardiovasc Interv. 2001;54:234–8.
19. Zamorano JL, Badano LP, Bruce C, et al. EAE/ASE recommendations for the use of echocardiography in new transcatheter interventions for valvular heart disease. Eur Heart J. 2011;32:2189–214.
20. Merin O, Bitran D, Fink D, Asher E, Silberman S. Mechanical valve obstruction caused by an occlusion device. J Thorac Cardiovasc Surg. 2007;133:806–7.
21. Garcia-Villarreal OA. Amplatzer devices are not geometrically adapted to close paravalvular leaks. Ann Thorac Surg. 2013;95:774.
22. Sorajja P, Cabalka AK, Hagler DJ, Rihal CS. Percutaneous repair of paravalvular prosthetic regurgitation: acute and 30-day outcomes in 115 patients. Circ Cardiovasc Interv. 2011;4:314–21.
23. Sorajja P, Cabalka AK, Hagler DJ, Rihal CS. Long-term follow-up of percutaneous repair of paravalvular prosthetic regurgitation. J Am Coll Cardiol. 2011;58:2218–24.

Difficult Cases and Complications from the Catheterization Laboratory: Case 1

5

Neil Ruparelia, Azeem Latib, and Antonio Colombo

5.1 Case Presentation

An 81-year-old lady presented to the Heart Team as an emergency with an episode of acute cardiac decompensation. Three years previously, she had undergone successful cardiac surgery with coronary artery bypass grafting (CABG) (saphenous vein graft – left obtuse marginal branch) with both mitral (25 mm Mosaic valve, Medtronic, Minnesota, USA) and aortic valve replacements (25 mm Epic valve, St. Jude, Minnesota, USA). She made an uneventful recovery from this surgery. Two years later, she presented as an emergency with bacterial endocarditis (*Streptococcus sanguinis*) affecting the aortic prosthesis that was successfully treated with prolonged ampicillin and gentamicin chemotherapy without the requirement for surgery. However, she was left with residual moderate aortic regurgitation (AR) in the absence of symptoms.

N. Ruparelia, DPhil, MRCP
Imperial College, London, UK

San Raffaele Scientific Institute, Milan, Italy

EMO-GV Centro Cuore Columbus, Via Buonarroti 48, 20145 Milan, Italy

A. Latib, MD • A. Colombo, MD (✉)
San Raffaele Scientific Institute, Milan, Italy

EMO-GV Centro Cuore Columbus, Via Buonarroti 48, 20145 Milan, Italy
e-mail: info@emocolumbus.it; colombo@emocolumbus.it
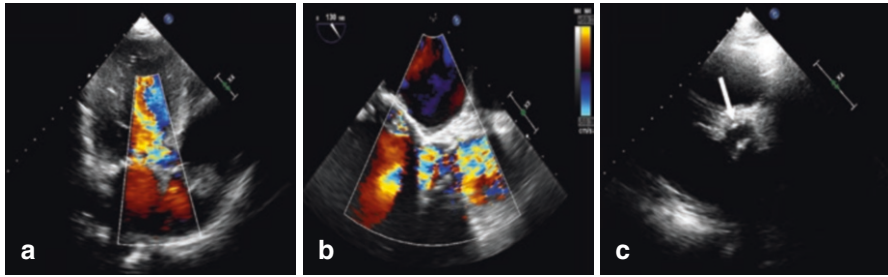
Fig. 5.1 Aortic valve assessment. Transthoracic echocardiogram confirmed aortic bioprosthesis dysfunction with severe aortic regurgitation (**a**), confirmed on transesophageal echocardiogram (**b**). A short-axis transthoracic view demonstrated the appearance of a mobile calcified mass (*arrow*) (**c**)

During this admission (1 year following the episode of endocarditis), in the acute setting, she was successfully managed with parenteral diuresis and optimal medical therapy consisting of beta-blockers, angiotensin-converting enzyme inhibitors, and potassium-sparing diuretics. When clinically stable, a transthoracic echocardiogram revealed severe central aortic regurgitation secondary to a perforated bioprosthetic valve leaflet, in the presence of moderate to severe aortic stenosis (mean gradient: 37 mmHg) (Fig. 5.1a, b, Video 5.1). Additionally, there was evidence of a calcified mobile structure attached to the aortic bioprosthesis (Fig. 5.1c (arrow), Video 5.2). The ejection fraction was calculated at 50 %, end-diastolic dimension 61 mm, and end-systolic dimension 42 mm. Pulmonary artery pressures were elevated at 65 mmHg.

In view of her emergency admission with cardiac decompensation in the context of aortic bioprosthesis dysfunction, she was discussed at the "Heart Team meeting." Due to her high surgical operative risk (Logistic EuroSCORE, 21 %; STS mortality, 11.33 %), it was decided that she would be best treated with transcatheter aortic valve implantation (TAVI).

5.2 Patient Work-Up

Further investigations were carried out to aid in procedural planning. Baseline hematology revealed a normal hemoglobin and platelet count and biochemistry confirmed normal renal and hepatic function. There was no biochemical evidence of ongoing inflammation. Other investigations including carotid Doppler ultrasound and pulmonary function tests were within normal limits.

Computed tomography (CT) confirmed the diameter of the inner ring of the aortic bioprosthesis to be 16.5 mm (Fig. 5.2a, b), the anatomy of the left ventricular outflow tract (LVOT) (Fig. 5.2c), and the position of the mitral bioprosthesis (Fig. 5.2d). The height of the left coronary ostium was 12 mm and the right coronary ostium was 14 mm. Assessment of the peripheral vasculature demonstrated a minimal lumen diameter (MLD) of 6.1 mm on the right and 5.7 mm on the left in the absence of significant calcification or tortuosity.
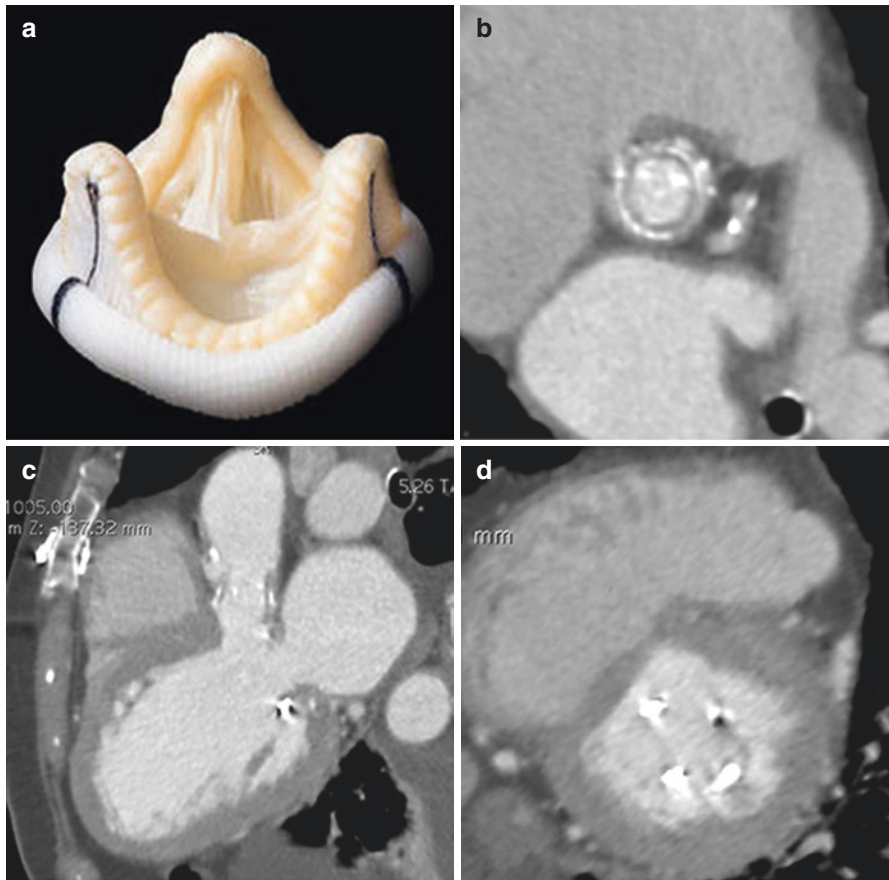
Fig. 5.2 Computed tomography. Appearance of St. Jude Epic bioprosthetic valve (**a**). Computed tomography of aortic bioprosthesis (**b**) and appearance of left ventricular outflow tract (LVOT) (**c**) and of mitral bioprosthesis (**d**)

5.3   Factors for Consideration

There were a number of different factors that require careful consideration when determining the optimal procedural strategy for this patient including:

- Choice of access site
- Device selection for a valve-in-valve (VIV) procedure in the presence of severe aortic regurgitation
- Device selection in view of the presence of a mitral bioprosthesis
- The requirement of cerebral protection in view of the appearance of a mobile calcified structure on the aortic bioprosthetic valve – a likely consequence of the previously treated episode of endocarditis

5.4   Procedural Planning

5.4.1   Access Site

The default vascular access site is now the transfemoral route, due to a number of advantages including the ability to perform the procedure under sedation, resulting in shorter procedure and recovery times [1, 2]. With improvements in the design of current TAVI transfemoral delivery systems, the currently recommended MLD is >5.5 mm for femoral access. Our patient had favorable femoral anatomy, and therefore, a transfemoral approach was chosen.

5.4.2   Valve-in-Valve Procedure

Redo sternotomy and surgical aortic valve replacement are associated with a mortality of approximately 5 % [3] and may rise to as high as 20 % in elderly patients with multiple comorbidities [4]. The global valve-in-valve (VIV) registry [5] demonstrated that TAVI treatment for bioprosthesis dysfunction is feasible and reported a procedural success rate of 93 % and 30-day mortality of 8.4 %. Our patient had a 25-mm Medtronic Epic valve in situ with an inner ring diameter of 17 mm suitable for a transcatheter VIV procedure.

5.4.3   Device Selection

The correct selection of device is critical to the ultimate success of any TAVI procedure but was even more critical in this case due to the number of different aspects that needed to be considered:

1. VIV procedures as opposed to the treatment of native valves are associated with a higher risk of coronary obstruction [5].
2. The presence of the bioprosthetic mitral valve was an important consideration due to the potential difficulty in obtaining an optimal position of the TAVI device.
3. The small annulus size of the bioprosthetic valve and the concern of a high post-procedural gradient following TAVI [5].

   In view of these concerns, we decided to use a Medtronic Evolut R 23-mm device. Firstly, the design of the valve with the constriction zone reduces the likelihood of coronary obstruction. Secondly, as opposed to other devices (e.g., Portico valve), the CoreValve is implanted in a supra-annular position that is associated with lower postprocedural gradients following VIV TAVI [6]. Finally, due to the presence of the mitral bioprosthesis, we were concerned about the possibility of not achieving optimal valve positioning at the first attempt [7]. The ability to reposition and completely resheath the Evolut R device in case of suboptimal position or coronary obstruction was particularly attractive.

5.4.4 Cerebral Protection

The use of cerebral protection devices has been of great interest recently in a bid to reduce the incidence of stroke with effects between 5 % and 7 % of patients at 1-year following TAVI [8], and 80 % of patients suffer silent cerebral injury when measured by magnetic resonance imaging [9]. One such strategy has been the use of cerebral protection devices, and a recent study has demonstrated that the use of the Claret embolic protection device (Claret Medical, Santa Rosa, California, USA) has been associated with a reduction in the volume of ischemic lesions following TAVI implantation [10], although the clinical significance of this finding is currently unclear. In view of the appearance of a mobile calcified lesion on the aortic bioprosthesis, it was felt that the use of a cerebral protection device was indicated and may reduce the risk of an embolic event following valve implantation, accepting that the Claret device does not protect the left vertebral artery.

In summary, based on subsequent investigations and patient-specific factors, it was decided that the patient would undergo transfemoral TAVI with a Medtronic Evolut R 23-mm valve and the use of a CLARET cerebral embolic protection device.

5.5 Procedure

The procedure was carried out under local anesthetic and sedation via the transfemoral route. Left femoral access was carried out under fluoroscopic guidance, and a 0.018″ wire was placed in the contralateral femoral artery ("crossover technique" [11]) prior to femoral puncture on that side which was the interventional side with the aim of maintaining control of the artery in the presence of a vascular complication. Following the placement of two ProGlide (Abbott Vascular, Santa Clara, California, USA) vascular closure devices, right radial arterial access was obtained followed by placement of a CLARET cerebral protection device (Fig. 5.3).

The valve was crossed with the aid of an Amplatz catheter and a straight tip 0.035″ wire. The wire was then exchanged for an Amplatz Super Stiff wire (Boston Scientific, Natick, MA, USA), which was positioned at the apex of the left ventricle. Aortography confirmed severe aortic regurgitation (Fig. 5.4a, Video 5.3), and invasive hemodynamic monitoring demonstrated near equalization of the left ventricular and aortic diastolic pressures further confirming the severity of the AR (Fig. 5.4b).

The 14 French Medtronic Evolut R transfemoral system was introduced via the right femoral artery over the Amplatz Super Stiff wire and was advanced across the bioprosthetic aortic valve. After partial unsheathing of the valve, aortography indicated that the valve was too low (Video 5.4) and was therefore resheathed and then redeployed in a higher, more optimal position.

Final aortography confirmed an excellent result with no evidence of AR (Fig. 5.5a, Video 5.5) with an associated improvement in hemodynamics (Fig. 5.5b) and no evidence of new conduction delay on surface electrocardiogram. Transthoracic echocardiography acutely confirmed excellent TAVI prosthesis function and a mean gradient of 19 mmHg (Fig. 5.6a). On removal of the CLARET
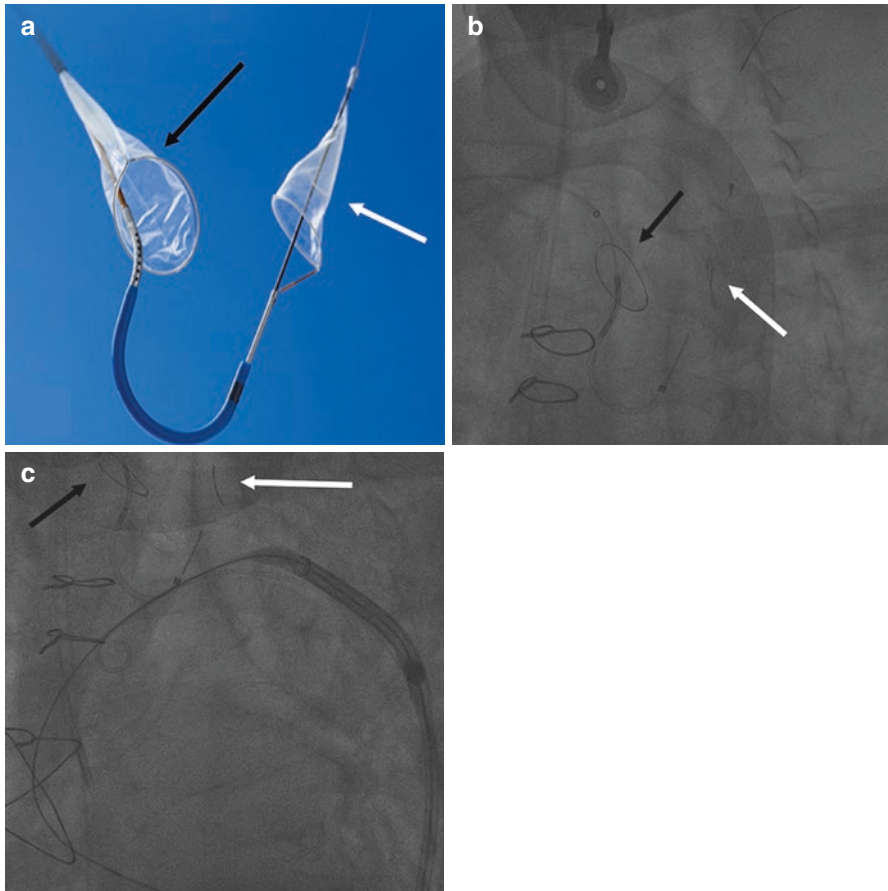
Fig. 5.3 Claret embolic protection device. Appearance of Claret embolic protection device (**a**) with appearance of proximal filter (*black arrow*) and distal filter (*white arrow*). Fluoroscopic appearance of deployment of Claret device demonstrating both proximal (*black arrow*) and distal (*white arrow*, **b**) filters. Fluoroscopic appearance of final position of device while deploying transcatheter aortic valve device (**c**)

cerebral protection device, there was evidence of minimal debris in the filter (Fig. 5.6b). The femoral sheaths were removed, with hemostasis achieved with successful deployment of the two ProGlide devices.

5.6 Clinical Course and Follow-Up

Following the procedure, the patient was transferred to the main ward. The patient made an uncomplicated recovery and was discharged home 4 days after the procedure. At 1-month follow-up, transthoracic echocardiography confirmed a well-functioning TAVI prosthesis with the patient symptomatically much improved (NYHA class I).
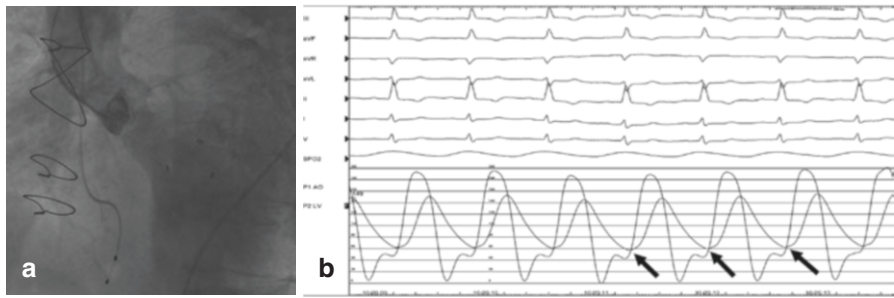
Fig. 5.4 Assessment of aortic regurgitation severity. Aortogram demonstrating severe aortic regurgitation (**a**). Invasive hemodynamic assessment demonstrating near equalization of end-diastolic pressures (*black arrows*), confirming severity of aortic regurgitation (**b**)
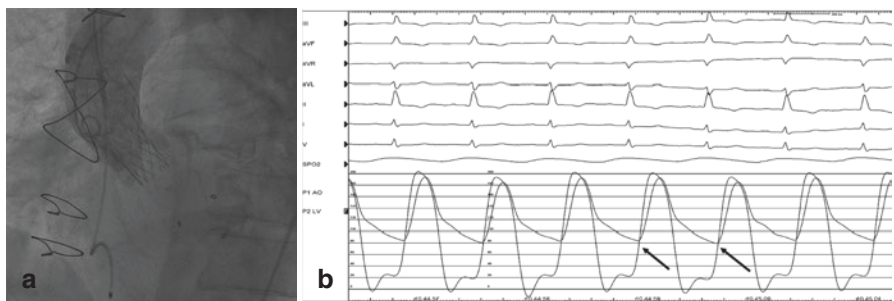
Fig. 5.5 Final result. Final aortography demonstrated an excellent result with no evidence of coronary obstruction or aortic regurgitation (**a**); this was associated with an improvement in hemodynamics (*black arrows*, **b**)
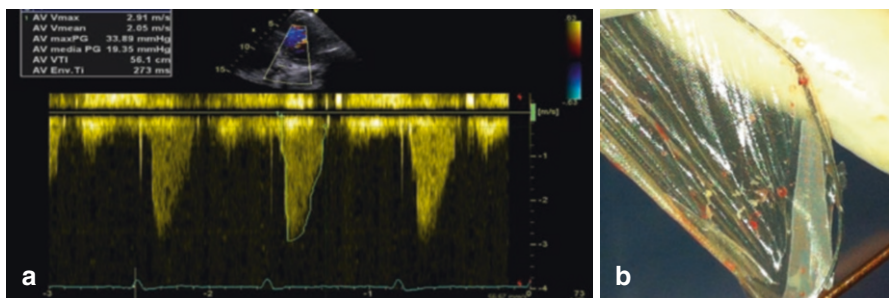
Fig. 5.6 Final echocardiogram and filter appearance. Postprocedural transthoracic echocardiogram demonstrated a mean aortic valve gradient of 19 mmHg (**a**) with no evidence of aortic regurgitation. On removal of the Claret device, there was no evidence of any debris in the filter (**b**)

> **Conclusion**
>
> This challenging case highlights the importance of the careful consideration of all technical aspects of the procedure to try and preempt the occurrence of any complication. With the aid of relevant preprocedural clinical assessment and imaging, we were able to carefully plan the procedure with the correct choice of TAVI and adjunctive devices which all contributed to achieving an optimal outcome.

References

1. Wiegerinck EM, Boerlage-van Dijk K, Koch KT, Yong ZY, Vis MM, Planken RN, Eberl S, de Mol BA, Piek JJ, Tijssen JG, Baan Jr J. Towards minimally invasiveness: transcatheter aortic valve implantation under local analgesia exclusively. Int J Cardiol. 2014;176:1050–2.
2. Durand E, Borz B, Godin M, Tron C, Litzler PY, Bessou JP, Bejar K, Fraccaro C, Sanchez-Giron C, Dacher JN, Bauer F, Cribier A, Eltchaninoff H. Transfemoral aortic valve replacement with the Edwards SAPIEN and Edwards SAPIEN XT prosthesis using exclusively local anesthesia and fluoroscopic guidance: feasibility and 30-day outcomes. J Am Coll Cardiol Intv. 2012;5:461–7.
3. Christiansen S, Schmid M, Autschbach R. Perioperative risk of redo aortic valve replacement. Ann Thorac Cardiovasc Surg Off J Assoc Thorac Cardiovasc Surg. 2009;15:105–10.
4. Vogt PR, Brunner-LaRocca H, Sidler P, Zund G, Truniger K, Lachat M, Turina J, Turina MI. Reoperative surgery for degenerated aortic bioprostheses: predictors for emergency surgery and reoperative mortality. Eur J Cardio Thorac Surg Off J Eur Assoc Cardiothorac Surg. 2000;17:134–9.
5. Dvir D, Webb J, Brecker S, Bleiziffer S, Hildick-Smith D, Colombo A, Descoutures F, Hengstenberg C, Moat NE, Bekeredjian R, Napodano M, Testa L, Lefevre T, Guetta V, Nissen H, Hernandez JM, Roy D, Teles RC, Segev A, Dumonteil N, Fiorina C, Gotzmann M, Tchetche D, Abdel-Wahab M, De Marco F, Baumbach A, Laborde JC, Kornowski R. Transcatheter aortic valve replacement for degenerative bioprosthetic surgical valves: results from the global valve-in-valve registry. Circulation. 2012;126:2335–44.
6. Azadani AN, Jaussaud N, Matthews PB, Ge L, Guy TS, Chuter TA, Tseng EE. Valve-in-valve implantation using a novel supravalvular transcatheter aortic valve: proof of concept. Ann Thorac Surg. 2009;88:1864–9.
7. Soon JL, Ye J, Lichtenstein SV, Wood D, Webb JG, Cheung A. Transapical transcatheter aortic valve implantation in the presence of a mitral prosthesis. J Am Coll Cardiol. 2011;58:715–21.
8. Smith CR, Leon MB, Mack MJ, Miller DC, Moses JW, Svensson LG, Tuzcu EM, Webb JG, Fontana GP, Makkar RR, Williams M, Dewey T, Kapadia S, Babaliaros V, Thourani VH, Corso P, Pichard AD, Bavaria JE, Herrmann HC, Akin JJ, Anderson WN, Wang D, Pocock SJ, Investigators PT. Transcatheter versus surgical aortic-valve replacement in high-risk patients. N Engl J Med. 2011;364:2187–98.
9. Kahlert P, Knipp SC, Schlamann M, Thielmann M, Al-Rashid F, Weber M, Johansson U, Wendt D, Jakob HG, Forsting M, Sack S, Erbel R, Eggebrecht H. Silent and apparent cerebral ischemia after percutaneous transfemoral aortic valve implantation: a diffusion-weighted magnetic resonance imaging study. Circulation. 2010;121:870–8.
10. Haussig, S, Mangner N, Dwyer MG, Lehmkuhl L, Lucke C, Woitek F, Holzhey DM, Mohr FW, Gutberlet M, Zivadinov R, Schuler G, Linke A. JAMA. 2016;316(6):592–601.
11. Buchanan GL, Chieffo A, Montorfano M, Maccagni D, Maisano F, Latib A, Covello RD, Grimaldi A, Alfieri O, Colombo A. A "modified crossover technique" for vascular access management in high-risk patients undergoing transfemoral transcatheter aortic valve implantation. Catheter Cardiovasc Interv Off J Soc Cardiac Angiography Interv. 2013;81:579–83.

Difficult Cases and Complications from the Catheterization Laboratory: Case 2

6

Difficult Cases and Complications from the Catheterization Laboratory: Percutaneous Treatment of Aortic Annulus and Left Ventricular Outflow Rupture During Transcatheter Aortic Valve Implantation

Salvatore Saccà, Tomoyuki Umemoto, Andrea Pacchioni, and Bernhard Reimers

6.1   Introduction

Transcatheter aortic valve implantation (TAVI) is now becoming an alternative therapy to surgical aortic valve replacement (SAVR) for the patient with high surgical risk. Preprocedural complications are still frequent, and they include not only vascular but also severe life-threatening complications such as stroke, heat block, coronary obstruction, improper prosthesis positioning, cardiac perforation, mitral valve injury, and annulus or aortic root rupture. Among these severe complications, annulus and aortic root rupture will induce catastrophic outcomes [1].

6.2   Case

An 85-year-old female was referred to our institution due to worsening chronic heart failure. Transthoracic echocardiography (TEE) showed severe aortic valve stenosis with decreased left ventricular systolic function (aortic valve area $0.6 \ cm^2/m^2$, LVEF 40 %). She had a history of chronic obstructive pulmonary disease and chronic renal failure. Due to estimated high operative risk (EuroSCORE 20 %), a TAVI approach was chosen by the Heart Team.

S. Saccà (✉) • T. Umemoto • A. Pacchioni
Department of Cardiology, Mirano Hospital, Mirano, Italy
e-mail: salvatoresacca@virgilio.it; michele.rinaldi@medtronic.com

B. Reimers
Cardiovascular Department, Humanitas Research Hospital, Rozzano, Milan, Italy

6.3   Procedural Summary

Computed tomography angiography (CTA) measurements showed the following: aortic valve annulus diameter, 21 × 26 mm; perimeter of area, 76.9 mm; and area, 458 mm² (Fig. 6.1). These measures are compatible both with 23-mm and 26-mm EDWARDS Sapien XT. We inserted a 6-Fr introducer sheath in her left common femoral artery (CFA) and advanced a pigtail catheter into her right CFA. Under the guidance with contrast injection, the right CFA was accessed, a 10-Fr Prostar (Abbott Vascular, Abbott Park, IL) was deployed, and a 10-Fr introducer sheath was introduced. A 0.018-in. V-18 guidewire (Boston Scientific, Natick, Massachusetts, USA) was delivered from left CFA into right SFA with crossover approach in case of perforation of right CFA by 18-Fr sheath introduction or occlusion/stenosis of right CFA after the closure by Prostar. After usual systemic heparinization (75 UI/kg), a pigtail catheter was introduced to the aortic root, and a transvenous temporary pacemaker was placed. The 10-Fr sheath was then exchanged for an 18-Fr sheath with Amplatz Super Stiff wire (Boston Scientific, Natick, Massachusetts, USA). The left ventricle (LV) was canalized by standard technique, and a reshaped Amplatz Super Stiff wire was introduced through a pigtail catheter. Then, balloon valvuloplasty was performed with 23-mm balloon (NuMed AB Medica, Italy) during rapid pacing, checking again annulus size (Fig. 6.2). A 26-mm prosthesis appeared to be the best choice. Subsequently, the Sapien XT prosthesis was advanced and positioned across the aortic valve (Fig. 6.3). Just after implantation of the Sapien XT prosthesis with 24-cc inflation, hemodynamic collapse suddenly occurred. While performing cardiac compression, aortogram revealed extravasation of contrast into the pericardial space (Fig. 6.4). Immediately we performed needle pericardiocentesis and pericardial drainage. After the hemodynamics slightly improved with pericardial drainage, aortic annulus and LV outflow tract rupture was revealed with close angiography using 6-Fr Amplatz left 1.0 guiding catheter (Fig. 6.5). Surgical repair was thought to be one of the options, but the patient was still in unstable hemodynamic status. Besides the ruptured hole seemed to be small, we decided to attempt to fix it by coil embolization. With intravenous epinephrine and reinfusion of the drained blood (totally about 1,000 cc), hemodynamics was somehow being maintained without percutaneous cardiopulmonary support device (PCPS). So we started coil embolization. At first, we engaged a 6-Fr Amplatz left 1.0 guiding catheter to the entry of the ruptured hole and injected a small amount of contrast in very gentle way in order to clarify the aortic annulus and LV outflow tract rupture. And then, a PROGREAT micro catheter (Terumo, Tokyo, Japan) was inserted into the ruptured hole. With this micro catheter, we started to deploy a VORTEX coil

Fig. 6.1 CT scan preoperative evaluation of annulus and left main ostium height. Annulus size fits in between Edwards Sapien 23 and 26 mm. Huge calcification in left ventricle outflow tract is clearly visible
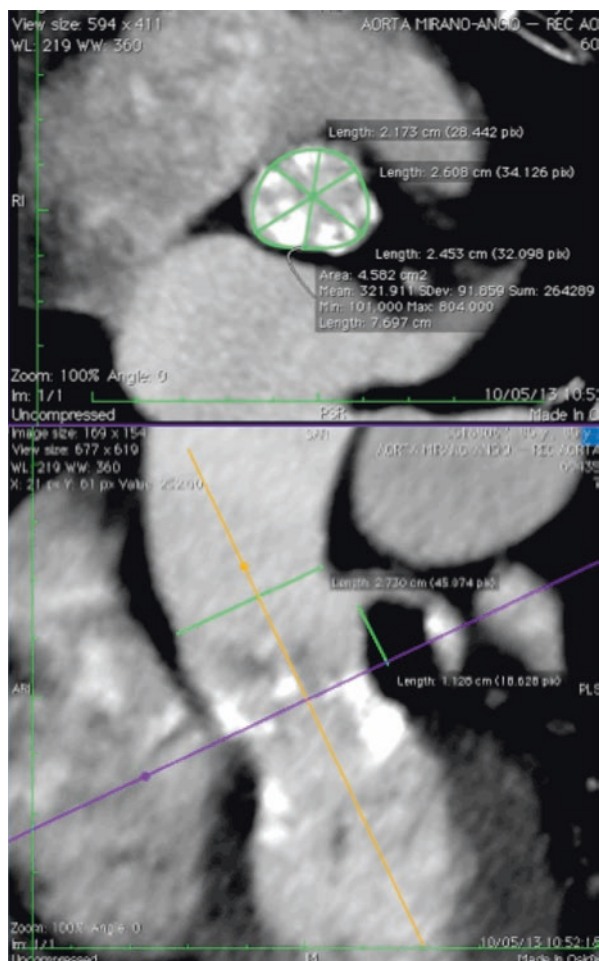
(Boston Scientific, Natick, Massachusetts) inside the pericardium. After the multiple VORTEX coil deployment (Fig. 6.6), we could gain the complete bleeding control confirmed by close aortography and left ventriculography (Fig. 6.7). The patient was transferred to the coronary care unit (CCU) after the procedure. She was intubated and subsequently underwent a tracheotomy but had a clear sensorium, and implanted Edwards Sapien XT prosthesis really worked well. Unfortunately, she experienced acute kidney failure and died due to massive intrapulmonary bleeding after bronchoscopy at day 27 in the CCU.

Fig. 6.2 Annulus size was checked again with injection during balloon valvuloplasty with 23-mm balloon. It appeared slightly small, so 26-mm valve was preferred
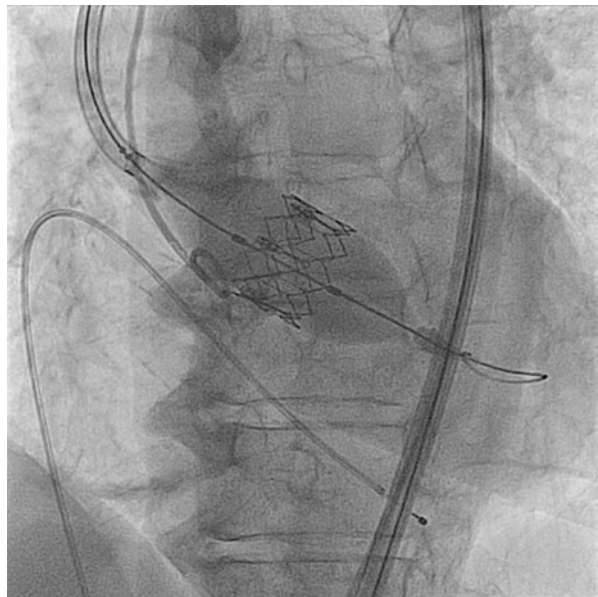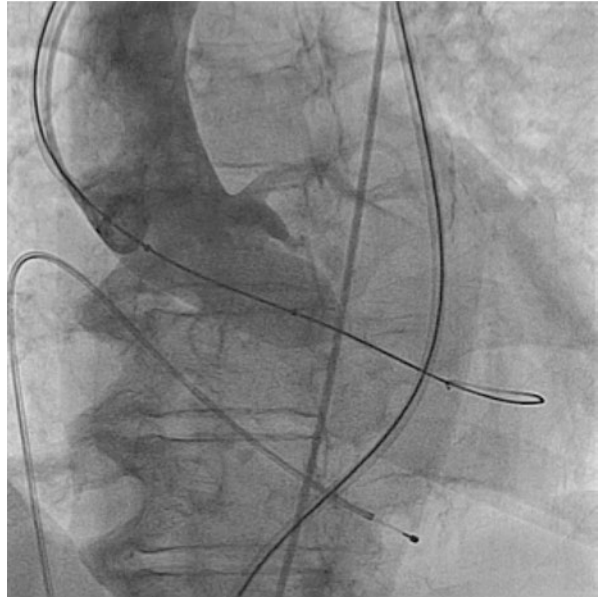
Fig. 6.3 Prosthesis deployment

Fig. 6.4 Aortogram
showed contrast medium
exited into pericardial
space (*black arrow*)
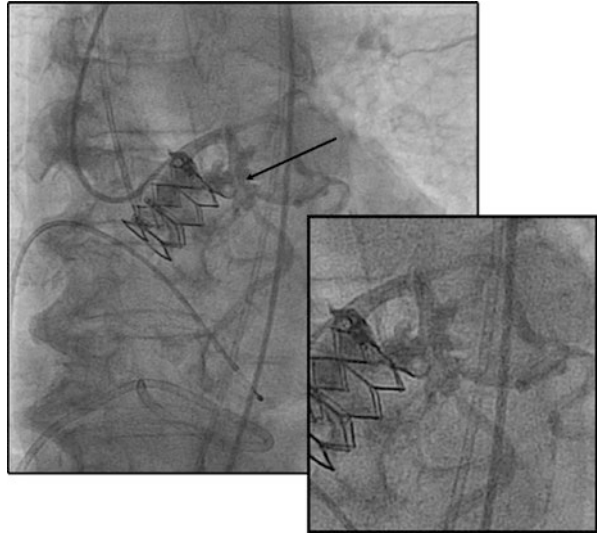
Fig. 6.5 Selective
catheterization with
contrast medium injection
through the breakdown
into the pericardial space
using 6-Fr Amplatz left 1.0
guiding catheter
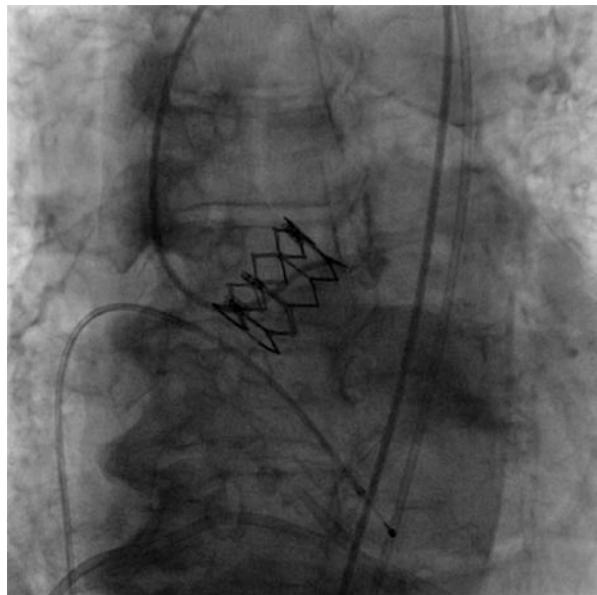
Fig. 6.6 Multiple coil embolizations into the pericardial space through the Amplatz left guiding catheter
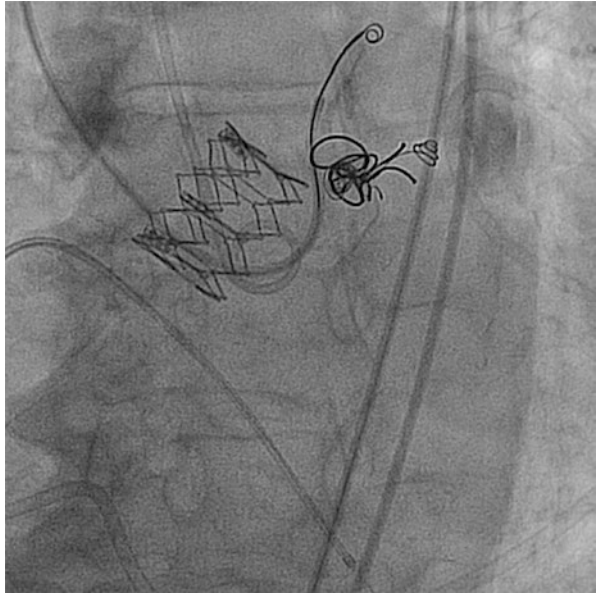
Fig. 6.7 Final angiogram showing complete sealing of the hole
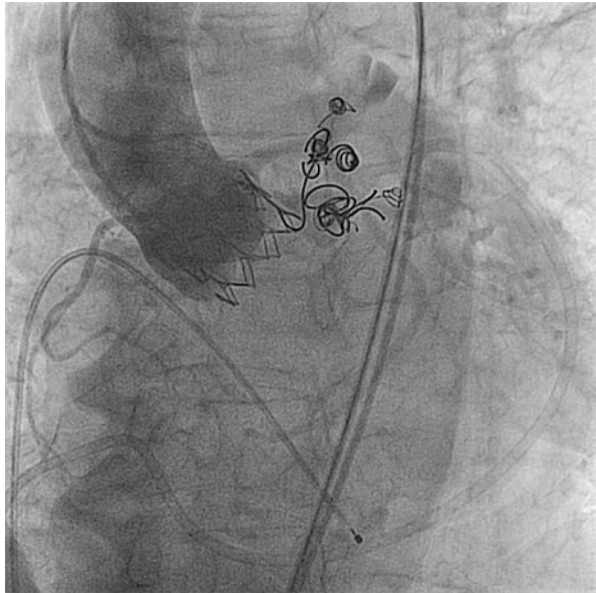
6.4   Discussion

Vascular complications after TAVI are frequent and reported as 22 % [2]. The incidence of catastrophic complications such as annulus or aortic root rupture is rarely reported and varies according to the papers as 0.6–4.2 % [1, 3–5]. Once annulus and aortic root rupture occurs, cardiac tamponade and hemodynamic collapse are instantaneous.

In the case described, there are two potential causes inducing aortic annulus and LV outflow tract rupture:

- A prosthesis oversized compared to the real annulus diameter. When we performed close remeasurement after the procedure, we realized we probably underestimated annulus perimeter and diameters. A smaller valve (e.g., Edwards Sapien XT 23 mm) should probably be fitted better (Figs. 6.8 and 6.9).
- Huge subaortic calcification (Fig. 6.1). We could see there was a big trunk of subvalvular calcification by CTA both in short- and long-axis views. Compared with the angiography just after the rupture, it seemed that perforation occurred around the mass of calcification.

Then how should we treat such a patient with a big subvalvular calcification? Self-expandable prosthesis might be one of the possible solutions, although paravalvular leakage might occur, which will lead to worse outcome because of aortic regurgitation.

So the most important thing is to measure the annulus with multiple imaging modalities including CTA and TEE and size precisely the prosthesis.

Once annulus and aortic root rupture occurred, first of all, you have to focus on the stabilization of hemodynamics with inotropic agents, needle pericardiocentesis, and PCPS if needed. Then you should perform a close angiography to clarify the damage of the aortic valve complex. If hemodynamics is stable, you can try surgical repair. But if the catastrophe is imminent, you should try a percutaneous management.

This is the first case report of successful management for the annulus or aortic root rupture with coil embolization. Of course there are possible complications including thromboembolism or coil migration, but coil embolization might be possibly effective as in this patient.

As conclusion, to avoid complications, it should be kept in mind that:

- Appropriate sizing of the prosthesis should be performed with multiple imaging modalities including CTA and TEE.
- A big mass of calcification around the aortic valve complex and a narrow sinotubular junction have a potential risk of annulus or aortic rupture.
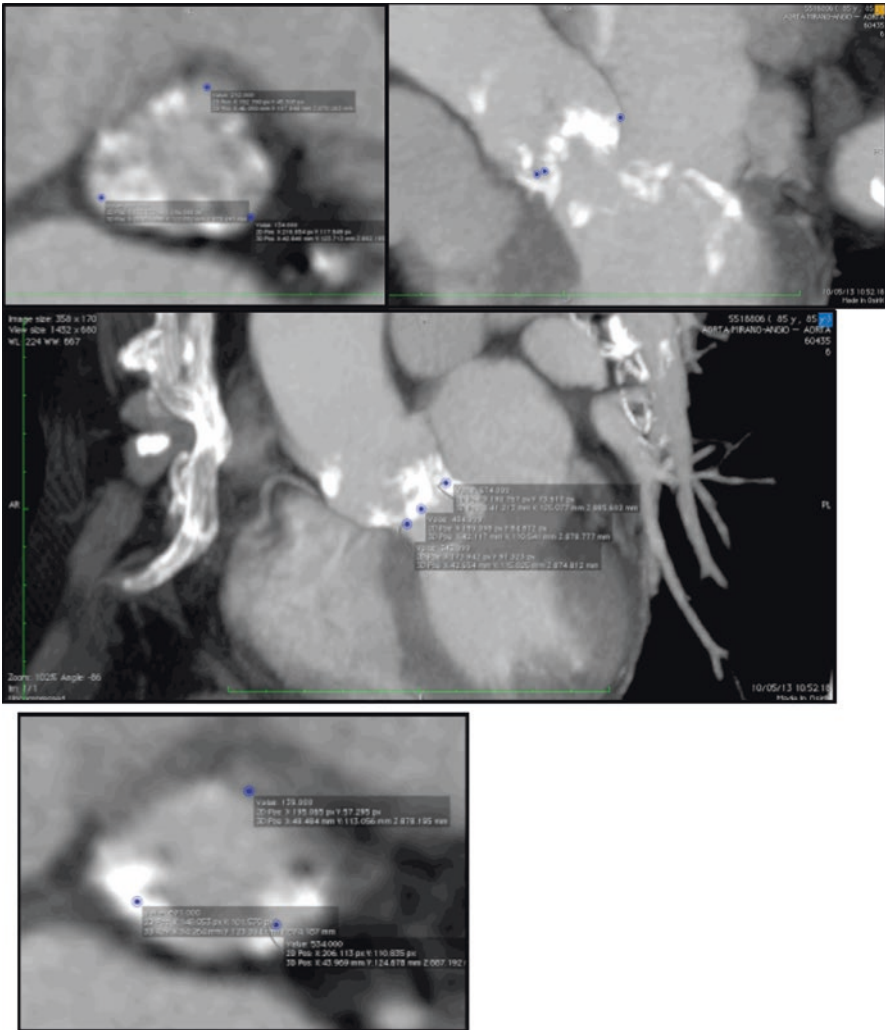
Fig. 6.8 Reevaluation of annulus size after TAVI; showing the erroneous measurements at first evaluation (*blue dots* representing the nadir of each valve cusps should be on the same axis when the annulus is correctly measured)

Fig. 6.9 With correct measurements, annulus size results smaller, leading to 23-mm valve choice
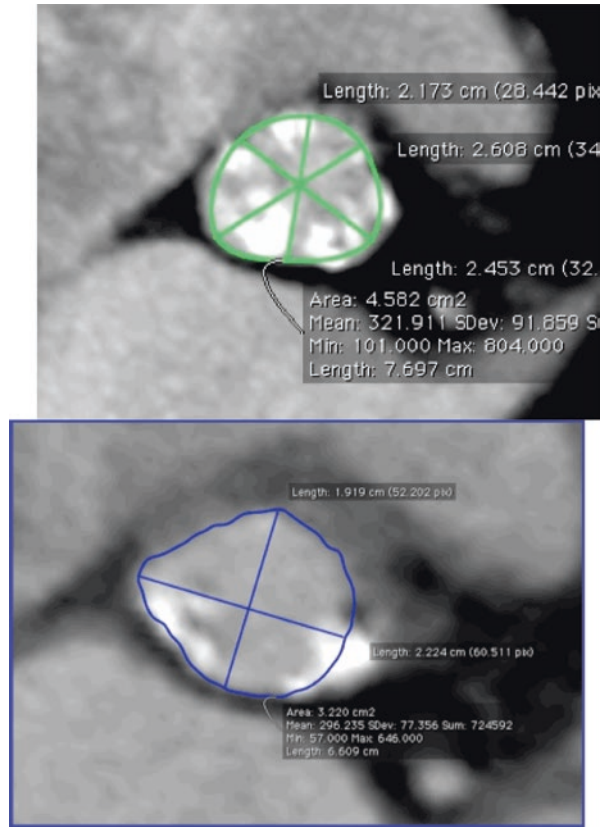
References

1. Barbanti M, Yang TH, Rodès Cabau J, et al. Anatomical and procedural features associated with aortic root rupture during balloon-expandable transcatheter aortic valve replacement. Circulation. 2013;128(3):244–53. doi:10.1161/CIRCULATIONAHA.113.002947.
2. Perrin N, et al. Management of vascular complications following transcatheter aortic valve implantation. Arch Cardiovasc Dis. 2015;108:491–501.
3. Gerhard S, et al. Ruptures of the device landing zone in patients undergoing transcatheter aortic valve implantation: an analysis of TAVI Karlsruhe (TAVIK) patients. Clin Res Cardiol. 2014;103(11):912–20.
4. Hayashida K, et al. Potential mechanism of annulus rupture during transcatheter aortic valve implantation. Catheter Cardiovasc Interv. 2013;82(5):E724–6.
5. Zhao QM, et al. Procedural results and 30-day clinical events analysis following Edwards transcatheter aortic valve implantation in 48 consecutive patients: initial experience. Chin Med J (Engl). 2012;125(16):2807–10.

Difficult Cases and Complications from the Catheterization Laboratory: Case 3 "The Importance of Being Prepared"

Chiara Fraccaro, Luca Nai Fovino, and Giuseppe Tarantini

7.1   The Patient

A 76-year-old male patient affected by severe symptomatic degenerative aortic stenosis was referred for evaluation to our Heart Team. He had a past medical history of arterial hypertension, smoking habit, chronic obstructive pulmonary disease, type 2 diabetes mellitus complicated by retinopathy, multivessel coronary artery disease treated by percutaneous revascularization on the left coronary artery, and normal left ventricular ejection fraction. Moreover, he was diagnosed with peripheral vascular disease and had been treated with bilateral percutaneous transluminal angioplasty on the popliteal arteries. The patient was symptomatic for mild exertional dyspnea (NYHA class III) and was judged at high risk for conventional aortic valve replacement (logistic EuroSCORE 15.80 %, EuroSCORE II 1.59 %, STS score morbidity/mortality 20.95 %) and therefore scheduled for TAVI.

7.2   Case Planning

Three-dimensional multidetector computed tomography (CT) aortic annulus measurements were: maximum annular diameter 28.5 mm, minimum annular diameter 22.5 mm, mean annular diameter 26 mm, perimeter 79 mm, area 4.65 cm^2, and area-derived diameter 24.33 mm. According to the company's recommendations, a 26 mm Edwards Sapien 3 valve prosthesis was selected. Moreover, CT scan (Fig. 7.1a–c) showed extensive circumferential calcification of the iliac-femoral arterial axis without significant tortuosity and minimum diameters of 6.0 mm (right) and 4.8 mm (left). Although no clear stenosis was present, neither the right nor the

C. Fraccaro • L. Nai Fovino • G. Tarantini (✉)

Interventional Cardiology, department of Cardiac, Thoracic and Vascular Sciences, University of Padua, Padua, Italy

e-mail: giuseppe.tarantini.1@unipd.it
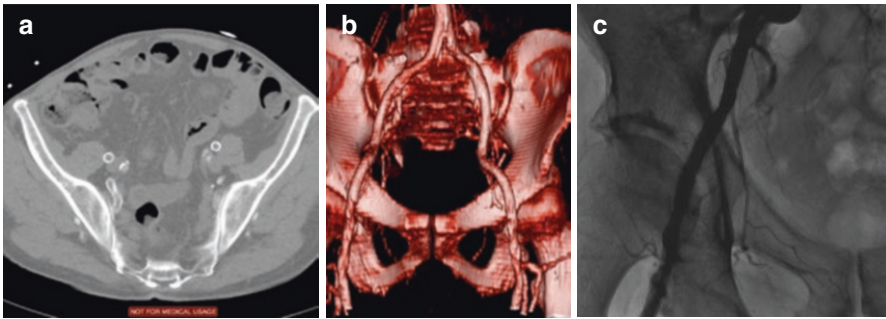
Fig. 7.1 Preoperative multimodality imaging evaluation of access site. Extensive circumferential calcification of the iliac-femoral arterial tree at multidetector computed tomography (panel A, B). No significant stenosis is documented at angiography (panel C)

left axes had diameters large enough to allow passage of the big introducer sheath needed. However, after careful examination of anatomical features by angiograms and CT scan, the patient was considered eligible to TAVI through minimal invasive transfemoral percutaneous approach, once performed a percutaneous angioplasty of the right common femoral artery (CFA).

7.3   The Procedure

Under local anesthesia and mild sedation, angioplasty (Mustang balloon dilation catheters 8×40 mm, 9×30 mm and 10×30 mm, Boston Scientific, United States) of the right CFA and external iliac arteries (EIAs) was performed with crossover technique from the contralateral groin, with guidewire placed distally in the superficial femoral artery (SFA). At control angiography, contrast medium extravasation from the right EIA was seen, and two covered stents (Advanta 8×38 mm, Rastatt, Germany) were placed (Fig. 7.2).

Right arterial access was then obtained by puncture of CFA under fluoroscopic guidance. After preparation of the vessel with a 9-F vascular sheath, a 10-F ProStar XL closure device (Abbott Vascular Devices, Redwood City, California) was inserted, and sutures were deployed, needles removed, and sutures secured using the pre-closure technique. A 16-F delivery sheath (Edwards eSheath) was then inserted over a stiff wire placed in the left ventricle. After valve predilation with a 23 mm balloon, the Edwards Sapien 3 26 mm valve prosthesis was successfully implanted with rapid ventricular pacing. The vascular access sheath was then removed, and the pre-laid sutures of the Prostar device were tied in place. The result was checked by angiography via the crossover sheath, with evidence of another contrast medium extravasation at the vessel entry site (Fig. 7.3). Thus, double covered stenting under fluoroscopic guidance was performed using the guidewire previously positioned into the distal
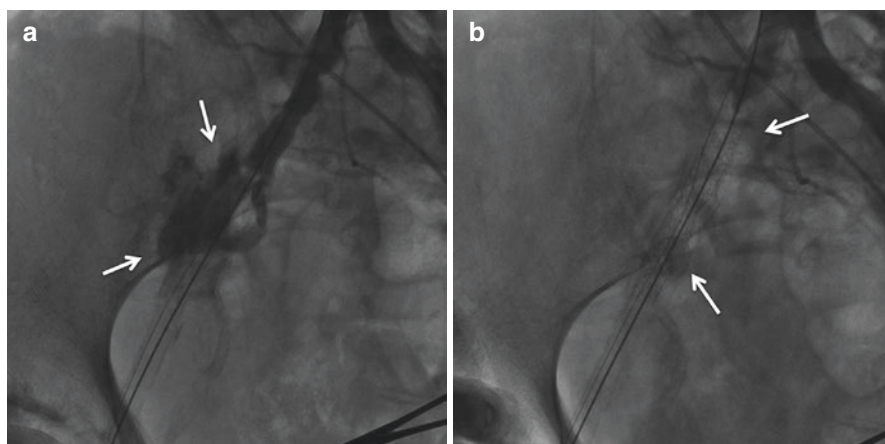
Fig. 7.2 Treatment of femoral artery injury with covered stenting. Arterial access site rupture with extravasation of contrast medium (*arrows*). Sealing of arterial rupture with implantation of covered stents (*arrows*)

SFA. Final control angiography showed no residual contrast medium extravasation. Prior to discharge, angio-CT scan showed stents' patency with complete sealing of vessel rupture (Fig. 7.4).

7.4 Case Analysis

Vascular complications such as iliofemoral dissection and rupture, puncture site stenosis/thrombosis/occlusion, artery avulsion, pseudoaneurysm, failed percutaneous closure, access site bleeding, and infections remain a major pitfall in transfemoral TAVI. The incidence of major VARC vascular complications ranges from 16 % in the PARTNER trial (using 22- and 24-F delivery system) [1] to 6 % in the SOURCE XT registry (using 18- and 19-F sheaths) [2], with an important impact on morbidity and mortality. The high prevalence of peripheral arterial disease together with the required antithrombotic treatment during the procedure further increases patient's risk. According to available literature, major predictors of such complications are small vessel dimensions, moderate or severe iliofemoral calcification, and poor center experience [3–5]. Therefore, preoperative multimodality imaging evaluation of the access site with aortic angiogram and CT scan is of paramount importance to minimize the risk of complications. In particular, multidetector CT is considered the gold standard for the evaluation of vessel size, degree of calcification, minimal luminal diameter, plaque burden, and vessel tortuosity and also for the identification of high-risk features including dissections and complex atheroma.
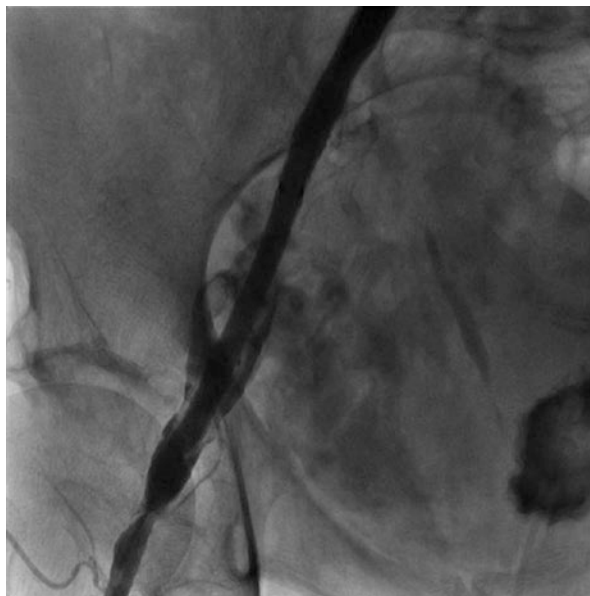
Fig. 7.3 Angiography of the right femoral artery showing contrast medium extravasation from the vascular entry site

In our case, we chose the transfemoral approach despite the fact that the iliofemoral vessels' diameters were at the lower tolerance limit and the femoral arteries were highly calcified. Notably, in the absence of atherosclerotic disease, the common femoral artery is compliant and can accommodate sheaths slightly larger than the artery diameter. When moderate or severe calcification is documented, the external sheath size should not extend the minimal artery diameter; this is particularly true in the presence of horseshoe or circumferential calcifications (such as in our case), which do not allow any vessel compliance. Improvements in percutaneous techniques and materials with reduction in delivery systems profile have extended eligibility criteria for transfemoral TAVI approach. For example, the new expandable introducer sheaths are designed to reduce vascular trauma since they allow for transient sheath expansion during the delivery system passage and reduce the time the access vessel is expanded.

Surgical treatment of access site rupture or dissection is feasible, but it is associated with treatment delay, prolonged hospitalization, and the risk of wound infections. Endovascular techniques, including the implantation of covered stent grafts, may allow for less invasive yet effective management of arterial injuries to rapidly stop severe bleeding. The only concern is that covered stent grafts implanted into the iliofemoral artery may be prone to stent fracture and flow obstruction.
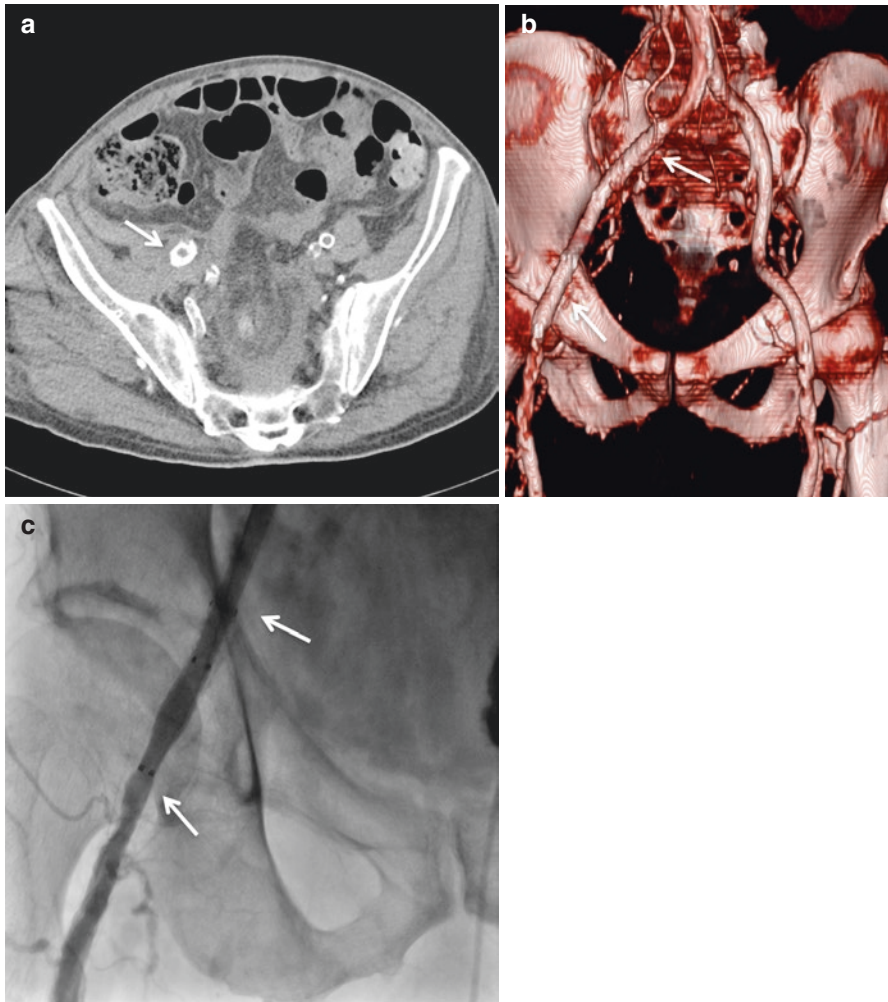
Fig. 7.4 Imaging follow-up assessment. Imaging follow-up assessment of vascular injury site by multidetector computed tomography and biplane angiography showing patency of the stent grafts (*arrows*) and the absence of significant restenosis

In conclusion, vascular complications in TAVI remain a major challenge for the interventional cardiologist. Accurate preoperative multimodality screening is mandatory to reduce such risk by selecting the most appropriate vascular access site. In most cases, percutaneous treatment of vascular complications is feasible with a high rate of technical success and good clinical outcomes. Stent patency and integrity should be verified at follow-up with both clinical and instrumental evaluations.

References

1. Leon MB, Smith CR, Mack M, et al. Transcatheter aortic-valve implantation for aortic stenosis in patients who cannot undergo surgery. N Engl J Med. 2010;363:1597–607.
2. Schymik G, Lefevre T, Bartorelli AL, et al. European experience with the second-generation edwards sapien xt transcatheter heart valve in patients with severe aortic stenosis 1-year outcomes from the source xt registry. Jacc Cardiovasc Interv. 2015;8:657–69.
3. Lange R, Bleiziffer S, Piazza N, et al. Incidence and treatment of procedural cardiovascular complications associated with trans-arterial and trans-apical interventional aortic valve implantation in 412 consecutive patients. Eur J Cardiothorac Surg. 2011;40:1105–13.
4. Hayashida K, Lefevre T, Chevalier B, et al. Transfemoral aortic valve implantation new criteria to predict vascular complications. Jacc Cardiovasc Interv. 2011;4:851–8.
5. Toggweiler S, Gurvitch R, Leipsic J, et al. Percutaneous aortic valve replacement. J Am Coll Cardiol. 2012;59:113–8.

Current and Next Generation of Transcatheter Valves

8

Francesco Bedogni, Mauro Agnifili, and Luca Testa

From the first quarter of 2014, a new generation of transcatheter valves (Fig. 8.1) has CE mark approval for clinical use in Europe and under scrutiny for FDA approval in the United States. These new valves aim to overcome or to reduce the major limitations of first-generation valves (Edwards XT and CoreValve) as paravalvular leak, vascular complications, cardiac rhythm disturbances, and stroke. We describe below the technical features and the first clinical results of the new transfemoral devices.

8.1   Medtronic Evolut R

The transcatheter aortic valve CoreValve Evolut R (Fig. 8.1a) available in sizes 23, 26, and 29 is constituted by a porcine pericardium valve with flaps engineered, obtained by suturing the three valve flaps (obtained from a single sheet of pericardium) to the support with the addition of a "skirt" which facilitates the closure and is shaped to obtain a better fluid dynamics. Support is nitinol self-expanding and is radiopaque. The valve is reduced to an extent of 18 Fr for its positioning, and then, once in place, it is re-expanded to a size between 18 and 20 mm for valve 23, 20 and 23 mm for valve 26, 23 mm for valve 3, and 26 mm for valve 29. The stent is a self-expandable nitinol with cells of diamond in shape and its radiopacity allows the correct positioning of the bioprosthesis; it is designed to have three levels of radial force; in particular in the stretch of inner flow, the radial force is such as to allow the valve to comply native annulus of the patient, to reduce losses paravalvular, and to prevent migration of the prosthesis. The two hooks positioned in the upper portion of the stent allow the loading of the valve. The valve CoreValve Evolut R is designed to be recaptured and repositioned during implant, for a maximum of two times. You

F. Bedogni (✉) • M. Agnifili • L. Testa
IRCCS Policlinico San Donato, Milan, Italy
e-mail: francesco.bedogni@grupposandonato.it
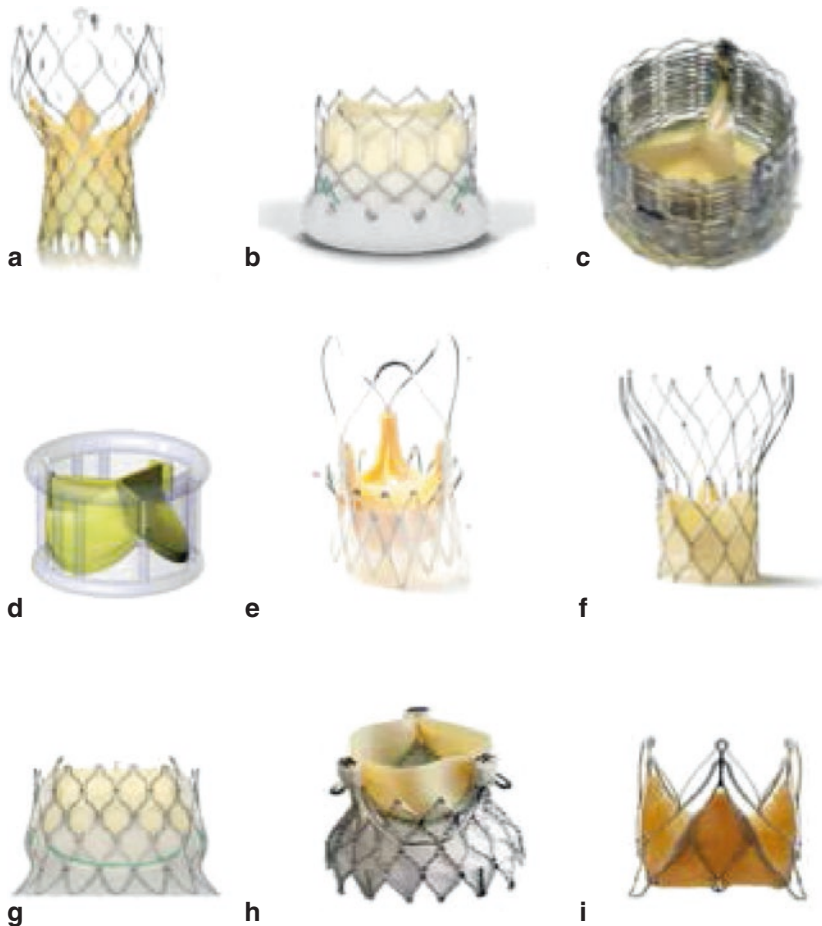
Fig. 8.1 New valves currently available for clinical use. Currently available and underdevelopment transcatheter valves (**a**) Medtronic Evolut (Medtronic Inc, Minneapolis, MN), USA). (**b**) Sapien 3 (Edwards Lifesciences, Irvine, CA, USA). (**c**) Lotus Medical (Boston Scientific Corporation, Natick, MA, USA) valve. (**d**) Direct Flow Medical valve (Direct Flow Medical, Santa Rosa, CA, USA). (**e**) Symetis Acurate (Symetis SA, Lausanne, Switzerland) valve. (**f**) Portico (St Jude Medical, St Paul, MN, USA) valve. (**g**) Centera (Edwards Lifesciences). (**h**) Engager (Medtronic Inc., Minneapolis, MN, USA) transapical valve. (**i**) Transapical JenaValve (JenaValve Technology, Munich, Germany)

can recapture the valve up to 80% of release. The valve design also allows a radial force constant regardless of the size of the native annulus patient, to mitigate any paravalvular regurgitation. The release system with system EnVeo with introducer InLine is necessary for the percutaneous insertion of the bioprosthesis and is formed by a catheter with an outer diameter of 18 Fr and 15 Fr in the distal part in the central part of the shaft, where the stability layer Accutrak is present. Along the proximal part of the delivery, the introducer InLine is present, with a diameter of 18 outer

Fr, which allows to implant the valve without further introducers. The distal part of the device has an atraumatic tip radiopaque. A protective sheath covers in nitinol and maintains bioprosthesis closed. Such sheathing also allows the valve to recapture most twice during implant by turning in the opposite part of the handpiece used to issue the same. This is possible up to 80 % of the opening. Evolut R is available since the fourth quarter of 2014, and very few clinical data are available until now. In CE study of 60 patients, Evolut R showed excellent procedural and 30-day outcomes and strong safety profile (0 % mortality rate) [1].

8.2   Edwards Sapien 3

The Edwards Sapien 3 transcatheter heart valve model (Fig. 8.1b) is the last evolution of balloon-expandable EVS valves. Available from the first quarter of 2014, it combines a stent in chromium-cobalt expandable with a radiopaque balloon, a pericardial three flaps of tissue valve, and an inner and outer skirt made of polyethylene terephthalate (PET). The heart valve Sapien 3 (S3) is available in three sizes (23, 26, and 29), but 20 mm will soon be ready. The valve is assembled with three strips of bovine pericardium. The Edwards Sapien 3 transcatheter heart valve can be implanted with three different approaches: transfemoral, transapical, and trans-aortic. Before implantation, the bioprosthesis is mounted on the delivery system balloon Commander, using a special compression device (crimper). The bioprosthesis is positioned and released at the site of the native aortic valve stenosis through inflating the balloon of the delivery system, which is subsequently removed. Expandable introducer Edwards eSheath 14 F for the valves 23 and 26 mm or 16 F for the valve 29 mm is used for femoral access, allowing a reduction of sheath size compared to Sapien XT. The release system is constituted by a catheter flexible carrier within which a balloon catheter is assembled. The balloon expands the bioprosthesis through a controlled volume of the mixture of contrast medium and saline. The flexible, load-bearing catheter Commander allows the alignment of the valve with the annulus plane through a controlled rotation of the handle and consequent flexion of the distal end. An important new feature of this valve is the presence of a skirt surrounding the distal part of the stent frame on the purpose to reduce the paravalvular leaks with a better contact with calcifications. First-in-man publication done in 2013 showed from the beginning that the S3 and delivery system might facilitate fully percutaneous implantation in a broader range of patients with the potential for more accurate positioning and less paravalvular regurgitation [2]. Recently, at ACC meeting held in San Diego on March 2015, S Kodali presented 30-day results of S3 implant in high- and intermediate-risk patients. Mortality rate and stroke rate were very low in both populations (cardiovascular mortality rate 1.4 % in high-risk and 0.9 % in intermediate-risk, stroke rate 0.9 in high-risk and 1.0 % in intermediate-risk patients) [3]. PARTNER 2 randomized trial is enrolling, and it will compare S3 results versus surgical results in intermediate-risk profile.

8.3   Boston (BSI) Lotus

The device Lotus™ (Fig. 8.1c) is a transcatheter valve system designed to be released retrogradely through a guide 0035″ available in three sizes 23, 25, and 27. This system consists of two main components: a bioprosthetic aortic valve premounted on a delivery system consisting of a catheter for the introduction and the valve itself. Such valve is premounted on the delivery system during the production phase. The valve Lotus™ in size from 23 mm is compatible with the introducer 18 Fr, while the same valve in sizes from 25 to 27 mm are compatible with the introducer 20 Fr. This valve consists of three flaps of bovine pericardium, supported by a structure realized by a single wire braided nitinol, which ends exactly in the central part with a tube crimped in tantalum, which assures a radiopaque marker on implantation. The three flaps are cut by patches of bovine pericardium fixed with glutaraldehyde and subsequently sutured together. The woven structure is drawn so as to shorten longitudinally and to expand radially at the time of deployment, and therefore, it is locked in this position by means of a safety mechanism. This mechanism allows the physician to lock the valve in position, unlock to recapture, release it again and reposition, or even withdraw it completely. The maximum height for all sizes of valves, at the time of complete release, is 19 mm. An outer coating of polyurethane-polycarbonate, called Adaptive Seal™, is designed to minimize paravalvular aortic regurgitation. The delivery system of the valve consists of three main components: an inner catheter (described as a multi-lumen catheter) which is connected to the valve, an external catheter (described as an external introducer), and a handpiece which is used to control the positioning and release of the valve itself. The major advantages of this system are the possibility of a complete resheathing until the valve is released and the presence of the outer adaptive membrane facilitating the contact with the native valve, compensating the anatomical variations, and minimizing the paravalvular leak. The still bulky delivery system is the major disadvantage of Lotus, but in the fourth quarter of 2015, the new trackable and lower profile delivery system would be available. The procedure of Lotus valve is shown in Fig. 8.2. Commercial use of BSI Lotus started in 2014, and results available until now are really encouraging especially in terms of reduction of paravalvular leaks compared to competitors [4, 5]. In REPRISE II CE-Mark Study designed to test safety and performance in extreme/high-risk patients, the device success (correct positioning of one valve in proper position without periprocedural mortality) was 99.2%. Six months of mortality rate was 8.4% and pacemaker rate 29.4%. In this study, only 1% of patients had more than mild paravalvular regurgitation, and no severe aortic regurgitation was reported. At EuroPCR 2015, Van Mieghem presented the first 250 interim analyses of RESPOND post-market safety and performance study. This single-arm registry is designed to enroll 1,000 patients in the real-world population with 23, 25, and 27 mm valve sizes. All-cause mortality was 2.0%, stroke was 3.3%, and no moderate or severe aortic regurgitation was reported. Even in this trial, the PM rate rises to 33.7% but with large difference among centers, and only one-third of patients are still PM dependent at 30 days [6].
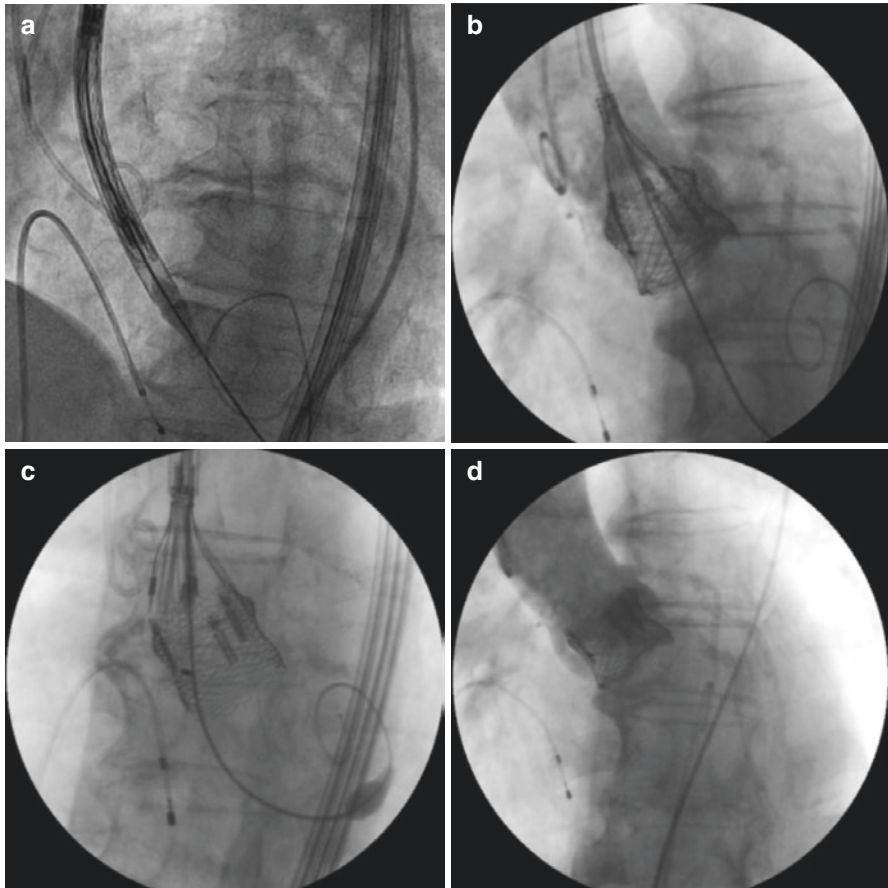
Fig. 8.2 (**a**) Delivery system containing the unexpanded Lotus prosthesis through the native valve. (**b**) Image showing the deployment of the valve. (**c**) Final detachment of Lotus valve. (**d**) Absence of aortic insufficiency on aortography after transcatheter implantation Lotus valve

8.4   Saint Jude Portico

The Portico valve (Fig. 8.1f) consists of a self-expandable nitinol frame with three bovine pericardial leaflets and a porcine pericardial sealing cuff. It is available in four sizes 23, 25, 27, and 29 accommodating annulus diameters between 19 and 27 mm. It can be fully recaptured, retrieved, and repositioned until 80–90 % of deployment. At this point, the annular section of the stent has full contact, allowing for assessment of placement and hemodynamic function prior to final release. In addition, the leaflets are designed to function at an intra-annular aortic position, which helps to maintain hemodynamic stability during deployment. A porcine pericardial sealing cuff is sewn around the stent frame to provide sealing and mitigate
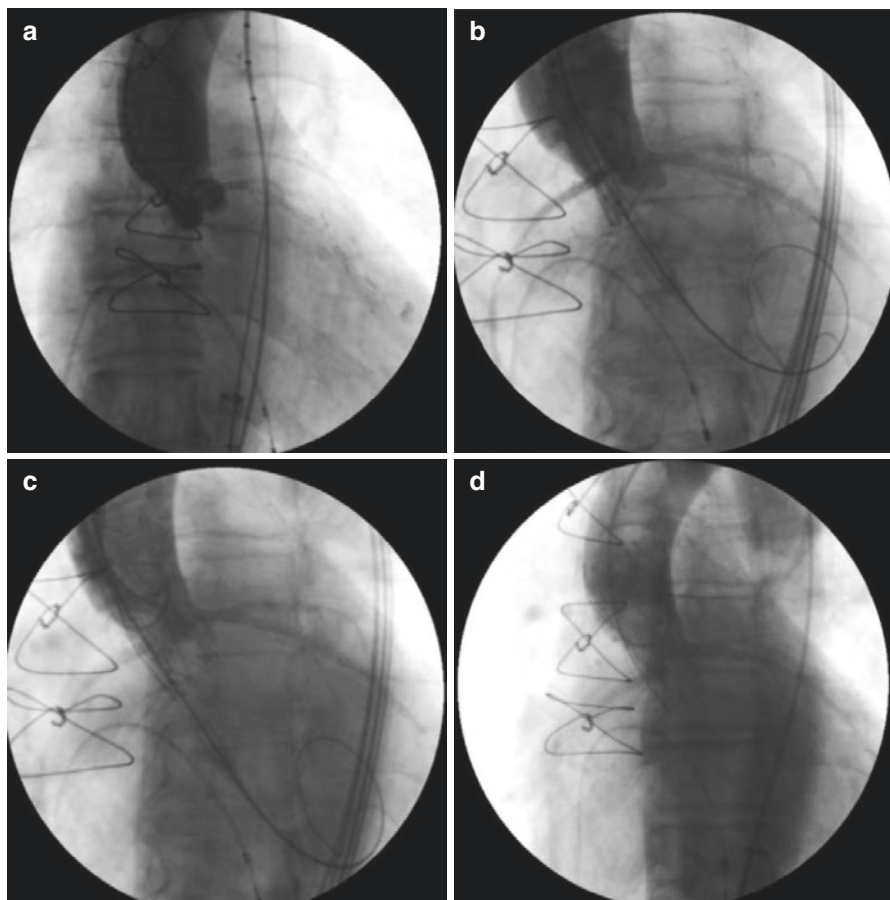
Fig. 8.3 (**a**) Baseline aortic angiography; (**b**) initial stage of prosthesis deployment; (**c**) final stage of prosthesis deployment; (**d**) Portico prosthesis fully deployed

paravalvular leaks. The nitinol frame has relatively large cells and a non-flared inflow section compared to CoreValve. Three retention tabs on the outflow section facilitate attachment to the delivery system. The valve can be prepared and loaded on the delivery system at room temperature without the use of cold saline. The Portico delivery system facilitates implantation of the Portico valve using transfemoral, transaxillary, or transaortic access methods. The over-the-wire, 0.035″ (0.89 mm) compatible system is designed to be flexible and facilitates gradual, controlled valve deployment (Fig. 8.3). If needed, the valve may be resheathed and repositioned up to two times, after which it should be retrieved and replaced by a new valve. A handle located on the proximal end of the delivery system includes the following features:

1. Two sliding mechanism buttons: Facilitate rapid travel of the protective sheath. The sliding mechanism is used to open the delivery system for valve loading and may be used to resheath the inner sheath of the delivery system prior to withdrawal from the descending aorta.
2. A deployment/resheathing wheel: Used to adjust the position of the protective sheath during valve loading and deployment.
3. Two locking buttons: Control movement of the sliding mechanism.
4. A release lever: Used to prevent unintended complete valve deployment before valve position is optimized.

The encouraging acute and 1-year results after implantation of Portico valve were presented by G. Manoharan at PCR and TCT 2014. 103 high-risk patients were treated: 30-day and 1-year mortality was 2.9 and 8.7 %, stroke rate 2.9 and 3.9 %, low PM implantation rate 9.7 and 10.7 %, and finally 11.7 % of moderate or severe aortic regurgitation [7]. A European post-market registry (PORTICO I) and a prospective randomized study for FDA approval in the United States are ongoing.

8.5   Direct Flow

The Direct Flow Medical Transcatheter Aortic Valve System (Fig. 8.1d) is comprised of three key components, the bovine pericardial bioprosthesis (implant), the sheathed delivery system (catheter), and the exchange system. Available since 2013, the Direct Flow Medical Transcatheter Aortic Valve is a nonmetallic bovine pericardial tissue leaflet heart valve. The bioprosthesis is provided in 23, 25, 27, and 29 mm sizes. The bioprosthesis is designed to be fully repositionable and retrievable prior to final deployment through the 18 F introducer, but it can't be resheathed. The bioprosthesis is designed to encircle and capture the native valve annulus, thereby ensuring positive anchoring of the bioprosthesis and minimizing potential paravalvular leaks, dislodgement, or migration. The bioprosthesis can be placed with minimal or no contrast. The bioprosthesis is available in sizes 23, 25, 27, and 29 mm configurations. The delivery system is an over-the-wire multiaxial catheter that is compatible with a standard 0.035″ guidewire. The system is designed to deliver the Direct Flow Medical bioprosthesis over the guidewire. The exchange system is a fluid pathway device and is used to exchange the polymer into the bioprosthesis after positioning. The exchange system is a three-part system. The first part is the Direct Flow Medical Radiopaque Exchange Solution (the "RES") that is used to fill the inflation channels of the bioprosthesis to provide visualization of the bioprosthesis during positioning in the native aortic annulus. The second is an exchange syringe used to replace the RES with the polymer using pressure in a closed loop system during the media exchange procedure. The third part is the proprietary Direct Flow Medical Polymer. The polymer is an epoxy-based material that is
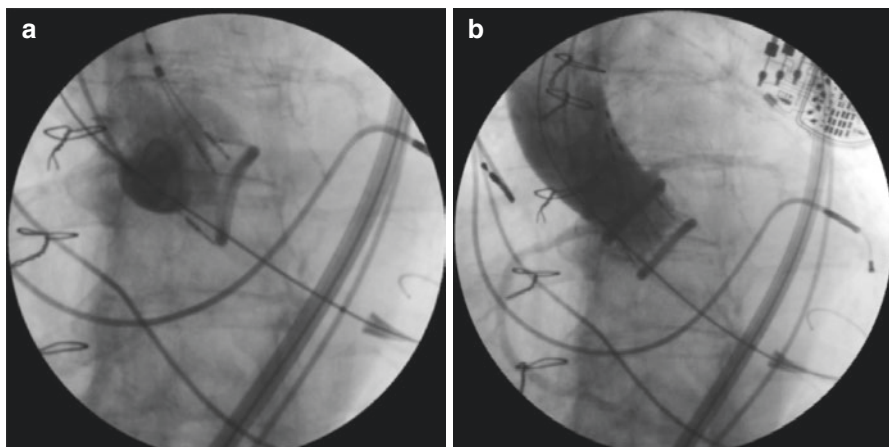
Fig. 8.4 (**a**) Direct flow implantation. Basal ring inflated; (**b**) absence of aortic insufficiency after transcatheter implantation of direct flow

injected into the inflation channels of the bioprosthesis in vivo. Once the polymer is inserted into the bioprosthesis, it will cure to create the structural frame of the bioprosthesis. Direct Flow implantation is shown in Fig. 8.4. Schofer published in 2014 the non-randomized multicenter DISCOVER CE trial [8]. There was 99 % freedom from all-cause mortality at 30 days (primary endpoint). VARC criteria defined 30-day combined freedom from patient safety event rate was 91 % and overall device success was 93 %. The post-implantation echocardiographic results demonstrated mild or no aortic regurgitation in 99 % (73 of 74) with a mean gradient of 12.6 ± 7.1 mmHg ($n = 72$) and effective orifice area of 1.50 ± 0.56 cm^2, and New York Heart Association functional class was I or II in 92 % of cases. The same author presented at EuroPCR 2014 the 1-year results of this trial that confirmed the safety and efficacy of this valve. Survival rate at 1 year was 90 % with no more than mild aortic regurgitation and 17 % PM rate. The Direct Flow prosthesis is no longer available.

8.6   Symetis Acurate Neo

The system consists of two components: the bioprosthetic aortic valve Acurate neo™ (Fig. 8.1e) and a disposable delivery system, the Acurate TFTM system. Acurate neo™ aortic bioprosthesis is composed of the following three elements: (1) a porcine pericardium valve, (2) a self-expanding nitinol stent at which the prosthetic valve is sutured, and (3) a double skirt in porcine pericardium sutured internally and externally to the surface of the stent. The femoral Acurate neo™ is available in three different sizes: 23 mm, 25 mm, and 27 mm from the first quarter of 2015. The delivery system has a usable length of 105 cm and is compatible with the introducer expandable Terumo Solopath 15 F or the introducer of the cook
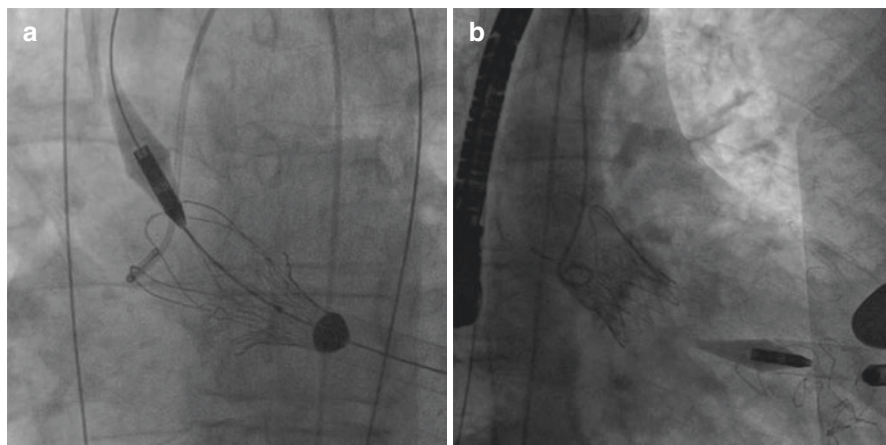
Fig. 8.5 Symetis Acurate procedure. (**a**) Deployment with its upper crown engaging the native leaflets. (**b**) Angiography after deployment showing the minimal paravalvular regurgitation prior to post-dilation

extra-large Check-Flo and 18 F with a guidewire of 0.0035″. The delivery system can be used with all three measures of the Acurate neo™. This valve is fixed first from aortic side and then delivered at the annular position (Fig. 8.5). It is a unique top to down deployment that allows an axial elf alignment even in angulated aortas. The valve works in a supra-annular position. The transapical CE mark trial was conducted between 2009 and 2011 in 90 patients with 80 % 1-year survival (107), and recently, transfemoral valve received the CE mark after the Acurate TF CE mark trial that achieved 3.4 % 30-day morality rate, 2.2 % stroke, 9.0 % PM rate, and only 4.9 % ≥ grade 2 paravalvular leak [9, 10].

References

1. Meredith IT, et al. Early results from the CoreValve Evolut R CE Study (2101–295). Presented at the annual meeting of the American College of Cardiology. March 14, 2015.
2. Binder RK, Rodés-Cabau J, Wood DA, Mok M, Leipsic J, De Larochellière R, Toggweiler S, Dumont E, Freeman M, Willson AB, Webb JG. A new balloon-expandable transcatheter heart valve. J Am Coll Cardiol Intv. 2013;6(3):293–300.
3. Kodali S on behalf of PARTNER investigators. American College of Cardiology (ACC) 2015 March 15, 2015; San Diego.
4. Meredith AM, et al. Reprise I. Euro Interv. 2014;9(11):1264–70.
5. Meredith et al. REPRISE II Trial JACC 2014.
6. Van Mieghem NM, on behalf of the RESPOND Investigators. First report from the RESPOND study: post-market evaluation of a fully repositionable and retrievable aortic valve in 250 patients treated in routine clinical practice. EuroPCR 2015.
7. Ganesh Manoharan On behalf of the Portico™ Valve CE Mark Investigators. Multicentre clinical study evaluating a novel resheathable self-expanding transcatheter aortic valve system preliminary results: acute and 1-year outcomes EuroPCR 2014 oral presentation.

8. Schofer J, Colombo A, Klugmann S, et al. Prospective multicenter evaluation of the direct flow medical transcatheter aortic valve. J Am Coll Cardiol. 2014;63(8):763–8.
9. Kempfert J, Holzhey D, Hofmann S, Girdauskas E, Treede H, Schröfel H, Thielmann M, Walther T. First registry results from the newly approved ACURATE TA™ TAVI system. Eur J Cardiothorac Surg. 2015;48(1):137–41.
10. Möllmann H, Diemert P, Grube E, Baldus S, Kempfert J, Abizaid A. Symetis ACURATE TF™ aortic bioprosthesis. Euro Interv. 2013;9:S107–10.

Part II

Mitral Valve Intervention

Severe Mitral Regurgitation Treatment: Percutaneous Options, Patient Selection, and Preoperative Evaluation

Michele Pighi and Anita W. Asgar

9.1 Introduction

Mitral regurgitation (MR) is one of the most common forms of valvular heart disease with a prevalence of up to 10 % in the aging population [1]. There are two forms of MR: primary in which the regurgitation occurs as a result of a structural abnormality of the MV apparatus and secondary, which occurs in the absence of intrinsic valve disease. Indications for intervention for both primary and secondary MR have been recently reviewed and published by both the ESC and ACC/AHA [2, 3]. According to these guidelines, MV surgery is the treatment of choice for patients with severe symptomatic primary MR (MR); however, despite this, a significant number of patients do not undergo MV (MV) surgery because of high surgical risk [3]. This is particularly prevalent in those with secondary MR and results in a significant impact on mortality [4].

There is an unmet need for lower-risk therapeutic options for those patients with primary MR at high surgical risk and those with secondary MR. As a result, this has become the focus of intense research over the past decade with two currently approved transcatheter mitral repair devices in Europe: the MitraClip and Carillon device.

We will describe these transcatheter options for the treatment of MR with emphasis on patient selection and the preoperative evaluation.

M. Pighi, MD (✉) • A.W. Asgar, MD
Montreal Heart Institute, 5000 Rue Bélanger, Montréal, QC H1T 1C8, Canada
e-mail: michele.pighi@hotmail.it
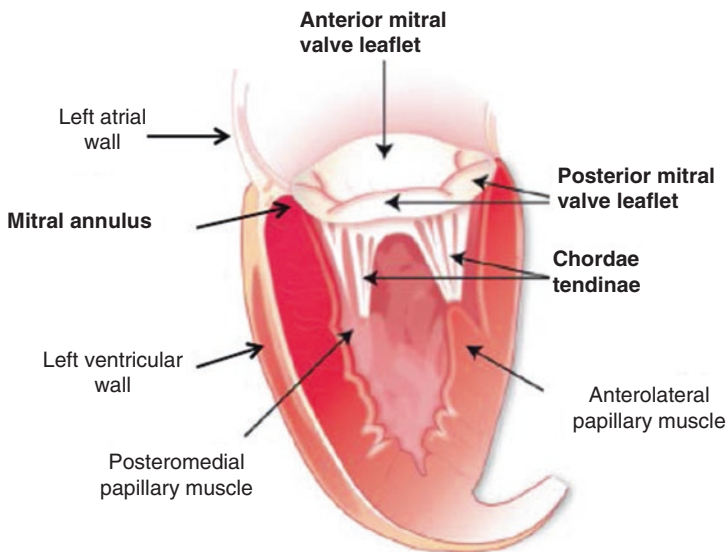
Fig. 9.1 Mitral apparatus. In bold the anatomical targets of the current commercially available percutaneous devices (Modified with permission from Asgar et al. [5])

9.2   Anatomy and Percutaneous Approaches for the Treatment of MR

9.2.1   Anatomical Targets

The normal function of the MV depends on six components: the mitral annulus [1], valve leaflets [2], chordae tendineae [3], papillary muscles [4], left ventricular wall [5], and the left atrial wall [6] (Fig. 9.1).

Each of these components represents a potential target for the treatment of MR. The following will focus on the description of the three anatomical structures (annulus, leaflets, and chordae tendineae) and the devices, which represent the current commercially available percutaneous options.

9.2.1.1 Mitral Annulus

The mitral annulus is a fibrous ring that connects with the leaflets. It is not a continuous ring around the mitral orifice but rather more D shaped [6]. The straight border of the annulus and anterior leaflet is posterior to the aortic valve which is located between the ventricular septum and the MV [6]. Annular dilation tends to occur along the septo-lateral axis resulting in poor leaflet apposition and MR.

Direct Approach (The Cardioband System)

Percutaneous annuloplasty approaches target the mitral annulus either directly at the level of the annulus or indirectly via the coronary sinus. Access to the annulus can be obtained either through transseptal puncture or retrogradely via the aortic

valve and the left ventricle (LV). These devices are implanted into the annulus to directly reduce its circumference.

The Cardioband system (Valtech, Israel) combines an annuloplasty implant with a transfemoral venous delivery system, by utilizing transseptal percutaneous placement of a series of small corkscrew anchors on the atrial side of the left atrium under transesophageal echocardiographic guidance. The anchors are connected by a Dacron sleeve that can be subsequently tensioned reducing the mitral annular circumference. Early results in humans, in a European CE Mark trial, showed a significant reduction of MR and an improvement in terms of functional class at the 6-month follow-up, leading to recent CE Mark approval.

The key aspect of this technology is careful preprocedural planning requiring computed tomography (CT) to assess the size of the annulus, the appropriate fluoroscopic projections, and the location of the transseptal puncture.

Indirect Approach (The Carillon System)

The anatomic relationship of the coronary sinus (CS) with the mitral annulus has stimulated much interest in using the CS to reduce mitral annular dimensions. The CS is located in the posterior portion of the coronary sulcus on the diaphragmatic or posterior surface of the heart and in many cases lies in close proximity to the mitral annulus.

The Carillon device (Cardiac Dimensions, Kirkland, Washington DC, USA) is a self-expandable nitinol device with semihelical distal and proximal anchors connected by a nitinol bridge that is placed in the coronary sinus via a jugular venous approach. Tension generated by this system results in cinching of posterior mitral annulus pushing it anteriorly.

The Carillon Mitral Annuloplasty Device European Union Study (AMADEUS) was the first investigation of a percutaneous coronary sinus-based intervention to reduce FMR [7]. This study enrolled 48 symptomatic patients with dilated cardiomyopathy, at least moderate FMR and a LVEF <40%. Of the 48 patients enrolled in the trial, 30 received the Carillon device. Eighteen patients did not receive a device because of access issues, insufficient acute MR reduction, or coronary artery compromise. The major adverse event rate was 13% at 30 days. At 6 months, the degree of MR reduction among five different quantitative echocardiographic measures ranged from 22 to 32%. Despite improvement of quality of life and functional indices, there was no significant change in left ventricular remodeling at 6 months. The device has been subsequently improved to increase resistance and reduce the risk of fracture. The device efficacy was tested in the Transcatheter Implantation of Carillon Mitral Annuloplasty Device (TITAN) trial [8], which included 53 patients, 36 of whom received the device. The TITAN trial revealed a mortality rate of 1.9% at 30 days after the procedure without other major complications. Successful device therapy showed significant reduction in MR grade, favorable LV remodeling, and improved quality of life when compared with the control group of subjects who did not receive implants [8].

9.2.1.2 MV Leaflets

The MV has been described as a continuous veil inserted around the circumference of the mitral orifice [9]. The free edges of the leaflets have several indentations, two
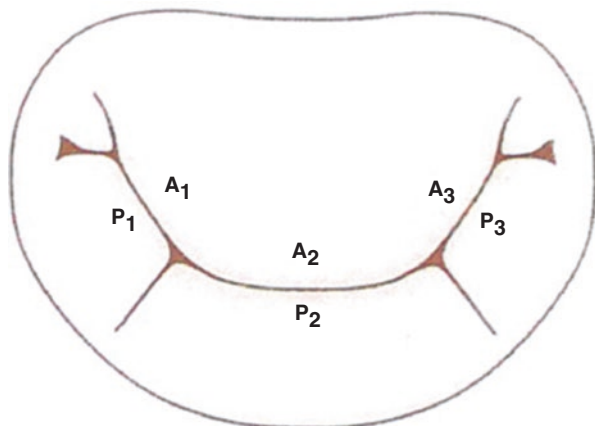
Fig. 9.2 Carpentier's classification of MV leaflet structure. The MV is viewed from the left atrium. *A* anterior, *P* posterior (Adapted with permission from Shah [11])

of which, the anterolateral and posteromedial commissures, divide the leaflets into anterior and posterior. The posterior leaflet is narrow and extends two-thirds around the left atrioventricular junction within the inlet portion of the ventricle. In adults, the posterior leaflet has three scallops (segments) along the elongated free edge. Carpentier's nomenclature [10] (Fig. 9.2) describes the most lateral segment as P1, which lies adjacent to the anterolateral commissure, P2 is central and can significantly vary in size, and the most medial is the P3 segment, which lies adjacent to the posteromedial commissure. The semicircular anterior leaflet of the MV is much broader than the posterior leaflet and comprises one-third of the annular circumference. The distinguishing feature of this leaflet is the fibrous continuity with the left and noncoronary cusps of the aortic valve and with the inter-leaflet triangle between the aortic cusps that abuts onto the membranous septum. The anterior leaflet is also divided into three regions: A1, A2, and A3 corresponding to the adjacent regions of the posterior leaflet.

Percutaneous Mitral Leaflet Repair (The MitraClip System)

The edge-to-edge repair has been used as a surgical technique for the treatment of MR since the early 1990s pioneered by Alfieri [12]. This technique involves suturing a portion of the anterior leaflet to the corresponding portion of the posterior leaflet, creating a point of permanent approximation of the two leaflets and resulting in a double orifice. The percutaneous technique is performed using the MitraClip system (Abbott Vascular, Abbott Park, IL, USA), which consists of applying a clip at the site of MR, thereby reproducing the edge-to-edge surgical technique. The MitraClip is a transvenous procedure performed under general anesthesia with TEE guidance. Following transseptal puncture, the clip is advanced via the guiding catheter into the left atrium and steered toward the mitral leaflets. Using TEE guidance, the site of MR is identified, and the clip is placed at the area of the regurgitant jet.

Once appropriately positioned, the clip is closed and the effect on MR is assessed. The clip can be opened and repositioned as required to achieve optimal MR reduction. Closure of the clip results in leaflet coaptation and the formation of a bridge between the anterior and posterior leaflets.

9.2.1.3 Chordae Tendineae

The mitral leaflets have fan-shaped chords running from the papillary muscles and inserting into the leaflets, the chordae tendineae. Depending on where they attach, there are three types of chordae tendineae. Primary chords attach to the free edge of the rough zone of both leaflets. Secondary chords attach to the ventricular surface in the region of the rough zone (i.e., body of the leaflet). The tertiary chords are found in the posterior leaflet (the only one which has a basal zone). These chords attach directly to the ventricular wall. The posteromedial papillary muscle gives chords to the medial half of both leaflets (i.e., posteromedial commissure, P3, A3, and half of P2 and A2). Similarly, the anterolateral papillary muscle chords attach to the lateral half of the MV leaflets (i.e., anterolateral commissure, A1, P1, and half of P2 and A2). Among the secondary chords of the anterior leaflet, there are two that are the largest and thickest. Termed strut cords, these arise from the tip of each papillary muscle and are thought to be the strongest.

Chordal Implantation (The NeoChord System)

Synthetic chord technology, designed mainly for degenerative MR (with posterior leaflet prolapse), can be implanted via a transapical or transseptal approach, and they are anchored between the left ventricular myocardium and the leaflet. In appropriate patients, MR can be reduced or abolished by adjusting the length of the chord. At present, NeoChord DS1000 (NeoChord, Inc, Minnetonka, MN) is the only CE marked chordal implantation system. The device is a transapically inserted tool that can capture a flail leaflet segment, pierce it with a needle, and attach a standard polytetrafluoroethylene artificial chord which is then anchored to the apical entry site with a pledgeted suture. The available clinical evidence is comprised of the Transapical Artificial Chordae Tendineae (TACT) trial [13] by Seeburger et al. which enrolled 30 patients at seven centers in Europe. Among the initial population, acute procedural success (placement of ≥1 NeoChord and reduction of MR from 3+/4+ to ≤2+) was achieved in 26 (86.7%) patients. Four patients did not receive repair with the device at the discretion of the surgeon. Major adverse events included one death and one minor stroke. At 30 days, 17 patients had an MR grade 2+ or greater.

9.3   Pathophysiology of MR

Appropriate systolic coaptation of the anterior and posterior mitral leaflets depends on the normal anatomy and function of the various components of the mitral apparatus: annulus, leaflets, chordae tendineae, papillary muscles, and left ventricular wall. MR consists of the retrograde flowing of blood from the LV to the left atrium

during ventricular systole, due to inadequate coaptation of the leaflets and to the pressure gradient between the two cavities.

According to the "pathophysiological triad" described by Carpentier and colleagues, three main types of MR can be distinguished based on the movement of the leaflets:

- Type I: normal leaflet motion
- Type II: leaflet prolapse or excessive motion
- Type III: restricted leaflet motion

Type I is often the result of mitral annulus dilation, secondary to left ventricular dilation (thus comprising patients with dilated cardiomyopathy or ischemic heart disease); this group also includes patients with leaflet perforation secondary to endocarditis.

Type II, instead, occurs following the stretching or rupture of the chordae tendineae, but it can also be observed in patients with coronaropathy, as they may suffer rupture or stretching of the papillary muscles.

Finally, type III is further divided into IIIa and IIIb depending on whether the restriction occurs during ventricular diastole or systole. It is associated with rheumatic disease, ischemic heart disease, and dilated cardiomyopathy.

A pathophysiological classification of MR is distinguished between two main forms, based on their etiology: primary or degenerative MR and secondary or functional MR.

9.3.1 Primary (Degenerative) MR

Organic or degenerative disease is defined as a spectrum of conditions in which infiltrative or dysplastic tissue changes cause elongation or rupture of the MV chordae, resulting in leaflet prolapse and usually associated with annular dilation [14]. At one end of the spectrum of organic mitral disease is fibroelastic deficiency, characterized by insufficient tissue in a normal-sized valve leaflets which are thinned and almost transparent and chordae which are flimsy and thin. MR is most frequently caused by rupture of a single chord associated with a single prolapsing segment, usually P2, resulting in Carpentier's type II leaflet dysfunction. The prolapsing segment may become distended and thickened by a localized myxomatous process in the chronic condition.

At the opposite end of the spectrum of degenerative MR is Barlow's disease, characterized by marked excess tissue involving multiple leaflet segments in an otherwise large valve. Leaflet tissue is thickened and redundant, with thick, elongated, mesh-like chordae which may or may not be ruptured [14].

MR severity depends on the number of prolapsing leaflet segments (Carpentier's type II). Finally, the pathophysiology of MR differs depending on whether valve damage is acute or the result of a chronic process. The causes that generally elicit primary acute MR are spontaneous rupture of the chordae tendineae, acute

endocarditis, or chest trauma [15]. In the acute stage, which usually occurs with a spontaneous chordae tendineae or papillary muscle rupture secondary to myocardial infarction, a sudden volume overload occurs on an unprepared LV and left atrium. The volume overload on the LV increases left ventricular stroke work. Increased left ventricular filling pressures, combined with the transfer of blood from the LV to the left atrium during systole, result in elevated left atrial pressures. This increased pressure is transmitted to the lungs resulting in acute pulmonary edema and dyspnea. In the case of chronic MR, there is plenty of time for the left atrium and LV to make compensatory changes allowing for increased atrial and pulmonary vein compliance.

Therefore, patients do not usually report the symptoms of pulmonary edema for many years. The chronic compensated phase results in eccentric left ventricular hypertrophy. The combination of increased preload and hypertrophy produces increased end-diastolic volumes, which, over time, result in left ventricular muscle dysfunction. This muscle dysfunction impairs the emptying of the ventricle during systole. The regurgitant volume and left atrial pressures increase, leading to pulmonary congestion, ultimately leading to pulmonary edema and, if left untreated, cardiogenic shock.

9.3.2   Secondary (Functional) MR

Traditionally functional MR has been described as a structurally normal MV with impaired function due to ventricular dilation and dysfunction. However, new insights in myocardial adaptation have also demonstrated abnormalities in the mitral leaflets. Indeed FMR is not simply a disease of ventricular dysfunction and might be better understood in terms of ventricular, subvalvular, and valvular interaction and adaptation [16, 17]. LV dilation due to ischemic or nonischemic cardiomyopathy secondarily impairs leaflet coaptation of a structurally normal MV, resulting in secondary MR. Specifically, LV dysfunction and remodeling lead to apical and lateral papillary muscle displacement, resulting in leaflet tethering, dilation and flattening of the mitral annulus, and reduced valve closing forces. Because these changes are dependent on loading conditions and the phase of the cardiac cycle, secondary MR is dynamic in nature [18]. The normal saddle shape of the annulus is important for maintaining normal leaflet stress. Loss of this shape and annular flattening with LV remodeling result in increased leaflet stress with secondary MR. In addition, LV systolic dysfunction reduces the strength of MV closing, which opposes the leaflet tethering forces created by papillary muscle displacement. These pathological changes culminate in failure of leaflet coaptation and decreased valvular closing forces due to LV dysfunction, resulting in MR [19]. MR can be further classified as either ischemic or nonischemic. In ischemic MR (the more frequent etiology), LV remodeling after myocardial infarction (MI) results in papillary muscle displacement, causing systolic tenting of the MV. Global left ventricular ejection fraction (LVEF) does not have to be reduced; regional wall motion abnormalities with remodeling may result in sufficient MV tethering to cause severe MR, despite

preserved LVEF [20]. Symmetric or asymmetric leaflet tethering may occur. Symmetric tethering is associated with substantial systolic dysfunction, global remodeling, and increased LV sphericity with a central regurgitant jet. Asymmetric tethering most frequently results from localized remodeling affecting the posterior papillary muscle, with posterior tenting of both leaflets (most pronounced at the medial or P3 portion of the posterior leaflet) causing a posteriorly directed asymmetric regurgitant jet (Carpentier's type IIIB). Mitral annular dilation typically occurs late in the pathophysiology of secondary MR and is often asymmetric, with greater involvement of the posterior annulus. Papillary muscle infarction is rarely the cause of secondary MR [21]. Nonischemic MR, most commonly due to long-standing hypertension or idiopathic dilated cardiomyopathy, is characterized by global LV dilation with increased sphericity and (typically) a centrally located regurgitant jet. Symmetric mitral annular dilation is greatest in the septal-lateral direction and correlates with the severity of LV dysfunction [22].

9.4 Patient Selection

9.4.1 Primary MR

In chronic primary MR, pathology of at least one of the components of the MV (leaflets, chordae tendineae, papillary muscles, annulus) causes valve incompetence with systolic regurgitation of blood from the LV to the left atrium. The anatomic substrate for degenerative MR spans the spectrum from diffuse myxomatous changes (Barlow's disease) to localized abnormalities associated with fibroelastic deficiency. The myxomatous degeneration of the MV is characterized by thickened (>5 mm), redundant leaflets and chordae tendineae, with bulging of the valve leaflets into the left atrium during systole.

According to the ACC/AHA valvular heart disease guidelines [3], primary MR is classified into one of the four categories shown in Table 9.1.

In regard to interventions for primary MR, the ACC/AHA guidelines recommend MV surgery for symptomatic patients with chronic severe primary MR (stage D) and LVEF >30 % and for asymptomatic patients with chronic severe primary MR and LV dysfunction (LVEF 30–60 % and/or LVESD $\geq$40 mm, stage C2) (class of recommendation, I; level of evidence, B).

Conversely, the guidelines suggest transcatheter MV repair may be considered for severely symptomatic patients (NYHA class III–IV) with chronic severe primary MR (stage D) who have favorable anatomy for the repair procedure and a reasonable life expectancy but who have a prohibitive surgical risk because of severe comorbidities and remain severely symptomatic despite guideline-directed medical therapy (GDMT) for HF (class of recommendation, IIb; level of evidence, B).

Table 9.1 Stages of primary MR

Grade	Definition	Valve anatomy	Valve hemodynamics	Hemodynamic consequences	Symptoms
A	At risk of MR	Mild MV prolapse with normal coaptation Mild valve thickening and leaflet restriction	No MR jet or small central jet area <20% LA on Doppler Small vena contracta <0.3 cm	None	None
B	Progressive MR	Severe mitral prolapse with normal coaptation Rheumatic valve changes with leaflet restriction and loss of central coaptation Prior IE	Central jet MR 20–40% LA or late systolic eccentric jet MR Vena contracta <0.7 cm Regurgitant volume <60 mL Regurgitant fraction <50% ERO <0.40 cm² Angiographic grade 1–2+	Mild LA enlargement No LV enlargement Normal pulmonary pressure	None
C	Asymptomatic severe MR	Severe MV prolapse with loss of coaptation or flail leaflet Rheumatic valve changes with leaflet restriction and loss of central coaptation Prior IE Thickening of leaflets with radiation heart disease	Central jet MR >40% LA holosystolic eccentric jet MR Vena contracta ≥0.7 cm Regurgitant volume ≥60 mL Regurgitant fraction ≥50% ERO ≥0.40 cm² Angiographic grade 3–4+	Moderate or severe LA enlargement LV enlargement Pulmonary hypertension may be present at rest or with exercise *C1*: LVEF >60% and LVESD <40 mm *C2*: LVEF ≤60% and LVESD ≥40 mm	None

Table 9.1 (continued)

Grade	Definition	Valve anatomy	Valve hemodynamics	Hemodynamic consequences	Symptoms
D	Symptomatic severe MR	Severe MV prolapse with loss of coaptation or flail leaflet Rheumatic valve changes with leaflet restriction and loss of central coaptation Prior IE Thickening of leaflets with radiation heart disease	Central jet MR >40 % LA holosystolic eccentric jet MR Vena contracta ≥0.7 cm Regurgitant volume ≥60 mL Regurgitant fraction ≥50 % ERO ≥0.40 cm^2 Angiographic grade 3–4+	Moderate or severe LA enlargement LV enlargement Pulmonary hypertension present	Decreased exercise tolerance Exertional dyspnea

Adapted with permission from Nishimura et al. [3]
ERO indicates effective regurgitant orifice, *IE* infective endocarditis, *LA* left atrium/atrial, *LV* left ventricular, *LVEF* left ventricular ejection fraction, *LVESD* left ventricular end-systolic dimension, and *MR* MR

In a similar way, the European guidelines suggest that percutaneous edge-to-edge procedure may be considered in patients with symptomatic severe primary MR, who fulfill the echo criteria for eligibility, are judged inoperable or at high surgical risk by a "Heart Team," and have a life expectancy greater than 1 year (class of recommendation, IIb; level of evidence, C).

9.4.1.1 Transthoracic/Transesophageal Echocardiographic Evaluation

Transthoracic echocardiography (TTE) is one of the most important diagnostic tests in clinical decision-making process for chronic primary MR. As per the ACC/AHA guidelines, TTE is indicated in patients with primary MR (stages B–D) to evaluate the MV apparatus and left ventricular function after a change in symptoms and (stages A–D) for baseline evaluation of left ventricular size and function, right ventricular function and left atrial size, pulmonary artery pressure, and mechanism and severity of primary MR (stages A–D). Thus, TTE represents the principal investigation and must include an assessment of severity, mechanism, and impact on right and left ventricular function [23].

Transesophageal echo (TEE) is not recommended for routine evaluation and follow-up of patients with chronic primary MR but is indicated when TTE images

are inadequate (e.g., MR due to infective endocarditis) and for a more precise quantitation of regurgitant severity. In particular, intraoperative TEE is indicated to establish the anatomic basis for chronic primary MR (stages C and D) and a standard imaging modality for guiding therapy of MR. Three-dimensional TEE may be helpful in further visualizing the abnormal MV anatomy. Moreover, intraoperative TEE is especially helpful in gauging the adequacy of repair.

Finally, the use of three-dimensional echocardiography is becoming more commonplace to evaluate valvular pathology, in particular, to characterize the nature of the flail or prolapsing segment, which represents essential information for predicting the likelihood of a successful repair (isolated P2 and A2 pathologies are more likely to be successfully repaired). Moreover, three-dimensional TEE has been extremely helpful in identifying involvement of multiple scallops, localizing MV clefs, and intraoperatively assessing the adequacy of MV repair.

9.4.1.2 Selection of the Appropriate Transcatheter Therapy

Transcatheter devices available for the treatment of primary MR are limited to the MitraClip system (Abbott Vascular, Menlo Park, CA, USA) and the NeoChord DS1000 (NeoChord, Inc, Minnetonka, MN).

MitraClip
According to the latest European Society of Cardiology (ESC) guidelines, percutaneous edge-to-edge procedure may be considered in patients with symptomatic severe primary MR, who fulfill the echocardiographic criteria for eligibility, are judged inoperable or at high surgical risk by a "Heart Team," and have a life expectancy greater than 1 year (class for recommendation, IIb; level of evidence, C).

In addition, the ACC/AHA guidelines state that transcatheter MV repair may be considered for severely symptomatic patients (NYHA class III–IV) with chronic severe primary MR (stage D) who have favorable anatomy for the repair procedure and a reasonable life expectancy but who have a prohibitive surgical risk because of severe comorbidities and remain severely symptomatic despite optimal GDMT for heart failure (class of recommendation, IIb; level of evidence, B).

As well as meeting the recommended guidelines for transcatheter therapy, it is necessary to further refine patient selection. Table 9.2 illustrates further clinical and anatomical inclusion and exclusion criteria for percutaneous valve repair using the MitraClip system according to the EVEREST II trial [24].

NeoChord
The only information about patient selection for the NeoChord DS1000 belong to the enrollment criteria used in the Transapical Artificial Chordae Tendineae (TACT) trial [13].

The main inclusion criteria were the presence of severe MR due to isolated Carpentier's type II prolapse of the posterior MV leaflet and no annulus dilation,

Table 9.2 Major inclusion and exclusion criteria for MitraClip system

Inclusion criteria
Age 18 years or older
Moderate-to-severe (3+) or severe (4+) chronic MV regurgitation with symptoms or without symptoms but left ventricular ejection fraction (LVEF) <60 % 01′ LV end-systolic diameter >45 mm
High-risk candidate for MV surgery including cardiopulmonary bypass
Primary regurgitant jet originating from malcoaptation of the A2 and P2 scallop of the MV. If a secondary jet exists, it must be considered clinically insignificant
Presence of sufficient leaflet tissue for a mechanical coaptation
Nonrheumatic/endocarditic valve morphology
Transseptal catheterization determined to be feasible by the treating physician
Exclusion criteria
Evidence of an acute myocardial infarction 12 weeks prior of the intended treatment
Need for any other cardiac surgery including surgery for coronary artery disease, atrial fibrillation, and pulmonic, aortic, or tricuspid valve disease
MV orifice area <4.0 cm^2
If leaflet flail is present:
Flail\width ≥15 mm
Flail gap ≥10 mm
If leaflet tethering is present:
Coaptation depth ≥II mm
Coaptation length <2 mm
Severe mitral l annular calcification
Any leaflet anatomy which may preclude clip implantation, proper clip positioning on the leaflets, or sufficient reduction in MR
Hemodynamic instability defined as systolic pressure <90 mmHg without afterload reduction or cardiogenic hock or the need for inotropic support or intra-aortic balloon pump
Need for emergency surgery for any reason
Systolic anterior motion of the MV leaflet
Hypertrophic cardiomyopathy
Echocardiographic evidence of intracardiac mass, thrombus, or vegetation
History of or active endocarditis
History of or active rheumatic heart disease
History of atrial-septal defect whether repaired or not
History of patent foramen ovale associated with clinical symptoms (e.g., cerebral ischemia) or previously repaired or when, in the judgment of the investigator, an atrial-septal aneurysm is present that may interfere with transseptal crossing
History of stroke or documented TIA within 6 month prior
Patients in whom transesophageal echocardiography is contraindicated

Table 9.3 Echocardiography methods to assess the degree of regurgitation

2D echo	Color	Pulsed wave Doppler	Continuous wave Doppler
MV morphology	Jet area	Regurgitant volume	Jet spectral analysis
Left atrial volume	Vena contracta	Regurgitant fraction	Systolic pulmonary artery pressure
LV dimension	Convergence area PISA-ERO area	ERO area A wave, E wave Pulmonary venous flow	

ERO indicates effective regurgitant orifice, *PISA* proximal isovelocity surface area

Table 9.4 Echocardiographic criteria for severe MR in primary and secondary disease of the MV

Parameter	Primary MR	Secondary MR
EROA	$\geq$0.4 cm^2	$\geq$0.2 cm^2
Regurgitant volume	$\geq$60 ml	$\geq$30 ml
Regurgitant fraction	$\geq$50%	$\geq$50%
Vena contracta	0.7 cm	–
Jet area	Central jet >40% LA or holosystolic eccentric jet	–

Modified with permission from Asgar et al. [5]
EROA indicates effective regurgitant orifice area, *LA* left atrium

with an indication for surgery. Conversely, key exclusion criteria included secondary MR, severe left ventricular dysfunction (left ventricular end-diastolic diameter >6.5 cm), anterior or bileaflet MV prolapse, permanent atrial fibrillation, and concomitant cardiac disease with an indication for surgical treatment.

9.4.2   Secondary MR

9.4.2.1 Transthoracic/Transesophageal Echocardiographic Evaluation

The echocardiographic pattern characterizing functional MR is the pathologic tethering of the MV leaflets in the absence of structural valvular abnormalities. An integrated approach (Table 9.3) to the quantitation of MR, incorporating semiquantitative and quantitative measures (such as assessment of the jet area, vena contracta diameter, effective regurgitant orifice area (EROA), regurgitant fraction and volume, and pulmonary venous flow patterns), is recommended by international guidelines [3] (Table 9.4).

Of note, functional MR is afterload dependent, and the determination of its severity must take into account left ventricular pressure. Therefore, it is important to stress that decision-making on the severity of MR not be made under general anesthesia which is associated with a predictable fall in systemic vascular resistance, leading to a dramatic reduction in the observed degree of regurgitation.

9.4.2.2 Selection of the Appropriate Transcatheter Therapy

To date, the most effective therapies for secondary MR are aimed at the underlying left ventricular dysfunction, including GDMT for heart failure [3] and cardiac resynchronization therapy (CRT) when appropriate [25]. The role of surgical and transcatheter MV repair or replacement as strategies to interrupt the progressive vicious cycle leading from left ventricular volume overload to increasing MR is less well established, although some patients may benefit symptomatically. Finally, mechanical left ventricular assist devices and heart transplantation should be taken into consideration in patients with severe heart failure and secondary MR refractory to standard therapies [5].

With respect to percutaneous options, the two currently available transcatheter devices for the treatment of secondary MR are the Carillon device (Cardiac Dimensions, Kirkland, Washington DC, USA) and the MitraClip system (Abbott Vascular, Menlo Park, CA, USA).

Carillon Device

Due to the limited availability and experience with the Carillon device, the only information about patient selection are the enrollment criteria of AMADEUS and TITAN trials. Inclusion criteria consist of dilated ischemic or nonischemic cardiomyopathy, at least moderate (2+) functional MR, left ventricular ejection fraction (<40 %; NYHA class II–IV; 6-min walk distance 150–450 m), and stable heart failure medication regimen (i.e., diuretic, beta-blocker, and angiotensin-converting enzyme inhibitor or angiotensin receptor blocker for 3 months). Key exclusion criteria were severe tricuspid regurgitation, renal insufficiency (serum creatinine 2.2 mg/dL), the presence of significant organic MV pathology, and pacing lead already in the coronary sinus (CS).

The main technical limitation of the Carillon device is the fact that CS does not have a fixed relationship with the mitral annulus, as has been confirmed in various anatomic and in vivo imaging studies [26, 27]. Moreover, a recent report by Sahni et al. [28], investigating the spatial relationship of the coronary sinus with the mitral annulus, in adult human cadaveric hearts, showed that the CS occupied the mitral annulus for an average distance of 3.2 ± 0.8 cm, after which it left the annulus toward the posterior left atrial surface in the majority of cases (90.8 %). However, in the 9.2 % of cases, the CS did not show any parallel and proximal relation with the

annulus, crossing it obliquely at one point, leading to an imprecise and indirect transmission of the tension created by the implanted annuloplasty device to the annulus, thus reducing the efficacy of MR reduction. These findings suggest that the success of percutaneous transvenous procedures is limited to cases where the CS courses oblique to the mitral annulus plane, where the coronary artery traverses deep to the CS, and when appropriate CS dimensions are present. Therefore, a careful preprocedural selection of candidates with a favorable anatomy and the design of devices with dimensions compatible to the coronary venous system are the keys to achieve procedural success.

MitraClip

The main criteria to assess technical feasibility of MitraClip are the following:

- Primary regurgitant jet originating from malcoaptation of the A2 and P2 scallop of the MV. If a secondary jet exists, it must be considered clinically insignificant.
- Presence of sufficient leaflet tissue for a mechanical coaptation.
- Nonrheumatic/endocarditic valve morphology.
- Transseptal catheterization determined to be feasible by the treating physician.

Conversely, the following criteria represent a contraindication at the use of MitraClip device:

- MV orifice area <4.0 cm^2
- Severe mitral annular calcification
- Any leaflet anatomy which may preclude clip implantation, proper clip positioning on the leaflets, or sufficient reduction in MR
- Patients in whom transesophageal echocardiography is contraindicated

The MitraClip has been commercially available in Europe since receiving CE Mark in 2008. As a result, there has been significant registry data published in mainly secondary MR which has demonstrated both safety and efficacy of the technique [29–31]. This evidence has resulted in specific recommendations for the management of secondary MR. In 2012 the ESC guidelines on valvular heart disease suggested consideration of MitraClip in symptomatic patients with severe secondary MR, despite GDMT and CRT, who are inoperable or at high risk [2] (class of recommendation, IIb; level of evidence, B). The 2013 ACCF/AHA HF guidelines also suggest consideration of MitraClip in symptomatic patients with severe secondary MR despite GDMT after "careful candidate selection" [25] (class of recommendation, IIb; level of evidence, B). Transcatheter MV repair for secondary MR did not receive an official recommendation in the 2014 ACCF/AHA valvular heart

disease guidelines, although it is recommended for severe primary MR in symptomatic patients at prohibitive risk for MV surgery [3] (class of recommendation, IIb; level of evidence, B).

Box. 9.1 Tips in the Box (How to Perform TEE Evaluation for Mitral Regurgitation)

TEE checklist for the evaluation of mitral regurgitation:

- Focus on mitral valve and leaflets and understanding mechanism of mitral regurgitation.
- Etiology: degenerative, functional, or mixed.
- Leaflets: flail, prolapse, restricted, cleft, etc.
- Left ventricular function: ejection fraction and left ventricular size.
- Left atrium size: mitral regurgitation acute vs. chronic.
- Subvalvular apparatus:
  – Chordal relationships: proximity and support
  – Papillary muscles
- Jet origin and location of the PISA.
- Atrial septum: atrial-septal defects, PFO, fossa size, aneurysm, etc.
- Other: thrombus in left atrial appendage, vegetation, calcium, etc. (Tables 9.5 and 9.6).

9.5 Future and Ongoing Challenges

Since the introduction and widespread diffusion of transcatheter aortic valve replacement, there has been an increasing interest to extend this approach to other valvular diseases. Transcatheter MV replacement (TMVR) may have potential to become an alternative to treat severe MR in high surgical risk patients [32]. To date, there are a number of off-label uses of percutaneous valves (Melody, Edwards Sapien, and Sapien XT) for degenerated surgical bioprostheses in the mitral position, so-called MV in valve [33]. Despite the success and relatively favorable outcomes of these experiences, the main problem remains in patients with diseased native MV. Indeed, one of the key obstacles in designing valves for TMVR is the difficulty in anchoring the bioprosthesis to the mitral annulus. Despite this, there are a growing number of TMVR options, in preclinical phase or early human experience, including different approaches such as transatrial, transapical, and transseptal. In the meantime, transcatheter mitral repair appears to be a safe alternative in high-risk patients with primary MR. Current clinical experience with secondary MR is also favorable; however, the results of randomized clinical trials will be important to understand the place of this therapy amid GDMT and CRT.

Table 9.5 Main transesophageal echocardiographic views for mitral regurgitation

TEE views	Features	Technical aspects
0° views		
Superior	*A1/P1* scallops Aortic valve LV outflow (LV foreshortened)	ME five-chamber view
Central	A2/P2 scallops LV cavity completely visualized Measurements: functional MR (coaptation length) degenerative MR (flail gap)	ME four-chamber view by advancing probe 1–3 cm
Inferior	A3/P3 scallops Coronary sinus Tricuspid valve	ME four-chamber view by further advancing the probe 1–3 cm
60–90° views		
Anterior	A1, A2, and A3 scallops	This view is obtained at the anterior side of the valve
Midline	P1, A2, and P3 scallops	This view is obtained at the midline of the valve
Posterior	P1, P2, and P3 scallops	This view is obtained at the posterior side of the valve
110–130° views		
Lateral	A1 and P1 scallops	This view is obtained at the lateral side of the valve
Central	A2 and P2 scallops	This view is of the central aspect of the valve
Medial	A3 and P3 scallops	This view is obtained at the medial side of the valve
Pulmonary veins' views		
Left upper vein (0–30°) Right upper vein (90–120°) Pulmonary vein flow	Presence of systolic flow reversal	Color flow and PW Doppler Color flow and PW Doppler PW Doppler
Transgastric short axis (0–20°)	Measure flail Jet origin MV orifice area	Color flow Doppler
3D "en face" view	To supplement and confirm the initial diagnosis	3D transgastric short axis

Table 9.6 TEE evaluation of anatomic measurements

Anatomic measurement	Characteristics	TEE assessment
Degenerative mitral regurgitation (DMR):		

Flail gap	The greatest distance between the ventricular side of the flail leaflet segment and the atrial side of the opposing leaflet edge	This distance is measured (in systole) perpendicular to the plane of the annulus in two views, and the largest measurement is used
		Assessment views:
		    Four-chamber long axis
		    LVOT

Flail width	The width of flail leaflet segment as measured along the line of coaptation in the transgastric short axis view	Measured in transgastric short axis view during systole
Functional mitral regurgitation (FMR):		
Vertical coaptation length	The vertical length of leaflets that is in contact, *or is available* for contact, during mid-systole in the atrial-to-ventricular direction	Simultaneous color and noncolor views are helpful to confirm the location of the regurgitant lesion and to measure the coaptation length
	Measure of the length of leaflet tissue available to be inserted into the arms of the MitraClip device	Assessment view: Four-chamber view

Central jet origin	Evaluation of the jet in A2/P2 region	Assessment views:
		    Two-chamber intercommissural
		    Transgastric short axis

Mitral valve area	Planimetry of the mitral orifice	Assessment view: Transgastric short axis
Calcification in the grasping area	Evidence of calcification in the grasping area (defined as the most distal 7 mm of available leaflet tissue) of the A2 and/or P2 scallops	Assessment view: Central 0°

References

1. Iung B, Vahanian A. Epidemiology of acquired valvular heart disease. Can J Cardiol. 2014;30(9):962–70.
2. Authors/Task Force Members, Vahanian A, Alfieri O, Andreotti F, Antunes MJ, Baron-Esquivias G, et al. Guidelines on the management of valvular heart disease (version 2012): the Joint Task Force on the Management of Valvular Heart Disease of the European Society of Cardiology (ESC) and the European Association for Cardio-Thoracic Surgery (EACTS). Eur Heart J. 2012;33(19):2451–96.
3. Nishimura RA, Otto CM, Bonow RO, Carabello BA, Erwin JP, Guyton RA, et al. 2014 AHA/ACC guideline for the management of patients with valvular heart disease: a report of the American College of Cardiology/American Heart Association Task Force on Practice Guidelines. J Am Coll Cardiol. 2014. pp. e57–185.

 4. Goel SS, Bajaj N, Aggarwal B, Gupta S, Poddar KL, Ige M, et al. Prevalence and outcomes of unoperated patients with severe symptomatic mitral regurgitation and heart failure: comprehensive analysis to determine the potential role of MitraClip for this unmet need. J Am Coll Cardiol. 2014;63(2):185–6.
 5. Asgar AW, Mack MJ, Stone GW. Secondary mitral regurgitation in heart failure: pathophysiology, prognosis, and therapeutic considerations. J Am Coll Cardiol. 2015;65(12):1231–48.
 6. Ho SY. Anatomy of the mitral valve. Heart. 2002.
 7. Schofer J, Siminiak T, Haude M, Herrman JP, Vainer J, Wu JC, et al. Percutaneous mitral annuloplasty for functional mitral regurgitation: results of the CARILLON mitral annuloplasty device European union study. Circulation. 2009;120(4):326–33.
 8. Siminiak T, Wu JC, Haude M, Hoppe UC, Sadowski J, Lipiecki J, et al. Treatment of functional mitral regurgitation by percutaneous annuloplasty: results of the TITAN Trial. Eur J Heart Fail. 2014;14(8):931–8.
 9. Harken DE, Ellis LB, Dexter L, Farrand RE, Dickson JF. The responsibility of the physician in the selection of patients with mitral stenosis for surgical treatment. Circulation. 1952;5(3):349–62.
10. Carpentier AF, Lessana A, Relland JYM, Belli E, Mihaileanu S, Berrebi AJ, et al. The "Physio-Ring": an advanced concept in mitral valve annuloplasty. ATS. 1995;60(5):1177–86.
11. Shah PM. Current concepts in mitral valve prolapse – diagnosis and management. J Cardiol. 2010;56(2):125–33.
12. Alfieri O, Maisano F, De Bonis M, Stefano PL, Torracca L, Oppizzi M, et al. The double-orifice technique in mitral valve repair: a simple solution for complex problems. J Thorac Cardiovasc Surg. 2001;122(4):674–81.
13. Seeburger J, Rinaldi M, Nielsen SL, Salizzoni S, Lange R, Schoenburg M, et al. Off-pump transapical implantation of artificial neo-chordae to correct mitral regurgitation: the TACT Trial (Transapical Artificial Chordae Tendineae) proof of concept. J Am Coll Cardiol. 2014;63(9):914–9.
14. Anyanwu AC, Adams DH. Etiologic classification of degenerative mitral valve disease: Barlow's disease and fibroelastic deficiency. Semin Thorac Cardiovasc Surg. 2007;19(2):90–6.
15. Fenster MS, Feldman MD. Mitral regurgitation: an overview. Curr Probl Cardiol. 1995;20(4):199–276.
16. Yiu SF, Enriquez-Sarano M, Tribouilloy C, Seward JB, Tajik AJ. Determinants of the degree of functional mitral regurgitation in patients with systolic left ventricular dysfunction: a quantitative clinical study. Circulation [Internet]. 2000;102(12):1400–6. Available from: http:// eutils.ncbi.nlm.nih.gov/entrez/eutils/elink.fcgi?dbfrom=pubmed&id=10993859&retmode=ref&cmd=prlinks.
17. Chaput M, Handschumacher MD, Tournoux F, Hua L, Guerrero JL, Vlahakes GJ, et al. Mitral leaflet adaptation to ventricular remodeling: occurrence and adequacy in patients with functional mitral regurgitation. Circulation. 2008;118(8):845–52.
18. Hung J. Mechanism of recurrent ischemic mitral regurgitation after annuloplasty: continued LV remodeling as a moving target. Circulation. 2004;110(11_Suppl_1):II–85–90.
19. Dal-Bianco JP, Levine RA. Anatomy of the mitral valve apparatus: role of 2D and 3D echocardiography. Echocardiogr Diagn Manag Mitral Valve Dis. 2013;31(2):151–64.
20. Kumanohoso T, Otsuji Y, Yoshifuku S, Matsukida K, Koriyama C, Kisanuki A, et al. Mechanism of higher incidence of ischemic mitral regurgitation in patients with inferior myocardial infarction: quantitative analysis of left ventricular and mitral valve geometry in 103 patients with prior myocardial infarction. J Thorac Cardiovasc Surg. 2003;125(1):135–43.
21. Agricola E. Echocardiographic classification of chronic ischemic mitral regurgitation caused by restricted motion according to tethering pattern. Eur J Echocardiogr. 2004;5(5):326–34.
22. Nagasaki M, Nishimura S, Ohtaki E, Kasegawa H, Matsumura T, Nagayama M, et al. The echocardiographic determinants of functional mitral regurgitation differ in ischemic and non-ischemic cardiomyopathy. Int J Cardiol. 2006;108(2):171–6.

23. Carabello BA, Williams H, Gash AK, Kent R, Belber D, Maurer A, et al. Hemodynamic predictors of outcome in patients undergoing valve replacement. Circulation. 1986;74(6):1309–16.
24. Mauri L, Garg P, Massaro JM, Foster E, Glower D, Mehoudar P, et al. The EVEREST II Trial: design and rationale for a randomized study of the evalve mitraclip system compared with mitral valve surgery for mitral regurgitation. Am Heart J. 2010;160(1):23–9.
25. Yancy CW, Jessup M, Bozkurt B, Butler J, Casey DE, Drazner MH, et al. 2013 ACCF/AHA guideline for the management of heart failure: a report of the American College of Cardiology Foundation/American Heart Association Task Force on Practice Guidelines. J Am Coll Cardiol. 2013. pp. e147–239.
26. Tops LF, Van de Veire NR, Schuijf JD, de Roos A, van der Wall EE, Schalij MJ, et al. Noninvasive evaluation of coronary sinus anatomy and its relation to the mitral valve annulus: implications for percutaneous mitral annuloplasty. Circulation. 2007;115(11):1426–32.
27. Maselli D, Guarracino F, Chiaramonti F, Mangia F, Borelli G, Minzioni G. Percutaneous mitral annuloplasty: an anatomic study of human coronary sinus and its relation with mitral valve annulus and coronary arteries. Circulation. 2006;114(5):377–80.
28. Sahni D, Randhawa A, Aggarwal A, Rohit MK. Spatial relationship of coronary sinus-great cardiac vein with adjoining anatomic structures: a key element in predicting the success of percutaneous transvenous mitral annuloplasty. J Heart Valve Dis. 2014;23(2):184–92.
29. Maisano F, Franzen O, Baldus S, Schäfer U, Hausleiter J, Butter C, et al. Percutaneous mitral valve interventions in the real world: early and 1-year results from the ACCESS-EU, a prospective, multicenter, nonrandomized post-approval study of the MitraClip therapy in Europe. J Am Coll Cardiol. 2013;62(12):1052–61.
30. Nickenig G, Estevez-Loureiro R, Franzen O, Tamburino C, Vanderheyden M, Lüscher TF, et al. Percutaneous mitral valve edge-to-edge repair: in-hospital results and 1-year follow-up of 628 patients of the 2011–2012 Pilot European Sentinel Registry. J Am Coll Cardiol. 2014;64(9):875–84.
31. Glower DD, Kar S, Trento A, Lim DS, Bajwa T, Quesada R, et al. Percutaneous mitral valve repair for mitral regurgitation in high-risk patients: results of the EVEREST II study. J Am Coll Cardiol. 2014;64(2):172–81.
32. De Backer O, Piazza N, Banai S, Lutter G, Maisano F, Herrmann HC, et al. Percutaneous transcatheter mitral valve replacement: an overview of devices in preclinical and early clinical evaluation. Circ: Cardiovasc Interv. 2014;7(3):400–9.
33. Cheung A, Webb JG, Barbanti M, Freeman M, Binder RK, Thompson C, et al. 5-year experience with transcatheter transapical mitral valve-in-valve implantation for bioprosthetic valve dysfunction. J Am Coll Cardiol. 2013;61(17):1759–66.

Techniques and Devices

10

Alessandro Candreva, Maurizio Taramasso,
and Francesco Maisano

10.1 Introduction

Due to an increased understanding of the functional anatomy of the mitral valve (MV) and the heterogeneous pathophysiology of mitral regurgitation (MR), over the past two decades, a huge variety of percutaneous treatment for MR have been successfully developed to treat high-risk patients who are usually not surgical candidate. In most cases, they represent the noninvasive conversion of a surgical procedure into a percutaneous one.

Differently from the aortic valve (AV), where a simpler geometry of the aortic root has allowed since the beginning of the development of successful transcatheter aortic valve replacement (TAVR) devices, in the field of transcatheter MV (TMV) interventions, the complex anatomical and functional rapports between the left ventricle (LV) and the MV led the engineering process mainly toward repairing techniques. Nevertheless, in the last years, many companies have focused their resources in developing percutaneous valve deployable in mitral position.

In the following, we will describe some of the available and forthcoming technologies in the field of TMV interventions, separating transcatheter MV repair (TMVRe) devices from transcatheter MV replacement (TMVR) devices.

10.2 Transcatheter MV Repair (TMVRe) Devices

The MV is a complex three-dimensional structure, comprehensive of a valvular and a subvalvular level fully "deployed" in the LV. A therapeutic approach to the mitral pathology cannot ignore this multilevel aspect. In effect, already in 1983, Carpentier described for surgical intervention on MV three possible levels of intervention [1]:

A. Candreva (✉) • M. Taramasso • F. Maisano
University Hospital of Zurich, Raemistrasse 100, 8091-CH Zurich, Switzerland
e-mail: alessandro.candreva@usz.ch

Table 10.1 Pathophysiological classification of transcatheter MV repair (TMVRe) devices

Transcatheter MV repair (TMVRe) techniques and devices	
Annuloplasty	
Indirect annuloplasty	Carillon (Cardiac Dimensions, Kirkland, WA, USA)
	MONARC (Edwards Lifesciences Corporation, Irvine, CA, USA)
	PS3 System (Ample Medical, Foster City, CA, USA)
	PTMA Device (Viacor, Wilmington, MA, USA)
	Valcare (Valcare Medical, Herzliya Pituach, Israel)
	Viacor (Viacor, Wilmington, MA, USA)
Direct annuloplasty	Accucinch (Guided Delivery Systems, Santa Clara, CA, USA)
	Cardioband (Valtech Cardio, Or Yehuda, Israel)
	Millipede system (Millipede LLC, Ann Arbor, MI, USA)
	Mitralign (Mitralign, Tewksbury, MA, USA)
	QuantomCor system (QuantomCor, San Clemente, CA, USA)
	ReCor system (ReCor Medical, Ronkonkoma, NY, USA)
Leaflet repair	MitraClip (Evalve, Menlo Park, CA, USA)
	MitraFlex (TransCardiac Therapeutics, Atlanta, GA, USA)
	Mobius (Edwards Lifesciences, Irvine, CA, USA)
	Percu-Pro (Cardiosolutions, Soughton, MA, USA)
	ThermoCool Smarttouch (Cordis, Bridgewater, NJ, USA)
Neochordae implantation	MitraFlex (TransCardiac Therapeutics, Atlanta, GA, USA)
	NeoChord (NeoChord, Wayzata, MI, USA)
	V-Chordal (Valtech Cardio, Or Yehuda, Israel)
LV remodeling devices	BACE (Mardil, Orono, MI, USA)
	iCoapsys (Myocor, Maple Grove, MN, USA)
	PARACHUTE (CardioKinetix, Menlo Park, CA, USA)

at the annular level, at the leaflet level, and at the subvalvular level (both on the chordal apparatus and on LV wall).

Therefore, in the repairing process both surgical and percutaneous, a good understanding of the valvular pathology in the preoperative phase is essential.

Consequently, transcatheter technologies of MV repair have been developed mainly aiming to a specific impaired valvular function (see Table 10.1):

- The annuloplastic techniques modify the annular dilation and deformation.
- The leaflet repair techniques may be addressed in both cases of poor leaflet coaptation and primary leaflet degeneration.
- The implantation of synthetic neochordae could be reparative in case of flail leaflet.
- By modifying the LV geometry, it is possible to restore reciprocal structural rapports within the valvular elements and consequently reduce MR.

Notably, in some cases, the addressed level of intervention does not correspond to the impaired one: for example, in case of a flailing leaflet, instead of implantation

of a neochorda, it is also possible to treat MR with a leaflet repair technique (such as MitraClip), according to a functional rather than anatomical repair approach.

In some other cases, a "multilevel" action may be performed: in case of LV remodeling devices, an extended geometrical deformation from the apical to the annular level may be achieved concomitantly to an improvement of the papillary muscle traction forces on leaflets.

Most of the TMVRe devices are delivered through a venous approach with consecutive transseptal puncture (see "Tips in the box: how to perform transseptal technique") or from venous jugular access. For some direct annuloplasty devices, a retrograde approach from the arterial root may be used. More invasive approaches, such as the transapical root, are used in specific cases (e.g., NeoChord).

In most TMVRe technologies, the clinical effect is achieved by the implantation of a device that exerts on the tissue a mechanical traction, whether only in few cases the delivering of some form of energy, which induced tissue modification through fibrosis on the target lesion, is used.

In the description of the different types of TMVRe, we will use a descending order, therefore from the valvular annulus to the apex of the heart.

For each technique, we will focus our attention on the most diffuse and tested devices.

10.2.1 Percutaneous Annuloplasty

An intervention addressed at reshaping a deformed (in most cases dilated) mitral annulus is defined as annuloplasty. This is mainly pursued by reducing septo-lateral (or anteroposterior) dimension of the mitral annulus. Of course, main indications to stand-alone annuloplasty are secondary or functional forms of MR.

Depending on the interaction between the annulus and the device, transcatheter MV annuloplasty (TMVA) may be classified as indirect and direct annuloplasty.

10.2.1.1   Indirect Transcatheter MV Annuloplasty

An indirect approach to the MV annulus consists in the transmission of traction forces on the MV annulus by modifying the perivalvular tissue without a direct contact with the annular fibers. This can be achieved in several manners.

The coronary sinus (CS) reshaping techniques or percutaneous transvenous mitral annuloplasty (PTMA) devices represent the first attempts to reduce MR by indirectly approaching the mitral annulus through the close CS. These techniques consist in the introduction in the CS of a steerable catheter, which delivers two anchors (proximal and distal). Once the anchors are expanded and fixed on site, the nitinol "bridge" between the two anchors is shortened, deflecting the posterior annulus anteriorly, thereby reducing the septo-lateral dimension. The MONARC (Edwards Lifesciences Corporation, Irvine, CA, USA) and the Carillon (Cardiac Dimensions, Kirkland, WA, USA; Fig. 10.1) are two similar devices that use the CS reshaping technique. Both devices went through a reengineering process in order to reduce complications (coronary artery compressions, coronary sinus dissections/perforations), to reduce implantation failure and to improve grade of MR reduction

Fig. 10.1 An example of indirect percutaneous annuloplasty, the Carillon device (Cardiac Dimensions, Kirkland, WA, USA) (From Feldman and Young [36]. Artwork by Craig Skaggs, with permission)
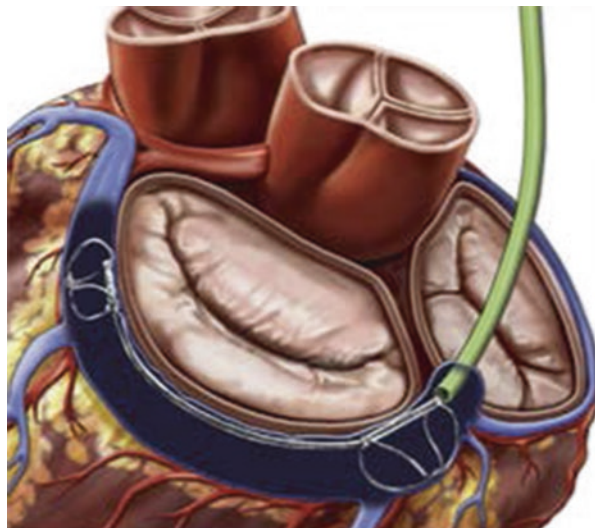
[2, 3]. Nevertheless, according to the Transcatheter Implantation of Carillon Mitral Annuloplasty Device (TITAN), device implantation rate remains only 68 %, with high rate of implantation failure and transient coronary compromise [4]. Carillon device obtained CE Mark in 2011. The results of the TITAN trial showed a significant reduction in FMR grade with a reduction in LV diastolic and systolic volumes compared to a control group composed of non-implanted patients. In addition, functional and performance status markedly improved for the implanted patients. The REDUCE FMR randomized trial will compare the Carillon device to optimal medical therapy in 120 heart failure patients with FMR. The first patient has been enrolled in June 2015.

The MONARC device is actually abandoned.

Another critic addressed to PTMA devices was that the partial obliteration of CS might theoretically jeopardize future attempts at implanting cardiac resynchronization devices. Nevertheless, initial experience has been reassuring about this [5].

The so-called asymmetric approach to CS reshaping is a complex approach where a PTMA is connected to an Amplatzer PFO occluder anchored in the atrial septum. The device that has been engineered using this method is the Percutaneous Septal Sinus Shortening System (PS3 System, Ample Medical, Foster City, California). Tension on the bridge reduced septo-lateral dimension.

10.2.1.2 Direct Transcatheter MV Annuloplasty

The direct approach differs from the indirect one, because the reshaping of the mitral annulus is achieved without the occupation of the CS. In this case, the use of mechanical forces or heat energy applied directed on the mitral annulus will permit a cinching of the annular fibers.

The direct approach to the mitral annulus could be from the ventricular or the atrial side.
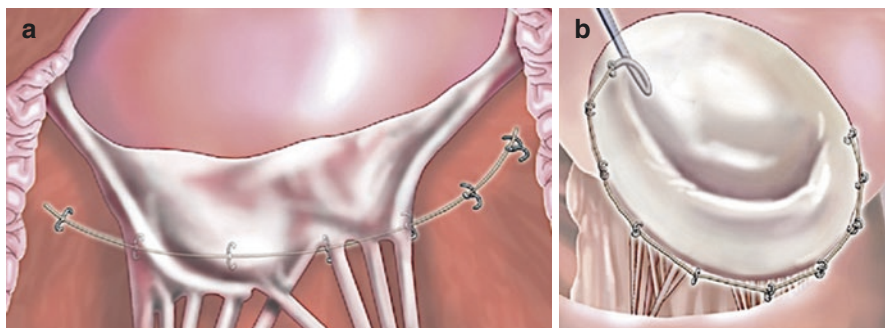
Fig. 10.2 The guided delivery systems Accucinch device is delivered through retrograde catheterization of the left ventricle. (*Left*) Anchors are placed in the posterior mitral annulus and (*right*) connected with a "drawstring" to cinch the annular circumference (From Feldman and Young [36]. Artwork by Craig Skaggs, with permission)

Techniques based on mechanical traction forces are, at the time, the most promising.

The Mitralign (Mitralign, Tewksbury, MA, USA) is a device based on anchors, which approach the posterior mitral annulus from the LV side. The anchors, connected to each other by a suture, are able to cinch the annulus by traction. Similarly, the Accucinch (Guided Delivery Systems, Santa Clara, CA, USA; Fig. 10.2) uses also a ventricular approach to place circumferentially 9–12 anchors that are able to cinch the posterior annulus.

The Cardioband (Valtech Cardio, Or Yehuda, Israel) is a transcatheter mitral sutureless and adjustable posterior direct annuloplasty system. This device represents the real percutaneous adaptation of the surgical annuloplasty with an incomplete ring. Through a transseptal approach, the placement of a variable number of small retrievable corkscrews permits the fixation of the adjustable Dacron sleeve in supra-annular position (Fig. 10.3). Annular dimensions are then tuned using the adjustment tool. Short- and midterm (up to 90 days) preclinical outcomes in porcine model are very promising [6]. First-in-man implantation has been recently reported [7].

The main concern pointed out against the direct TMVA devices is the risk of accidental damage or perforation of neighboring cardiac structures (coronary sinus, left atrium, and MV leaflets). However, preliminary results showed that direct annuloplasty is a very safe approach. Moreover, compared to CS annuloplasty, direct approach bases on a solid surgical background.

On the other hand, the energy-mediated cinching approach for direct TMVA applies heat to cause the fibrosis and the cinching of the mitral annulus. This category includes:

- The QuantomCor System (QuantomCor, Lake Forest, CA, USA), which uses radiofrequency energy
- The ReCor (ReCor Medical, Ronkonkoma, NY, USA), which delivers high-intensity focused ultrasound
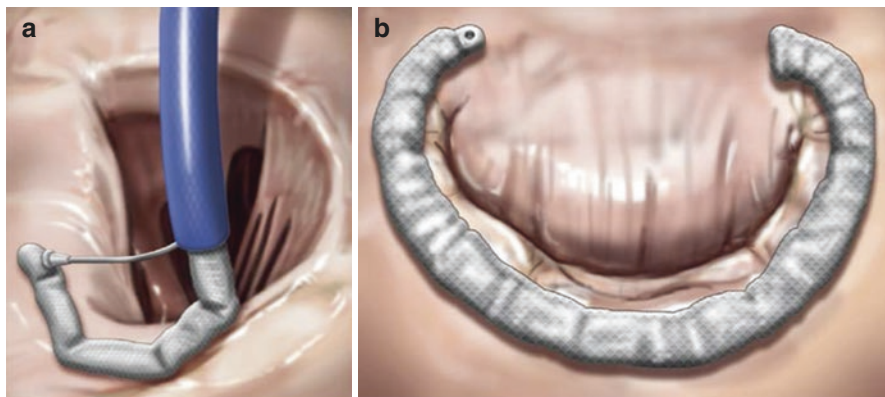
Fig. 10.3 Valtech Cardioband. (**a**) Sequential corkscrew fixation through the transseptal guide catheter. (**b**) Complete deployed Cardioband (Dracon) after the final adjustment using an adjusting tool (From Feldman and Young [36]. Artwork by Craig Skaggs, with permission)

In this case, the limitation reported is a not precise control of the energy distribution and a possible resulting mitral stenosis.

10.2.2 Percutaneous Leaflet Repair

Percutaneous leaflet repair can be done with the following three approaches: increasing leaflet coaptation, modifying leaflet area, and physically occupying regurgitant orifice.

10.2.2.1   Leaflet Coaptation
Several devices have been developed in order to reintegrate or sometimes enhance leaflet coaptation.

Taking again in consideration the Carpentier's classification for MR [1], an insufficient leaflet coaptation resulting in a significant MR may be secondary to several mechanisms: a dilated annulus (type I), an excessive leaflet motion in case of MV prolapse/flail (type II), or a limited systolic leaflet motion due to chordal tethering by LV dilation (type IIIb). The first and the third features depict mainly a functional disease, while the second feature is more consistent of a myxomatous or damaged valve. In all these cases, an intervention addressed at increasing leaflet coaptation may represent a valid solution in reducing MR.

Conversely, in the remaining type of MR (type IIIa), an impaired systolic and diastolic leaflet motion results in most cases in an enhanced leaflet coaptation and in elevated transvalvular gradient measures that could represent a contraindication to a percutaneous approach aimed at increase leaflet coaptation.

Most of the devices operating on leaflet coaptation basically work by "clipping" two MV scallops together. In this way, the regurgitant orifice is partially obliterated. The final result is the creation of a double orifice valve. This concept comes directly

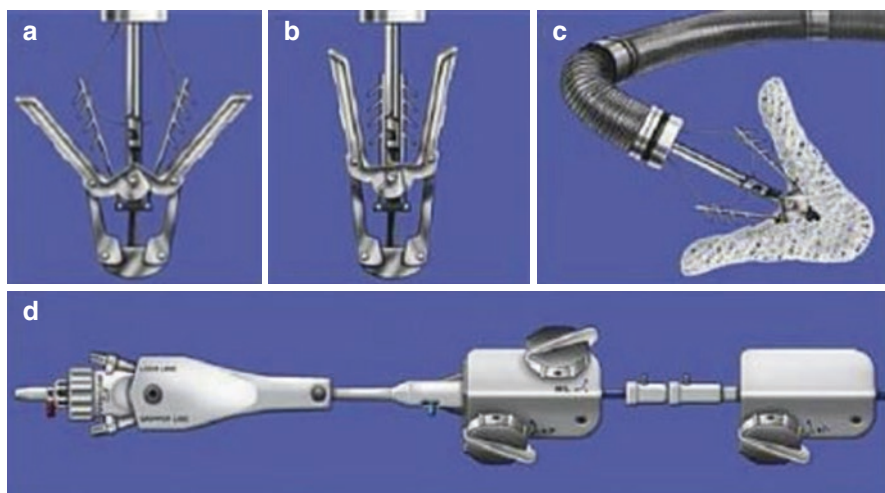**Fig. 10.4** The MitraClip system. (**a**) Device in open configuration. When the leaflets are grasped, the barbed configuration of the grippers helps to fix the leaflets within the clip arms. (**b**) Device in close configuration. A fine wire, which runs through the grippers, permits the closure of the device. This operation is reversible at any time before clip deployment. (**c**) The partially open clip is shown with its polyester fabric covering. (**d**) Remote control system. The steering knobs are shown on the *right-hand* side for maneuvering the clip within the left atrial cavity. The isolated knob at the far *left* of the picture is the one used to open and close the clip, and, close to it, the release mechanism (From Feldman and Young [36]. Artwork by Craig Skaggs, with permission)

from the surgical edge-to-edge technique, also worldwide known as Alfieri's technique [8]. The only device clinically available in this category is the MitraClip (Evalve, Menlo Park, CA, USA); the Mobius device (Edwards Lifesciences, Irving, California) has been abandoned secondary to serious suture dehiscence and technical difficulties occurred [9], and the MitraFlex (TransCardiac Therapeutics, Atlanta, Georgia) is still in a preclinical phase. The latter one could also be used to deliver a neochorda to the MV (see further).

The MitraClip system represents the transcatheter conversion of the surgical Alfieri's stitch [8]. This percutaneous treatment consists in the union of free edges (edge to edge) of the leaflet by applying a cobalt-chromium mixture clip (Fig. 10.4) on the beating heart. The clip includes two arms and two "grippers" adjacent to each arm to independently secure the leaflets following grasping. Arms and grippers are covered with polyester to enhance healing.

The procedure is performed under general anesthesia and is guided by transesophageal real-time 3D echocardiography and fluoroscopy. Conscious sedation and intracardiac echocardiographic guidance may be considered in selected patients [10, 11].

The MitraClip is implanted through a sequence of standardized steps via peripheral venous access at the groin (Fig. 10.5). After transseptal puncture (see Box 10.1), a 24-Fr steerable clip delivery system (CDS) delivers the clip on the left atrium. The device is then advanced to the annular level through a sophisticated triaxial remote
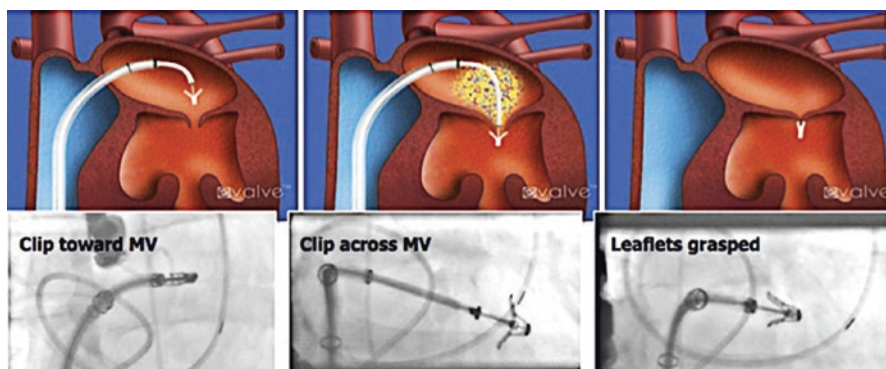
Fig. 10.5 Basic steps of MitraClip implantation procedure (Feldman, JACC 2011; with permission)

catheter control system (Fig. 10.4), which allows the CDS to move in four directions.

An optimal coaxial alignment with the annular plane is critical for an optimal MitraClip implantation. At the regurgitant orifice, clip arms are opened and positioned perpendicular to the line of coaptation. Then, the clip is advanced in the LV and then slowly retracted again toward the valvular level. By doing this, a progressive contact with the MV leaflet is achieved. In the following, the barbed grippers are lowered and the clip arms are closed. A consensual movement of the MitraClip and MV leaflet indicates a successful leaflet engagement. If a satisfactory reduction of MR is achieved without a significant increase in transvalvular mitral gradient, the clip can be deployed. Otherwise, arms and grippers can be reopened at any time before device deployment and the device can be repositioned. In some cases, the implantation of one or two additional clips could be indicated. Once the procedure is completed, vascular closure is performed, and the patient is weaned from general anesthesia.

With more than 20,000 implantation worldwide, randomized trials and national registries demonstrated safety, feasibility, and efficacy of the MitraClip procedure in selected high surgical risk patients with both degenerative and functional etiologies [12–14], and the latest European and North American guidelines recommend (see Table 10.2) this device in symptomatic severe mitral regurgitation in high surgical risk patients on optimal medical treatment [15–18].

10.2.2.2 Leaflet Ablation

ThermoCool (Biosense Webster, Inc., Diamond Bar, California) is a radiofrequency ablation catheter that through regional fibrosis reduces the excessive leaflet motion in a degenerated MV. Severe damage to leaflets and adjacent cardiac structures might occur [19].

10.2.2.3 Space Occupier

Percu-Pro® (Cardiosolutions, Soughton, MA, USA) is a balloon-shaped space occupier that, through a transapical approach, is anchored at the LV apex. It then

Table 10.2 Recommendations for the use of MitraClip according to the latest European and American guidelines

Recommendations for the use of MitraClip	Class	Level
The percutaneous MitraClip procedure may be considered in patients with symptomatic severe secondary MR despite optimal medical therapy (including CRT if indicated), who fulfill the echo criteria of eligibility, who are judged inoperable or at high surgical risk by a team of cardiologists and cardiac surgeons, and who have a life expectancy greater than 1 year[a]	IIb	C
Percutaneous edge-to-edge procedure may be considered in patients with symptomatic severe primary MR who fulfill the echo criteria of eligibility, are judged inoperable or at high surgical risk by a "heart team," and have a life expectancy greater than 1 year[a]	IIb	C
Transcatheter mitral valve repair may be considered for severely symptomatic patients (NYHA class III to IV) with chronic severe primary MR (stage D) who have favorable anatomy for the repair procedure and a reasonable life expectancy but who have a prohibitive surgical risk because of severe comorbidities and remain severely symptomatic despite optimal GDMT for HF[b]	IIb	B
MitraClip for FMR is of uncertain benefit and should only be considered after careful candidate selection and with a background of guideline-directed medical therapy[c]	IIb	B
In patients with an indication for valve repair but judged inoperable or at unacceptably high surgical risk, percutaneous edge-to-edge repair may be considered in order to improve symptoms[d]	IIb	B

Abbreviations: *MR* mitral regurgitation, *CRT* cardiac resynchronization therapy, *NYHA* New York Heart Association, *GDMT* guideline-determined medical therapy
[a]Adapted from The Joint Task Force on the Management of Valvular Heart Disease of the European Society of Cardiology (ESC), the European Association for Cardio-Thoracic Surgery (EACTS), Vahanian et al. [37]
[b]Adapted from Nishimura et al. [16]
[c]Adapted from Yancy et al. [17]
[d]Adapted from McMurray et al. [18]

acts like a "buoy" that automatically centered itself across the MV orifice to provide a surface for leaflet coaptation. This has been preclinically tested in both DMR and FMR (no available published literature).

As a "spacer," it may induce mitral stenosis.

10.2.3 Percutaneous Neochordae Implantation

Chordal implantation consists in embedding onto the LV myocardium of synthetic chords, which reaches the leaflet edge on the opposite end. This procedure may be performed both via transapical (see Fig. 10.6) and transseptal routes. By varying the length of the chord, it is possible to optimize leaflet coaptation. This approach is mainly direct to treat flailing leaflet and other forms of DMR.

The MitraFlex (TransCardiac Therapeutics), the NeoChord DS1000 (NeoChord, Inc., Minnetonka, Minnesota), and the V-Chordal (Valtech Cardio, Or Yehuda, Israel) are examples of devices which use this technology.
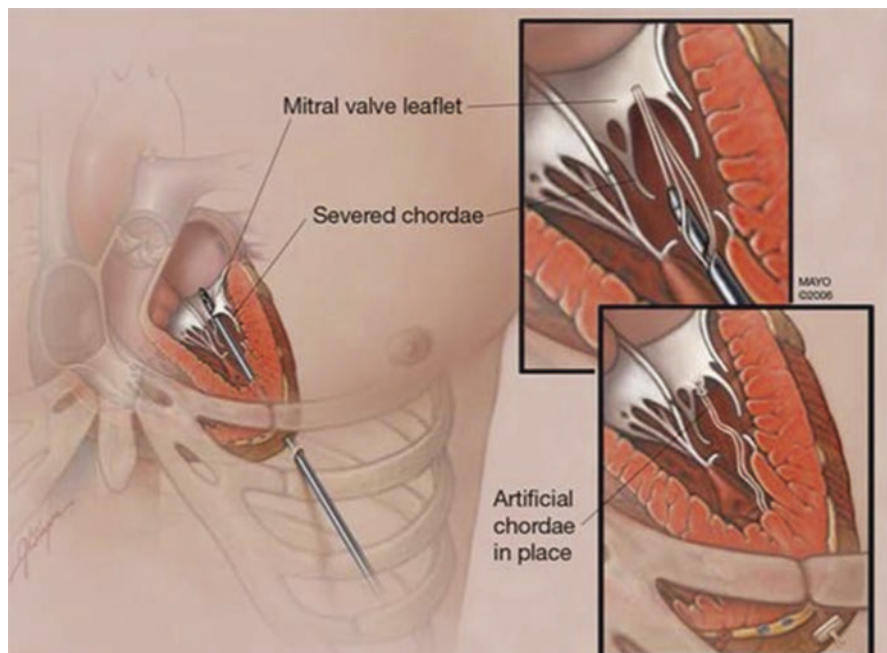
Fig. 10.6 The NeoChord device (NeoChord, Inc., Minnetonka, Minnesota) implanted from a transapical approach (Chiam and Ruiz, JACC 2011; with permission)

In the Transapical Artificial Chordae Tendinae (TACT) trial, the implantation of the NeoChord DS1000 system was demonstrated to be safe and feasible, even though a high recurrence of significant MR was documented already at 30 days [20].

10.2.4 Percutaneous Left Ventricle Remodeling Devices

The remodeling of the LV by reducing the anteroposterior dimension is a possible solution to indirectly decrease MR. This is secondary to the reduction of the septo-lateral annular distance and to the approaching of LV papillary muscles to the leaflets. This approach seems suitable mainly for FMR (Table 10.3).

The Coapsys (Myocor, Maple Grove, Minnesota) device is a percutaneous (sub-xiphoid) technique, which places pads on either side of the LV with a cord passing through the LV cavity to apply tension to the annulus and basal LV wall.

Despite the positive results of the Randomized Evaluation of a Surgical Treatment for Off-Pump Repair of the Mitral Valve (RESTORE-MV) trial [21], this device is no longer manufactured.

The Basal Annuloplasty of the Cardia Externally (BACE, Mardil, Orono, MI, USA) is a silicon band that is placed around the beating heart, at the atrioventricular groove. This device requires a mini-thoracotomy.

Table 10.3 List of transcatheter MV replacement (TMVR) devices known at a most advance stage of development

Transcatheter MV replacement (TMVR) devices
CardiAQ (CardiAQ Valve Technologies, Winchester, MA, USA)
Cardiovalve (Valtech Cardio Ltd, Or Yehuda, Israel)
Double-Crowned Mitral Valve Implantation (Zhejiang University, Hangzhou, China and Centre Hospitalier Universitaire Vaudois (CHUV), Lausanne, Switzerland)
Endovalve-Herrmann prosthesis (Endovalve, Princeton, NJ, USA)
Fortis (Edwards Lifesciences, Irvine, CA, USA)
Gorman (The Trustees of The University of Pennsylvania, Philadelphia, PA, USA)
HighLife (HighLife Medical, CA,US)
MedtronicTranscutaneous Mitral Valve (Medtronic, Minneapolis, MN, USA)
MitralSeal (Avalon Medical Ltd., Stillwater, Minneapolis, US)
MitrAssist (MitrAssist Medical Ltd, Misgav, Israel)
MiVAR (Trinity College Dublin, EIRE)
NaviGate Cardiac Structures (NaviGate Cardiac Structures, Cleveland, OH, USA)
Tendyne (Tendyne Medical, Baltimore, MD, US)
Tiara (Neovasc, Inc., Richmond, British Columbia, Canada)

10.3   Transcatheter MV Replacement (TMVR) Devices

Until now, there is not extensive clinical evidence concerning TMVR. Most of the TMVR devices (Table 10.4) are still in the preclinical or in the early clinical phase, and most of the published literature consists of case reports.

From these reports, however, it is possible to demonstrate that the approach is feasible and promising in not operable patients with impossibility or failure of a TMVRe procedure [22] and in case of failure of a previous implanted mitral surgical bioprosthesis or an annular device (namely, "valve in valve" and "valve in ring," respectively) [23–28].

At a structural level, all the prosthetic models tested for MV are composed of four elements:

- The occluding component guarantees the unidirectional blood flow through the cardiac chambers. It consists generally of three bovine or porcine pericardial membrane leaflets (in case of MitrAssist only two).
- The supporting frames are in most of cases composed of self-expandable nitinol, which has demonstrated better adaptability to the geometrical complexity of the mitral annulus than balloon-expandable frames. The latter ones (e.g., the NaviGate Cardiac Structures device) could represent an option in case of rheumatic disease and diffuse annular calcification.
- The anchoring system is aimed at maintaining the deployed valve in position and at avoiding embolization and also minor dislocations, which could result in paravalvular leakage (PVL). As mentioned above, the lack of hard calcified native annulus doesn't allow the radial reaction forces of the expanded supporting

Table 10.4 Transcatheter mitral valve replacement devices

	CardiAQ prosthesis		Medtronic transcatheter mitral valve
	CardiAQ Valve Technologies Inc., Winchester, Massachusetts, US		*Medtronic Inc., Minneapolis, US*
	Frame: self-expandable, made of superelastic Ni-Ti alloy		**Frame:** self-expandable, made of
	Leaflets: glutaraldehyde-fixed porcine pericardium		superelastic Ni-Ti alloy
	Anchoring: atrial and ventricular flanges (Fig. 10.1c)		**Leaflets:** glutaraldehyde-fixed pericardium
	Delivery: transseptal/transapical (Fig. 10.2a,b)		**Anchoring:** atrial flange and native valve anchors (Fig. 10.1b)
	Trials: first in human in 2012		**Delivery:** left atriotomy (Fig. 10.2c)
			Trials: animals only
	Cardiovalve		**MitralSeal**
	Valtech Cardio Ltd, Or Yehuda, Israel		*Avalon Medical Ltd., Stillwater, Minneapolis, US*
	Frame: self-expandable, made of superelastic Ni-Ti alloy		**Frame:** self-expandable, made of superelastic Ni-Ti alloy
	Leaflets: glutaraldehyde-fixed pericardium		**Leaflets:** glutaraldehyde-fixed pericardium
	Anchoring: atrial flange (full details not currently available)		**Anchoring:** atrial flange and ventricular tethers (Fig. 10.1a)
	Delivery: not specified		**Delivery:** transapical (Fig. 10.1b)
	Trials: animals only		**Trials:** animals only
	Double-crowned mitral valve implantation		**MitrAssist**
	Zhejiang University, Hangzhou, China and CHUV, Lausanne, Switzerland		*MitrAssist Medical Ltd., Misgav, Israel*
	Frame: self-expandable, made of superelastic Ni-Ti alloy		**Frame:** superelastic Ni-Ti alloy
	Leaflets: porcine pulmonary and aortic homografts		**Leaflets:** glutaraldehyde-fixed pericardium
	Anchoring: atrial ventricular flanges (Fig. 10.1c)		**Anchoring:** atrial flange and native valve anchors (Fig. 10.1b)
	Delivery: Left atriotomy (Fig. 10.2c)		**Delivery:** Not specified
	Trials: animals only		**Trials:** animals only

Table 10.4 (continued)

	Endovalve		MiVAR
	Micro Interventional Devices, Langhorne, Pennsylvania, US		*Trinity College Dublin, EIRE*
	Frame: self-expandable, made of superelastic Ni-Ti alloy]		**Frame:** self-expandable, made of superelastic Ni-Ti alloy
	Leaflets: glutaraldehyde-fixed pericardium		**Leaflets:** glutaraldehyde-fixed pericardium
	Anchoring: arrowhead anchors		**Anchoring:** atrial cage (Fig. 10.1e)
	Delivery: transapical (Fig. 10.2b)		**Delivery:** not specified
	Trials: animals only		**Trials:** animals only
	Fortis		Navigate cardiac structures
	Edwards Lifesciences		*NaviGate Cardiac Structures Inc., Cleveland, Ohio, US*
	Frame: self-expandable, made of superelastic Ni-Ti alloy		**Frame:** balloon expandable, made of cobalt-chromium alloy
	Leaflets: glutaraldehyde-fixed bovine pericardium		**Leaflets:** glutaraldehyde-fixed pericardium
	Anchoring: atrial flange and native valve anchors (Fig. 10.1b)		**Anchoring:** atrial and ventricular flanges (Fig. 10.1c)
	Delivery: transapical (Fig. 10.2b)		**Delivery:** transseptal (Fig. 10.1a)
	Trials: first in human in 2014		**Trials:** none currently reported
	Gorman		Tendyne
	The Trustees of The University of Pennsylvania, Philadelphia, US		*Tendyne Medical Inc., Baltimore, Maryland, US*
	Frame: self-expandable, made of superelastic Ni-Ti alloy		**Frame:** self-expandable, made of superelastic Ni-Ti alloy
	Leaflets: glutaraldehyde-fixed pericardium		**Leaflets:** glutaraldehyde-fixed bovine pericardium
	Anchoring: atrial and ventricular flanges (Fig. 10.1c)		**Anchoring:** atrial flange and ventricular tethers (Fig. 10.1a)
	Delivery: Left atriotomy (Fig. 10.2c)		**Delivery:** transapical (Fig. 10.2b)
	Trials: animals only		**Trials:** first in human in 2013

(continued)

Table 10.4 (continued)

	Highlife		Tiara
	HighLife Medical Inc., California, US		*Neovasc Inc., Richmond, British Columbia, Canada*
	Frame: self-expandable, made of superelastic Ni-Ti alloy		**Frame:** self-expandable, made of superelastic Ni-Ti alloy
	Leaflets: glutaraldehyde-fixed pericardium		**Leaflets:** glutaraldehyde-fixed bovine pericardium
	Anchoring: atrial and ventricular flanges (Fig. 10.1c)		**Anchoring:** atrial flange and native valve anchors (Fig. 10.1b)
	Delivery: Left atriotomy (Fig. 10.2c)		**Delivery:** Transapical (Fig. 10.1b)
	Trials: animals only		**Trials:** first in human in 2013

Representation of the devices known at a most advanced stage of development and description of their main features (From Preston-Maher et al. Cardiovascular Engineering and Technology. June 2015 (Open access article))

frame to maintain the valve fixed in position. A higher level of radial forces could also push the anterior MV leaflet in the LV outflow tract (LVOT), resulting in subaortic gradient or LVOT obstruction, as well as in an impingement of the aortic valve function by deforming the aorto-mitral curtain. Therefore, several types of alternative solutions have been engineered. These mainly consist of several types of atrial flanges and anchors, which can be fixed on the ventricle wall or by grasping the MV leaflets (Fig. 10.7a–c). Acting as proximal and distal constraints, flanges and anchors fix the device by counteracting axial forces. Alternative approaches were proposed: the Endovalve uses barb springs that penetrate the tissue from the atrial side (Fig. 10.7d), while in case of MiVAR valve, an atrial nitinol cage (Fig. 10.7e) keeps the valve in position.

- The presence of an external sealing component may help to minimize PVL.

Even though a venous transfemoral route would permit to avoid the dangerous ventricular navigation close to the subvalvular apparatus, most of the tested valves use the transapical route. In both cases large delivery systems up to 24 Fr are used.

10.3.1 Challenges in TMVR

Differently from the aortic side, where the TAVR has reached nowadays the full approval of the international scientific community, entering in the guidelines as a safe and effective procedure for a surgical risk patients for severe aortic stenosis [15, 16], the placement of a prosthetic valve in mitral position is still an open challenge and a "hot topic" of discussion in the international interventional meetings. Many reasons for that could be pointed out.

Firstly, the complex three-dimensional structure of the MV, comprehensive subvalvular apparatus fundamental for a synergic ventricular contraction, and the
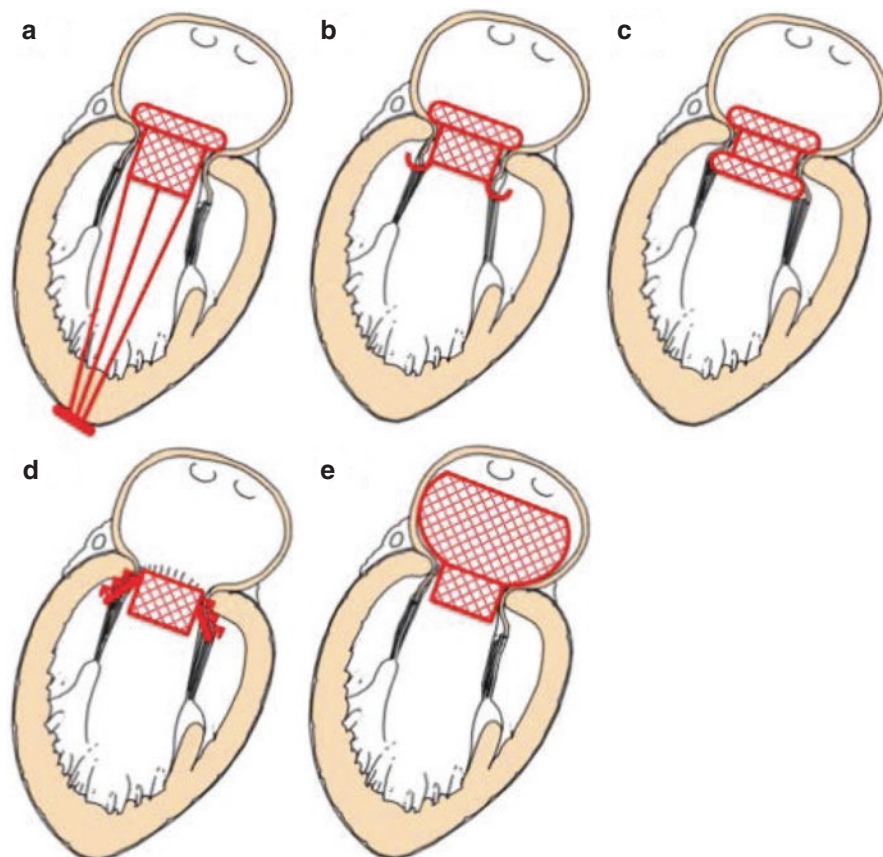
Fig. 10.7 Anchoring systems for percutaneous mitral valve replacement (PMVRe) devices. (**a**) Atrial flange and ventricular tethers, (**b**) atrial flange and native valve anchors, (**c**) atrial and ventricular flanges, (**d**) subannular hooks, and (**e**) atrial cage (From Preston-Maher et al. Cardiovascular Engineering and Technology. June 2015 (Open access article))

presence of a large poorly calcified ring under critical loading conditions are responsible for the difficulty of firmly anchoring a bioprosthetic valve in mitral position. Consequently, also the risk of failure (PVL) or periprocedural complications (chordal engaging, leaflet damage, LVOT obstruction) is for the MV higher.

Notably, balloon-expandable TAVR devices have been successfully deployed in calcific mitral annuli [26].

Secondly, the need of bigger valves forces the employment of larger delivery systems from 24 to 33 Fr, which could need "more invasive" routes than the transfemoral one, such as the transapical and transaortic, or a left atriotomy. The use of combined routes (transapical-transseptal) has also been described [29].

Further concerns have been addressed at the new anchoring systems. Even though big atrial flanges may prevent PVL, ventricular anchors may be displaced by

LV remodeling with resulting loss of caudal constraint. Therefore, clamping the native leaflets seems a more promising option. Moreover, it has been observed that by capturing the native anterior leaflet, the risk of LVOT obstruction is lower [30].

Lastly, given a bigger transvalvular pressure difference between the two left cardiac chambers than between the LV and aorta, the risk and also the predictable impact of transmitral PVL may be also accentuated. Therefore, atrial flanges, ventricle anchors, and sealing components have to be engineered at eliminating gaps between the bioprosthesis and the annulus. A saddle-shaped design could improve valve adaptation at the annular level [31].

In conclusion, the role of TMVI in comparison to the actual established role of TMVRe is difficult to foresee. In a recent review [32], a group of experts compared clinical and technical advantages and disadvantages of the two approaches. In current practice, surgical replacement and repair are complementary rather than competitive. Given the embryonic state of the art for TMVI and the rapid evolution in device development, the complementary role of TMVRe and TMVI must be considered speculative.

Box 10.1. Tips in the Box: How to Perform Transseptal Technique
Transseptal puncture is a crucial step of left-sided structural interventions. The puncture should be done within the limits of the fossa ovalis. For this purpose, a pullback technique is conventionally performed until a "jump" is observed at fluoroscopy. This corresponds usually to a visible tenting on the fossa ovalis at transesophageal echocardiography (TEE).

Mitral valve interventions benefit from precise localization of the puncture according to the etiology of the disease and to the device. For this purpose, TEE guidance is mandatory. The localization of the tenting on the fossa prior to puncture responds to precise anatomical and TEE landmarks. A puncture can be superior (cranial) or inferior (caudal), as identified in the bicaval view at TEE. It can be anterior or posterior (in respect to the aorta), as identified at short axis at the base view, and it can be finally high or low (in respect to the annulus) according to the four-chamber TEE view.

For MitraClip therapy, the transseptal puncture has to be tailored to patient-specific anatomy and the underlying etiology. In primary MR, when the mechanism of regurgitation is prolapse, the puncture needs to be done high enough (respect the annular level) to allow sufficient backward travel of the clip to pull on the leaflets once grasped. This is usually achieved by a superior and posterior puncture. In functional regurgitation, since the leaflet coaptation is lowered, transseptal puncture should be done at a lower height. This is achieved by a more inferior and anterior puncture, as compared to degenerative MR. Position of the puncture also varies according to the location of the target. For example, in case of posteromedial commissure flail/prolapse, an inferior and posterior puncture may be beneficial to achieve enough height and a straight trajectory to the target.

In case of transcatheter direct annuloplasty (Cardioband, Valtech Cardio), a low puncture is more efficient to get more support during the implant.

Inferior puncture is also preferable in case of combined mitral interventions with left appendage closure.

Transseptal puncture can be challenging in patients with convex septum or in those with previous septal interventions. The presence of multiple pacing electrodes can also be a challenge.

In terms of transseptal catheterization material, there are several options. The classic Brockenbrough needle and Mullins catheter are the standard solution [33]. More operators are now using braided catheters initially developed for electrophysiology. In case of challenging puncture, the use of radiofrequency catheters can be beneficial, since they allow precise crossing without the risk of sliding cranially while advancing the needle for puncture [34]. As an alternative, the use of cautery on the needle serves for the same purpose [35].

Bibliography

 1. Carpentier A. Cardiac valve surgery – the "French correction". J Thorac Cardiovasc Surg. 1983;86(3):323–37.
 2. Harnek J, Webb JG, Kuck KH, Tschope C, Vahanian A, Buller CE, et al. Transcatheter implantation of the MONARC coronary sinus device for mitral regurgitation: 1-year results from the EVOLUTION phase I study (Clinical Evaluation of the Edwards Lifesciences Percutaneous Mitral Annuloplasty System for the Treatment of Mitral Regurgitation). JACC Cardiovasc Interv. 2011;4(1):115–22.
 3. Siminiak T, Hoppe UC, Schofer J, Haude M, Herrman JP, Vainer J, et al. Effectiveness and safety of percutaneous coronary sinus-based mitral valve repair in patients with dilated cardiomyopathy (from the AMADEUS trial). Am J Cardiol. 2009;104(4):565–70.
 4. Siminiak T, Wu JC, Haude M, Hoppe UC, Sadowski J, Lipiecki J, et al. Treatment of functional mitral regurgitation by percutaneous annuloplasty: results of the TITAN Trial. Eur J Heart Fail. 2012;14(8):931–8.
 5. Hoppe UC, Brandt MC, Degen H, Dodos F, Schneider T, Stoepel C, et al. Percutaneous mitral annuloplasty device leaves free access to cardiac veins for resynchronization therapy. Cathet Cardiovasc Interv: Off J Soc Card Angiography Interv. 2009;74(3):506–11.
 6. Maisano F, Vanermen H, Seeburger J, Mack M, Falk V, Denti P, et al. Direct access transcatheter mitral annuloplasty with a sutureless and adjustable device: preclinical experience. Eur J Cardiothorac Surg: Off J Eur Assoc Cardiothorac Surg. 2012;42(3):524–9.
 7. Maisano F, La Canna G, Latib A, Denti P, Taramasso M, Kuck KH, et al. First-in-man transseptal implantation of a "surgical-like" mitral valve annuloplasty device for functional mitral regurgitation. JACC Cardiovasc Interv. 2014;7(11):1326–8.
 8. Alfieri O, Maisano F, De Bonis M, Stefano PL, Torracca L, Oppizzi M, et al. The double-orifice technique in mitral valve repair: a simple solution for complex problems. J Thorac Cardiovasc Surg. 2001;122(4):674–81.
 9. Webb JG, Maisano F, Vahanian A, Munt B, Naqvi TZ, Bonan R, et al. Percutaneous suture edge-to-edge repair of the mitral valve. EuroIntervention: J EuroPCR Collab Work Group Interv Cardiol EurSoc. 2009;5(1):86–9.
10. Ussia GP, Barbanti M, Tamburino C. Feasibility of percutaneous transcatheter mitral valve repair with the MitraClip system using conscious sedation. Cathet Cardiovasc Interv: Off J Soc Card Angiography Interv. 2010;75(7):1137–40.

11. Maisano F, Godino C, Giacomini A, Denti P, Arendar I, Buzzatti N, et al. Clinical trial experience with the MitraClip catheter based mitral valve repair system. Int J Cardiovasc Imaging. 2011;27(8):1155–64.

12. Feldman T, Kar S, Rinaldi M, Fail P, Hermiller J, Smalling R, et al. Percutaneous mitral repair with the MitraClip system: safety and midterm durability in the initial EVEREST (Endovascular Valve Edge-to-Edge REpair Study) cohort. J Am Coll Cardiol. 2009;54(8):686–94.

13. Mauri L, Foster E, Glower DD, Apruzzese P, Massaro JM, Herrmann HC, et al. 4-year results of a randomized controlled trial of percutaneous repair versus surgery for mitral regurgitation. J Am Coll Cardiol. 2013;62(4):317–28.

14. Maisano F, Franzen O, Baldus S, Schafer U, Hausleiter J, Butter C, et al. Percutaneous mitral valve interventions in the real world: early and 1-year results from the ACCESS-EU, a prospective, multicenter, nonrandomized post-approval study of the MitraClip therapy in Europe. J Am Coll Cardiol. 2013;62(12):1052–61.

15. Vahanian A, Alfieri O, Andreotti F, Antunes MJ, Baron-Esquivias G, Baumgartner H, et al. Guidelines on the management of valvular heart disease (version 2012). The joint task force on the management of valvular heart disease of the European Society of Cardiology (ESC) and the European Association for Cardio-Thoracic Surgery (EACTS). G Ital Cardiol. 2013;14(3):167–214.

16. Nishimura RA, Otto CM, Bonow RO, Carabello BA, Erwin 3rd JP, Guyton RA, et al. 2014 AHA/ACC guideline for the management of patients with valvular heart disease: a report of the American College of Cardiology/American Heart Association Task Force on Practice Guidelines. J Am Coll Cardiol. 2014;63(22):e57–185.

17. Yancy CW, Jessup M, Bozkurt B, Butler J, Casey Jr DE, Drazner MH, et al. 2013 ACCF/AHA guideline for the management of heart failure: a report of the American College of Cardiology Foundation/American Heart Association Task Force on Practice Guidelines. J Am Coll Cardiol. 2013;62(16):e147–239.

18. McMurray JJ, Adamopoulos S, Anker SD, Auricchio A, Bohm M, Dickstein K, et al. ESC Guidelines for the diagnosis and treatment of acute and chronic heart failure 2012: the task force for the diagnosis and treatment of acute and chronic heart failure 2012 of the European Society of Cardiology. Developed in collaboration with the Heart Failure Association (HFA) of the ESC. Eur Heart J. 2012;33(14):1787–847.

19. Williams JL, Toyoda Y, Ota T, Gutkin D, Katz W, Zenati M, et al. Feasibility of myxomatous mitral valve repair using direct leaflet and chordal radiofrequency ablation. J Interv Cardiol. 2008;21(6):547–54.

20. Seeburger J, Rinaldi M, Nielsen SL, Salizzoni S, Lange R, Schoenburg M, et al. Off-pump transapical implantation of artificial neo-chordae to correct mitral regurgitation: the TACT Trial (Transapical Artificial Chordae Tendinae) proof of concept. J Am Coll Cardiol. 2014;63(9):914–9.

21. Grossi EA, Woo YJ, Patel N, Goldberg JD, Schwartz CF, Subramanian VA, et al. Outcomes of coronary artery bypass grafting and reduction annuloplasty for functional ischemic mitral regurgitation: a prospective multicenter study (Randomized Evaluation of a Surgical Treatment for Off-Pump Repair of the Mitral Valve). J Thorac Cardiovasc Surg. 2011;141(1):91–7.

22. Lawrie GM. Mitral valve: toward complete repairability. Surg Technol Int. 2006;15:189–97.

23. Seiffert M, Conradi L, Baldus S, Schirmer J, Knap M, Blankenberg S, et al. Transcatheter mitral valve-in-valve implantation in patients with degenerated bioprostheses. JACC Cardiovasc Interv. 2012;5(3):341–9.

24. Seiffert M, Franzen O, Conradi L, Baldus S, Schirmer J, Meinertz T, et al. Series of transcatheter valve-in-valve implantations in high-risk patients with degenerated bioprostheses in aortic and mitral position. Cathet Cardiovasc Interv: Off J Soc Card Angiography Interv. 2010;76(4):608–15.

25. Nunez-Gil IJ, Goncalves A, Rodriguez E, Cobiella J, Marcos-Alberca P, Maroto L, et al. Transapical mitral valve-in-valve implantation: a novel approach guided by three-dimensional

transoesophageal echocardiography. Eur J Echocardiogr: J Work Group Echocardiogr Eur Soc. 2011;12(4):335–7.

26. Cheung AW, Gurvitch R, Ye J, Wood D, Lichtenstein SV, Thompson C, et al. Transcatheter transapical mitral valve-in-valve implantations for a failed bioprosthesis: a case series. J Thorac Cardiovasc Surg. 2011;141(3):711–5.

27. de Weger A, Ewe SH, Delgado V, Bax JJ. First-in-man implantation of a trans-catheter aortic valve in a mitral annuloplasty ring: novel treatment modality for failed mitral valve repair. Eur J Cardiothorac Surg: Off J Eur Assoc Cardiothorac Surg. 2011;39(6):1054–6.

28. Maisano F, Reser D, Pavicevic J, Nietlispach F, Gamperli O, Schmid M, et al. Successful first-in-man Melody transcatheter valve implant in a dehisced mitral annuloplasty ring transapical valve-in-ring implant. EuroIntervention: J EuroPCR Collab Work Group Interv Cardiol Eur Soc Cardiol. 2014;10(8):961–7.

29. Kliger C, Al-Badri A, Wilson S, Weiss D, Jelnin V, Kronzon I, et al. Successful first-in-man percutaneous transapical-transseptal Melody mitral valve-in-ring implantation after complicated closure of a para-annular ring leak. EuroIntervention: J EuroPCR Collab Work Group Interv Cardiol Eur Soc Cardiol. 2014;10(8):968–74.

30. Rabbah JP, Saikrishnan N, Siefert AW, Santhanakrishnan A, Yoganathan AP. Mechanics of healthy and functionally diseased mitral valves: a critical review. J Biomech Eng. 2013;135(2):021007.

31. Jensen MO, Hagege AA, Otsuji Y, Levine RA, Leducq Transatlantic MN. The unsaddled annulus: biomechanical culprit in mitral valve prolapse? Circulation. 2013;127(7):766–8.

32. Maisano F, Alfieri O, Banai S, Buchbinder M, Colombo A, Falk V, et al. The future of trans-catheter mitral valve interventions: competitive or complementary role of repair vs. replacement? Eur Heart J. 2015.

33. Brockenbrough EC, Braunwald E, Ross Jr J. Transseptal left heart catheterization. A review of 450 studies and description of an improved technic. Circulation. 1962;25:15–21.

34. Sakata Y, Feldman T. Transcatheter creation of atrial septal perforation using a radiofrequency transseptal system: novel approach as an alternative to transseptal needle puncture. Cathet Cardiovasc Interv: Off J Soc Card Angiography Interv. 2005;64(3):327–32.

35. Maisano F, La Canna G, Latib A, Godino C, Denti P, Buzzatti N, et al. Transseptal access for MitraClip(R) procedures using surgical diathermy under echocardiographic guidance. EuroIntervention: J EuroPCR Collab Work Group Interv Cardiol EurSoc. 2012;8(5):579–86.

36. Feldman T, Young A. Percutaneous approaches to valve repair for mitral regurgitation. J Am Coll Cardiol. 2014;63:2057–68.

37. Vahanian A, et al. Guidelines on the management of valvular heart disease (version 2012). Eur Heart J. 2012;33(19):2451–96.

Perivalvular Leakage: Percutaneous Treatment Options

11

Gabriele Pesarini and Flavio Ribichini

11.1 Introduction

Widespread diffusion of biomedical technologies and interventional options in developed countries have progressively changed the natural history and improved the dismal prognosis of patients with degenerative cardiovascular diseases, leading to an increasing contingent of surviving patients that age with different and complex comorbidities. Furthermore, invasive treatments may in turn generate unique complications and novel pathological conditions often requiring demanding approaches. In this view, prosthetic paravalvular leakage (PVL) represents a paradigm of a surgically induced pathology that may be acquired early or late after valvular surgery and, although the majority of cases are mild to moderate, may also be life-threatening in its severe forms. Redo surgery, when medical therapy fails to maintain heart compensation or good quality of life, has been the established destination treatment for severe cases. However, as previously stated, the increasing age and complexity of patients as well as the high risk of failure when suturing a compromised tissue have raised the need to develop feasible and effective percutaneous alternatives.

Mitral valve surgery is mainly driven by mitral regurgitation. Recognizing a degenerative etiology in the majority of cases, especially among older people, this pathology represents the second reason for heart valve surgery worldwide [1]. Ischemic, infectious, or rheumatic etiologies are also involved in the onset of mitral regurgitation requiring surgery, while mitral stenosis frequently has rheumatic origin and may be subject to percutaneous valvuloplasty in case of favorable anatomic features [2]. Percutaneous treatment of postsurgical mitral PVL is among the most difficult and technically challenging structural interventions and requires high levels of expertise and confidence with different endovascular procedures, as well as multidisciplinary approaches and multimodality imaging integration.

G. Pesarini (✉) • F. Ribichini
Department of Cardiology, University of Verona, Verona, Italy
e-mail: gabriele.pesarini@ospedaleuniverona.it

153

11.2 Epidemiology, Onset, and Symptoms

A certain degree of PVL is not infrequent after cardiac valve replacement and valvular ring surgery, with quite a wide range between 5 % and 17 % [3, 4]. In mitral valve surgery, PVLs are usually more common than in aortic procedures (7–17 % vs. 2–10 %) [3], and in fact prosthetic mitral position represents a risk factor for PVL itself. Some surgical series with transesophageal echocardiogram analyses report even higher incidence, up to 32 % of patients [5]. Surgical techniques involving continuous sutures or sutures without pledgets are also at higher risk [3, 6]. More generally, any condition that may increase the sutured tissue friability – such as calcifications, previous or acquired infections, ischemia, and redo surgery – can raise the risk of developing PVL [7]. The time range of mitral PVL onset is also very wide: in fact PVL can occur immediately or early after the operation or very late (also decades after), even without relevant signs of acquired endocarditis [8].

With the advent of endovascular techniques for valve replacement, such as the transcatheter aortic valve implantation (TAVI), the prosthetic PVL became no more an exclusive of open heart surgery. After TAVI, PVL is relatively common: in fact various degrees of aortic leakage from trivial to severe were reported in up to 70 % of cases [9]. Furthermore, recent insights on large series report 14 % of moderate to severe PVL after TAVI and confirm the detrimental effect of its presence and severity on patients' outcome [10]. This phoenomenon is changing over time and is clearly linked to the type of prosthesis, the anatomy of the ventricle-aortic complex and the operator's experience. In a near future, the ongoing development of mitral percutaneous and transapical valve implantation techniques will give interventionalists the possibility of performing mitral procedures on a large scale, and the PVL problem may arise as a consequence of these advancements [11, 12].

Multiplanar reconstruction CT scan has proved useful to clarify the size, shape, and position of the leak.

Clinical manifestation of mitral PVL ranges from no symptoms to fatigue and dyspnea to overt heart failure in severe cases: the underlying conditions and comorbidities of the patient do often influence the severity of these symptoms. Furthermore, as blood is accelerating and backflowing through an irregularly shaped passage next to a surgically placed prosthesis, hemolytic anemia with reduced levels of haptoglobin may be an important phenomenon driving patients' symptoms and requiring accurate monitoring and repeated blood transfusions. In recent series, the presence of hemolytic anemia after mitral has been linked with poor prognosis, suggesting a more aggressive approach for these patients [13].

11.3 Diagnosis

The presence of mitral PVL may be clear immediately or early after the surgical intervention. Technical success should be constantly monitored during surgery usually via transesophageal echocardiography: this also contributes to the intraoperative correction of inadequate surgical results, if feasible. Predischarge or postsurgical

echocardiography in the rehab usually permits to formulate the correct diagnosis of early-onset cases. As the majority of PVLs are initially of trivial or mild severity, no particular clinical features or objective sings are usually evident at this stage. These early forms are most often associated with the technical aspects of the valve surgery.

Late forms may derive from suture dehiscence, remodeling of annular calcifications, or mitral endocarditis: scheduled control echocardiograms or the onset of the previously cited symptoms (see above) usually unveils these cases. In moderate to severe forms, a pansystolic murmur may be appreciated over the left side of the sternum with radiation sign relative to the direction of the jet associated with the regurgitation. Heart failure due to volume overload may be present in over 85 % of symptomatic patients, and the majority of these patients are in NYHA class III or IV [14]. Hemolysis presents in 30–75 % of the patients and may be identified using standard laboratory assays, particularly elevated serum lactate dehydrogenase, reduced levels of haptoglobin, and elevated reticulocytes in hemo-competent subjects [15]. History or signs/symptoms of previous endocarditis are of crucial importance in patients with prosthetic valves and warrant in-depth analyses to rule out secondary PVLs.

Of course, imaging techniques have a key role in the diagnosis of mitral PVLs and, as previously stated, may be indicated after clinical suspect or may unveil asymptomatic PVLs at scheduled controls. Being the most diffused, cheapest, and less invasive of the imaging techniques, transthoracic echocardiography (TTE) with color Doppler imaging is usually the first method to reveal the presence of PVL and estimate its severity. Three-dimensional TTE may be used to better define the anatomic and spatial characteristics of the leak, but may often be limited by patients' echogenicity and compliance. Therefore, transesophageal echocardiography (TEE), especially with its 3D applications, is usually performed during the diagnostic path of PVLs and may permit adequate localization, planimetry, measurement, and shape definition of the defect [16]. However, spatial resolution may still be insufficient for defining small defects or fissures. For the estimate of PVL's functional severity, both qualitative (jet width and density, reversal of flow in the pulmonary veins during systole) and quantitative (regurgitant volume and fraction, vena contracta, proximal isovelocity surface area) parameters are useful, but the dispersion of the jets against the atrial walls may cause visual underestimation of the regurgitation [17]. Due to their multiple jets and extreme eccentricity, the assessment of the severity of multiple mitral PVLs may be very difficult: reporting the proportion of the areas of regurgitation to the prosthetic annulus circumference, are usually defined as mild the PVLs occupying <10 %, moderate those between 10 % and 20 %, and severe PVLs involving >20 % of circumference [18]. Alternatively, some specialists calculate the regurgitant blood volume by comparing mitral blood volume with the aortic, if that valve is competent. However, acoustic shadowing due to patients' characteristics or artifacts induced by the presence of a mechanical valve, as well as technical limitation and low temporal-spatial resolution of available 3D applications, may limit the echocardiogram's precision, requiring other methods for better diagnosis and quantification.

Diagnostic angiography is currently rarely used to determine the key features of PVLs, as it is not capable of native 3D evaluation and has limited spatial resolution. Furthermore, even if multiple acquisitions and balloon sizing were formerly adopted

for aortic PVL assessment, mitral apparatus is not adequate for these approaches, and therefore, alternative methods should be used.

Computed tomography (CT) with the administration of contrast media and gating to ECG leads may be of great help in diagnosing PVL presence and severity and planning possible interventions. In fact, with the application of a protocol similar to that used for coronary angio-CT and 3D/4D reconstruction post-processing, CT scan permits outstanding visualization of the defect(s), detailed shape definition, and precise size measurements. It is also possible to appreciate the contrast actually flowing through the PVL [19]. However, severe calcifications or the presence of metallic prostheses may interfere with CT quality and, in some cases, limit the precision of the measurements. Furthermore, the risk associated with radiations must be taken into account, especially for younger individuals.

Magnetic resonance imaging (MRI) may be of help in highly experienced centers to quantify the regurgitant volume through the PVL; however, the high costs, the necessary high level of expertise, and the contraindication in patients with mechanical prosthetic valves limit MRI use in routine leak evaluation [20, 21].

Whatever being the diagnostic tool, it is not infrequent to find severe PVLs in patients with previous repeated chest surgery or at very high risk for redo operations. These patients are prone to develop severe events and, if not treated, are known to have a dismal prognosis. Therefore, percutaneous reduction or closure of PVLs has been developed as a chance to approach these complex cases, and recent evidences report satisfying results after successful intervention [22], even if no randomized clinical trials have been conducted so far.

11.4   Imaging Guidance for Percutaneous Intervention

Procedural success for mitral PVL reduction or closure procedures is strictly linked to the correct anatomical definition of the defect(s). Given the complex morpho-functional nature of the mitral valvular apparatus, a high degree of confidence with multimodal imaging is required for the operator, and collaboration with adequately trained echocardiographers is crucial for the result [23]. TEE with 3D applications is usually the method of choice for procedural guidance, even if intracardiac echocardiography (ICE) is being successfully used, especially when it is important to avoid general anesthesia in particularly frail or complex patients. However, the procedure itself may be long and technically complex, and therefore, sedation is often required. The first diagnostic step is to confirm that no active endocarditis or intracardiac thrombi that may dislodge are evident; otherwise, the procedure should be postponed. Furthermore, the presence of a leak that has extended to more than one third of the annulus circumference or a rocking prosthesis usually defines a disease phase too advanced to be successfully addressed via the percutaneous approach.

To establish a common language and reference in describing the anatomy during procedures, usually echocardiographic images are oriented following a "surgical view" from the left atrium [24] (Fig. 11.1). In this view, mitral valve is regarded as a "clock face," where the 12 o'clock position is set on the anterior
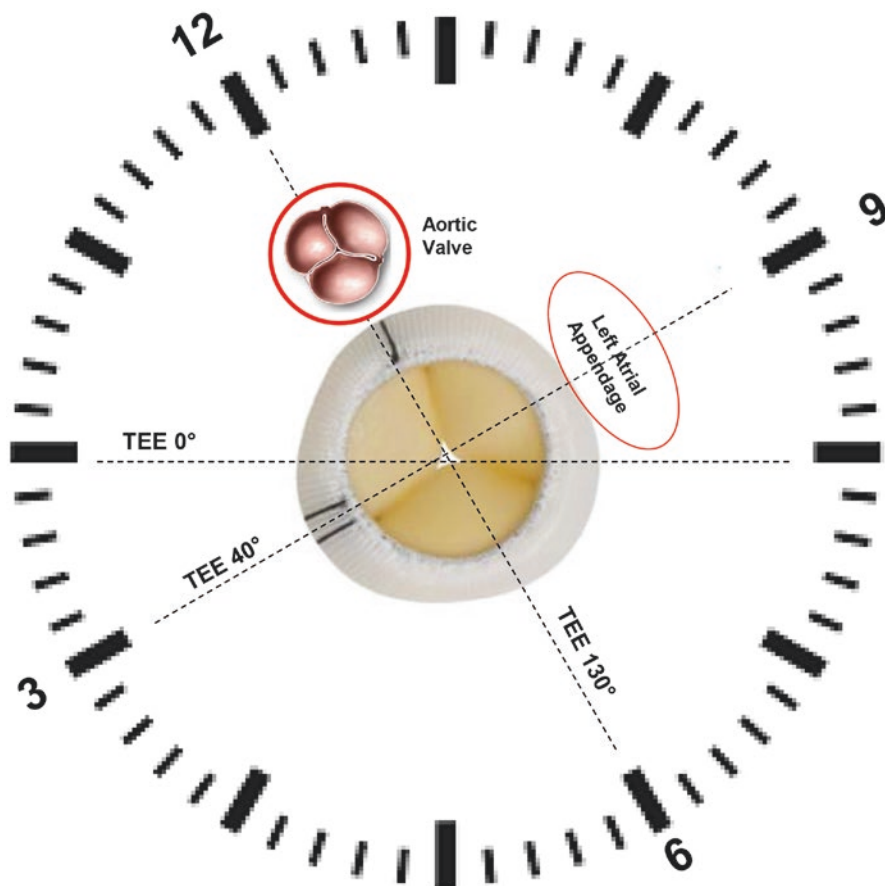
Fig. 11.1 "Clock face" orientation of the mitral prosthesis as seen from the left atrial "surgical" approach. Twelve o'clock corresponds to the junction with the aortic valve, while 9 o'clock is set as facing the left atrial appendage. *Dashed lines* represent transesophageal echocardiographic sections as seen from the left ventricle

mitral ring at the junction with the aortic valve, and the 9 o'clock position is defined as facing the left atrial appendage. An eight-quadrant method to easily define the location of the defect(s) has been also developed [25], taking as reference three points: the aortic valve as anterior, the left atrial appendage as anterolateral, and the interatrial septum as anteromedial. In surgical series, mitral PVLs are mostly found on anteromedial and posterolateral quadrants [26], but different locations are also well documented in percutaneous experiences [14]. The interventionalist needs to "map" the position of PVL using the "clock face" or quadrant method, taking into account that in the classic angiographic left anterior oblique (LAO) projection, the valve is seen as it would be regarded from the left ventricle: Fig. 11.1 also demonstrates TEE interrogation planes for each section of the mitral valve in this view.

After carefully confirming the position, size, and shape of PVL(s), the use of echo imaging is essential and integral for the whole procedure and result evaluation. In transseptal approaches, TEE guides the choice of the puncture site, even if some centers routinely use ICE to accomplish this task, and this choice is based on the location of the defect to close. Standard high puncture of the interatrial septum is adequate for pointing toward lateral PVLs, while medial defects are usually more accessible with posterior and lower punctures. As sometimes the anatomy of previously operated patients is somehow distorted or interatrial septum is fibrotic or patched, the puncture site and device crossing should be followed very carefully with both echo and fluoro imaging.

Fluoroscopy should be used with radiation protection in mind, and therefore, it is generally a good idea to start with reduced frame rates (i.e., 7.5/s), raising them if needed. The operator should search and make note of the two basic projections that permit to display the prosthetic valve tangentially (usually a right anterior oblique – RAO) and en face (usually a left anterior oblique – LAO) by fine-adjusting the gantries on the basis of the sewing ring. These projections are key to compare fluoroscopic with echocardiographic images and permit the correct placement of wires and devices through the PVL and not through the prosthesis. Radiologic characteristics, inner and outer dimensions, and leaflet peculiarities of the prosthesis itself are taken into account to correctly interpret the imaging and plan the procedure. With mechanical prostheses, the risk of interfering with the mobile elements during the procedure or after releasing occluder devices is a clue aspect to evaluate, and any problem should be diagnosed intraprocedurally in order to promptly correct it.

Integration with CT scan acquired previously in the diagnostic phase is under evaluation and successfully used in some centers. CT images are overlaid on the fluoro images after defining common reference points and seem to be promising in guiding devices' route during the procedure [27].

11.5 Mitral PVL Closure Techniques

11.5.1 The Antegrade Transseptal Approach

This is the most common approach for mitral PVL closure and will be described in detail with the most common possible variants. After adequate infusion of local anesthetics, the femoral vein is accessed and cannulated to perform echo-guided interatrial septum puncture, choosing the puncture site as previously reported. During the whole procedure, the activated clotting time should be frequently checked and maintained above 250–300 s by heparin administration. Sometimes the use of radiofrequency or electrocautery devices is needed to facilitate the passage through a fibrous or altered septum. Additionally, to safely pass hardened septums and avoid any damage to the left atrial walls, the use of dedicated guidewires able to assume J-shape after crossing, such as the SafeSept transseptal guidewire (Pressure Products Medical Supplies Inc, San Pedro, CA), may be useful and allow more gentle maneuvers. The septum is then dilated as usual and a telescopic system

is advanced through it: most often it is helpful to use a steerable device as the Agilis NxT Introducer (St. Jude Medical, St. Paul, MN), an 8.5 French sheath available in three distal curve sizes to adapt best for pointing toward the PVL site. If the operator prefers, an ordinary angiographic guiding catheter may be directly introduced without the sheath: the choice is based on the anatomy, but usually Judkins right, Hockey stick, or internal mammary are best suited. The advantage of using a steerable sheath consists in the possibility of maneuvering complex telescopic setups to achieve three-dimensional orientation of the devices to fine-direct the selected guidewire across the defect. In fact, catheters of decreasing size can be telescoped together and rotated/advanced independently: typically a 6-Fr 100 cm multipurpose guiding with another 5-Fr longer (125 cm) multipurpose diagnostic or an angled catheter of choice inside [28]. Sometimes, the use of an angled 4-Fr glide catheter (120 cm by Terumo Medical) may be of help in particular situations such as postero-medial PVLs [29]. Anyway, the use of such an equipment usually allows complete probing of the mitral valvular ring.

Of course, the next procedural step consists in crossing the true lumen of the identified PVL with a guidewire in order to gain access to the left ventricular side and proceed. An angled, extra-stiff, and exchange long 0.035″ idrophilic guide (e.g., Glidewire by Terumo Medical) is therefore advanced through the defect with fine rotation by dedicated torquer, while available imaging modalities (RAO/LAO angio views, TEE, or ICE) are carefully monitored to avoid intravalvular crossing. Once ensured correct positioning, the guidewire is advanced deeply into the left ventricle to form a loop avoiding any wall damage, pointing toward the outflow tract, and entering the ascending aorta where it will be finally advanced down to the descending thoracic part in order to the minimize the risk of displacement/loose of position. In some difficult cases, especially when the PVL is particularly small or fissure-like, the use of a regular 0.014″ coronary guidewire may be an option.

After crossing the PVL with the wire, the operator needs to advance the catheter(s) of his telescopic system through the defect: this maneuver should be performed very cautiously due to the risk of losing the position or damaging the structures as relevant force is needed to be accomplished. Therefore, at this point, the need for higher support should be determined, and additional techniques may be used to gain it. Most commonly, an arteriovenous loop is created by accessing the contralateral femoral artery and advancing a snare to capture the wire parked in the descending aorta for externalization and fixing. This technique usually guarantees extremely high support for the rest of the procedure.

The next step depends on the choice of the occluder device(s) to be used; in fact, while smaller devices like the Amplatzer Vascular Plug II (AVP II; St. Jude Medical, St. Paul, MN) up to 12 mm can pass quite easily though a 6-Fr guiding catheter, other devices of larger dimensions usually require catheters of higher diameters. The force required to advance a 6-Fr catheter through the defect may be a good indicator for the size of the device to start with, selecting smaller ones for difficult crossings. On the contrary, when the defect is large, the common choice is to advance a dedicated sheath like a 9- or 10-Fr Amplatzer TorqVue delivery into the

ventricle for bulky occluders. If necessary, the interatrial septum may be further dilated prior crossing with this larger stuff.

The preferred method for defect reduction or closure should be selected and preplanned on the basis of the PVL morphological characteristics, whenever possible. In fact, when the PVL is small and oblong or crescentic, it is often more advisable to account for the use of multiple smaller devices, while round and bigger defects are commonly best addressed with single larger occluders [7]. Figure 11.2 describes the characteristics of the most commonly used commercial devices for PVL closure. Ductal, septal, and muscular VSD occluders from Amplatzer may also
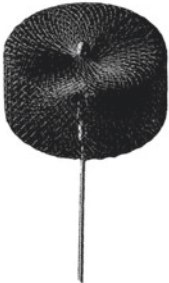
	Amplatzer Vascular Plug Single-lobe device constituted by a nitinol mesh,available in diameters from 4 to 16 mm with lengths of 7-8mm and compatible with 5-8Fr guiding catheters,depending on the diameter.
	Amplatzer Vascular Plug II Multi-lobes Nitinol device that bares multiple contact-points with the target structure.It is available in diameter sizes from 3 to 22mm and its length varies from 6 to 18mm accordingly. Smaller devices accomodate into a 5-Fr guiding,while bigger ones require 9 Fr catheters.
	Amplatzer VSD Occluder Self-expandable Nitinol device made by two discs linked toghether by a connecting waist available in diameter 4-18mm that will accomodate into a 5-9Fr releasing device. It has the advantage of an inner fabric layer for better sealing, but is stiff and may have higher rates of hemolysis.

Fig. 11.2 Commonly used devices for percutaneous paravalvular leak closure. Of note, there are no devices specifically designed for this purpose up to date

	Amplatzer ASD Occluder Self-expandable Nitinol originally designed for atrial septal defect clusere. It has two discs of different diameters (Left>Right) from 16 to 54mm and may be delivered by a 6-12Fr Sheath .
	Amplatzer PDA Occluder Originally designed for Patent Ductus Arteriosus closure,this Nitinol device has a cone - shape, has polyester tissue growth-promoting coating and is easy to deploy. However , the limited sizes of its cylindical body (from 5 to 14mm) represent a limitation.

Fig. 11.2 (continued)

be chosen when appropriate, but due to the higher stiffness of their nitinol structure and bigger sizes, these may be more prone to develop postprocedural hemolysis [14]. Of note, as none of these devices are specifically designed for PVL closure to date, and due to the great anatomical variety of periprosthetic defects, the use of this material remains off-label, and great care should be taken when planning their use.

The next phase is the release of the selected device across the mitral PVL: with the guiding catheter or sheath inside the left ventricle, the distal portion of the occluder is advanced and opens into the cavity. Then the whole system is very carefully retracted against the mitral valvular ring, and the operator starts a controlled release of the device by gently pushing the device while continuing the retraction of the sheath. Collaboration with the echocardiographer is crucial to identify interference with the prosthesis at this stage, when it is possible to readvance the sheath and retry with a different orientation. If manipulation is not sufficient for avoiding valve dysfunction, a different or smaller occluder may be selected and tried. When satisfied with the behavior of the device, the release can be completed proceeding with the retraction of the sheath, and final detach from the delivery system may be accomplished. Of course, the interaction between the occluder type and the PVL anatomy determines the shape that it will assume when released: in particular, the proximal portion may open and extend in the atrial structure or may remain compressed within the PVL channel. In either case, the device stability and adequate occlusion should be carefully assessed prior to final release.

If more than one device are needed, several techniques may be used to avoid losing the position into the left ventricle through the leak. In particular, when a multiple occluder procedure was previously planned, a multiple-guidewire approach may be chosen: a 20-Fr venous femoral introducer is needed to limit access bleeding, and two (or even three) 0.032″ extra-stiff guidewires are advanced through the crossing guiding catheter (typically the 6-Fr multipurpose) that is then carefully removed after wire placement into the left ventricle or aorta if possible. Afterward, two independent telescopic systems (again, typically a 5-Fr diagnostic into a 6-Fr guiding catheters) are mounted onto the wires and then advanced through the leak to permit simultaneous device delivery.

When multiple devices are not planned or the defect is not big enough for the above-described simultaneous-delivery technique, a sequential approach may be used. This time when the hydrophilic wire is in place in the descending aorta, a 0.032″ or 0.035″ stiff wire is advanced into the left ventricle through the guiding catheter. Then, another sheath (typically an 8-Fr Cook Flexor Shuttle Sheath by Cook Medical) is placed into the LV and permits delivery of the first device. The sheath is then removed leaving the occluder attached to its delivery cable and readvanced through the extra-stiff wire, allowing for repeated sequential occluder delivery. Alternatively, an arteriovenous loop can be obtained as previously described, and the tension and support offered by the hydrophilic externalized wire may be controlled by a second operator. Like in the previous technique, a sheath is needed and this time advanced directly onto the arteriovenous loop wire to deliver in sequence the desired number of occluders [7, 30]. For sequential delivery techniques, the need for smaller catheters as the leak gets reduced by the devices should be taken into account. Caution must be used when manipulating the externalized wire for more support, as damages on the vessels, prosthesis impingement, or anatomy distortion may occur and complicate the procedure. A useful tip is to remember controlling the aortic pressure shape, as excessive wire tension induces aortic regurgitation and therefore lowers diastolic pressure: of course, this condition should be eliminated as soon as possible by releasing the tension on the wire. A step-by-step description of the usual transseptal antegrade technique is detailed in Fig. 11.3.

11.5.2 The Transaortic Retrograde Approach

Crossing a mitral PVL may be achieved also accessing the arterial system by the femoral route and proceeding retrogradely following the path aorta-left-ventricle-PVL-left atrium. However, when selecting this approach, the operator commonly faces two major problems: the first is that directing the hydrophilic wire through the PVL from the ventricular cavity most often is difficult and requires acutely angled or retroflexed catheters (e.g., Amplatzer, left coronary bypass) and the second deals with the low support of this configuration that many times requires contralateral venous access, septal puncture with wire snaring, and arteriovenous loop realization. Furthermore, in patients with mechanical aortic prosthesis, this technique is inadvisable. Therefore, this approach is usually considered for aortic rather than mitral PVL treatment.
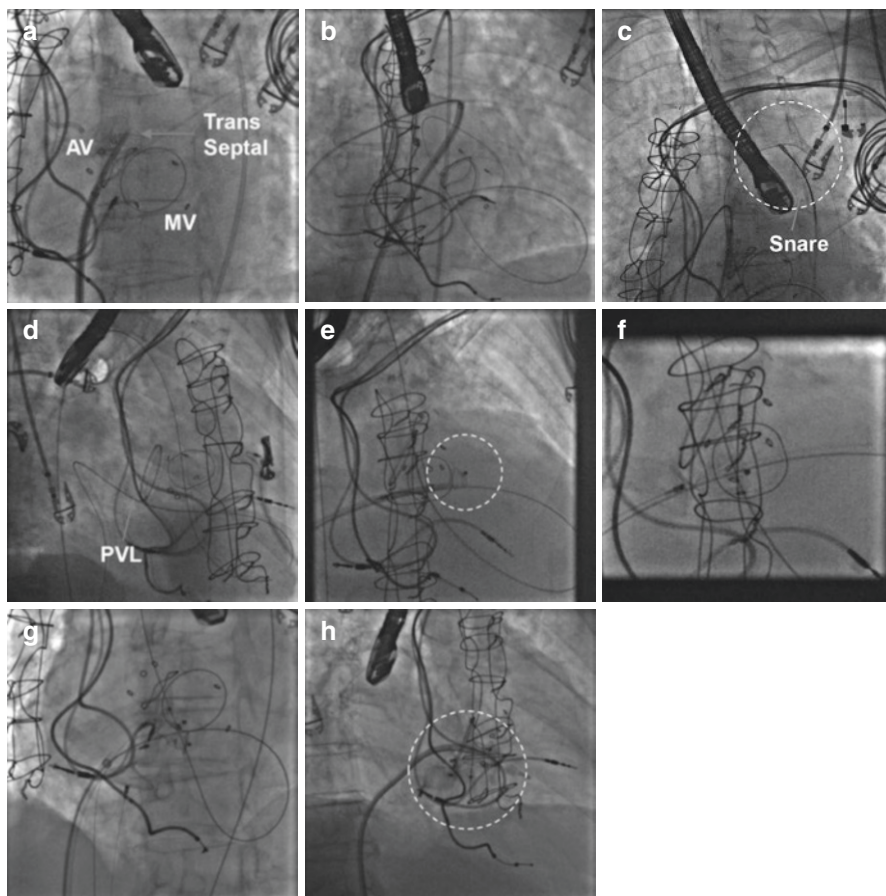
Fig. 11.3 Angiographic detail of key points in transseptal technique mitral PVL closure. (**a**) Transseptal procedure and advancement of the sheath into the left atrium. (**b**) An hydrophilic wire (Terumo Glidewire) was advanced through the PVL into the left ventricle (in this particular case just by the use of a Judkins right catheter instead of a steerable system) and then parked in the ascending aorta. (**c**) A snare device was advanced via the contralateral femoral artery access to capture the wire. (**d**) Arteriovenous loop was completed by wire externalization through the femoral artery in order to obtain a very high support circuit. (**e**) Initial delivery of an Amplatzer Vascular Plug II device through the wide PVL. (**f**) When in place, the single device was not sufficient to determine acceptable result. (**g**) Delivery of a second Amplatzer Vascular Plug II through the PVL with sequential technique. Notice that both devices were still connected with the delivery systems. (**h**) Final angiographic result with the two devices in place. In this case also, a tricuspid valvuloplasty with an Inoue balloon was performed

11.5.3 The Transapical Approach

Percutaneous puncture of the left ventricular apex or surgical access with a minithoracotomy to expose the apex itself and allow for surgical closure/repair represents another possible approach in particular situations, especially in medial PVLs where it is impossible to direct the catheters and wire toward the leak or in patients

with previous positioning of atrial defect closure devices. Sometimes, snaring the wire through the transapical access is the only way to realize the loop to gain adequate support for device placement. In general, for the percutaneous puncture, it is required to limit the introducer size to 5 or 6 French to reduce the risk of apical leak after removal, even if up to 20 % of these procedures require pericardial drainage or other surgical management [31]. Finally, some operators have suggested the possibility of closing the apical puncture via arterial sealing devices (Prostar and ProGlide by Abbott) or by PDA occluder stuff [32].

11.6   Evaluating the Acute Results

The main goal of the procedure is to obtain adequate reduction or interruption (especially in the case of severe hemolytic anemia) of the regurgitant flow through the PVL without altering the function of the leaking prosthesis. Intraoperative TEE should generally address the first question and define the need for additional devices/procedures or device repositioning. Of note, temporary spatial distortions of the interatrial septum may occur while the occluder is attached to its release cable, and therefore, echo images should be interpreted accordingly, trying to minimize device's tethering. Also, it may be of worth measuring the left atrial pressure, particularly the "V" wave, before and after the deployment of the selected occluder to evaluate the acute hemodynamic result. 3D-TEE images and fluoroscopy in different projections should also be acquired to rule out the possibility of prosthetic leaflet impingement before the definitive release of the device and at the end of the procedure.

11.7   Procedural Complications

Prosthetic leaflet impingement may occur in up to 5 % of cases and must be immediately evaluated with fluoroscopy and 3D-TEE: the operator may try recapture and replacement of the occluder, but if this procedure is not effective after multiple attempts, smaller devices or occluders with different shapes should be used instead of the originally selected device. In almost 1 % of cases, the occluder can embolize: trying to avoid this rare but severe complications requires the operator to carefully push and pull the chosen device after placement but before final release. If embolization occurs, snaring techniques may be attempted to achieve occluder removal from the femoral sheath. The procedure may suffer of the risks in common with all the transseptal interventions, if this approach is selected, and therefore, adequate TEE or ICE guidance is of great help. In case an A-V loop is requested for additional support, operators must be aware that excessive tension may cause the wire to damage or even cut vessels or heart structures, while too low force may impede adequate advancements of the devices. Of course, common cares should be applied to prevent and manage vascular access site bleedings. Finally, an activated clotting time of 300 s or more during the procedure is of help in minimizing the risk for thrombotic complications.

11.8 Procedural Outcomes

Percutaneous PVL closure is often a complex procedure, chosen for inoperable symptomatic patients with severe anemia or advanced heart failure and may therefore result as lifesaving in these subjects otherwise doomed to dismal prognosis if leaved under medical therapy alone. Although success rates of mitral PVL closure are slightly inferior compared to aortic procedures, available data suggest that the procedure is feasible and the need for emergency/urgent surgery is very low (less than 1%). Stroke occurs in around 3% of patients and vascular complications/bleeding in 5% of cases. Some authors define as procedural success a residual leakage of 1+ or less at TEE evaluation [15, 33], and this goal is generally achieved in 77–90% of cases. The degree of residual mitral regurgitation seems to be a significant predictor of the long-term outcomes of the patients. A recent meta-analysis reported that even reducing PVL by ≥1 grade of regurgitation seems to be associated with reduced cardiac mortality and improved functional class in respect to patients with failed procedures [22]. From the limited published series involving very compromised patients, mortality rate at 30 days varies between 5% and 9%, and 3-year survival seems to be around 65%, with hemolysis persistent reduction in around a half of subjects and improvement of heart failure in >70% of cases [14, 15, 22, 33].

Conclusions

Mitral PVL closure represents one of the most challenging procedures for the interventional cardiologist, both because of the particularly severe conditions of the patients undergoing this intervention and the technical difficulties requiring multiple skills in vascular and structural fields. In particular, correct execution and interpretation of advanced multimodal imaging is crucial before and during the procedure. Therefore, multidisciplinary collaboration (the "Heart Team") is essential for procedural success and for the growth of all the operators, individually and as a team. Percutaneous PVL closure is a feasible and relatively safe procedure right now even if it's oriented mainly to unoperable patients and limited long-term data are available. Future directions will include larger series and improved comprehension of the hemodynamic and prognostic impact of PVL closure owing to better patient selection and technology advancements. In fact, while today operators must rely on catheters and occluders aimed to other objectives, the development of specifically designed devices will improve their practice of tomorrow.

References

1. Iung B, Baron G, Butchart EG, Delahaye F, Gohlke-Barwolf C, Levang OW, Tornos P, Vanoverschelde JL, Vermeer F, Boersma E, Ravaud P, Vahanian A. A prospective survey of patients with valvular heart disease in Europe: the euro heart survey on valvular heart disease. Eur Heart J. 2003;24:1231–43.

2. Iung B, Nicoud-Houel A, Fondard O, Akoudad H, Haghighat T, Brochet E, Garbarz E, Cormier B, Baron G, Luxereau P, Vahanian A. Temporal trends in percutaneous mitral commissurotomy over a 15-year period. Eur Heart J. 2004;25:701–7.

3. Ionescu A, Fraser AG, Butchart EG. Prevalence and clinical significance of incidental para-prosthetic valvar regurgitation: a prospective study using transoesophageal echocardiography. Heart. 2003;89:1316–21.

4. Rallidis LS, Moyssakis IE, Ikonomidis I, Nihoyannopoulos P. Natural history of early aortic paraprosthetic regurgitation: a five-year follow-up. Am Heart J. 1999;138(2 pt 1):351–7.

5. Hwang HY, Choi JW, Kim HK, Kim KH, Kim KB, Ahn H. Paravalvular leak after mitral valve replacement: 20-year follow-up. Ann Thorac Surg. 2015;100(4):1347–52.

6. Englberger L, Schaff HV, Jamieson WR, Kennard ED, Im KA, Holubkov R, Carrel TP, AVERT Investigators. Importance of implant technique on risk of major paravalvular leak (PVL) after St. Jude mechanical heart valve replacement: a report from the Artificial Valve Endocarditis Reduction Trial (AVERT). Eur J Cardiothorac Surg. 2005;28:838–43.

7. Eleid MF, Cabalka AK, Malouf JF, Sanon S, Hagler DJ, Rihal CS. Techniques and outcomes for the treatment of paravalvular leak. Circ Cardiovasc Interv. 2015;8(8):e001945.

8. Misawa Y, Saito T, Konishi H, et al. When and how does nonstructural mechanical prosthetic heart valve dysfunction occur? Jpn J Thorac Cardiovasc Surg. 2003;51:355–60.

9. Tarantini G, Gasparetto V, Napodano M, Fraccaro C, Gerosa G, Isabella G. Valvular leak after transcatheter aortic valve implantation: a clinician update on epidemiology, pathophysiology and clinical implications. Am J Cardiovasc Dis. 2011;1(3):312–20.

10. Jerez-Valero M, Urena M, Webb JG, Tamburino C, Munoz-Garcia AJ, Cheema A, Dager AE, Serra V, Amat-Santos IJ, Barbanti M, Immè S, Alonso Briales JH, Al Lawati H, Benitez LM, Cucalon AM, Garcia del Blanco B, Revilla A, Dumont E, Barbosa Ribeiro H, Nombela-Franco L, Bergeron S, Pibarot P, Rodés-Cabau J. Clinical impact of aortic regurgitation after trans-catheter aortic valve replacement: insights into the degree and acuteness of presentation. JACC Cardiovasc Interv. 2014;7(9):1022–32.

11. Buzzatti N, Taramasso M, Latib A, Denti P, Guidotti A, Alfieri O, Maisano F. Transcatheter mitral repair and replacement: state of the art and future directions. J Heart Valve Dis. 2014;23(4):492–505.

12. Cheung A, Webb J, Verheye S, Moss R, Boone R, Leipsic J, Ree R, Banai S. Short-term results of transapical transcatheter mitral valve implantation for mitral regurgitation. J Am Coll Cardiol. 2014;64(17):1814–9.

13. Cho IJ, Hong GR, Lee S, Byung-Chul C, Ha JW, Chung N. Predictors of prognosis in patients with mild to moderate paravalvular leakage after mitral valve replacement. J Card Surg. 2014;29(2):149–54.

14. Ruiz CE, Jelnin V, Kronzon I, Dudiy Y, Del Valle-Fernandez R, Einhorn BN, Chiam PT, Martinez C, Eiros R, Roubin G, Cohen HA. Clinical outcomes in patients undergoing percuta-neous closure of periprosthetic paravalvular leaks. J Am Coll Cardiol. 2011;58:2210–7.

15. Sorajja P, Cabalka AK, Hagler DJ, Rihal CS. Percutaneous repair of paravalvular prosthetic regurgitation: acute and 30-day outcomes in 115 patients. Circ Cardiovasc Interv. 2011;4:314–21.

16. Kronzon I, Sugeng L, Perk G, Hirsh D, Weinert L, Garcia Fernandez MA, Lang RM. Real-time 3-dimensional transesophageal echocardiography in the evaluation of post-operative mitral annuloplasty ring and prosthetic valve dehiscence. J Am Coll Cardiol. 2009;53:1543–7.

17. Kliger C, Eiros R, Isasti G, Einhorn B, Jelnin V, Cohen H, Kronzon I, Perk G, Fontana GP, Ruiz CE. Review of surgical prosthetic paravalvular leaks: diagnosis and catheter-based clo-sure. Eur Heart J. 2013;34:638–48.

18. Zoghbi WA, Chambers JB, Dumesnil JG, Foster E, Gottdiener JS, Grayburn PA, Khandheria BK, Levine RA, Marx GR, Miller Jr FA, Nakatani S, Quinones MA, Rakowski H, Rodriguez LL, Swaminathan M, Waggoner AD, Weissman NJ, Zabalgoitia M. Recommendations for evaluation of prosthetic valves with echocardiography and doppler ultrasound: a report from

the American society of echocardiography's guidelines and standards committee and the task force on prosthetic valves. J Am Soc Echocardiogr. 2009;22:975–1014.

19. Jelnin V, Co J, Muneer B, Swaminathan B, Toska S, Ruiz CE. Three dimensional ct angiography for patients with congenital heart disease: scanning protocol for pediatric patients. Catheter Cardiovasc Interv. 2006;67:120–6.

20. Hundley WG, Li HF, Willard JE, Landau C, Lange RA, Meshack BM, Hillis LD, Peshock RM. Magnetic resonance imaging assessment of the severity of mitral regurgitation. Comparison with invasive techniques. Circulation. 1995;92:1151–8.

21. Sherif MA, Abdel-Wahab M, Beurich HW, Stocker B, Zachow D, Geist V, Tolg R, Richardt G. Haemodynamic evaluation of aortic regurgitation after transcatheter aortic valve implantation using cardiovascular magnetic resonance. EuroIntervention. 2011;7:57–63.

22. Millán X, Skaf S, Joseph L, Ruiz C, García E, Smolka G, Noble S, Cruz-González I, Arzamendi D, Serra A, Kliger C, Sia YT, Asgar A, Ibrahim R, Jolicœur EM. Transcatheter reduction of paravalvular leaks: a systematic review and meta-analysis. Can J Cardiol. 2015;31(3):260–9.

23. Perloff JK, Roberts WC. The mitral apparatus. Functional anatomy of mitral regurgitation. Circulation. 1972;2:227–39.

24. Krishnaswamy A, Tuzcu EM, Kapadia SR. Paravalvular leak closure. In: Rogers J, Lasala J, editors. Interventional procedures for structural heart disease. Philadelphia: Elsevier; 2014.

25. Spoon DB, Malouf JF, Spoon JN, Nkomo VT, Sorajja P, Mankad SV, Lennon RJ, Cabalka AK, Rihal CS. Mitral paravalvular leak: description and assessment of a novel anatomical method of localization. JACC Cardiovasc Imaging. 2013;6:1212–4.

26. De Cicco G, Russo C, Moreo A, Beghi C, Fucci C, Gerometta P, et al. Mitral valve periprosthetic leakage: anatomical observations in 135 patients from a multicentre study. Eur J Cardiothorac Surg. 2006;30:887–91.

27. Krishnaswamy A, Tuzcu EM, Kapadia SR. Three-dimensional computed tomography in the cardiac catheterization laboratory. Catheter Cardiovasc Interv. 2011;77:860–5.

28. Rihal CS, Sorajja P, Booker JD, Hagler DJ, Cabalka AK. Principles of percutaneous paravalvular leak closure. JACC Cardiovasc Interv. 2012;5:121–30.

29. Yuksel UC, Tuzcu EM, Kapadia SR. Percutaneous closure of a postero-medial mitral paravalvular leak: the triple telescopic system. Catheter Cardiovasc Interv. 2011;77:281–5.

30. Krishnaswamy A, Kapadia SR, Tuzcu EM. Percutaneous paravalvular leak closure – imaging. Techniques and outcomes. Circ J. 2013;77:19–27.

31. Pitta SR, Cabalka AK, Rihal CS. Complications associated with left ventricular puncture. Catheter Cardiovasc Interv. 2010;76:993–7.

32. Jelnin V, Dudiy Y, Einhorn BN, Kronzon I, Cohen HA, Ruiz CE. Clinical experience with percutaneous left ventricular transapical access for interventions in structural heart defects a safe access and secure exit. J Am Coll Cardiol Intv. 2011;4:868–74.

33. Sorajja P, Cabalka AK, Hagler DJ, Rihal CS. The learning curve in percutaneous repair of paravalvular prosthetic regurgitation: an analysis of 200 cases. JACC Cardiovasc Interv. 2014;7:521–9.

Difficult Cases and Complications from Catheterization Laboratory: MitraClip Therapy in a Patient with Lack of Leaflet Coaptation

12

Marianna Adamo, Claudia Fiorina, Salvatore Curello, Ermanna Chiari, Giuliano Chizzola, Elena Pezzotti, Rosa Mastropierro, and Federica Ettori

12.1 Clinical History

This is the case of a 43-year-old male with history of hypertension, insulin-dependent diabetes, and cocaine abuse. On June 2010, he was admitted at our department because of an inferior acute myocardial infarction (AMI) treated with primary percutaneous coronary intervention (PCI) on the right coronary artery. A chronic occlusion of the distal left anterior descending artery was detected without indication to coronary revascularization. Two days after the primary PCI, a cardio-embolic stroke occurred due to a left atrial thrombosis.

The echocardiography examination, performed 2 months later, showed a postinfarction dilated cardiomyopathy (EDV 183 ml and EDD 70 mm) with severe left ventricular dysfunction (LVEF 29 %) (Fig. 12.1) and severe functional mitral regurgitation (MR) (Fig. 12.2 and Video 12.1) due to a central jet (A2-P2) with annulus dilation (40×44 mm) and lack of leaflet coaptation mainly owing to a posterior mitral leaflet retraction (Fig. 12.3 and Video 12.2). A severe pulmonary hypertension was estimated with a systolic pulmonary artery pressure of roughly 80 mmHg.

There was no indication to cardiac resynchronization therapy (CRT), therefore a monocameral ICD was implanted on August 2010.

M. Adamo • C. Fiorina • S. Curello • E. Chiari • G. Chizzola • E. Pezzotti • R. Mastropierro F. Ettori (✉)
Cardiothoracic Department, Spedali Civili, Piazzale Spedali Civili, 1, 25100 Brescia, Italy
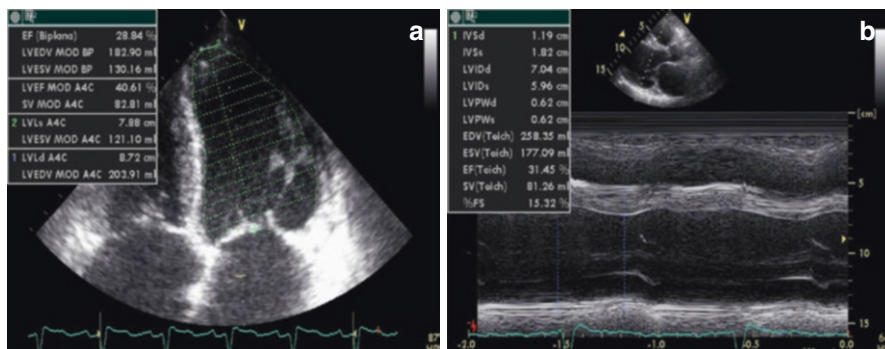e-mail: fedettori@libero.it

Fig. 12.1 Left ventricle volumes and ejection fraction (**a**) and left ventricle diameters (**b**). A two-dimensional transthoracic echocardiography at baseline shows a postinfarction dilated cardiomyopathy with severe left ventricle dysfunction and dilation

Fig. 12.2 Mitral regurgitation. Color Doppler examination reveals severe mitral regurgitation (4+) with a central jet extending to the atrial roof
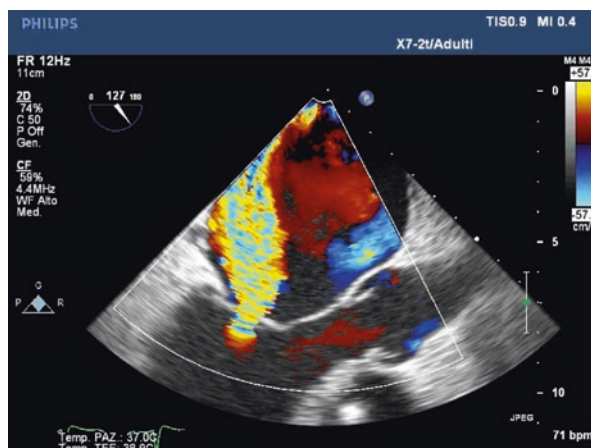
No symptoms occurred until July 2011 when the patient was admitted at our department due to acute heart failure.

Although an optimal medical therapy achievement, in the following months, a functional NYHA class III–IV persisted and hospitalizations due to acute heart failure occurred. In particular, five hospitalizations for a total of 78 days of in-hospital stay were counted between July 2011 and February 2012.

The right cardiac catheterization confirmed a severe postcapillary pulmonary hypertension (systolic and diastolic pulmonary pressure of 80 and 43 mmHg, respectively; capillary wedge pressure of 51 mmHg) and a severe reduction of cardiac output (1.8 l/min/m²).

A severe disorder of functional status was evident at the cardiopulmonary test with a peak VO_2 of 7.9 mL/min/Kg and a VE/VCO_2 slope of 56. The distance walked at the 6-min walking test (6MWT) was 348 m.

Fig. 12.3 Baseline coaptation. Baseline echocardiography shows complete absence of leaflet coaptation
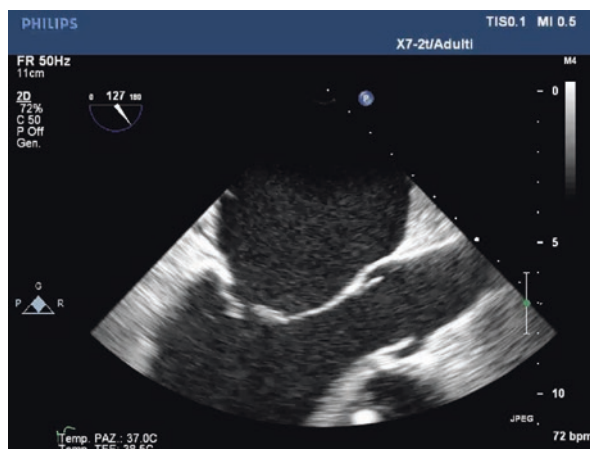
It was not possible to include the patient in waiting list for heart transplantation owing to the history of cocaine abuse and previous stroke. Because of the high surgical risk, the Heart Team decided, on February 2012, to consider the percutaneous mitral valve repair with MitraClip system despite the complete absence of leaflet coaptation.

12.2 Preparation to MitraClip Procedure

Pharmacological agents and mechanical support were used to restore the leaflet coaptation allowing MitraClip therapy.

The patient was treated with intravenous diuretic and vasodilator drugs in order to reduce the left ventricle preload. In particular, 500 mg/day of furosemide and 2 ml/h of nitrate were infused for 48 h. However, no improvement of leaflet coaptation was observed.

The second step was the administration of an inotropic support (enoximone 5γ/Kg/min) in order to modify the ventricle geometry increasing the contractility. Nevertheless, after 24 h, it was still not enough.

As a last step, an intra-aortic balloon pump (IABP) was implanted in order to further decrease left ventricle pre- and post-load; 24 h later, the echocardiography showed a coaptation depth of 20 mm and a coaptation length less than 2 mm but enough to try a leaflet grasping with the MitraClip device.

12.3 MitraClip Procedure

The procedure was performed with IABP and enoximone infusion.

At the transesophageal echocardiography, after anesthesia induction, a coaptation length of 2 mm and a coaptation depth of 18 mm were detected (Fig. 12.4 and Video 12.3).

Fig. 12.4 Coaptation after drugs, IABP, and anesthesia. A sufficient coaptation length is detected at the TEE performed after enoximone, IABP placement, and anesthesia induction
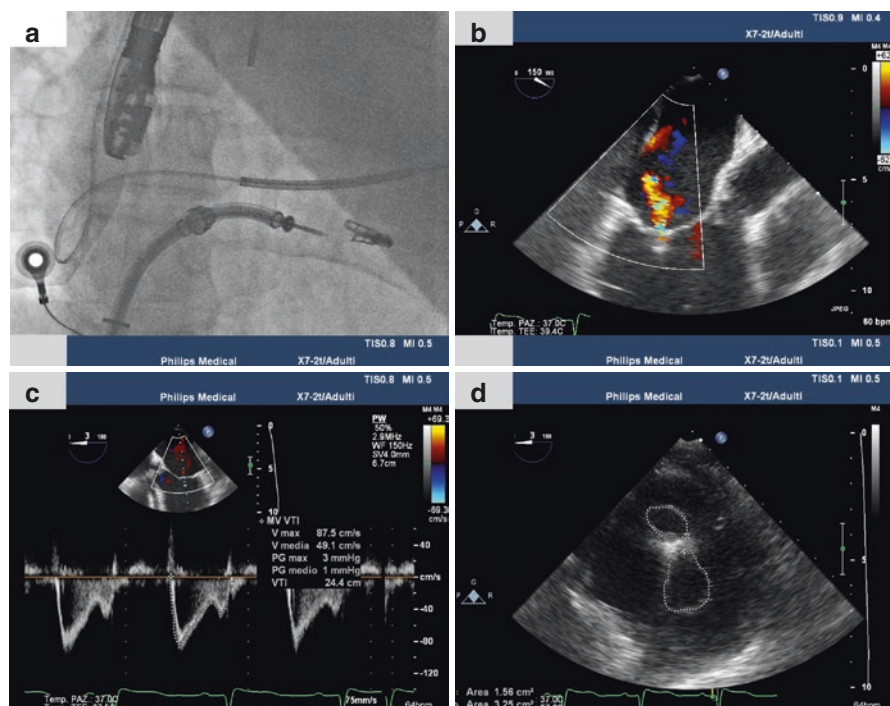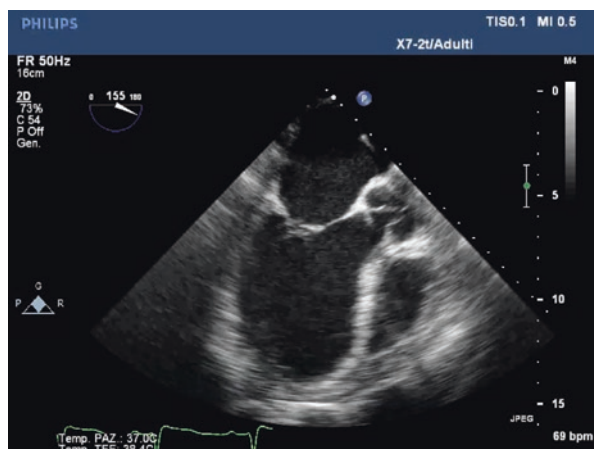
Fig. 12.5 Results after first clip placement. The fluoroscopic snapshots show the successful implantation of the first clip (**a**) with a residual moderate mitral regurgitation (**b**), a low mean gradient (**c**), and a large double mitral orifice (**d**) at the echocardiography

A first clip was implanted in central position, between A2 and P2 leaflets, resulting in a moderate regurgitation with a mitral valve area >4 cm^2 and a mean transvalve gradient of 1 mmHg (Fig. 12.5). Therefore, a second clip was placed, very close and lateral to the first one, with an excellent final result: trivial MR, mean
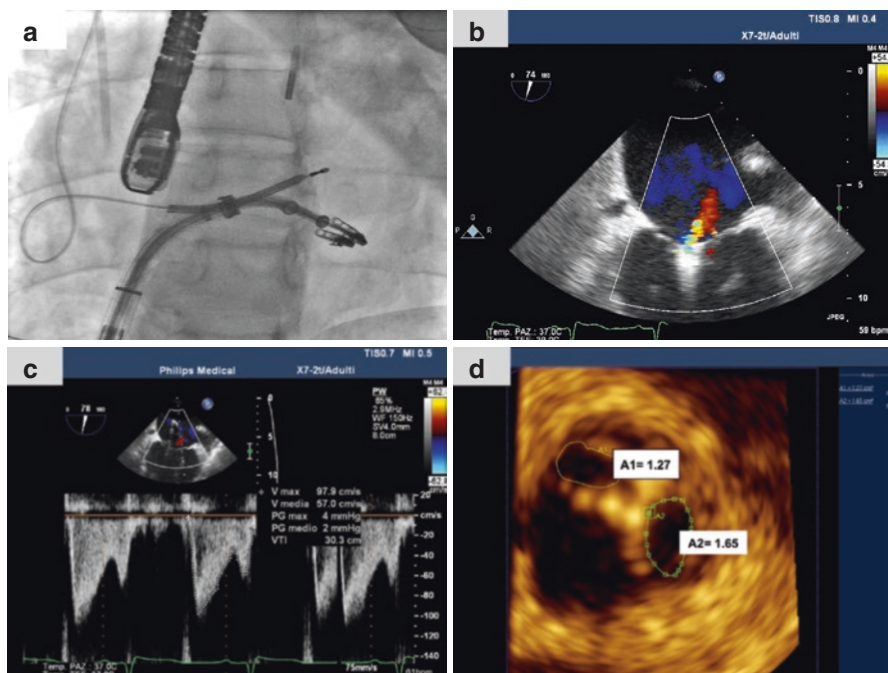
Fig. 12.6 Final result. The fluoroscopic snapshots show the successful implantation of the second clip very close and lateral to the first one (**a**) with a residual trivial mitral regurgitation (**b**) and absence of mitral stenosis (**c**, **d**) at the echocardiography

gradient 2 mmHg, valve area about 3 cm^2 (Fig. 12.6), and normalization of S/D ratio on pulmonary veins.

No complication occurred during the procedure. The patient was weaned from IABP and pharmacological supports at 2 and 6 days, respectively. He was discharged 9 days after MitraClip implantation on functional NYHA class II and with a mild MR.

12.4   Follow-Up

The clinical, echocardiographic, and hemodynamic parameters detected during the follow-up and compared with the baseline are displayed in Table 12.1.

At 1-month follow-up, the patient was on functional NYHA class I. The echocardiographic evaluation showed mild MR with significant reduction of systolic pulmonary artery pressure.

A significant improvement of functional status and hemodynamic parameters was noted at cardiopulmonary test and right cardiac catheterization performed after 1 year from the procedure.

A reverse remodeling with slight improvement of LVEF was observed at 2-year follow-up.

Table 12.1 Clinical, echocardiographic, and hemodynamic parameters at baseline and follow-up

	Pre-MitraClip	Follow-up		
		1 month	1 year	2 years
Echocardiography				
MR (+)	4	1	1	1
EROA (mm^2)	45	12	13	11
LVEF (%)	29	32	33	41
EDD (mm)	70	67	67	67
Left atrial area (cm^2)	35	27	23	23
sPAP (mmHg)	80	40	36	30
NYHA (class)	IV	I	I	I
Hospitalizations (days)	78	0	0	0
6MWT (meters)	348	441	460	458
Cardiopulmonary test				
Peak VO$_2$ (ml/min/Kg)	7.9	–	12.2	15.3
VE/VCO$_2$ slope	56	–	33.6	36
Cardiac catheterization				
PAP (mmHg)	80/43	–	32/11	–
CWP (mmHg)	51	–	9	–
Cardiac index (l/min/m^2)	1.8	–	2.2	–

EDD end-diastolic volume, *EROA* effective regurgitant orifice area, *LVEF* left ventricle ejection fraction, *MR* Mitral regurgitation, *6MWT* 6-min walking test, *NYHA* New York Heart Association, *sPAP* systolic pulmonary artery pressure, *CWP* capillary wedge pressure

Mitral regurgitation degree (mild) and functional NYHA class (I) have been stable until the recent 3-year follow-up. No heart failure hospitalizations occurred after MitraClip implantation.

12.5   Discussion

In patients with functional mitral regurgitation (MR) due to severe annulus and/or left ventricle dilation, the mitral leaflet coaptation could be absent or incomplete and/or the tethering toward the papillary muscles extreme.

They are usually patients on refractory, advanced, or end-stage heart failure who, according with the most recent evidence, could benefit by percutaneous mitral valve repair with MitraClip system [1–3]. However, if the coaptation length is less than 2 mm and/or the coaptation depth more than 11 mm, the EVEREST criteria would limit the MitraClip treatment [4, 5].

Recently, Attizzani et al. [6] reported similar 1-year safety and efficacy end points in patients with expanded echocardiographic characteristics (LVEF <25 %, EDD >55 mm, coaptation depth <11 mm or flail width ≥15 mm) compared with those who completely fulfill the EVEREST criteria.

Nevertheless, the coaptation length remains a broad issue and one of the anatomical criteria, which still limit the percutaneous mitral valve repair with MitraClip device.

In our experience, it could be possible to restore the mitral leaflet coaptation on patients with coaptation length absent or less than 2 mm and/or with insufficient coaptation depth, yielding them a chance to be treated.

The reported case is just one out of a series of patients with incomplete or missing mitral leaflet coaptation that we have systematically treated using MitraClip device with positive results.

Pharmacological and mechanical supports, reducing left ventricle pre- and/or post-load and increasing cardiac contractility, have an essential role to improve leaflet coaptation and prepare the valve apparatus to the grasping.

12.5.1 Drugs

Patients should undergo MitraClip procedure as to compensate as possible. However, they could be on refractory heart failure (like in the above case), and the continuous infusion of diuretic drug at high dose (i.e., furosemide >250 mg/day) could be necessary in order to reduce the cardiac overload. Continuous infusion of nitrate could be useful to decrease the left ventricle preload and the pulmonary artery pressure. Low doses of nitroprusside, compatibly with the systemic blood pressure, working even on artery vessels, would reduce the left ventricle post-load. Dopamine, dobutamine, or, if concomitant beta-blocker therapy, enoximone could be used in order to increase the left ventricle contractility and to induce a temporary remodeling of mitral valve apparatus, which could improve the leaflet coaptation.

Diuretics, vasodilators, and inotropic agents may be used in association, if tolerated.

12.5.2 Intra-aortic Balloon Pump

When the pharmacological agents are ineffective to allow the leaflet coaptation, a mechanical support could be used. The IABP decreases both pre- and post-load reducing oxygen consumption and left ventricle wall tension and increasing diastolic and decreasing systolic pressures. Its role could be essential, especially in patients on refractory heart failure. We usually wait at least 24 h to detect any effect.

12.5.3 Anesthesia

The peripheral vasodilation and the hypotension induced by anesthesia during the MitraClip intervention could be useful to improve the leaflet coaptation. Often, if the coaptation length is present but incomplete and/or the coaptation length insufficient, the anesthesia could be enough to allow a comfortable grasping.

12.5.4 Weaning

A gradual weaning from pharmacological and/or mechanical supports is advisable after the procedure in order to allow left ventricle restoration avoiding suddenly overload.

Conclusions

Pharmacological and mechanical supports could be used to improve mitral leaflet coaptation in patients with severe MR and coaptation length ≤2 mm and/or coaptation depth >11 mm, who would be otherwise excluded from MitraClip treatment.

References

1. Franzen O, van der Heyden J, Baldus S, et al. MitraClip® therapy in patients with end-stage systolic heart failure. Eur J Heart Fail. 2011;13(5):569–76.
2. Neuss M, Schau T, Schoepp M, et al. Patient selection criteria and midterm clinical outcome for MitraClip therapy in patients with severe mitral regurgitation and severe congestive heart failure. Eur J Heart Fail. 2012;5:786–95.
3. Adamo M, Barbanti M, Curello S, et al. Effectiveness of MitraClip therapy in patients with refractory heart failure. J Interv Cardiol. 2015;28(1):61–8.
4. Feldman T, Kar S, Rinaldi M, et al. Percutaneous mitral repair with the MitraClip system: safety and midterm durability in the initial EVEREST (Endovascular Valve Edge-to-Edge Repair Study) cohort. J Am Coll Cardiol. 2009;54:686–94.
5. Feldman T, Foster E, Glower DD, for the EVEREST II Investigators, et al. Percutaneous repair or surgery for mitral regurgitation. N Engl J Med. 2011;364:1395–406.
6. Attizzani GF, Ohno Y, Capodanno D, et al. Extended use of percutaneous edge-to-edge mitral valve repair beyond EVEREST (Endovascular Valve Edge-to-Edge Repair) criteria: 30-day and 12-month clinical and echocardiographic outcomes from the GRASP (Getting Reduction of Mitral Insufficiency by Percutaneous Clip Implantation) registry. JACC Cardiovasc Interv. 2015;8(1 Pt A):74–82.

Difficult Cases and Complications from Catheterization Laboratory: A Case of Mitral Cleft

13

A.S. Petronio and C. Giannini

13.1 Background

The mitral valve is a complex structure with two leaflets which vary in shape and length usually named anterior and posterior. During systole, the leaflets meet to close the ventricle, the line of coaptation, which occurs along the leaflet edge more similar to a smile. According to the Carpentier's definition, the anterior and posterior leaflets are divided in three scallops (A1, A2, A3 and P1, P2, P3) one opposite to the other from the medial commissure to the lateral one. Each scallop is separated from the other by an indentation called more commonly cleft, two for the anterior and two for the posterior leaflet. These indentations are usually more pronounced in the posterior leaflet than in the anterior, where, on the other hand, congenital pathological clefts are more frequently associated with congenital atrioventricular septal defect and more complex congenital disease in young subjects [1].

A wide variability in the number and position of standard clefts has been described, ranging from small ones that only help to recognize the scallops to others more evident and deep and involved in the mechanism of regurgitation [2]. These so-called deviant cleft needs to be recognized to allow an exact evaluation of the disease and its resolution.

Three-dimensional transesophageal echocardiography (3D TEE) gives a complete visualization of the mitral apparatus in any plane orientation. During clinical evaluation, screening 3D TEE helps in defining the extent and location of the pathology and the severity of valvular dysfunction [3]; during surgery, it allows the cardiac surgeons to visualize the location and extent of complex mitral valve lesions, commissural pathology, and clefts. Nowadays, 3D TEE improved success rate not only during mitral surgical repair but also with percutaneous valve procedure [4].

A.S. Petronio, MD, FESC (✉) • C. Giannini, MD, PhD
Dipartimento Cardiotoracico e Vascolare, S.D.Emodinamica, AOUP, Pisa 56124, Italy
e-mail: as.petronio@gmail.com

During the first experiences with percutaneous mitral valve repair by MitraClip, the presence of a cleft was considered as a complex anatomy not suitable for percutaneous treatment. In the last years, however, there have been a few reports of cases demonstrating the feasibility of mitral clipping despite the presence of a cleft [5].

This is a description of a case of isolated cleft in a subject with severe mitral regurgitation and left ventricular dysfunction.

13.2   Case Description

An 81-year-old man, who underwent coronary artery bypass in 2007, presented at our hospital with severe dyspnea [New York Heart Association (NYHA) grade III]. The medical history included atrial fibrillation, arterial hypertension, hyperlipidemia, cerebrovascular disease, severe chronic renal failure with right atrophic kidney, and stented left renal artery. He also had a single-chamber ICD implanted in 2008 for ventricular arrhythmia.

Transthoracic echocardiography (TTE) showed a severe functional mitral regurgitation (vena contracta 0.7 cm) due to symmetric mitral leaflet tethering. An enlarged left ventricle (LV) (end-diastolic and end-systolic diameter 70 mm and 49 mm, respectively) with reduced ejection fraction (EF 28 %) and a severely elevated systolic pulmonary pressure (sPAP 60 mmHg) were also found.

As first step, the patient was treated with optimal medical therapy according to the current ESC guidelines for the management of valvular heart disease in chronic heart failure (diuretics, beta-blockers, aldosterone antagonists). ACE inhibitors were excluded because of renal artery stenosis.

In the following months, the clinical status progressively worsened to NYHA class grade III, with several hospitalizations for decompensated heart failure. Two independent surgeons refused redo surgery because of prohibitive risk (Logistic EuroScore 66 %, STS Score 13 %). Therefore, he was referred for a less invasive approach using the percutaneous repair procedure. Two-dimensional and 3D TEE was performed to investigate mitral valve morphology. Two TEEs confirmed a severe mitral regurgitation due to deep symmetric tethering with a central jet and two commissural jets (Fig. 13.1). The 3D TEE visualized the presence of a cleft in the P2 region of the posterior mitral valve leaflet (Fig. 13.2).

In particular, the central jet did not arise from inside the cleft in the posterior leaflet, but rather from its free edge.

13.3   Procedure Description

From the beginning, we planned to deploy two clips both for the increased annulus diameters (SL: 38 mm; IC: 37 mm) with borderline coaptation and for the presence of a deep cleft in the P2 region of the posterior mitral valve leaflet. As no jet was coming from the indentation of the cleft, we decided to position the clips on both sides of mitral cleft and perpendicular to the rim to avoid any distortion of the leaflet
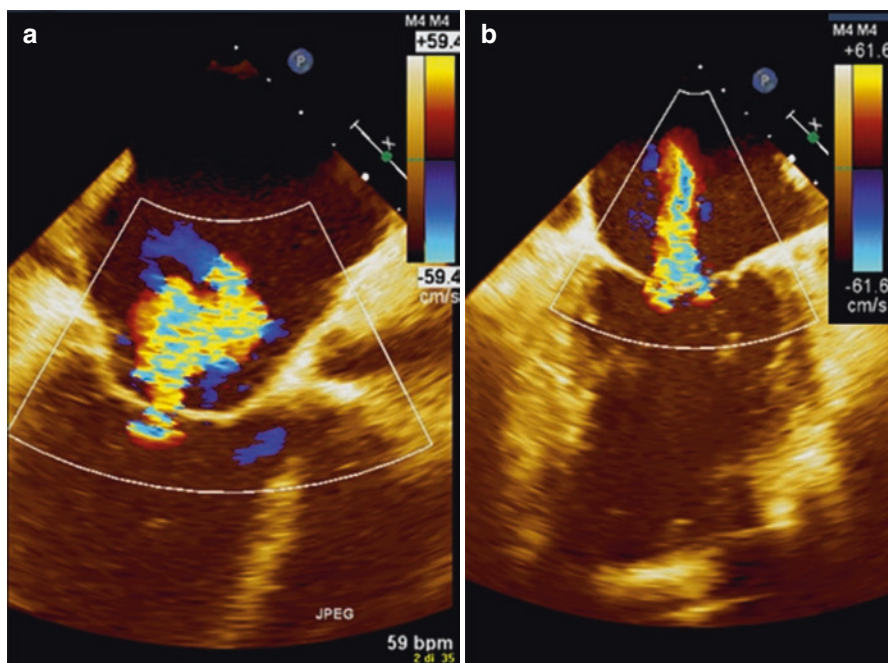
Fig. 13.1 Two-dimensional TEE images showing the presence of a severe mitral regurgitation due to deep symmetric tethering with a central jet (**a**) and two commissural jets (**b**)
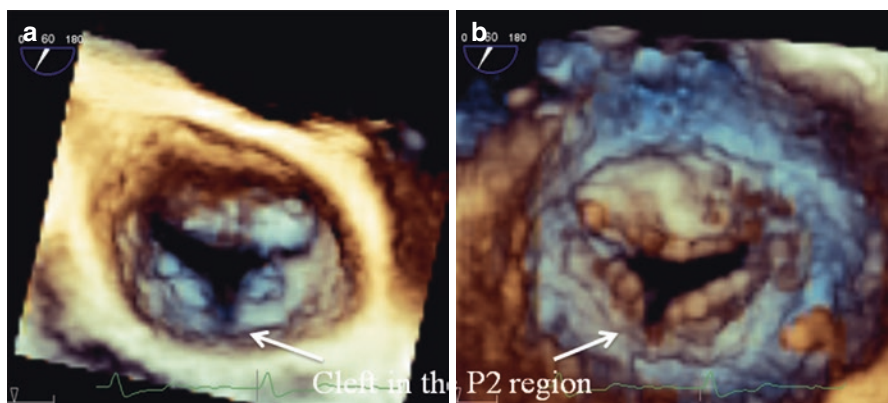
Fig. 13.2 Three-dimensional TEE images showing the presence of a deep cleft in the P2 region of the posterior mitral valve leaflet from the atrial (**a**) and ventricular (**b**) view

and the consequent risk of increased regurgitation (Fig. 13.3). The presence of a jet inside the cleft could favor a "reverse V" shape of the two clips.

The procedure was performed under general anesthesia and was guided by TEE (two- and three-dimensional) and fluoroscopy (Figs. 13.4 and 13.5). At the end of

Fig. 13.4 Three-dimensional TEE image showing implantation of the first clip at the P2/P3 region (**a**). Two-dimensional TEE image showing the origin of a moderate residual jet lateral to the first clip (**b**)

procedure, TEE demonstrated mild residual mitral regurgitation with the two clips placed on both sides of the mitral cleft (Fig. 13.6).

Procedure lasted less than 2 h, and the patient was extubated immediately in the cath lab and transferred to the cardiac intensive care unit for one night. No adverse events occurred during hospital stay. TTE confirmed a mild residual MR with a
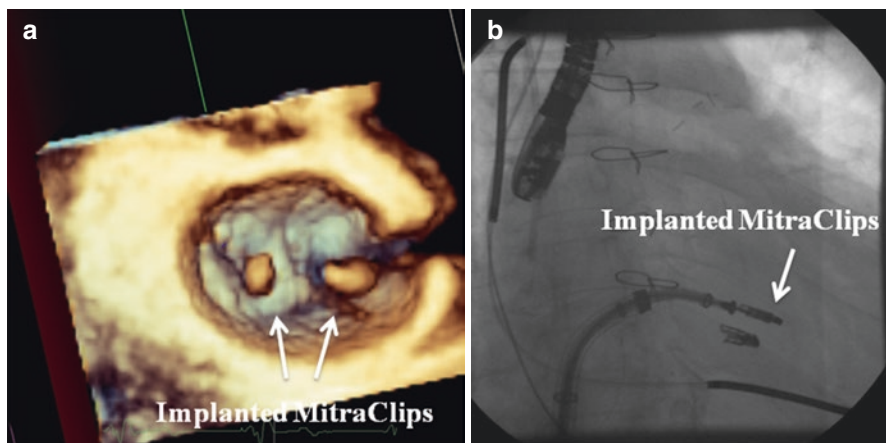
Fig. 13.5 Three-dimensional TEE image of the final result showing the two implanted clips on both sides of the mitral cleft (**a**). Fluoroscopic result after implantation of two clips (**b**)
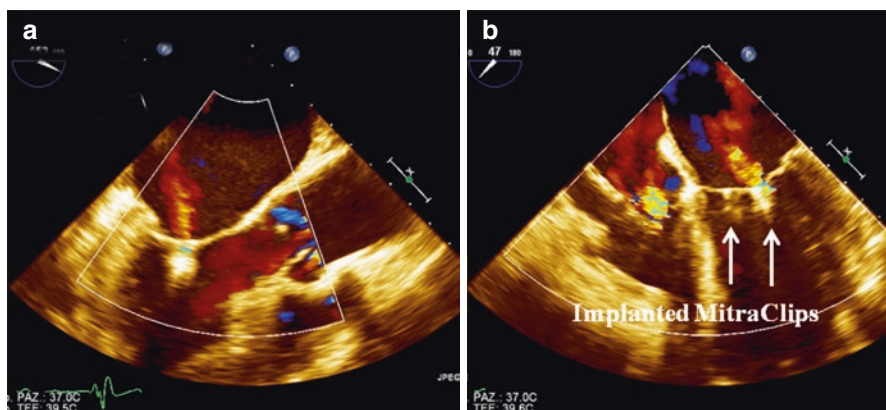
Fig. 13.6 Two-dimensional TEE images showing a significant reduction in the mitral regurgitation jet after implantation of two clips

concomitant slight improvement in LV function (EF 33 %) and a significant reduction in systolic pulmonary arterial pressure (sPAP 45 mmHg).

Three months after the procedure, the patient remained free of any cardiovascular events with improved NYHA class grade II. He reached 526 m during the SMWT and 30 points in the MLHF questionnaire. On physical examination, the patient showed mild peripheral edema. Echocardiography confirmed the stability of mitral regurgitation and LV function. BNP went down to 865 pg/ml.

At 12-month follow-up, the clinical and echocardiographic status was stable: NYHA class II, SMWT 530 m, MLHF questionnaire 30 points, mild residual mitral regurgitation, LV-EF 33 %, and sPAP 40 mmHg.

Conclusions

This case confirms the possibility to correct a severe mitral regurgitation in the presence of a cleft with the MitraClip procedure by the guidance of 3D echocardiography that determines the correct technical position of the two grasp and avoids any leaflet distortion.

References

1. Séguéla PE, Houyel L, Acar P. Congenital malformations of the mitral valve. Arch Cardiovasc Dis. 2011;104(8–9):465–79.
2. Quill JL, Hill AJ, Laske TG, Alfieri O, Iaizzo PA. Mitral leaflet anatomy revisited. J Thorac Cardiovasc Surg. 2009;137(5):1077–81.
3. Grewal J, Mankad S, Freeman WK, Click RL, Suri RM, Abel MD, Oh JK, Pellikka PA, Nesbitt GC, Syed I, Mulvagh SL, Miller FA. Real-time three-dimensional transesophageal echocardiography in the intraoperative assessment of mitral valve disease. J Am Soc Echocardiogr. 2009;22(1):34–41.
4. Guarracino F, Baldassarri R, Ferro B, Giannini C, Bertini P, Petronio AS, Di Bello V, Landoni G, Alfieri O. Transesophageal echocardiography during MitraClip® procedure. Anesth Analg. 2014;118(6):1188–96.
5. Willemsen HM, van den Heuvel A, Schurer R, van Melle J, Natour E. Mitral cleft repair by mitraclipping. Eur Heart J. 2014;35(16):1021.

Difficult Cases and Complications from Catheterization Laboratory: Successful Percutaneous Mitral Valve Repair with Three MitraClip Devices in a Complex Case of Severe Functional Mitral Regurgitation

14

G. Grassi and F. Ronco

14.1 Case Report

A 62-year-old man with non-ischemic dilated cardiomyopathy (DCM) was referred to our center for evaluation of percutaneous mitral valve repair (PMVR) as he had developed significantly reduced left ventricular ejection fraction (LVEF) and severe functional mitral valve regurgitation (MR).

DCM was first diagnosed in 2002, when the patient was admitted for acute heart failure. Coronary angiography showed absence of atheromasic disease, and the only remarkable finding was the chronic alcohol abuse. Despite the alcohol withdrawal, however, heart failure progressed through the years needing cardiac resynchronization therapy and sudden death prophylaxis by implantation of a biventricular defibrillator (CRT-D). In the following years, his symptoms were stable (NYHA I–II) despite evidence of progressive depression of LVEF and worsening mitral regurgitation (MR) on serial echocardiograms. In late 2014, he complained of progressive breathlessness and needed to be hospitalized on several occasions with acute decompensated congestive cardiac failure. In March 2015, he underwent coronary angiography and reimplantation of the left lead of the CRT-D device. There was no evidence of coronary artery disease. Two months later, a repeat echocardiogram showed that his LVEF and mitral valve

G. Grassi (✉) • F. Ronco
Emodinamica e Cardiologia Interventistica, Dipartimento Cardiovascolare, ULSS 12
Veneziana, Venice, Italy
e-mail: giuseppe.grassi@ulss12.ve.it

Fig. 14.1 Severe MR at basal TTE in apical four-chamber view
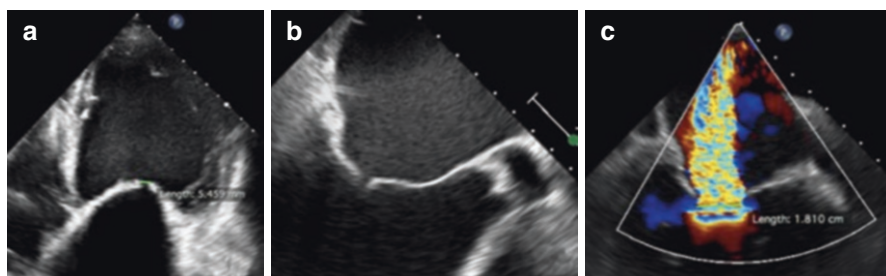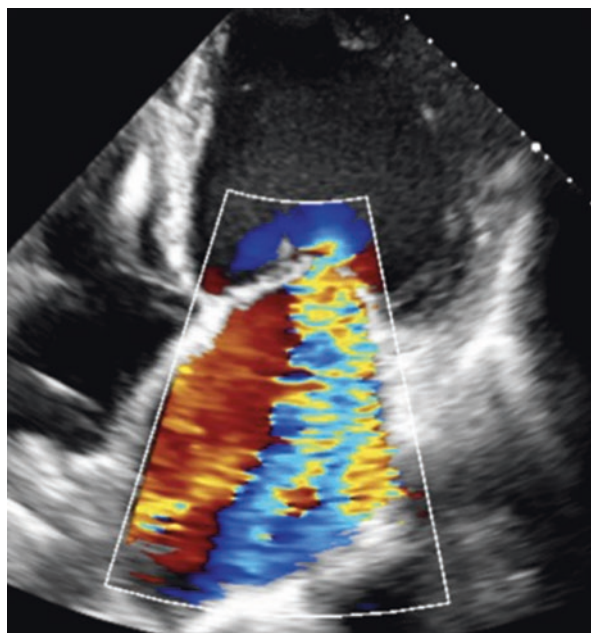
Fig. 14.2 Coaptation gap at basal TTE (**a**) and TEE (**b**). Flail width measured at TEE intercommissural view (**c**)

regurgitation had worsened. His estimated ejection fraction was 20 % and his mitral valve regurgitation was 4+/4. The risks associated with a surgical mitral valve replacement were considered to be too high given his severe left ventricular dysfunction. As an alternative, percutaneous mitral valve replacement (PMVR) therapy was proposed. As part of general screening, a transesophageal echocardiogram (TEE) was performed which confirmed severe MR due to severe bileaflet tethering (Fig. 14.1, Video 14.1). A coaptation gap of 5 mm was seen in the A2-P2 position and the jet width was 18 mm (Fig. 14.2a–c, Videos 14.2 and 14.3). Following a multidisciplinary discussion about the complexity, feasibility, risks, and potential outcomes of the intervention, a decision was made to proceed with PMVR in our institution.
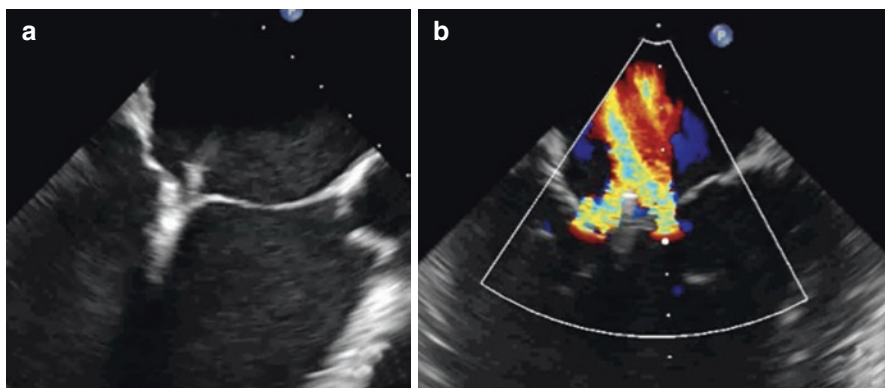
Fig. 14.3 Grasping of both leaflets in LVOT view (**a**) resulting in a splitted jet of moderate to severe MR (**b**)

14.2   The Procedure

The procedure was performed under general anesthesia by a multidisciplinary team consisting of interventional cardiologists, a cardiologist with special expertise in cardiac imaging, cardiac anesthesiologist, nurses, and a technician. The patient was carefully monitored and hemodynamically optimized. To assess the feasibility of a traditional approach, grasping in the A2-P2 position was attempted.

After six failed attempts to grasp the leaflet in A2-P2 position, we optimized conditions by temporarily ceasing mechanical ventilation and also took advantage of a compensatory pause following an extrasystole. This facilitated successful grasping of the leaflet in A2-P2 position and deployment of a clip. Mild improvement of the MR from 4+ to 3+ was noted with the jet split (Fig. 14.3a, b, Videos 14.4). A second clip was placed in a medial position close to the first one, resulting in a consistent reduction of the medial jet (Fig. 14.4, Video 14.5). Finally, a third clip was placed laterally to the first clip which led to a sustained improvement of the MR from 4+ to 1+ (Fig. 14.5a–c, Videos 14.6, 14.7, and 14.8), with a transmitral gradient of 2 mmHg. The patient was successfully weaned from mechanical ventilation and discharged home 5 days later. At time of discharge, the severity of his MR was assessed as 1+/4 by TTE (Fig. 14.6, Video 14.9).

At follow-up 1 month later, repeat echocardiography showed that the result was maintained (MR 1+ over 4). In addition, the patient felt significantly better and reported symptoms consistent with functional class NYHA 1 only.

14.3   Discussion

Mitral valve surgery remains the gold standard of care for patients with severe MR [1]. In this particular case, traditional surgery was considered to be associated with an unacceptably high risk of mortality and morbidity. The EVEREST high-risk study
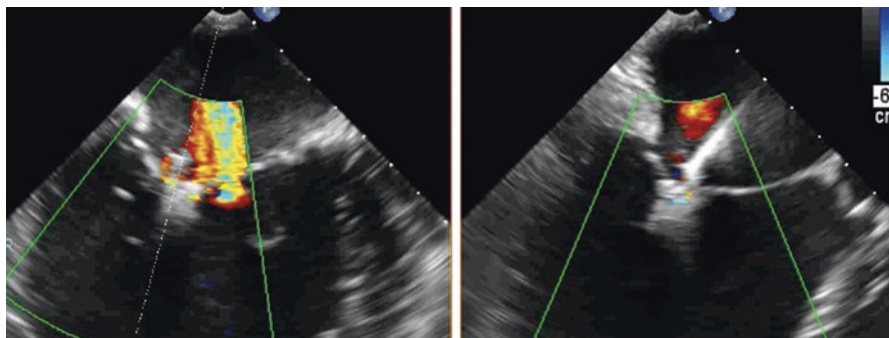
Fig. 14.4 X-plane view of the second MitraClip placed medially to the first. The medial jet was significantly reduced; the lateral jet is still present
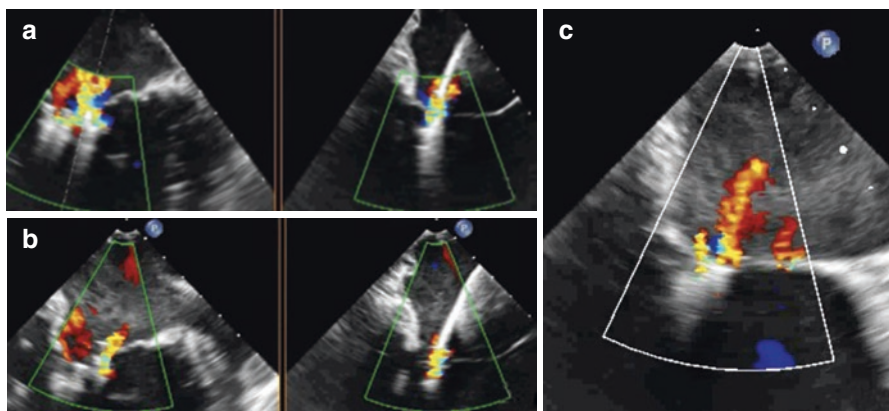
Fig. 14.5 Grasping (**a**) and deployment (**b**) of the third clip laterally to the first. Finally, the residual jet is mild (**c**)

previously showed that patients with severe predominantly functional MR in whom surgical repair or valve replacement was considered to be too risky, had a better outcome if treated with PMVR versus medical therapy [2]. Similar results were found in the REALISM Study and in the ACCESS-EU Registry [3, 4].

TEE evaluation is crucial in the patient selection process. A coaptation length of at least 2 mm and coaptation depth <11 mm are considered necessary. The coaptation gap should be ≤7 mm between the anterior and posterior leaflets, and the jet width should not exceed 15 mm. There should be some tissue between both leaflets to be used as target for the clips.

In our particular case, the valve anatomy was considered to be borderline for the PMVR approach with concerns about the coaptation gap and jet width.

Previous reports described various tips and tricks to improve the chances of procedural success in case of problems with bileaflet grasping. Apnea with temporary cessation of mechanical ventilation is one. It is widely used to limit chest excursion and movements of the clip delivery system during grasping. Some operators have
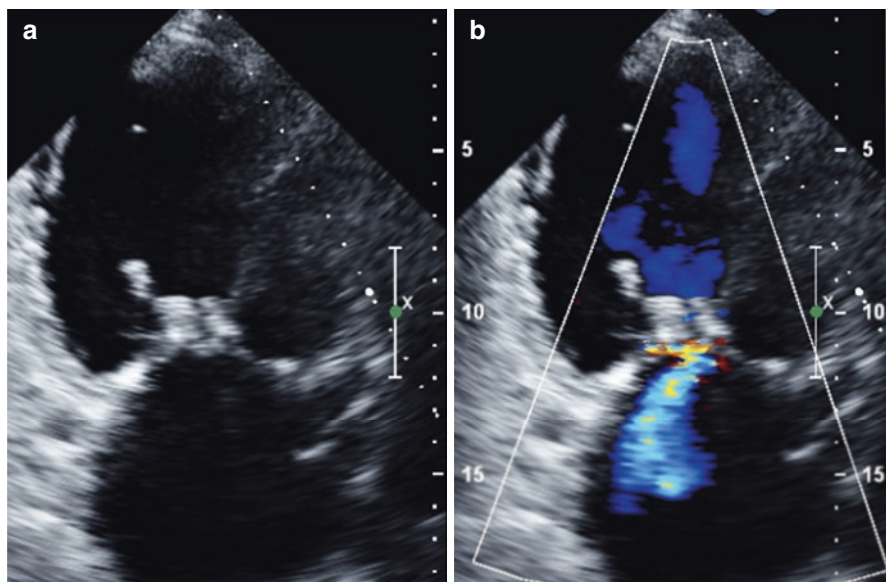
Fig. 14.6 Predischarge TTE showing persistence of good procedural result with mild MR

described the use of an intra-aortic balloon pump to decrease end left ventricular diastolic volume and to gain some coaptation. Rapid pacing has also been used to grasp still leaflets [5]. Ussia et al. described the annulus remodeling repair technique which is a multiple clip approach consisting of implantation of two clips starting from a commissure [6]. The aim is to reduce the annular perimeter and to improve the coaptation between A2 and P2, favoring the grasping of a third clip in the middle scallops which results in a double orifice mitral valve. Differently, Kische et al. previously described a strategy of "zipping by clipping" in a case of severe coaptation gap: medial to lateral approximation of the tethered leaflets was obtained by intentional deployment of four MitraClip devices with creation of a lateral neo-orifice with apparent acute clinical success [7].

In our case, we took advantage of a pause following an extrasystole during apnea to grasp the leaflets in the A2-P2 position after initial attempts during mechanical ventilation had failed. Given the severity of the jet width, two further clips were implanted medially and laterally close to the first one. The end result was a double orifice mitral valve with mild residual MR. In case of failure, "the plan B" was to proceed with a bailout strategy to remodel the annulus by implanting one or two clips close to the commissures and reducing the annular perimeter as described by Ussia et al. This method aims to improve the A2-P2 coaptation.

Conclusion

Severe functional MR with complex anatomy requires a certain grade of expertise in the technique of PMVR. Good procedural and clinical results can be achieved with different strategies and "tips and tricks."

References

1. Joint Task Force on the Management of Valvular Heart Disease of the European Society of Cardiology (ESC), European Association for Cardio-Thoracic Surgery (EACTS), Vahanian A, Alfieri O, Andreotti F, Antunes MJ, Barón-Esquivias G, Baumgartner H, Borger MA, Carrel TP, De Bonis M, Evangelista A, Falk V, Iung B, Lancellotti P, Pierard L, Price S, Schäfers HJ, Schuler G, Stepinska J, Swedberg K, Takkenberg J, Von Oppell UO, Windecker S, Zamorano JL, Zembala M. Guidelines on the management of valvular heart disease. Eur Heart J. 2012;33:2451–96.
2. Whitlow PL, Feldman T, Pedersen WR, Lim DS, Kipperman R, Smalling R, Bajwa T, Herrmann HC, Lasala J, Maddux JT, Tuzcu M, Kapadia S, Trento A, Siegel RJ, Foster E, Glower D, Mauri L, Kar S, on behalf of the EVEREST II Investigators. Acute and 12-month results with catheter-based mitral valve leaflet repair the EVEREST II (Endovascular Valve Edge-to-Edge Repair) high risk study. J Am Coll Cardiol. 2012;59:130–9.
3. Lim S, Reynolds MR, Feldman T, Kar S, Herrmann HC, Wang A, Whitlow PL, Gray WA, Grayburn P, Mack MJ, Glower DD. Improved functional status and quality of life in prohibitive surgical risk patients with degenerative mitral regurgitation after transcatheter mitral valve repair. J Am Coll Cardiol. 2014;64:182–92.
4. Maisano F, Franzen O, Baldus S, Schäfer U, Hausleiter J, Butter C, Ussia GP, Sievert H, Richardt G, Widder JD, Moccetti T, Schillinger W. Percutaneous mitral valve interventions in the real world early and 1-year results from the ACCESS-EU, a prospective, multicenter, non-randomized post-approval. J Am Coll Cardiol. 2013;62:1052–61.
5. Paranskaya L, Turan I, Kische S, Nienaber C, Ince H. Rapid pacing facilitates grasping and MitraClip implantation in severe mitral leaflet prolapse. Clin Res Cardiol. 2012;101:69–71.
6. Ussia GP, Cammalleri V, Sergi D, De Vico P, Romeo F. Annulus remodeling and double orifice repair using a multiple clip approach in complex mitral valve anatomy. JACC Cardiovasc Interv. 2014;7:53–4.
7. Kische S, Nienaber C, Ince H. Use of four MitraClip devices in a patient with ischemic cardio-myopathy and mitral regurgitation: "zipping by clipping". Catheter Cardiovasc Interv. 2012;80:1007–13.

Part III

Left Appendage Closure

Percutaneous Left Atrial Appendage Closure: Rational, Patient Selection, and Preoperative Evaluation

15

Marco Mennuni, Carlo Penzo, Giuseppe Ferrante, Giulio Stefanini, and Bernhard Reimers

15.1 Introduction

Atrial fibrillation (AF) is the most common arrhythmia, affecting 1–2 % of worldwide population, the incidence is 0.05 % cases per year, and it is expected to more than double by 2050 in the western countries [1]. AF presence increases the risk of embolic stroke by four- to fivefold [2] and results in stroke incidence of 2–5 % per year in untreated patients [3]. Such disabling complication is mainly related to thrombus formation within the left atrial appendage (LAA) [4]. Furthermore, among patients with AF and history of stroke, the rate of new embolic events may increase up to 12 % per year if patients are not on oral anticoagulants and is at 3 % per year in patients who are properly under medical treatment [2].

15.2 Rational

Oral anticoagulant drugs are an effective treatment to prevent embolic events in patients with AF; however, several drawbacks limit their applicability as well as the patient's compliance and the bleeding risk [3]. In daily practice, the decision on oral anticoagulant starting in AF patient is challenging. The physician's choice is based on balancing patient thromboembolic and bleeding risks. For this purpose, several risk score calculators have been developed, such as the $CHADS_2$ and the HAS-BLED risk score [4, 5]. However, overlap in bleeding and thrombotic risk factor is often observed in complex patients, making the choice of the most appropriate therapy tricky. As per European Society of Cardiology recommendation, the risk of

M. Mennuni • G. Ferrante • G. Stefanini • B. Reimers
Cardiovascular Department, Humanitas Research Hospital, Rozzano, Milan, Italy

C. Penzo (✉)
Cardiovascular Department, Mirano Hospital, Mirano, Italy
e-mail: carlopenzo78@gmail.com

Table 15.1 CHA$_2$DS$_2$-VASc risk score

	Risk factors	Points
C	Congestive heart failure (or left ventricular ejection fraction <40%)	1
H	Hypertension: blood pressure above 140/90 mmHg or treatment	1
A$_2$	Age ≥75 years	2
D	Diabetes mellitus	1
S$_2$	Prior stroke or thromboembolism	2
V	Vascular disease (peripheral artery disease, myocardial infarction, aortic plaque)	1
A	Age 65–74 years	1
Sc	Sex category (i.e., female sex)	1

Table 15.2 HAS-BLED risk score

	Risk factors	Points
H	Hypertension: (>160 mmHg systolic)	1
A	Abnormal renal function: dialysis, transplant, Cr >2.6 mg/dL	1
	Abnormal liver function: cirrhosis or bilirubin >2× normal or AST/ALT/AP >3× normal	1
S	Stroke (prior history of stroke)	1
B	Bleeding (prior major bleeding or predisposition to bleed)	1
L	Labile INR (unstable value, time in therapeutic range <60%)	1
E	Elderly (age >65 years)	1
D	Prior alcohol or drug usage history	1
	Medication usage predisposing to bleeding (i.e., antiplatelet agents or NSAID)	1

stroke should be calculated by CHA$_2$DS$_2$-VASc risk score, a more recent and implemented version of CHADS$_2$ score (Table 15.1) [6]. An additive score more or equal than two indicates high risk of thromboembolism.

The HAS-BLED risk score is the recommended tool to assess the risk of bleeding in patients with AF (Table 15.2) [6]. An additive score more or equal than three indicates high risk of bleeding.

15.2.1 Oral Anticoagulant Limitation

Current guidelines, based on several randomized controlled trials, suggest to treat patient with AF, elevated stroke risk, and bleeding risk not prohibitive, with chronic anticoagulation – traditionally with warfarin and, more recently, with direct thrombin and factor Xa inhibitors. Although warfarin is highly effective, it requires a frequent INR monitoring and dose adjustment due to its narrow therapeutic range. As a result, bleeding risk and variable compliance result into the exclusion of 14–44% of treatable patients from oral anticoagulant therapy [7]. Moreover, only

55 % of treated and well-adherent patients remain in therapeutic range during warfarin therapy [8].

Novel oral anticoagulants (NOAC) do not require INR monitoring and therefore are associated with a priori higher patient compliance. Furthermore, they have a favorable stroke/bleeding risk profile, driven by reductions in the rates of stroke and intracranial hemorrhage [9]. However, higher risk of GI bleeding observed with NOAC counterbalances the overall risk of bleeding, resulting to similarity between warfarin and novel molecules.

15.2.2 NOAC Limitation

In terms of patient compliance, randomized controlled trials comparing NOAC vs. warfarin, such as the RELY (dabigatran vs. warfarin) [10], ROCKET-AF (rivaroxaban vs. warfarin) [11], ARISTOTLE (apixaban vs. warfarin) [12], and ENGAGE AF-TIMI 48 (edoxaban vs. warfarin) [13] study, NOAC interruption, owing to side effects or low compliance, occurred in 10 %, 24 %, 25 %, and 34 %, respectively, during the study period. Therefore, a sizable proportion of patients still remain at high risk of stroke because of undertreatment. Moreover, the increased bleeding risk, especially among older patients and/or those who are on antiplatelet medications, and the required lifelong pill compliance prompted the development of alternative strategies for stroke prevention.

15.2.3 LAA Occlusion

Percutaneous LAA occlusion is a novel therapy to prevent stroke in patient with atrial fibrillation. The LAA, due to its trabeculae and blood stasis, is the most common site of thrombus generation in patients with AF [14]. Surgical exclusion of LAA has been previously used to reduce the risk of embolic events in patients with AF [15]. Percutaneous left atrial appendage occlusion (LAA) has been developed as a less invasive procedure to prevent stroke in patient with AF who cannot tolerate oral anticoagulation [9, 10]. This catheter-based technique provides an atrial endoluminal mechanical orifice obstruction. In 2002, the first case of percutaneous LAA closure was reported with the use of the PLAATO system (percutaneous left atrial appendage), a nitinol self-expandable cage with lateral hook, covered by ePTFE membrane. This device was implanted in few non-randomized series which showed good clinical results in terms of embolic event reduction: at 5 years stroke rate was 3.3 % compared to an expected rate of 6.6 % based on CHADS$_2$ score [16]. However, it was recalled from the market due to its complex and risky implantation technique, which resulted in high rate of procedural complication such as vessel perforation, cardiac tamponade, and device embolization [16–21].

Currently, three percutaneous LAA closure devices are available on the market: the Watchman™ (Boston Scientific, Natick, MA, USA), the Amplatzer™ Cardiac Plug (St. Jude Medical, Minneapolis, MN, USA), and WaveCrest.

The Watchman is a nitinol cage partially covered by a polyethylene terephthalate (PTFE) membrane, with lateral small barbs which anchor the device to LAA minimizing the risk of dislodgment. It is the only device studied in a randomized fashion. The Watchman Left Atrial Appendage System for Embolic Protection in Patients with Atrial Fibrillation (PROTEC-AF) trial was the first randomized study to investigate a LAA occlusion device. It included 707 patients with non-valvular AF and at least 1 CHADS$_2$ risk factor, who were randomized 2:1 to LAA closure with the use of the Watchman device or warfarin [22]. This study found that LAA closure was non-inferior to warfarin with respect to the combined risk of death, stroke, or embolism (8.4 % vs. 13.9 %) and the single risk of overall (12.3 % vs. 18.5) and cardiovascular death (3.7 % vs. 9.0 %) at early- and long-term follow-up [23].

The Prospective Randomized Evaluation of the Watchman LAA Closure Device in Patients with Atrial Fibrillation Versus Long-Term Warfarin Therapy (PREVAIL) trial was a confirmatory randomized study which demonstrates an improved safety compared to PROTECT-AF trial [24]. The most comprehensive study on Watchman was a recent individual patient-level meta-analysis of 2,406 patients including two randomized and two non-randomized trial (PROTECT-AF, PREVAIL, and their respective registries) with a mean follow-up of 2.7 years. The analysis found that the LAA occlusion with Watchman device provides similar benefit to warfarin for the composite efficacy end point of stroke, embolism, or cardiovascular death. In terms of single end points, the device provides an advantage for cardiovascular death (1.1 % vs. 2.3 % per year, hazard ration 0.48, $p = 0.006$) and bleeding events (hemorrhagic strokes 0.15 % vs. 0.96 % per year, hazard ratio 0.22; $p = 0.004$; and non-procedural bleeding 6.0 % vs. 11.3 %, hazard ratio 0.51; $p = 0.006$) compared with warfarin. This is balanced by a slight increase in ischemic stroke rate in device-treated group (1.6 % vs. 0.9 % per year, hazard ratio 1.95, $p = 0.05$) [25].

The Amplatzer Cardiac Plug – Amulet – is a second-generation device made of a nitinol lobe and disk connected by a short flexible waist, laid of polyester fabric. Such device is based on pacified principle: the main lobe is placed into the LAA body, and the disk covers the LAA orifice. The safety and efficacy were reported in few registries, which demonstrate good clinical performance, at least comparable to PROTECT-AF results. The procedural success varied from 95 to 100 %; embolization and pericardial effusion were 1–2 %. At the follow-up, the death rate was 6–9 % and stroke rate was 2–3 % [3, 26–29].

The Coherex WaveCrest (Coherex Medical Inc., Salt Lake City, UT, USA) device is made by a nitinol structure without exposed metal; it has a foam layer facing the LAA to promote the rapid endothelialization and PTFE layer facing the LAA to reduce thrombus formation. The device can be delivered and then fixed by actionable lateral hooks once the correct position is obtained. CE Marking was granted in 2013, and the device is now available in Europe. Currently, no clinical data have been published, but a phase 2 clinical study has been recently completed (clinicalTrials.gov Identifier: NCT02239887).

15.3   Patient Selection

The indication for LAA occlusion is summarized in Fig. 15.1. Based on European Society of Cardiology guidelines, the LAA occlusion is recommended (class IIb with level of evidence B) when high risk of stroke is present (CHA_2DS_2-VASc more than two or $CHADS_2$ more than one), and oral anticoagulation is not possible, as well as previous life-threatening bleeding events or high risk of bleeding under oral anticoagulation (increased HAS-BLED score, patient with coronary artery disease requiring prolonged dual antiplatelet therapy plus oral anticoagulation, or patient with end-stage renal failure) [6].

A recent expert consensus document indicated LAA occlusion in patient with high risk of stroke even when oral anticoagulation is possible [3]. Based on the Watchman device studies, this is the only indication based on two randomized trials comparing LAA occlusion vs. warfarin and patient-level meta-analysis demonstrating a similar effect of local LAA therapy and systemic oral anticoagulation (see above) [25].

Moreover, a cost-effectiveness evaluation should be assessed during the patient selection. Recent data demonstrated that the LAA occlusion is cost-effective compared to warfarin and NOAC after 7 and 16 years, respectively, and the LAA local therapy beats costs of NOAC at 5 years and the costs of warfarin at 10 years [30]. Such data might change lifetime horizon into the patient selection, and they might be considered during daily practice.
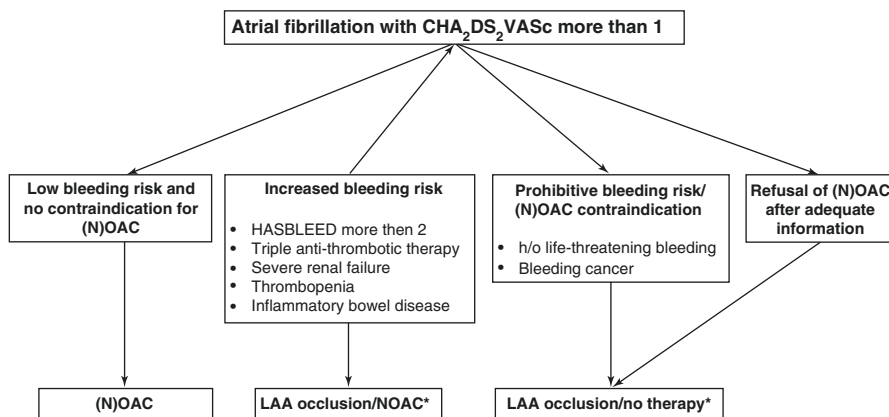
Fig. 15.1 Algorithm of stroke prevention adapted by EHRA/EAPCI expert consensus statement on catheter-based left atrial appendage occlusion [3]

15.4   Preoperative Evaluation

Adequate multimodality imaging evaluation is essential for a precise and safe LAA closure. Transesophageal echocardiography (TEE) and computerized tomography (CT) are the most common imaging modalities to visualize LAA. TEE is the gold standard for imaging of LAA during the occlusion work-up. However, CT availability is increasing among centers.

In the preprocedural evaluation, the first goal is to rule out the presence of thrombus within LAA. Fluttering or mobile thrombus in LAA is an absolute contraindication for LAA occlusion with any device, due to the risk of thrombus dislodgment during the device delivery. Currently, TEE is the reference modality to detect thrombus formation or sludge in the LAA [31]. Nevertheless, in some patients, the presence of *pectinate* muscle makes the thrombus detection challenging, and it may result in a false detection. CT scanner with delayed acquisition is a validated alternative to TEE with high sensitivity and specificity for the detection of LAA thrombi [32, 33].

The second step is to assess the morphology of LAA and the choice of device size for LAA closure. In some cases, LAA closure may not be feasible owing to large ostia, presence of early lobe, or early and severe main lobe bending.

Using the TEE, the LAA is viewed from the mid-esophageal window at least in four 45° different planes (e.g., 0°, 45°, 90°, and 135°). A three-dimensional (3D) echocardiography can better characterize the LAA morphology and presence of multiple lobes. The choice of the device size is based on the LAA ostium width and on the main lobe depth.

The LAA ostium width is measured from the left circumflex coronary artery to 1–2 cm from the edge of the warfarin ridge (at 0°) and from the mitral annulus to a point 1–2 cm from the ridge (45°, 90°, and 135°).

The depth of the LAA is detected from the ostium to the apex of the LAA main lobe. Each device has his own sizing: Watchman device can be used with LAA ostium from 17 to 31 mm (device size 21–33 mm); the ACP Amulet may be used for landing zones up to 31 mm (device size 16–34 mm). The device size should be 10–20 % larger than the landing zone diameter. Both LAA morphology and sizing can be evaluated by CT scanner with a dedicated acquisition and multiplanar reconstruction protocol. The CT scanner may well visualize both right and left atrial anatomies and generate a virtual implantation (transseptal puncture and device placement) through dedicated software.

Conclusion

Left atrial appendage occlusion represents an alternative local treatment for stroke prevention in patients with atrial fibrillation at high risk of both stroke and bleeding. The TEE and CT scan are valuable tools to evaluate the size and the morphology of LAA to achieve an optimal device choice and delivery.

References

1. Stewart S, Hart CL, Hole DJ, et al. Population prevalence, incidence, and predictors of atrial fibrillation in the Renfrew/Paisley study. Heart. 2001;86(5):516–21.
2. Peritz DC, Chung EH. Left atrial appendage closure: an emerging option in atrial fibrillation when oral anticoagulants are not tolerated. Cleve Clin J Med. 2015;82(3):167–76.
3. Meier B, Blaauw Y, Khattab AA, et al. EHRA/EAPCI expert consensus statement on catheter-based left atrial appendage occlusion. Europace. 2014;16(10):1397–416.
4. Gage BF, Waterman AD, Shannon W, et al. Validation of clinical classification schemes for predicting stroke: results from the National Registry of Atrial Fibrillation. JAMA. 2001;285(22):2864–70.
5. Pisters R, Lane DA, Nieuwlaat R, et al. A novel user-friendly score (HAS-BLED) to assess 1-year risk of major bleeding in patients with atrial fibrillation: the Euro Heart Survey. Chest. 2010;138(5):1093–100.
6. Camm AJ, Lip GY, De Caterina R, et al. Focused update of the ESC guidelines for the management of atrial fibrillation: an update of the 2010 ESC guidelines for the management of atrial fibrillation. Developed with the special contribution of the European Heart Rhythm Association. Eur Heart J. 2012;33(21):2719–47.
7. Onalan O, Lashevsky I, Hamad A, et al. Nonpharmacologic stroke prevention in atrial fibrillation. Expert Rev Cardiovasc Ther. 2005;3(4):619–33.
8. Baker WL, Cios DA, Sander SD, et al. Meta-analysis to assess the quality of warfarin control in atrial fibrillation patients in the United States. J Manag Care Pharm. 2009;15(3):244–52.
9. Ruff CT, Giugliano RP, Braunwald E, et al. Comparison of the efficacy and safety of new oral anticoagulants with warfarin in patients with atrial fibrillation: a meta-analysis of randomised trials. Lancet. 2014;383(9921):955–62.
10. Connolly SJ, Ezekowitz MD, Yusuf S, et al. Dabigatran versus warfarin in patients with atrial fibrillation. N Engl J Med. 2009;361(12):1139–51.
11. Patel MR, Mahaffey KW, Garg J, et al. Rivaroxaban versus warfarin in nonvalvular atrial fibrillation. N Engl J Med. 2011;365(10):883–91.
12. Granger CB, Alexander JH, McMurray JJ, et al. Apixaban versus warfarin in patients with atrial fibrillation. N Engl J Med. 2011;365(11):981–92.
13. Giugliano RP, Ruff CT, Braunwald E, et al. Edoxaban versus warfarin in patients with atrial fibrillation. N Engl J Med. 2013;369(22):2093–104.
14. Al-Saady NM, Obel OA, Camm AJ. Left atrial appendage: structure, function, and role in thromboembolism. Heart. 1999;82(5):547–54.
15. Kanderian AS, Gillinov AM, Pettersson GB, et al. Success of surgical left atrial appendage closure: assessment by transesophageal echocardiography. J Am Coll Cardiol. 2008;52(11):924–9.
16. Block PC, Burstein S, Casale PN, et al. Percutaneous left atrial appendage occlusion for patients in atrial fibrillation suboptimal for warfarin therapy: 5-year results of the PLAATO (Percutaneous Left Atrial Appendage Transcatheter Occlusion) study. JACC Cardiovasc Interv. 2009;2(7):594–600.
17. Sievert H, Lesh MD, Trepels T, et al. Percutaneous left atrial appendage transcatheter occlusion to prevent stroke in high-risk patients with atrial fibrillation: early clinical experience. Circulation. 2002;105(16):1887–9.
18. El-Chami MF, Grow P, Eilen D, et al. Clinical outcomes three years after PLAATO implantation. Catheter Cardiovasc Interv. 2007;69(5):704–7.
19. Park JW, Leithauser B, Gerk U, et al. Percutaneous left atrial appendage transcatheter occlusion (PLAATO) for stroke prevention in atrial fibrillation: 2-year outcomes. J Invasive Cardiol. 2009;21(9):446–50.
20. Ussia GP, Mule M, Cammalleri V, et al. Percutaneous closure of left atrial appendage to prevent embolic events in high-risk patients with chronic atrial fibrillation. Catheter Cardiovasc Interv. 2009;74(2):217–22.

21. De Meester P, Thijs V, Van Deyk K, et al. Prevention of stroke by percutaneous left atrial appendage closure: short term follow-up. Int J Cardiol. 2010;142(2):195–6.
22. Holmes DR, Reddy VY, Turi ZG, et al. Percutaneous closure of the left atrial appendage versus warfarin therapy for prevention of stroke in patients with atrial fibrillation: a randomised non-inferiority trial. Lancet. 2009;374(9689):534–42.
23. Reddy VY, Sievert H, Halperin J, et al. Percutaneous left atrial appendage closure vs warfarin for atrial fibrillation: a randomized clinical trial. JAMA. 2014;312(19):1988–98.
24. Holmes Jr DR, Kar S, Price MJ, et al. Prospective randomized evaluation of the Watchman left atrial appendage closure device in patients with atrial fibrillation versus long-term warfarin therapy: the PREVAIL trial. J Am Coll Cardiol. 2014;64(1):1–12.
25. Holmes Jr DR, Doshi SK, Kar S, et al. Left atrial appendage closure as an alternative to warfarin for stroke prevention in atrial fibrillation: a patient-level meta-analysis. J Am Coll Cardiol. 2015;65(24):2614–23.
26. Nietlispach F, Gloekler S, Krause R, et al. Amplatzer left atrial appendage occlusion: single center 10-year experience. Catheter Cardiovasc Interv. 2013;82(2):283–9.
27. Khattab AA, Meier B. Transcatheter left atrial appendage closure for stroke prevention among atrial fibrillation patients. Expert Rev Cardiovasc Ther. 2012;10(7):819–21.
28. Lopez-Minguez JR, Eldoayen-Gragera J, Gonzalez-Fernandez R, et al. Immediate and one-year results in 35 consecutive patients after closure of left atrial appendage with the amplatzer cardiac plug. Rev Esp Cardiol (Engl Ed). 2013;66(2):90–7.
29. Urena M, Rodes-Cabau J, Freixa X, et al. Percutaneous left atrial appendage closure with the AMPLATZER cardiac plug device in patients with nonvalvular atrial fibrillation and contraindications to anticoagulation therapy. J Am Coll Cardiol. 2013;62(2):96–102.
30. Reddy VY, Akehurst RL, Armstrong SO, et al. Time to cost-effectiveness following stroke reduction strategies in AF: warfarin versus NOACs versus LAA closure. J Am Coll Cardiol. 2015;66(24):2728–39.
31. Klein AL, Grimm RA, Murray RD, et al. Use of transesophageal echocardiography to guide cardioversion in patients with atrial fibrillation. N Engl J Med. 2001;344(19):1411–20.
32. Hur J, Kim YJ, Nam JE, et al. Thrombus in the left atrial appendage in stroke patients: detection with cardiac CT angiography – a preliminary report. Radiology. 2008;249(1):81–7.
33. Shapiro MD, Neilan TG, Jassal DS, et al. Multidetector computed tomography for the detection of left atrial appendage thrombus: a comparative study with transesophageal echocardiography. J Comput Assist Tomogr. 2007;31(6):905–9.

Device Selection According to Anatomy

16

Marco Michieletto

Percutaneous occlusion of the left atrial appendage (LAA) with a device offers an alternate method of reducing thromboembolic risk in patients with atrial fibrillation at increased risk for thromboembolic stroke and who cannot safely receive antico-agulation [1]. There are currently two commercially available devices for the left atrial appendage: Amplatzer Cardiac Plug (St. Jude Medical Inc., MN, USA) and Watchman LAA closure device (Boston Scientific Natick, MA, USA) (Fig. 16.1).

Echocardiographic imaging plays an important role in the selection of the patient according to anatomy, in verifying the presence of exclusion criteria to the proce-dure such as presence of a thrombus inside the left atrial appendage, and in device selection.

Multiplanar transesophageal echocardiography (TEE) is performed to define LAA size and anatomy. The LAA is imaged from the mid-esophageal view through 180° (in particular at 0°, 45–60°, 90°, and 120–135°) to define the maximum LAA width and maximum depth of the dominant lobe. The need of a complete 180° scan is due to the highly variable anatomy of the LAA, showing the presence of more than one lobe in 80 % of left atrial appendages (Fig. 16.2) [2]; it is not unusual that a LAA that shows one lobe at 45–60° then reveals the presence of more than one lobe or a "broccoli-like" aspect at 120–135° (Fig. 16.3); moreover, the ostium of the LAA is typically oval shaped; therefore, diameters on the various planes can vary significantly, in some cases up to a 12 mm difference between the diameters obtained at 0° and 135° [3].

A further help for the visualization of the LAA, in particular for determination of shape and dimension of the orifice, comes from the 3D TEE [4, 5]; the two main modalities to perform this exam are [3]:

M. Michieletto
Cardiology, Mirano, Italy
e-mail: marco.michieletto@ulss13mirano.ven.it
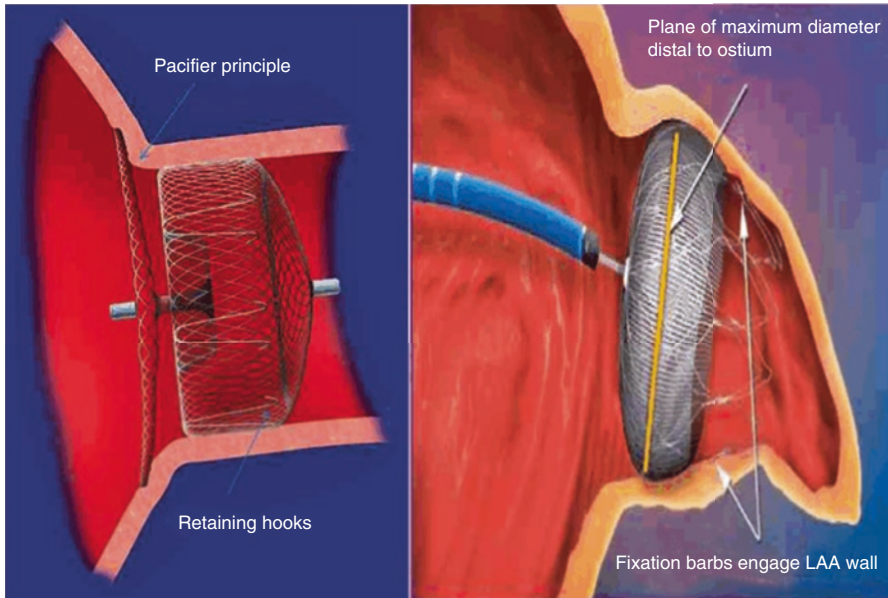
Fig. 16.1 Amplatzer Cardiac Plug (St. Jude Medical Inc., MN, USA) (*left panel*) and Watchman LAA closure device (Boston Scientific Natick, MA, USA) (*right panel*) (Image Courtesy of Boston Scientific)
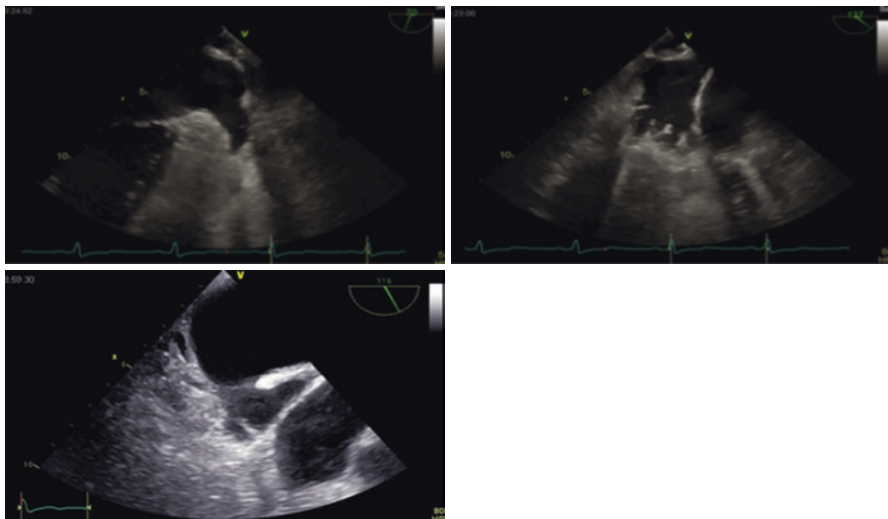

Fig. 16.2 TEE imaging of the most frequent shapes of LAA showing "windsock-type" shape in the *upper panel*, "broccoli-type" shape in the *middle panel*, and "chicken wing-type" shape in the *lower panel. LAA* left atrial appendage (Courtesy of L. Lanzoni)
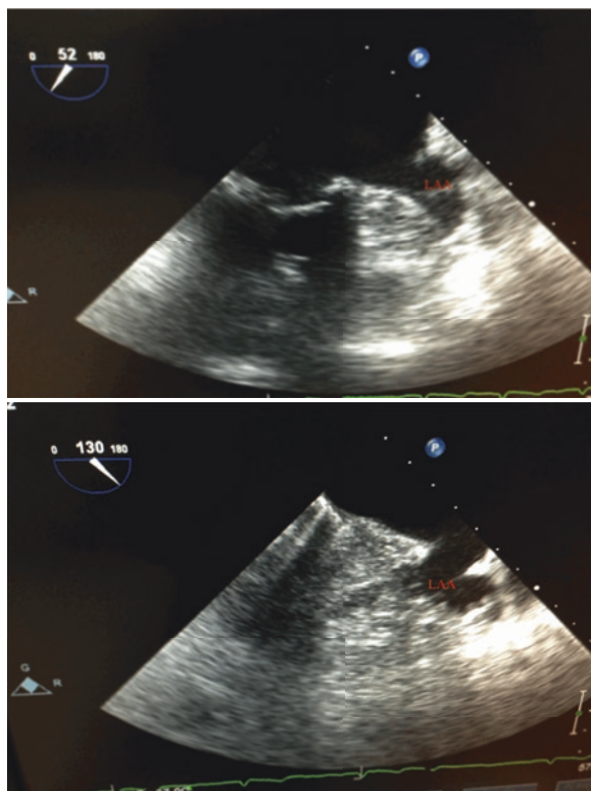
Fig. 16.3 TEE imaging of LAA showing one lobe at 52° (*upper panel*) and "broccoli-like" aspect at 130° (*lower panel*). *LAA* left atrial appendage

- The three-dimensional zoom mode that generates a data set which size is manually adjusted to incorporate the region of interest. The advantage of this technique is that image is presented in real time and can be rotated without any further manipulation of the probe (Fig. 16.4).
- The three-dimensional full volume mode that generates a data set acquired over four to seven cardiac cycles that display a larger volume of cardiac structures. The image has to be processed with cropping along any plane and rotating in all three axes, focusing the cardiac structures that have to be investigated (Fig. 16.5).

Multidetector computed tomography (MDCT) with contrast injection is an alternative to echocardiography, producing high-quality 3D images of the LAA anatomy, with a sensitivity for the detection of LAA thrombi comparable with TEE [6]; in our department, we don't use MDCT to avoid further radiation exposure or contrast administration. As an alternative, some authors use cardiac magnetic resonance imaging (MRI) to study the LAA; however, the role of this methodology needs to be better defined [7].

Fig. 16.4 TEE three-dimensional zoom mode of the orifice LAA, showing oval shape. *Red lines*: diameters of LAA orifice

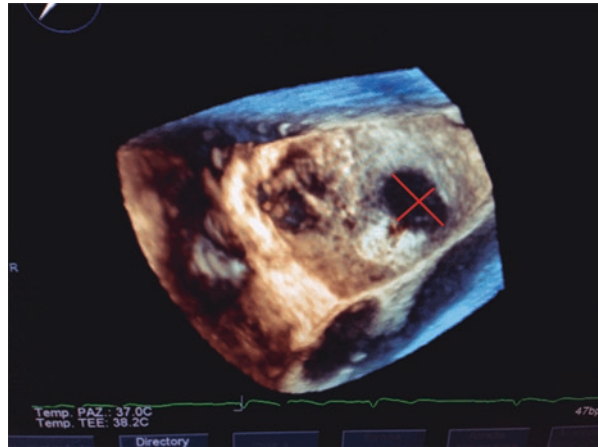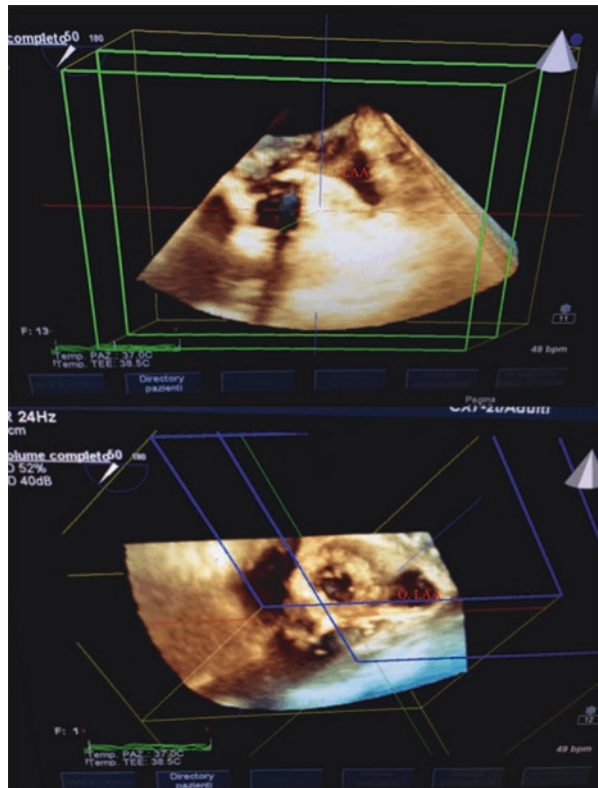**Fig. 16.5** TEE three-dimensional full volume mode of the LAA (*upper panel*) and processed image, cropped along superior plane and rotated to visualize the orifice (*lower panel*). *LAA* left atrial appendage, *O.LAA* orifice of left atrial appendage

During the procedure, after the transseptal puncture, comparison of TEE measurements with angiography (two projections) is usually performed in our department (Fig. 16.6).

The two commercially available devices need the following measurements:

1. Amplatzer Cardiac Plug: the measurement will be taken at the orifice of the LAA, with a second measurement for the landing zone of the stabilizer disk (lobe), which is located 10 mm from the orifice into the left appendage. This device cannot be used if the landing zone is less than 10-mm width. According to Table 16.1, from the measurement of the maximum diameter of the landing zone, a device size that corresponds to the lobe diameter will be chosen; particular care has to be given to the measurement of the orifice of the LAA, to be sure that the disk diameter exceeds the diameter of the orifice and completely covers it (for device size 16–22, the disk diameter exceeds 4 mm the lobe diameter; for device size 24–30, the disk diameter exceeds 6 mm the lobe diameter).

2. Watchman LAA closure device: the measurement will be taken from the level of the circumflex artery (at 0°) or at the mitral plane level (45–60°, 90°, 135°), to a point around 2 cm below the ridge of the pulmonary vein. Measurement of LAA length has to be obtained from every view, to assure that the dimensions are within the available device range (Table 16.2). This device cannot be used if the length of the LAA does not match the length of the device which corresponds to the diameter of the device that needs to be positioned. It is important to also obtain the measurement of the diameter of the orifice of the LAA, because sometimes the device has to be positioned less deeply due to anatomical anomalies, such as the presence of twigs, like in the case in Fig. 16.7.

In our department, the TEE study before the occlusion procedure will follow this protocol:

1. Visualization of LAA at 45–60°, 90°, and 135° to exclude the presence of thrombi and to visualize the shape
2. Measurement of diameters of LAA at 45–60°, 90°, and 135° (Fig. 16.8):
   • At orifice level (and measurement of the length of LAA from that plane)
   • One centimeter from the orifice into the left appendage
   • Two centimeters from the orifice into the left appendage (and measurement of the length of LAA from that plane)
3. Optional visualization of the LAA by three-dimensional zoom mode and full volume mode

During the procedure, TEE measurement will be compared with angiography, and then the type and the size of the device will be decided.

Fig. 16.6 Comparison of
TEE measurements of
LAA (*upper panel*) with
angiography (*lower panel*).
LAA left atrial appendage

Table 16.1 Amplatzer Cardiac Plug device selection

Max. landing zone width (mm)	Device size/lobe diameter (mm)	Disc diameter (mm)
12.6–14.5	16	20
14.6–16.5	18	22
16.6–18.5	20	24
18.6–20.5	22	26
20.6–22.5	24	30
22.6–24.5	26	32
24.6–26.5	28	34
26.6–28.5	30	36

Table 16.2   Watchman LAA closure device selection

Max LAA ostium (mm)	Device diameter (mm)	Device length (mm)
17–19.9	21	20.2
20–22.9	24	22.9
23–25.9	27	26.5
26–28.9	30	29.4
29–31.9	33	31.6

LAA left atrial appendage
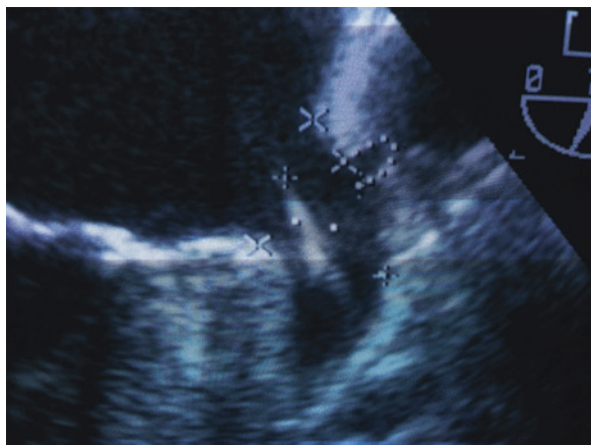
Fig. 16.7   Twig (*dot line*) into LAA, proximal to the usual landing zone of the Watchman LAA closure device. *LAA* left atrial appendage

Fig. 16.8 Measurement of diameters of LAA at 45–60° (*upper panel*), 90° (*middle panel*), and 135° (*lower panel*) at the orifice level (*red lines*) (and measurement of the length of LAA from that plane, *blue lines*), at 1 cm from the orifice into the left appendage (*green lines*), and at 2 cm from the orifice into the left appendage (*yellow lines*) (and measurement of the length of LAA from that plane, *orange lines*)
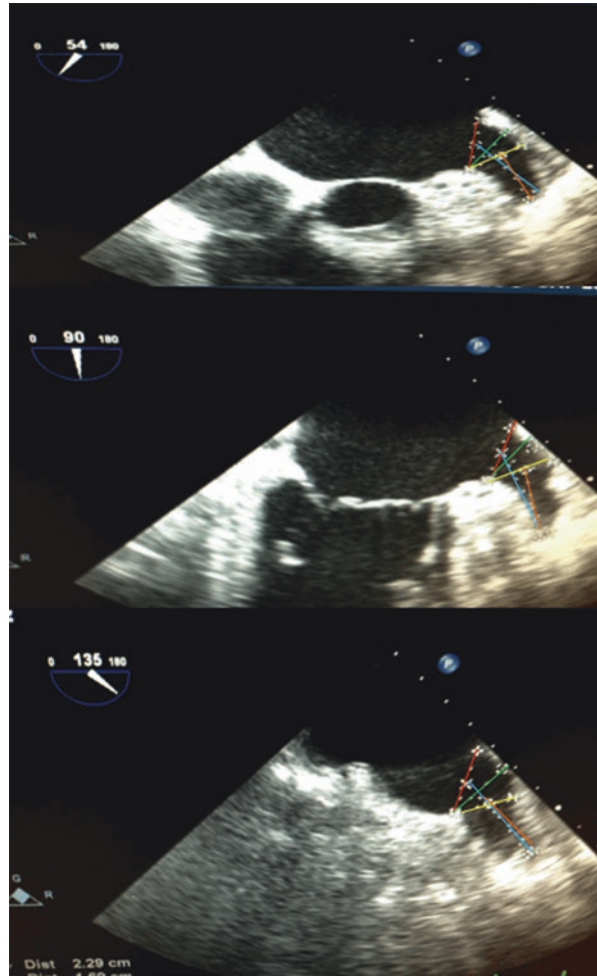
References

1. Holmes DR, Reddy VY, Turi ZG, Doshi SK, Sievert H, Buchbinder M, Mullin CM, Sick P, PROTECT AF investigators. Percutaneous closure of the left atrial appendage vs. warfarin therapy for prevention of stroke in patients with atrial fibrillation: a randomised non-inferiority trial. Lancet. 2009;374:534–42.
2. Veinot JP, Harrity PJ, Gentile F, Khandheria BK, Bailey KR, Eickholt JT, Seward JB, Tajik AJ, Edwards WD. Anatomy of the normal left atrial appendage: a quantitative study of age-related changes in 500 autopsy hearts: implications for echocardiographic examination. Circulation. 1997;96:3112–5.
3. Perk G, Biner S, Kronzon I, Saric M, Chinitz L, Thompson K, Shiota T, Hussani A, Lang R, Siegel R, Kar S. Catheter-based left atrial appendage occlusion procedure: role of echocardiography. Eur Heart J Cardiovasc Imaging. 2012;13(2):132–8. Epub 2011 Sep 8.

4. Shah SJ, Bardo DM, Sugeng L, Weinert L, Lodato JA, Knight BP, Lopez JJ, Lang RM. Real-time three-dimensional transesophageal echocardiography of the left atrial appendage: initial experience in the clinical setting. J Am Soc Echocardiogr. 2008;21:1362–8.
5. Nucifora G, Faletra FF, Regoli F, Pasotti E, Pedrazzini G, Moccetti T, Auricchio A. Evaluation of the left atrial appendage with real-time three-dimensional transesophageal echocardiography: implications for catheter-based left atrial appendage closure. Circ Cardiovasc Imaging. 2011;4(5):514–23.
6. Garcia MJ. Tomography: a word of caution detection of left atrial appendage thrombus by cardiac computed. J Am Coll Cardiol Img. 2009;2:77–9.
7. Mohrs, Nowak B, Petersen SE, Welsner M, Rubel C, Magedanz A, Kauczor HU, Voigtlaender T. Thrombus detection in the left atrial appendage using contrast- enhanced MRI: a pilot study. AJR. 2006;186:198–205.

Left Atrial Appendage Closure – Techniques and Devices

17

Marius Hornung, Jennifer Franke, Sameer Gafoor, and Horst Sievert

The history of percutaneous occlusion of the left atrial appendage (LAA) for stroke prevention started back in 2001 with the first implantation of the percutaneous LAA transcatheter occlusion system (PLAATO; Appriva Medical, Sunnyvale, CA, USA) [1]. The PLAATO device was a self-expanding nitinol cage covered with a polytetrafluoroethylene membrane, anchoring in the LAA using hooks positioned on the struts of the cage (Fig. 17.1). Despite favorable clinical results with an annual ischemic stroke rate substantially lower than predicted by CHADS$_2$ score (3.8 % vs. 6.6 %) [2], the manufacturer discontinued the development of the device in 2006. This was the result of the strict and therefore costly requirements of the FDA, which is why approval of the occluder on the American market did not appear possible. But the development of other endo- and epicardial systems for LAA closure continued. This section presents requirements and techniques for the occlusion of the LAA considering commercially available devices to which CE Mark or FDA approval was granted.

17.1 Preprocedural Imaging and Medication

Prior to the implantation of an LAA occlusion device, all patients must undergo preprocedural imaging to explore the anatomy of the LAA and to exclude thrombi in the left atrium and the LAA. The standard imaging technique is 2D and 3D transesophageal echocardiography (TEE). TEE enables measurement of the LAA ostium, the landing zone of the elected occlusions device, and the length of the LAA body, and it allows to characterize the shape of the LAA, especially when there are multiple lobes (number, shape, and localization). Some operators are using additional preprocedural imaging like computed tomography angiography or magnetic

M. Hornung, MD • J. Franke, MD • S. Gafoor, MD • H. Sievert, MD (✉)
CardioVascular Center Frankfurt, Frankfurt, Germany
e-mail: info@cvcfrankfurt.de

Fig. 17.1 The PLAATO occluder – a self-expanding nitinol cage with hooks on the struts of the cage for anchoring in the LAA. The whole occluder is covered with a polytetrafluoroethylene membrane

resonance imaging. Further important preprocedural information include the anatomical orientation of the LAA body axis, as this has important implications for the location of the transseptal puncture. Most commonly, TEE is performed immediately prior to the intervention. The authors recommend the whole procedure (transseptal puncture, LAA measurement, and device implantation) to be done under echocardiographic guidance (TEE or intracardiac echocardiography, ICE).

No later than 48 h prior to the procedure, patients should receive loading doses of 500 mg aspirin and 600 mg clopidogrel (for patients without previous regular intake). Antibiotic prophylaxis should be administered before and after the procedure. Femoral venous access is obtained under local anesthesia, and transseptal puncture is performed under TEE (or ICE) and fluoroscopic guidance. The procedure is usually performed under local anesthesia at the right femoral access site and slight sedation using midazolam or propofol, if needed. Sedation is foremost needed due to the application of TEE. The usage of ICE may eliminate the need of sedation.

17.2 Transseptal Puncture

The first crucial step of the procedure is the transseptal puncture. After local anesthesia of the femoral access site, an 8-French transseptal sheath is inserted into the right femoral vein and advanced into the right atrium. Through this sheath, a transseptal needle is advanced to the intra-atrial septum. The transseptal puncture is indicated in the posterior and inferior segment of the fossa ovalis to facilitate an anterior superior trajectory that optimizes device delivery for most LAAs. As the height of

the puncture depends on the orientation of the LAA, the puncture should always be done under echocardiographic guidance. In cases with rather cranial orientation of the LAA axis, the puncture site should be rather low and is best seen in bicaval view (90° in TEE). In cases with an anterior or rather caudal orientation of the LAA axis, the puncture should be done in the upper part of the septum. But independent from orientation of the LAA axis, all transseptal punctures should be carried out as far posterior as possible to facilitate access to the LAA. This can best be controlled in 45° view in TEE. Subsequent to transseptal puncture, the transseptal sheath is advanced though the puncture into the left atrium, and the needle is pulled back into the sheath. After echocardiographic exclusion of a pericardial effusion, 10,000 units of heparin should be administered to achieve an activated clotting time (ACT) of at least 250 s. The transseptal needle is exchanged for either a 0.035-in. stiff wire placed in the left upper pulmonary vein or a transseptal pigtail guidewire placed in the left atrium. Next, the transseptal sheath is exchanged over the wire for the occluder specific delivery sheath.

Independent from the LAA occlusion device chosen, the most effective and safe method to avoid air embolism is to wait for adequate back bleeding while holding the proximal end of the delivery catheter below zero. Furthermore, continuous saline infusion through the side arm of the sheath and slow removal of the dilator are recommended to avoid air embolism caused by air suction through the valve of the sheath during removal of the sheath dilator.

17.3   Watchman (Boston Scientific Corporation, Marlborough, MA, USA)

The Watchman system is the most commonly implanted LAA occlusion system worldwide. The first procedure was performed in August 2002. Since then, the device has repeatedly been technically modified. The occluder consists of a nitinol frame structure with ten fixation anchors along its waist. When fully deployed, the nitinol frame has a parachute-like configuration (Fig. 17.2). The proximal part of the system, which faces the left atrium after implantation, is covered with a thin polyethylene terephthalate (PET) membrane which is designed to reduce post-implant thrombus formation on the occluder, thus to allow faster endothelialization.

After successful transseptal puncture, the Watchman access sheath is introduced to the left side of the heart, and a pigtail catheter (5 Fr or 6 Fr) is introduced through the access sheath and advanced into the LAA to perform an angiography and make the necessary measurements. We take the fluoroscopic measurements in a caudal RAO projection. Furthermore, additional LAA measurements should be done by TEE in at least four views (0°, 45°, 90°, and 135°) with the ostium of the left circumflex artery as the essential landmark. Measurement should be done from the edge of the LCX to the opposite wall of the LAA, perpendicular to the axis of the LAA. We recommend an occluder size about 20 % bigger than the largest diameter measured to achieve the compression rate needed to engage the fixation barbs of the Watchman device into the wall of the LAA.

Fig. 17.2 The Watchman occluder – the parachute-like configuration of the nitinol frame carries ten fixation barbs along its waist. The part facing the left atrium is covered with a polyethylene terephthalate (PET) membrane

Fig. 17.3 The Watchman occluder delivery sheaths – the *double-curved* access sheath, the *single-curved* access sheath, and the *anterior curve* access sheath (from *left* to *right*)

The Watchman system consists of three parts: the specific transseptal access sheath with an outer 14-Fr diameter (inner diameter 12 Fr), the 12-Fr delivery catheter, and the Watchman device, which comes preloaded within the delivery catheter. The access sheath is available in three different shapes to facilitate the device placement depending on the orientation of the LAA: a single-curved, a double-curved, and an anterior curved sheath (Fig. 17.3). The access sheath with a dilator is advanced into the left atrium. Once in place, the dilator is removed, and the pigtail catheter is then advanced into the LAA. This allows atraumatic tracking of the access sheath into the LAA.

Knowledge of the specific markers on the access sheath is mandatory for correct device placement. There are four markers, one distal marker at the tip of the sheath
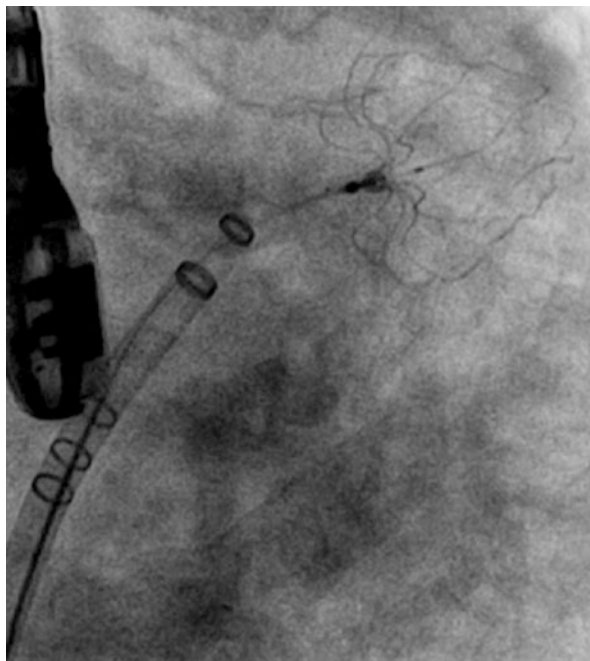
Fig. 17.4 Fluoroscopy of a deployed Watchman occluder – the deployed Watchman occluder on the right side is still connected with the delivery catheter. On the *left* side, the delivery sheath is shown, with its three radiopaque markers for optimizing occluder positioning before deployment

as well as three more markers placed more proximally (Fig. 17.4). The three proximal markers provide information on the placement of the most proximal part of the occluder, facing the left atrium when fully deployed. Depending on the size of the chosen occluder, its proximal end will align with one of these markers: the largest device size (33 mm) aligns with the most proximal placed marker, the 27-mm device aligns with the middle marker, and the smallest device (21 mm) aligns with the most distal of the three markers. The 30-mm and the 24-mm devices align between the markers, respectively. Knowledge of these specifications is important in order to place the access sheath correctly. Depending on the selected occluder size, the appropriate marking of the access sheath should align with the imaginary connecting line between the distal edge of the LCX and the opposite wall of the LAA, perpendicular to the LAA axis.

While introducing the delivery catheter into the access sheath, the delivery catheter with the closure device is continuously or intermittently flushed with heparinized saline to avoid air bubbles and air embolism. The delivery catheter is advanced under fluoroscopic guidance until its distal marker almost aligns with the distal marker of the access sheath. The access sheath must then be pulled back gently until the operator feels a click. This interlocks the access sheath with the delivery catheter. After checking the position of the delivery system fluoroscopically, the occluder can be deployed. The interlocked access and delivery sheath are pulled back while

holding the delivery cable of the device in a stable position. This allows the device to deploy while still being fixed to the delivery system. The combined delivery system allows complete retrieval of a deployed occluder in case of insufficient placement. When optimal device position, sizing, and device seal are ensured in angiography and in TEE, a last test of stability, a tug test, should be performed before releasing the occluder. For this purpose, the delivery core wire is gently pulled under simultaneous injection of contrast medium to see the movement of the LAA together with the occluder. After successfully passing this test, the device is released from the delivery system by turning the core wire counterclockwise five times. We recommend final contrast injections as well as a final control with TEE in all four views (0°, 45°, 90°, and 135°) to check for residual leaks.

Within the PROTECT-AF trial [3], combined oral anticoagulation with warfarin and with aspirin was continued for at least 45 days after the implantation of the Watchman system to facilitate device endothelialization and to reduce the risk of thrombus formation. If TEE after 45 days showed successful occlusion of the LAA, warfarin was stopped, and an oral dual antiplatelet therapy with 100 mg of aspirin and 75 mg of clopidogrel was started until 6 months of follow-up, from which point aspirin alone was continued indefinitely. The ASAP trial tested the implantation of the Watchman device without temporary post-interventional anticoagulation [4]. The patients received aspirin and clopidogrel for 6 months, followed by lifelong aspirin daily. The rate of device associated thrombus formation within 6 months after Watchman implantation was not increased when compared to the patients examined in the PROTECT-AF trial. Therefore, the authors of this chapter recommend a dual antiplatelet therapy with 100 mg of aspirin and 75 mg of clopidogrel for 6 months after the implantation. In case of successful occlusion of the LAA and missing evidence of thrombus formation on the occluder, thereafter we stop clopidogrel and aspirin.

17.4   Amplatzer Cardiac Plug/Amulet (St. Jude Medical, Inc., St. Paul, MN, USA)

After other non-dedicated Amplatzer devices have been used for LAA closure, the Amplatzer Cardiac Plug (ACP) was developed as a device designed especially for percutaneous occlusion of the LAA in 2008. The ACP consists of a distal lobe and a proximal disk, connected by a stretchable waist (Fig. 17.5). It is built of a self-expanding nitinol frame including two polyester patches. After its deployment, the distal lobe is placed in the neck of the LAA, while the proximal disk covers the ostium of the LAA. The lobe has six pairs of barbed stabilization wires on its outer circumference to secure itself to the walls of the LAA, thus reducing the risk to device embolization. The polyester filling of the ACP facilitates endothelialization and decreases blood flow through the occluder. It is available in sizes from 16 to 30 mm in 2 mm steps, according to the outer diameter of the lobe. The proximal disk extends the lobe by 4 mm for device sizes from 16 to 22 mm and by 6 mm for device sizes from 24 to 30 mm.

Fig. 17.5 Amplatzer LAA occlusion devices – the Amplatzer Cardiac Plug (*left*) and its second generation, the Amulet device (*right*) – technical differences are displayed in Table 17.1

The delivery system of the ACP consists of three parts: a loader, a delivery cable, and the delivery sheath. First antegrade loading of the device into the delivery system is required. A temporary loading cable is attached to the thread on the distal end of the lobe, and a delivery cable has to be attached to the thread on the proximal side of the disk; after that, the ACP device is pulled into the loader and through the loader until it reaches the connector of the loader. The loading process is performed in antegrade fashion to compress the hooks of the lobe with their arms down to ensure their functionality after deployment in the LAA. Then the loading cable is unscrewed, and the connector of the loader is attached to the delivery sheath. While unscrewing the loading cable, the tip of the lobe must be held firmly in order not to screw the delivery cable off at the same time, too. The loading process must be carried out completely submerged in a container with saline. Thereafter the delivery sheath should be flushed with saline meticulously to avoid air embolism. The delivery sheath itself, the Amplatzer TorqVue 45 × 45°, has two 45° bends facing anterior at its distal end to facilitate the entering of the LAA after successful transseptal puncture. The sheath size ranges from 9 Fr for the 16 mm ACP, over 10 Fr for the 18–22-mm versions of the ACP, up to 13 Fr for all devices with a size of 24 mm or bigger.

In January 2013 CE Mark approval was granted to the Amulet device (Fig. 17.5), the second generation of the ACP. As an alteration, the newer Amulet device comes preloaded in the delivery sheath to ensure easier and faster use. The Amulet is available in sizes up to 34 mm: the proximal disk extends the lobe by 6 mm in device sizes from 16 to 22 mm and by 7 mm in sizes from 25 to 34 mm. A possible advantage of this larger disk may be improved sealing of the ostium of the LAA. Furthermore, the lobe is longer when compared to that of the ACP (7.5 mm in Amulet sizes 16–22 mm and 10 mm in Amulet sizes 25–34 mm compared to 6.5 mm in any size of the ACP device). In combination with an increased number of hooks (ten pairs instead of six for the sizes 28–34 mm), this seems beneficial in positioning

Table 17.1 Comparison of the Amplatzer Cardiac Plug and the Amulet occluder

	ACP								Amulet							
Sizes (mm)	16	18	20	22	24	26	28	30	16	18	20	22	25	28	31	34
Disk diameter	Lobe + 4 mm				Lobe + 6 mm				Lobe + 6 mm				Lobe + 7 mm			
Lobe length (mm)	6.5								7.5				10			
Waist length (mm)	4								5.5				8			
Sheath diameter (Fr)	9	10			13				12					14		
Pairs of stabilizing wires	6								6		8				10	

and anchoring the device in the LAA. The required delivery sheath size for the Amulet device is slightly bigger when compared to the ACP devices: 12 Fr for Amulet occluders from 16 to 25 mm and 14 Fr for occluders with a lobe diameter of 28, 31, and 34 mm (Table 17.1).

The device size selection should be made by angiographic and echocardiographic measurement of the landing zone of the distal lobe and the ostium of the LAA. The landing zone of the distal lobe should be measured 1–2 cm distally to the plane of the LAA ostium. For choosing the optimal occluder size, we recommend an oversizing of about 20 % with regard to measured diameter of the landing zone of the lobe.

Pulling back the delivery sheath while holding the device in position deploys the distal lobe of the occluder. Deployment of the lobe should be carried out carefully to ensure the entire lobe is within the neck of the LAA, and at least two-thirds of the lobe should be located distal to the left circumflex artery. Depending on the individual anatomic findings, sometimes it is not possible to position the whole lobe of the occluder perpendicular to the axis of the LAA neck, so that the device may extend into the lobe of the LAA. After satisfactory positioning of the lobe, the proximal disk is deployed by further pulling back of the retrieval sheath. Successful implantation is defined by proper compression of the lobe, separation of the lobe and the disk on angiography, concave shape of the disk, and correct angulation of the lobe and disk in relation to the plane of the LAA ostium (Fig. 17.6). In case of unsatisfying positioning, the device can be recaptured. The occluder should not be resheathed completely, as this may cause damage or distortion of the hooks. To know how far the occluder may be resheathed, the lobe has radiopaque markers slightly proximal to the insertion point of the hooks. Up to these markers, the device can be taken safely back into the delivery catheter for repositioning.

17.5 Coherex WaveCrest® Left Atrial Appendage Occlusion System (Coherex Medical, Salt Lake City, UT)

Subsequent to the WaveCrest I trial of the WaveCrest Left Atrial Occlusion System, CE Mark approval was granted in August 2013. The device is designed for positioning in the ostium of the LAA without the necessity of catheter manipulation deep in

Fig. 17.6 Fluoroscopy of a successfully implanted ACP occluder – successfully implanted ACP occluder with proper compression of the lobe, separation between the lobe and the disk, *concave* shape of the disk
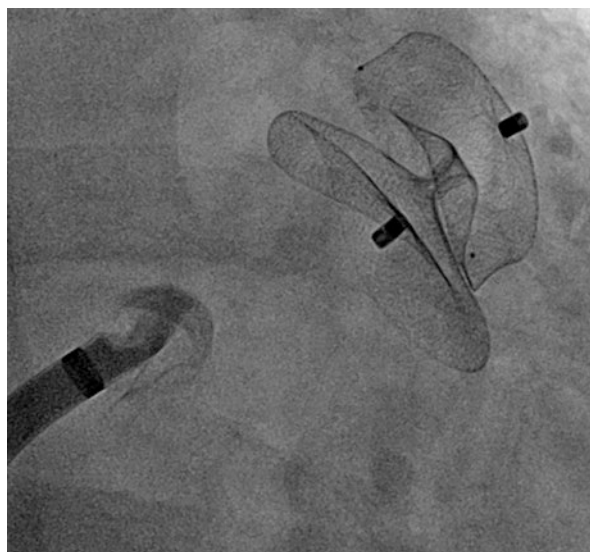
body of the LAA, which has thin walls and is filled with pectinate muscle, potentially reducing the risk of perforation. The implant is made up of two separate components: the occluder and the retractable anchor system, which deploys distal to the occluder. The occlusive membrane is a composite construction. The surface of the membrane that is exposed to the left atrium is covered with expanded polytetrafluoroethylene (ePTFE) membrane to minimize thrombogenicity and facilitate endothelialization (Fig. 17.7). Ten inter-anchor struts make up the distal part of the device when deployed. There are ten bidirectional microtines and ten monodirectional microtines to create a total of 30 points of tissue interaction. Five of the ten anchors have radiopaque tantalum markers to help the operator visualize anchor position. This device is unique in its design with separate steps for occluder positioning and anchoring. The occluder is deployed in the ostium of the LAA, and the anchors are only deployed once the operator is satisfied with the position and closure. If it is necessary to reposition the occluder, the anchors and the occluder are completely retrievable to allow full or partial recapture, enabling the device to be repositioned at any time during the implant procedure. The occluder is available in three sizes with diameters of 22, 27, and 32 mm.

There are four different models of the 15-French WaveCrest Delivery Sheath available to assist in a coaxial placement of the WaveCrest Occluder: 60°, 75°, 90°, and 90°s (with a distal superior angle). The 75° sheath is appropriate for most LAA anatomies. The 90° sheath is useful in LAAs with a rather horizontal or inferior trajectory, and the 60° and 90°s sheaths are of advantage in case of a superior trajectory of the LAA. After a successful transseptal puncture, a contrast injection is helpful to select the correct sheath shape. Once the delivery sheath is across the septum, the dilator and the guidewire are removed. A pigtail catheter may be advanced through the delivery sheath lumen to facilitate positioning in the LAA ostium. This

Fig. 17.7 The Coherex WaveCrest occluder – the part of the occluder facing the left atrium is covered with an ePTFE membrane. Ten interlinked anchor struts build a total of 30 points of tissue interaction

step is optional since the delivery sheath is only advanced just distal to the LAA ostium. Deep engagement of the delivery sheath in the LAA is not necessary or recommended. The delivery sheath has a soft distal tip with two radiopaque markers, 5 and 15 mm from the tip. These markers are used to assist the operator with better visualization and correct positioning of the delivery sheath in the ostium of the LAA.

TEE examination should include measurement of the anticipated landing zone in at least four projections (0°, 45°, 90°, and 135°). The landing zone is adjacent to the edge of the left circumflex coronary artery. The sizing chart included on the product label has recommendations for device size selection depending on the diameter of the anchor landing zone in TEE long- and short-axis views. Oversizing the device is unnecessary and may diminish the stability of the anchors or cause improper deployment of the occluder.

Initial preparation of the WaveCrest device for use includes retracting the anchors before the device is collapsed into the loader, which constrains the device for

insertion into the delivery sheath. After flushing the delivery system with heparinized saline, the implant and the loader are submerged under heparinized saline, while the implant is pulled into the loader. The loader then is advanced into the rotating hemostatic valve of the delivery sheath. The proximal portion of the delivery sheath includes a clear introduction window. If air is observed in this window, it must be aspirated through the delivery sheath flush port before further advancement of the device. The device can then be advanced to the distal tip. The occluder is then unsheathed completely for optimal positioning under fluoroscopic and TEE guidance. Supplementary contrast injection through the delivery sheath may facilitate the positioning. If the system has assumed the desired position, the anchors can be deployed for fixation. The radiopaque anchor core is visible when the anchors are extended but is hidden within the occluder hub and delivery catheter when the anchors are retracted (Fig. 17.8). Five to 10 mm of space distal to the anchors is ideal for unimpeded anchor extension. As the LAA ostium is not planar, anchor engagement in the area of the posterior wall of the LAA may require additional manipulation. Anchor engagement should be checked in multiple fluoroscopic and TEE views. Before final release of the implant, a stability test is recommended. The delivery sheath is pulled back approximately 2 cm from the occluder. A contrast injection through the delivery catheter into the distal LAA is used in conjunction with the tug test to help the operator assess stability and occlusion. If the implant is
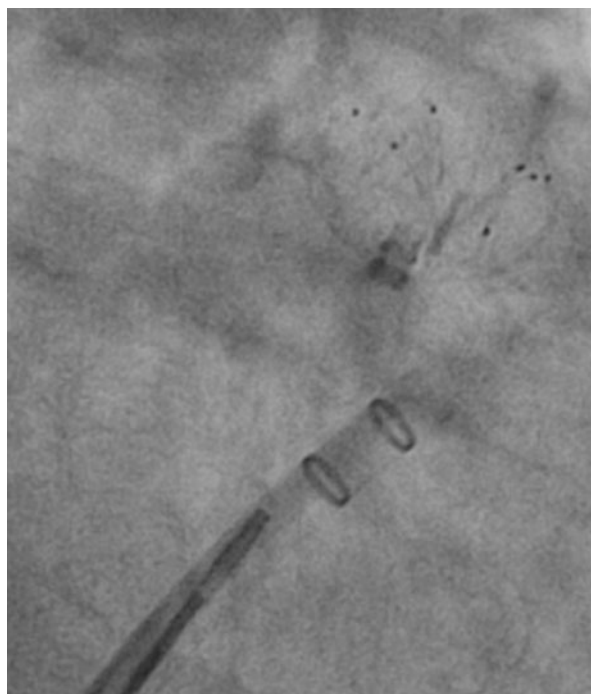

Fig. 17.8 The deployed Coherex WaveCrest – the released Coherex WaveCrest occluder in the *upper right* corner with its radiopaque tantalum markers incorporated into the anchor struts

not in a stable position or is not occlusive, the anchors may be retracted and the device fully recaptured and redeployed.

Finally, the WaveCrest occluder is released by first unscrewing of the anchor actuator knob and subsequently pressing the anchor release button. The anchor actuator is then pulled proximally while holding the delivery catheter stationary, causing the implant to detach.

Dual antiplatelet therapy with aspirin and clopidogrel is recommended for 6 weeks. A TEE examination to test for LAA occlusion should be performed at 45 days post-implant. The physician may then elect to stop clopidogrel therapy; however, aspirin should be continued indefinitely.

17.6   Lariat (SentreHEART, Red Wood City, CA, USA)

The Lariat device is a minimally invasive closed-chest LAA ligation technique that mimics the surgical ligation of the LAA to achieve permanent closure without the necessity of an endocardial implant. The system consists of the following components: a 0.025-in. endocardial and a 0.035-in. epicardial guidewire (both with magnetic tips), a 15-mm compliant balloon catheter, a 12-Fr suture delivery device, a suture-tightening device, and a suture cutter (Fig. 17.9). The procedure uses an anterior pericardial access as well as a transseptal approach to place a guidewire with a
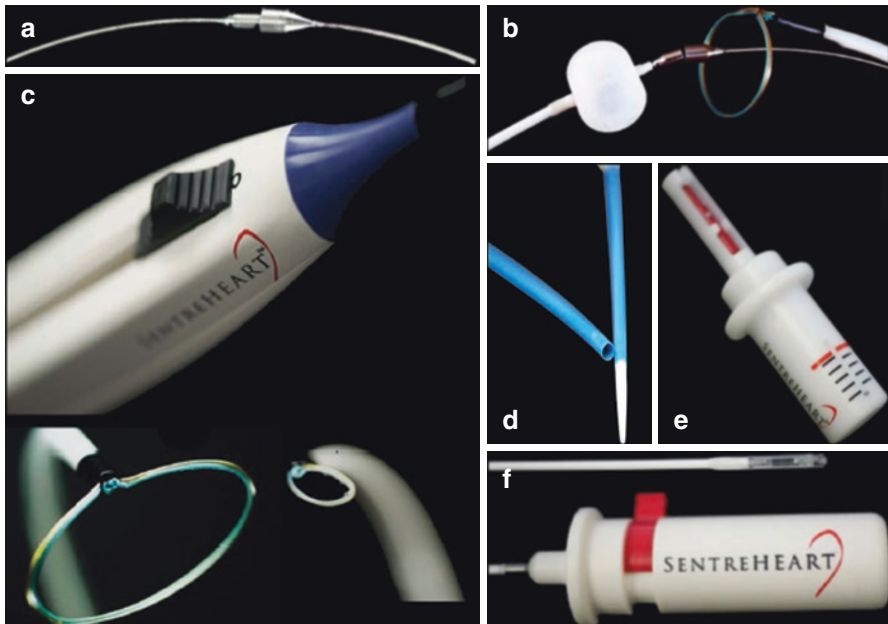

Fig. 17.9 The components of the Lariat system – the endo- and epicardial guidewires (**a**), the 15-mm compliant balloon catheter (**b**), the 12-Fr suture delivery device (**c**), the epicardial guide cannula (**d**), the suture-tightening device (**e**), and the suture cutter (**f**)

magnetic tip in the most distal part of the LAA. A magnetic counterpart wire is placed epicardially, and both wires are connected using their magnetic tips. These wires are then used to place the Lariat snare over the wire over the LAA. After confirmation of complete capture of the LAA with TEE and contrast injection, the snare is closed to achieve sealing of the LAA.

The success of the procedures starts with proper patient selection. As a certain pericardial space is required to achieve pericardial access and position the suture device freely over the LAA, patients with a history of open chest surgery, pericarditis, pectus excavatum, or any other conditions that may lead to pericardial adhesions have relative contraindications for this technique. An additional preprocedural imaging with computed tomography angiography may be reasonable not only to rule out the presence of LAA thrombus but also to check for further anatomic exclusion criteria: LAA width of more than 40 mm, a superior orientation of the LAA with the LAA apex directed behind the pulmonary trunk, the presence of a multilobed LAA in which the different lobes orient in different planes exceeding 40 mm, or a posteriorly rotation of the heart. In the presence of these anatomical features, the sling cannot be positioned over the LAA to guarantee complete sealing.

Pericardial access is achieved using a 17-gauge pericardial needle. The anterior-posterior fluoroscopic view is used to align the needle toward the lateral aspect of the cardiac silhouette, and the 90° left lateral view ensures that the puncture is on the anterior surface of the right ventricle. The injection of small amounts of contrast allows seeing tenting of the pericardium prior to puncture. Pericardial access is verified when the characteristic appearance of a small amount of contrast can be seen in the pericardial space and a 0.035-in. guidewire can be placed inside. Next, a 14-Fr, soft-tipped epicardial sheath is placed, and the guidewire is exchanged for the 0.035-in. magnetic-tipped guidewire of the Lariat system. An epicardial puncture performed too far medially may make the handling of the Lariat suture device more difficult.

Transseptal puncture is recommended under TEE guidance as previously described for the endocardial LAA occlusion devices. Next, an angiography of the left atrium and the LAA is performed to visualize the ostium of the LAA and its morphology. Contrast injection is done through the transseptal sheath or a pigtail catheter positioned in the LAA. Then, the 0.025-in. endocardial magnetic guidewire is advanced through the balloon catheter into the most anterior aspect of the LAA and connected with its epicardial counterpart. The EndoCATH balloon catheter (SentreHEART, Red Wood City, CA, USA) is placed at the ostium of the LAA for identification of the proper landing zone of the suture and for support during its placement. The interconnected guidewires serve a rail for the Lariat device snare. Proper placement of the snare at the LAA ostium is supported by inflation of the balloon on the balloon catheter. The snare can be opened and closed multiple times to ensure proper sealing of the LAA. Once TEE and angiography confirm complete closure of the LAA, the endocardial components (balloon catheter and guide wire) are removed, the TenSure Suture Tightener (SentreHEART, Red Wood City, CA, USA) is advanced epicardially, and the suture is cut near the LAA ostium using the SureCut Suture Cutter (SentreHEART, Red Wood City, CA, USA). A pigtail

catheter is left as a pericardial drain overnight which can be removed after echocardiographic exclusion of a relevant pericardial effusion on the following day.

As there is no foreign body left behind inside the heart, there is no need for post-interventional continuation of anticoagulation. However, the majority of the patients treated with the Lariat device so far received aspirin or clopidogrel after LAA ligation because of other concomitant diseases.

The high rates of technical success of the established LAA occlusion systems in combination with low periprocedural complication rates stimulated rapid development of new LAA occlusion devices. New techniques should facilitate device delivery and assure optimal positioning, minimizing the risk of appendage perforation, thrombus formation, or incomplete closure. Many new devices are under investigation in preclinical and first human trials.

References

1. Sievert H, Lesh MD, Trepels T, et al. Percutaneous left atrial appendage transcatheter occlusion to prevent stroke in high-risk patients with atrial fibrillation: early clinical experience. Circulation. 2002;105(16):1887–9.
2. Bayard YL, Omran H, Neuzil P, et al. PLAATO (Percutaneous Left Atrial Appendage Transcatheter Occlusion) for prevention of cardioembolic stroke in non-anticoagulation eligible atrial fibrillation patients: results from the European PLAATO study. EuroIntervention J EuroPCR Collab Working Group Interv Cardiol Eur Soc Cardiol. 2010;6(2):220–6.
3. Holmes DR, Reddy VY, Turi ZG, et al. Percutaneous closure of the left atrial appendage versus warfarin therapy for prevention of stroke in patients with atrial fibrillation: a randomised non-inferiority trial. Lancet. 2009;374(9689):534–42.
4. Reddy VY, Mobius-Winkler S, Miller MA, et al. Left atrial appendage closure with the Watchman device in patients with a contraindication for oral anticoagulation: the ASAP study (ASA Plavix Feasibility Study With Watchman Left Atrial Appendage Closure Technology). J Am Coll Cardiol. 2013;61(25):2551–6.

Difficult Cases and Complications from the Catheterization Laboratory: Left Atrial Appendage Perforation During Percutaneous Closure

18

Salvatore Saccà and Tomoyuki Umemoto

18.1   Introduction

PROTECT-AF trial proved that percutaneous left atrial appendage (LAA) closure was not inferior to anticoagulant therapy in preventing stroke [1–3]. In patients with contraindication to oral anticoagulant therapy (OAT) or with stroke despite appropriate OAT, percutaneous LAA closure could be an option. Possible periprocedural complications include stroke, puncture site bleeding, and cardiac tamponade.

18.2   Case Report

A 77-year-old lady, with well-functioning bioprosthetic aortic valve (cardiac surgery performed in 2004 for severe aortic stenosis), chronic atrial fibrillation (CHADSVASC 4, HASBLED 3), and hypertension, developed spontaneous intracranial subdural bleeding after 6 months of underdosed OAT (INR below 2). Since anticoagulation is clearly contraindicated in this patient, we decided to perform a percutaneous LAA closure with Watchman Left Atrial Appendage Occlusion Device (Boston Scientific, Natick, MA, USA).

S. Saccà (✉) • T. Umemoto
Department of Cardiology,
Mirano Hospital,
Mirano, Italy
e-mail: salvatoresacca@virgilio.it

18.3 Procedural Summary

Dual antiplatelets (aspirin 100 mg/day, clopidogrel 75 mg/day) were started 5 days before the procedure. The procedure was performed under local anesthesia with transesophageal echocardiography (TEE) guidance. To exclude possible three coronary vessel diseases, a coronary angiography was performed, showing absence of significant disease. A transseptal puncture was performed with 8-Fr Swartz guiding introducer and BRK-1 transept needle (St. Jude Medical, Plymouth, MN, USA). Then, after usual systemic heparinization (100 UI/kg), we advanced 6-Fr pigtail catheter having a radiopaque marker into the LAA through the introducer and performed injection in order to calibrate the size of LAA (Fig. 18.1). With the calibration by angiogram and TEE, we chose a 27 mm Watchman device. We inserted a 0.035-in. Amplatz Super Stiff wire (Boston Scientific, Natick, MA, USA) into the left atrium through the pigtail catheter. With this wire, we changed the 8-Fr Swartz guiding introducer to the Watchman Access System double curve 14-Fr introducer (Boston Scientific, Natick, MA, USA). Firstly, we gently advanced the pigtail catheter in the LAA and then, keeping it still, the 14-Fr introducer (a sort of telescope technique). We injected contrast with this 14-Fr introducer in order to check the position (Fig. 18.2). At this time, no contrast medium was visible in the pericardium, but we needed the introducer a little bit more advanced to deliver the Watchman device in appropriate position. After we advanced the introducer using a pigtail catheter, angiography was performed and showed extravasation of fluid into the pericardial space (Fig. 18.3, black arrow). We realized that LAA perforation occurred, fortunately without immediate clinical consequences. Immediately we advance the Watchman device and deployed it. After the deployment of the device inside LAA, another angiography was performed to check whether bleeding into the pericardial space stopped. As we could see no contrast medium exited into LAA anymore under deployment of Watchman device, we released the device completely (Figs. 18.4 and 18.5). After release of the Watchman device, we could confirm complete closure of LAA by left atrium angiogram (Fig. 18.6) and reverse heparin effect by protamine infusion. As transthoracic echocardiography (TTE) and TEE revealed few amount of pericardial effusion and hemodynamics was quite stable, the procedure was completed by sheath removal and venous puncture site closing by a cross-stitch. Total procedure time was 110 min. Total fluoroscopy time was 13 min. TTE at 2 h after the procedure revealed no pericardial effusion.

18.4 Discussion

AF induces more than 15 % of cerebral ischemic stroke [4–6]. For prevention of thromboembolic events in AF, anticoagulant therapy is one of the effective methods. Although warfarin is proved to be effective, there are some critical problems such as narrow therapeutic profile, multiple medication and food integration, and worsening bleeding disease [7]. Novel oral anticoagulants (NOAC) are also
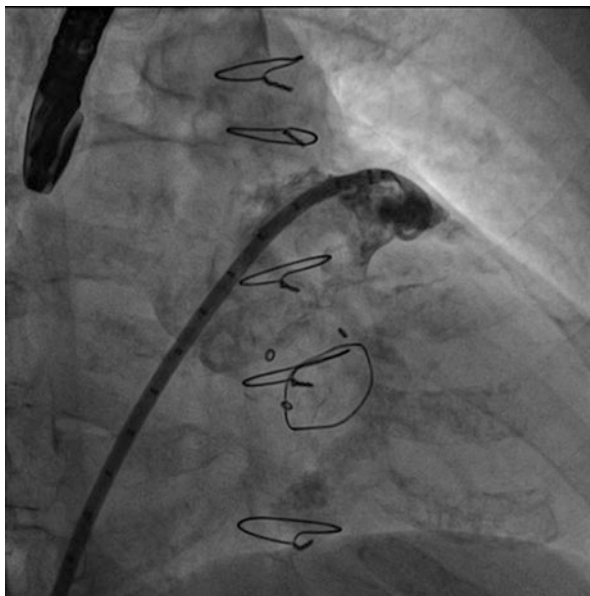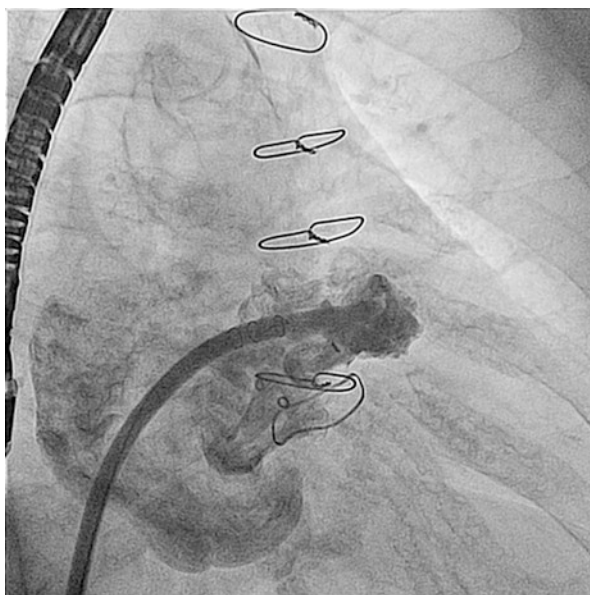
Fig. 18.1 Baseline angiogram of LAA

Fig. 18.2 Angiogram of LAA by sheath introducer

effective for preventing the stroke. For the patient who cannot keep the target range of INR by warfarin, NOAC will be an alternative. But it's still controversial if NOAC therapy is safe for patients with bleeding complication, even with INR below therapeutic threshold.

Fig. 18.3 LAA
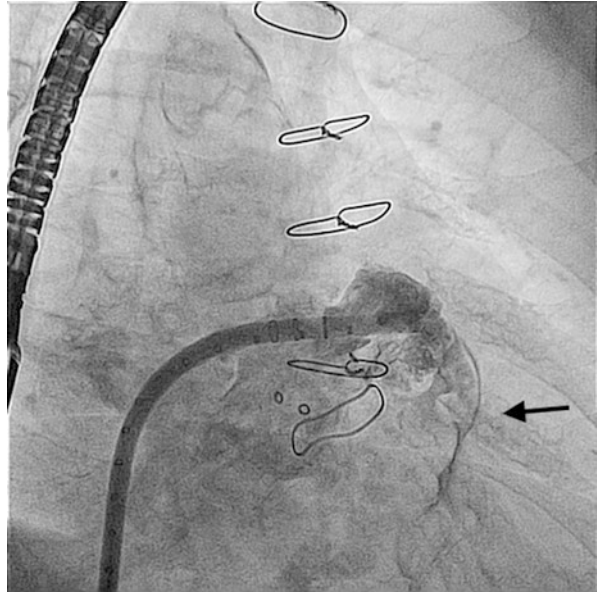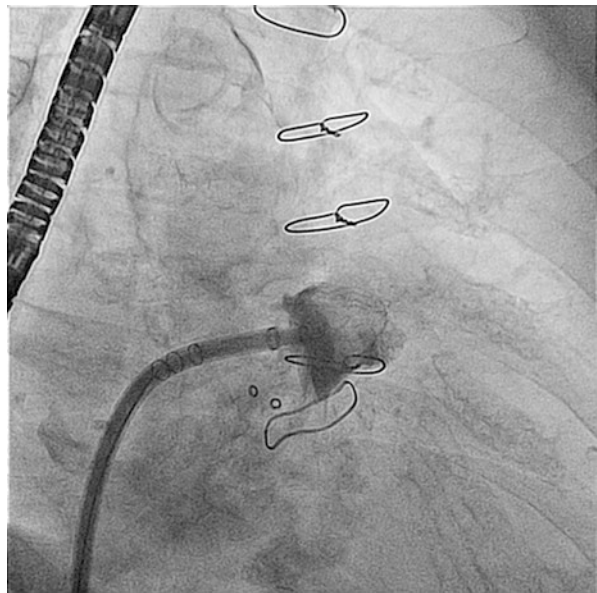perforation (*black arrow*)

Fig. 18.4 No leakage
before release the device

On the other hand, LAA is the site where most of thromboembolism come from, so mechanical approaches to close the LAA both surgically and percutaneously were developed [8–13].

Complications during percutaneous LAA closure include vascular complications, periprocedural stroke, LA or LAA perforation, dislocation of the device,

Fig. 18.5 Release the
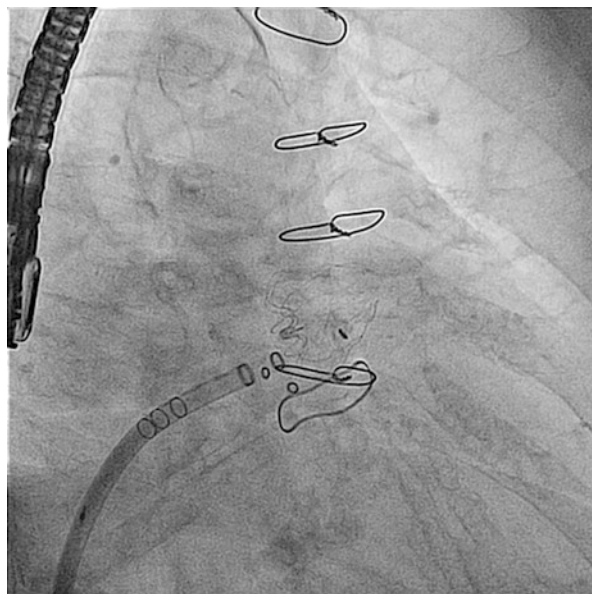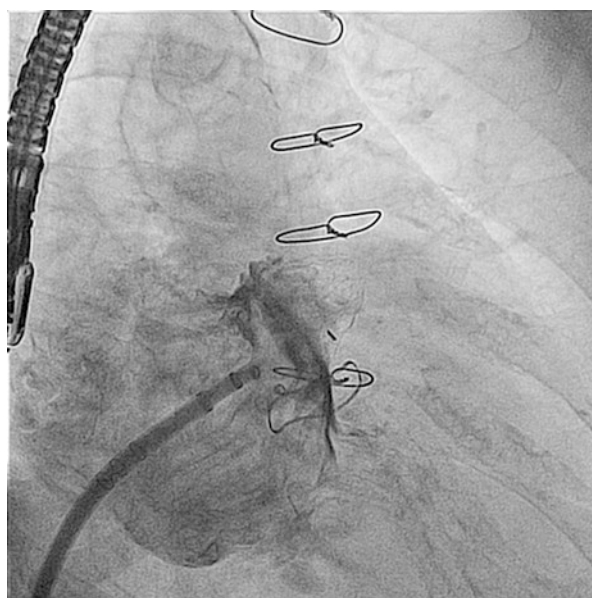Watchman device

Fig. 18.6 Final angiogram

post-procedural mitral regurgitation, and peridevice leakage. According to
PROTECT-AF trial, the reported incidence of serious pericardial effusions
(defined as the need for percutaneous or surgical drainage) during LAA closure is
4.8 % [1]. LAA perforation during LAA closure procedure can be caused by

introducer or closure device itself. It is usually difficult to recognize LAA perfora-tion because the perforating sheath becomes a plug of the perforated hole. With a little bit of pullback of the perforating sheath, the hole becomes visible. The most important thing is that a pigtail catheter should be used when advancing the 14-Fr introducer. Set the pigtail catheter a little bit outside the 14-Fr introducer that should prevent as much as possible the edge of the introducer from touching LAA wall directly. Advancement must be done gently as much as possible to avoid the damage of LAA wall.

In the case described, we advanced the 14-Fr introducer with pigtail catheter very gently. Nevertheless, LAA perforation occurred, since LAA wall is very thin and LAA perforation during this procedure might be ineluctable complication. If perforation occurs during LAA closure procedure and it is immediately recog-nized, first of all, the LAA closure device should be deployed immediately. After that, left atrium angiography, TTE, or TEE should be performed in order to check pericardial effusion and needle pericardiocentesis if needed. Reverse of heparin effect by protamine administration should be considered after measurement of activated clotting time. If bleeding into the pericardial space persists, surgical repair is the remaining option.

References

1. Holmes DR, et al. Percutaneous closure of the left atrial appendage versus warfarin therapy for prevention of stroke in patients with atrial fibrillation: a randomised non-inferiority trial. Lancet. 2009;374(9689):534–42.
2. Reddy VY, et al. Percutaneous left atrial appendage closure for stroke prophylaxis in patients with atrial fibrillation: 2.3-Year Follow-up of the PROTECT AF (Watchman Left Atrial Appendage System for Embolic Protection in Patients with Atrial Fibrillation) Trial. Circulation. 2013;127(6):720–9.
3. Reddy VY, et al. Percutaneous left atrial appendage closure vs warfarin for atrial fibrillation: a randomized clinical trial. JAMA. 2014;312(19):1988–98.
4. Sandercock P, Bamford J, Dennis M, et al. Atrial fibrillation and stroke: prevalence in different types of stroke and influence on early and long term prognosis (Oxfordshire Community Stroke Project). BMJ. 1992;305:1460–5.
5. Wolf PA, Benjamin EJ, Belanger AJ, Kannel WB, Levy D, D'Agostino RB. Secular trends in the prevalence of atrial fibrillation: the Framingham Study. Am Heart J. 1996;131:790–5.
6. Kannel WB, Wolf PA, Benjamin EJ, Levy D. Prevalence, incidence, prognosis, and predispos-ing conditions for atrial fibrillation: population-based estimates. Am J Cardiol. 1998;82:2N–9.
7. Bungard TJ, Ghali WA, Teo KK, McAlister FA, Tsuyuki RT. Why do patients with atrial fibril-lation not receive warfarin? Arch Intern Med. 2000;160(1):41–6.
8. Blackshear JL, Odell JA. Appendage obliteration to reduce stroke in cardiac surgical patients with atrial fibrillation. Ann Thorac Surg. 1996;61(2):755–9.
9. Aberg H. Atrial fibrillation: I, a study of atrial thrombosis and systemic embolism in a nec-ropsy material. Acta Med Scand. 1969;185(5):373–9.
10. Stoddard MF, Dawkins PR, Prince CR, Ammash NM. Left atrial appendage thrombus is not uncommon in patients with acute atrial fibrillation and a recent embolic event: a transesopha-geal echocardiographic study. J Am Coll Cardiol. 1995;25(2):452–9.

11. Sievert H, Lesh MD, Trepels T, et al. Percutaneous left atrial appendage transcatheter occlusion to prevent stroke in high-risk patients with atrial fibrillation: early clinical experience. Circulation. 2002;105(16):1887–9.
12. Sick PB, Schuler G, Hauptmann KE, et al. Initial worldwide experience with the WATCHMAN left atrial appendage system for stroke prevention in atrial fibrillation. J Am Coll Cardiol. 2007;49(13):1490–5.
13. Park JW, Bethencourt A, Sievert H, et al. Left atrial appendage closure with Amplatzer cardiac plug in atrial fibrillation: initial European experience. Catheter Cardiovasc Interv. 2011;77(5):700–6.

Difficult Cases and Complications from the Catheterization Laboratory: Left Atrial Appendage Closure Step-By-Step

19

Francesco Versaci, Stefano Nardi, Antonio Trivisonno, Angela Rita Colavita, Salvatore Crispo, Luigi Argenziano, Elpidio Pezzella, Anna De Fazio, Giampiero Vizzari, and Francesco Romeo

A 68-year-old man with hypertension, dyslipidemia, chronic kidney disease, and history of hemorrhagic stroke was admitted to our hospital because of atrial fibrillation (AF). After transesophageal echocardiography (TEE) that excluded the presence of left atrial appendage (LAA) thrombus, he underwent electrical cardioversion with sinus rhythm restoration. Nevertheless, he presented at 1-month follow-up visit with atrial fibrillation. Due to the history of hemorrhagic stroke and the subsequent contraindication to anticoagulation therapy, he was identified as a candidate to percutaneous closure of LAA. TEE was performed before the procedure to rule out the presence of LAA thrombus and to assess the dimensions and the morphology of the LAA. The procedure was performed under general anesthesia and TEE guidance. After transseptal puncture of the fossa ovalis, a 22-mm Amplatzer Cardiac Plug (ACP) (AGA, St. Jude Medical)

F. Versaci, MD (✉)
Department of Cardiovascular Disease, Tor Vergata University, Rome, Italy

Department of Cardiovascular Disease, Ospedale "Antonio Cardarelli",
Contrada Tappino, 86100 Campobasso, Italy
e-mail: francescoversaci@yahoo.it

S. Nardi, MD, PhD • L. Argenziano • E. Pezzella
Department of Cardiovascular Disease, Pineta Grande Hospital, Castel Volturno, Italy

A. Trivisonno • A.R. Colavita • S. Crispo • G. Vizzari
Department of Cardiovascular Disease, Ospedale "Antonio Cardarelli",
Contrada Tappino, 86100 Campobasso, Italy

A. De Fazio
Department of Cardiovascular Disease, Ospedale "Giovan Battista Grassi", Rome, Italy

F. Romeo
Department of Cardiovascular Disease, Tor Vergata University, Rome, Italy

231

device was advanced in the LAA through a dedicated delivery system (12-Fr Amplatzer TorqVue 45×45 Delivery Sheath – AGA, St. Jude Medical). Once the correct implanting zone was localized, the device was released under fluoroscopic and echocardiographic guidance. A check for pericardial effusion at the end of the procedure was done by transthoracic echo (TTE). The patient was discharged the day after the procedure with long-term therapy with a daily 100-mg aspirin and 75-mg clopidogrel for 3 months. Endocarditis antibiotic prophylaxis was also recommended for at least 6 months (Figs. 19.1, 19.2, 19.3, 19.4, 19.5, 19.6, 19.7, 19.8, and 19.9).

Fig. 19.1 Transesophageal echocardiography (TEE) was performed before the procedure to rule out the presence of left atrial appendage (LAA) thrombus and to assess the dimensions and the morphology of the LAA
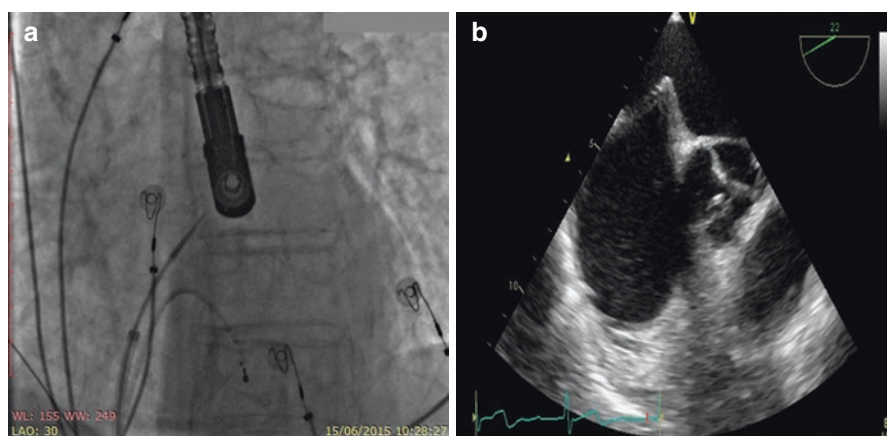

Fig. 19.2 Through the right femoral vein, an 8-Fr Mullins-style introducer (62 cm Preface sheath; Biosense Webster) was placed in the superior vena cava, and a Brockenbrough 71-cm transseptal needle (BRK™; St. Jude Medical) was advanced through the introducer (**a**). TEE was performed in order to obtain a precise puncture of the fossa ovalis and to check the "tenting" phenomenon when the introducer was correctly pushed inside the fossa toward the left atrium (**b**). The transseptal puncture was performed in the lower limbus of the fossa ovalis and in its middle part by pushing the needle without advancing the introducer
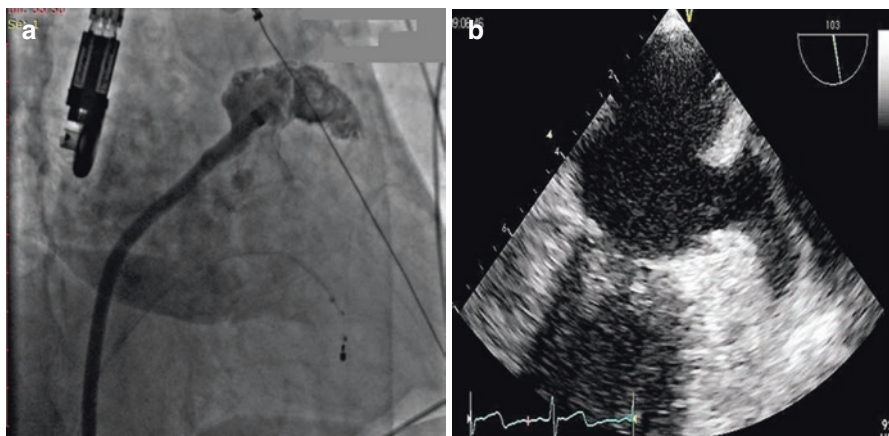
Fig. 19.3 The dedicated delivery system, 12-Fr Amplatzer TorqVue 45×45 Delivery Sheath (AGA, St. Jude Medical), was advanced in the left atrium over an Amplatz Super Stiff $0.035'' \times 260$ cm, short J tip guidewire (Boston Scientific). Atrium angiography was performed in RAO cranial view to size the LAA (**a**). TEE showed LAA ostium (transducer rotation at $87–105°$) (**b**)
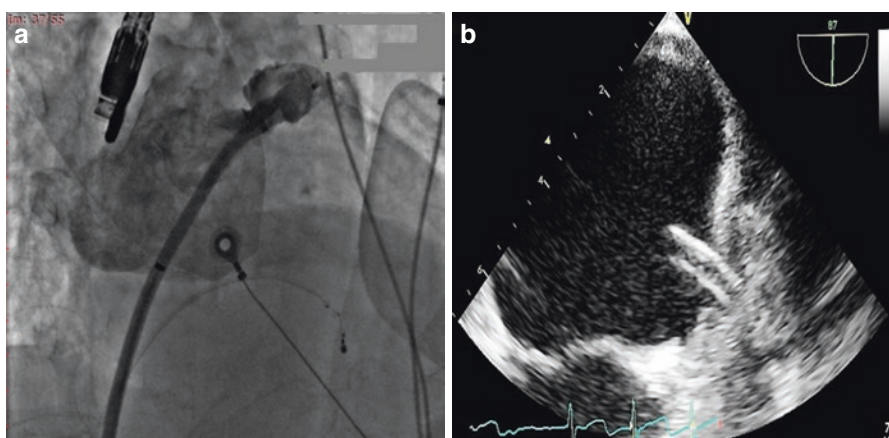

Fig. 19.4 A preloaded 22-mm Amplatzer Cardiac Plug (ACP) (AGA, St. Jude Medical) device was introduced in the delivery sheath and placed into the LAA, reaching the chosen landing zone under fluoroscopy guidance. The ACP lobe was advanced to obtain a "ball shape" (**a**). TEE view (transducer rotation at $79–90°$) (**b**)
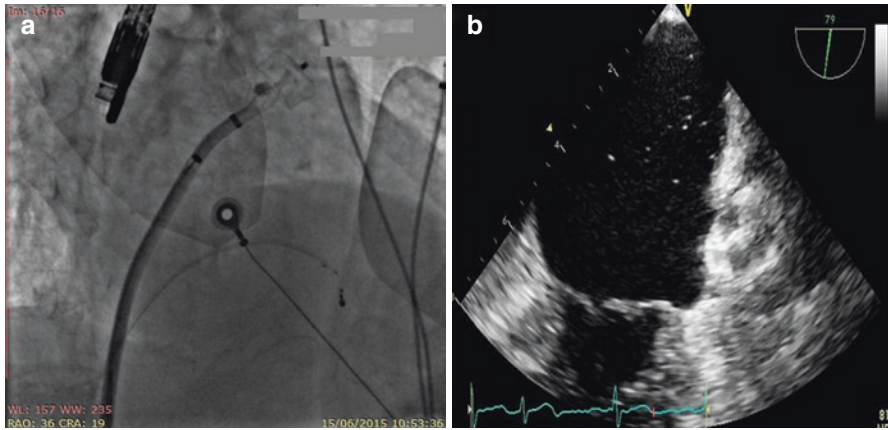
Fig. 19.5 Once the correct implanting zone was localized, the delivery cable was held in place while retracting the sheath to expose the lobe completely. The goal was to have the lobe of the device completely inside the LAA, with a slight deformation of its body (tire shape) (**a**). TEE view (transducer rotation at 79–90°) (**b**)
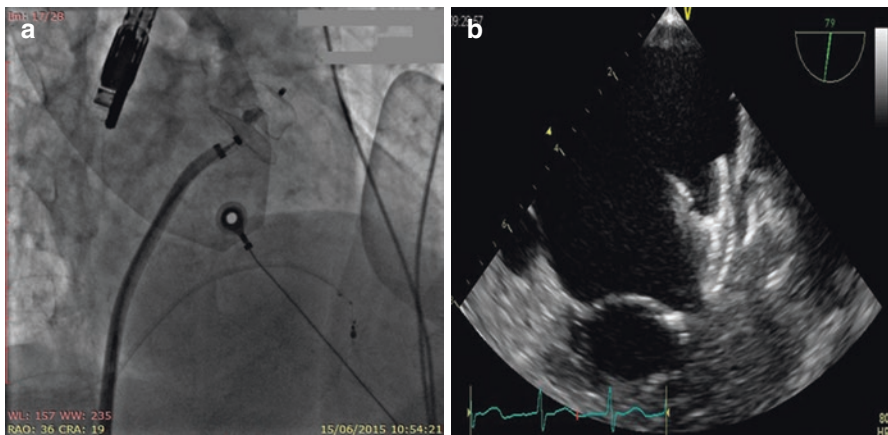
Fig. 19.6 While the device cable was maintained on traction, the delivery sheath was retracted to release the proximal disk (**a**). TEE view (transducer rotation at 79–90°) (**b**)
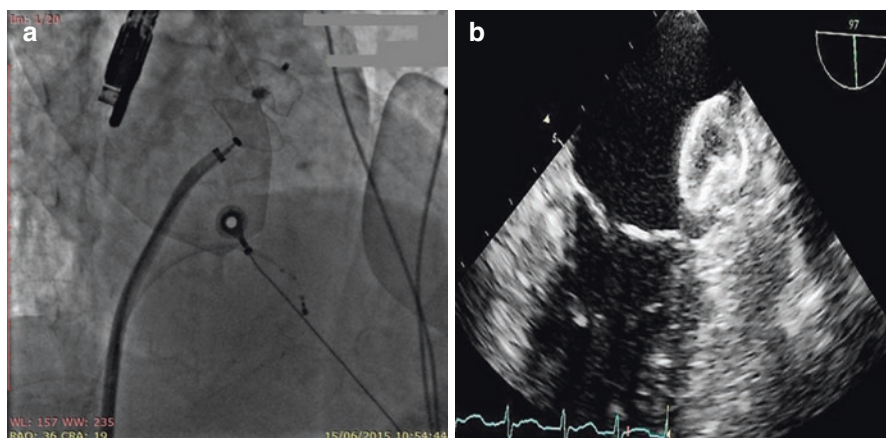
Fig. 19.7 As device embolization was reported as a possible complication, to verify the device stability before its release, the proximal disk was kept on traction for 3 min (**a**). TEE view (transducer rotation at 80–100°) (**b**)
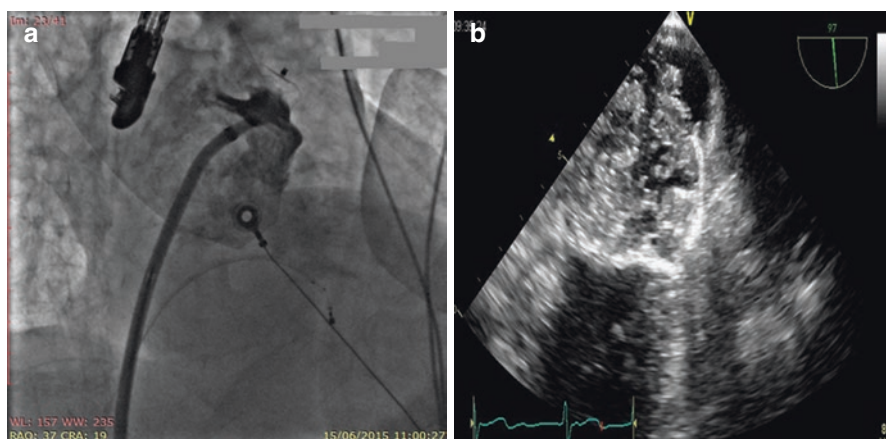
Fig. 19.8 Contrast media injection through the delivery sheath confirmed the correct position of the device and the effectiveness of LAA occlusion (**a**). TEE view (transducer rotation at 80–100°) (**b**)

Fig. 19.9 After confirmation of correct device position, it was released by turning the delivery cable vice counterclockwise (**a**). TEE view (transducer rotation at 80–100°) (**b**)

Part IV

Patent Foramen Ovale Closure

Percutaneous Options, Patient Selection, and Preoperative Evaluation

20

Gianluca Rigatelli

20.1 Introduction

Interatrial communications usually include a range of different atrial septal pathologies varying from patent foramen ovale (PFO) to true defects of interatrial septum within the fossa ovalis, the secundum atrial septal defects (ASD), and defects of interatrial septum outside the region of fossa oval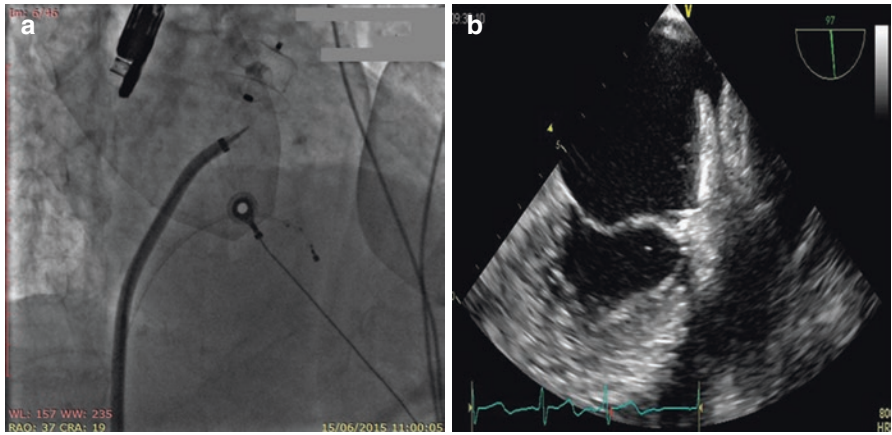is, such as the ostium primum defect and the sinus venosus defect. The PFO, defined as an incomplete adherence of septum primum and septum secundum at the level of the fossa ovalis, is a common finding in the general population with a prevalence of about 25 % [1]. It is mostly a benign condition, and its incidental finding in asymptomatic patients doesn't require any specific therapy. On the other hand, PFO is the main cause of right-to-left cardiac shunts followed by pulmonary arteriovenous fistulas, and it is potentially a risk factor for paradoxical embolism. Pathophysiology of right-to-left shunt in PFO patients, despite an unfavorable pressure gradient between the right and left atrium, has been postulated being caused by and confirmed by cardiac magnetic resonance flow studies [2]. Classical clinical presentations of patent foramen ovale include cryptogenic stroke, decompression syndrome, platypnea-orthodeoxia syndrome, and peripheral embolism. Other associations, like migraine with aura, have been suspected and are still matter of investigation. While many techniques and devices have been developed to make the transcatheter closure an effective and safe therapeutic option for this kind of patients, there is no complete agreement on which is the best management of this patients.

G. Rigatelli
Section of Congenital Heart Disease Interventions, Cardiovascular Diagnosis and Endoluminal, Interventions Unit, Rovigo General Hospital,
viale Tre Martiri, 45100 Rovigo, Italy
e-mail: jackyheart71@yahoo.it

20.2 PFO Pathophysiology in Otherwise Healthy Subjects

Several possible hypotheses have been postulated to explain the mechanism of right-to-left shunt in presence of normal cardiac pressures [3]. Firstly, despite the mean right atrial pressure is normally lower than the mean left atrial pressure, a physiologic transient spontaneous reversal of the left-to-right atrial pressure differential is present during early diastole and during isovolumetric contraction of the right ventricle of each cardiac cycle [4]; this reversal gradient may drastically increase under substantial hemodynamic changes caused by physiologic maneuvers that increase the right atrial pressure such as posture, inspiration, cough, or Valsalva maneuver or under some pathologic conditions resulting in high pulmonary vascular resistances [5], such as acute pulmonary embolism [6], hypoxemia due to obstructive sleep apnea [7], severe chronic obstructive pulmonary disease [8], right ventricular infarction [9], and positive end-expiratory pressure during neurosurgical procedures in the sitting position [10], causing right-to-left shunting when they are coupled with a secondary PFO.

Secondly, another anatomo-physiologic theory to explain the right-to-left shunting with both normal atrial and pulmonary vascular pressures involves the "flow phenomenon," i.e., a preferential blood flow streaming from the inferior vena cava toward the atrial septum as a part of the remnant prenatal circulatory pattern [11], but there is still only limited understanding of its potential significance in relation to right atrial anatomy and physiology. Thirdly, in the same way, a physiologic change in the relationship of right- and left-sided chamber compliance [12] that is probably exacerbated with age, with the right-sided chambers becoming stiffer than the left-sided counterpart, has been advocated.

Finally, an anatomic disarray of the inferior vena cava relative to the atrial septum due to mediastinal shift or heart counterclockwise rotation and/or distortion, following an ascending aorta enlargement [13], right pneumonectomy [14], or pericardial effusion [15], may result in an atypically horizontal reorientation of the plane of the atrial septum, which overlies the inlet of the inferior vena cava into the right atrium, facilitating part of the flow to stream directly into the left atrium via a PFO.

20.3 Percutaneous Options

As for secundum ASD, double-umbrella devices are the most used device for catheter-based therapy of PFO. These devices are usually composed by two disks of nitinol meshes connected by a single nitinol joint or by a mixed nitinol wires and tissue patches (PTFE, Dacron, etc.), which can be easily inserted into a catheter of varying size, ranging from 8 to 12 F. The catheter is usually passed through the PFO, and the device is firstly expanded in its left disk and then, after withdrawing the system, toward the fossa ovalis and interatrial septum in its right disk. The device is subsequently released by screwing the connecting cable or by cutting a connecting tender. Over the past 20 years, different alternative techniques and devices have been proposed, two of them deserving a brief description.

A "nothing behind" system, applying the radiofrequency energy or thermal ablation onto the surfaces of the fossa ovalis using a vacuum device to appose the fossa ovalis to the catheter, was aimed to fusing the two layers, the septum primum and the septum secundum, which anatomically form the PFO, in order to close the PFO without a metallic prosthesis. The system (PTfx) developed in the mid-2000s, didn't reach the market, because of a 63% incidence of ineffective closure requiring a second treatment [16].

The use of a sort of stent (Flatstent, Coherex Inc., Salt Lake City, USA) designed to be positioned within the tunnel formed by the septum secundum and septum primum components of the PFO has been developed in the mid-2000s in order to minimize the amount of implanted foreign material, reducing the risk of related complications such as thrombosis or erosion of the adjacent structures. It has been tested in a number of small studies and compared to the traditional devices finally suggesting that it can be useful and effective in tunnelized PFO with >4 mm tunnel and diameter less than 12 mm [17, 18].

20.4   Patient Selection

Patient selection for device-based PFO closure is probably one of the most complex and debated issues in interventional cardiology nowadays.

20.4.1 PFO and Stroke

While the relationships between PFO and paradoxical embolism is well known since the eighteenth century, the demonstration of a true increasing of risk of paradoxical embolism into the brain in patients with PFO is still controversial. In the 1990s and in the early 2000s, the early studies seemed to suggest an increased risk of stroke in patients with PFO, especially in patients with PFO and atrial septal aneurysm giving the basis for device development (Table 20.1).

Unfortunately in the late 2000s, the studies aimed to confirm the superiority of mechanical device closure over medical therapy with antiplatelet and anticoagulant agents, in particular the CLOSURE I and MIST [25, 26], failed to demonstrate even an equivalence, turning back the question about a real increase of risk of stroke related to the presence of PFO, despite large non-randomized series from different authors in different parts of the world have suggested a net benefit of mechanical closure over medical therapy.

Although many reasons have been claimed to be confounding factors in the design and enrollment process of these negative or inconsistent trials, and despite the results of some studies raised subsequently, such as the CODICIA study [27], TACET study [28], and the PC trial [29], which again suggested that PFO with or without septal aneurysm confers risk factor for stroke, and closure is ineffective, very recently, the RESPECT trial seems to shed light on.

The Randomized Evaluation of Recurrent Stroke Comparing PFO Closure to Established Current Standard of Care Treatment (RESPECT) trial [30])

Table 20.1 Results of the early studies about correlation between PFO and stroke recurrence

Author	Year	No. of patients	Findings
Mugge [19]	1995	195	Patients with ASA and shunt showed a high frequency of previous clinical events (65 %)
Bogousslavsky [20]	1996	140	The stroke or death rate was 2.4 % per year, but only eight patients had a recurrent infarct of 1.9 % per year
Cujec [21]	1999	90	Patients with PFO had a significantly higher rate of recurrent cerebral ischemic events than those without PFO. The attributable risk of PFO in recurrent neurological events was 7 %/patient/year
Mas [22]	2001	581	The risk of recurrent stroke was 2.3 % among the patients with patent foramen ovale alone, 15.2 % among the patients with both patent foramen ovale and atrial septal aneurysm, and 4.2 % among the patients with neither of these cardiac abnormalities
Mattioli [23]	2001	606	Atrial septal aneurysm predicted the presence of a patent foramen ovale. Multivariate analysis showed that atrial septal aneurysm was an independent predictor of an embolic event. A PFO was present in 95 % of patients with atrial septal aneurysm and cerebral ischemia aged less than 45 years
Lamy [24]	2002	581 (267 with PFO)	Patients with PFO were younger (OR, 0.95; 95 % CI, 0.93–0.97) and less likely to have traditional risk factors such as hypertension, hypercholesterolemia, or current smoking. Features suggestive of paradoxical embolism, such as Valsalva-provoking activities or deep vein thrombosis, were not more frequent in patients with PFO

evaluated patients 18–60 years old affected by nonfatal stroke randomized 499 to device closure using the Amplatzer device and 481 to medical therapy (aspirin 46.5 %, warfarin 25 %) over a period of follow-up of 8 years with a mean of 3 years. Despite the raw count, the intent to treat resulted in a nonsignificant difference between the two-arm, the per-protocol, and the as-treated analysis demonstrating for the first time a reduction of recurrence of stroke of 63.4 and 72.7 % with an immediate, procedural, and effective closure rates very high (>93 %). The analysis of the number needed to treat (NNT) demonstrated that 24 patients would need to be treated with the device in order to prevent one stroke over a 5-year period of time.

Although the results are not widely accepted, the most recent meta-analysis including this last trial, differently from the past, demonstrated a net benefit of closure over medical therapy (Tables 20.2 and 20.3).

Table 20.2 Results of the most recent meta-analysis about PFO/stroke, device closure/medical therapy

Author	Year	Studies considered or number of pts.	Findings
Ma [31]	2014	12 case control + 6 cohort	Case-control studies showed strong association between PFO and CS, but cohort studies failed to demonstrate a significant association
Khan [33]	2013	3 trials	PFO closure is beneficial as compared to medical therapy in the prevention of recurrent neurological events
Capodanno [32]	2014	2,231	Pooling trials of the Amplatzer PFO Occluder device resulted in a significant reduction of stroke (HR 0.44, 95 % CI: 0.20–0.95; $p=0.04$)
Pickett [34]	2014	2,303	Pooled hazard ratio was 0.67 in favor of closure. The use of the Amplatzer™ PFO Occluder resulted in significant stroke prevention benefit over medical therapy alone: hazard ratio = 0.44
Stortecky [35]	2015	2,963	The probability to be best in preventing strokes was 77.1 % for Amplatzer, 20.9 % for Helex, 1.7 % for Starflex, and 0.4 % for medical therapy
Patti [36]	2015	3,311	Patent foramen ovale closure was associated over the long term with significant net clinical benefit versus both antiplatelet and anticoagulant therapies; such benefit was driven by 50 % relative reduction of stroke and/or transient ischemic attack versus antiplatelet therapy and by 82 % relative reduction of major bleeding versus anticoagulant therapy

Table 20.3 Extra-cerebral PFO-related conditions

Conditions
Platypnea-orthodeoxia
Unexplainable hypoxemia
Extra-cerebral embolization
Hypoxemia in OSAS
Migraine with aura

OSAS obstructive sleep apnea syndrome

It appears clear that this trial helped at least to identify patients who may benefit from PFO closure: patients with recurrent stroke or stroke at first appearance in the absence of all other causes of stroke have been included nowadays in most advance protocols, even driven by some cost-effectiveness studies which suggest a cost-effective positive balance for device closure [37].

20.4.2 PFO and Other Conditions

Paradoxical embolism has been suggested as cause or mediator of a variety of different syndromes (Table 20.4), of whom migraine with aura and PFO causing life-threatening hypoxemia in patients with left ventricular assist device or heart transplantation deserve a separated brief discussion.

Different speculations have been argued on the causality of PFO and migraine attacks. Two main hypotheses have been put forward: first the shunt could allow microemboli or substances such as serotonin and norepinephrine to bypass filtration by the lungs and circulate through the brain and provoke migraine [38]. Second, the inheritance of PFO and migraine as lateralization defect: during embryonic development, any pineal gland displacement in respect to the medial line due to a deviation from the optimal serotonin levels may promote both migraine and incomplete closure of the fossa ovalis [39].

Recently, a certain degree of LA dysfunction, such as impairment of active or passive emptying or perhaps conduit function, has been suggested to be present in patients with PFO, especially those with atrial septal aneurysm [40], contributing to create the hemodynamic conditions for fibrin deposit or microthrombus formation just inside the left atrium, on the atrial aneurysm surface, or within the tunnel. Cortical spreading depression, a slow propagating wave of neuronal depolarization followed by neural suppression, has been suggested to be the main substrate for migraine, but its pathobiology is not completely understood. Most series of migrainous patients submitted to PFO closure reporting a certain amount of improvement faced to patients with severe disabling and refractory migraine and included patients with previous paradoxical embolism or at high-risk or paradoxical embolism. This might suggests that future studies should be probably conceived keeping in mind that not all patients with PFO have the same risk of paradoxical embolism and not all the patients with PFO suffered from significant migraine. Indeed, it is likely that the same factors influencing the risk of paradoxical embolism may play a role in the genesis of migraine and in particular in migraine with aura, a form of migraine

Table 20.4 RoPE score calculation

Characteristic	Points	Score
No history of hypertension	1	Maximum score 10
No history of diabetes	1	Minimum score 0
No history of stroke or TIA	1	
Nonsmoker	1	
Cortical infarct on imaging	1	
Age		
18–29	5	
30–39	4	
40–49	3	
50–59	2	
60–69	1	
≥70	0	

particularly linked with cortical spreading depression. Although actually there is no fully clear evidence to include migraine with aura patients in the selection process, however, in case of very severe migraine refractory to medical optimal therapy and permanent right-to-left shunt, there might be space for device-based therapy [41].

Complications relating to left ventricular assist devices (LVAD) are prone to cause hemodynamic instability. In particular, patients may experience life-threatening hypoxemia despite adequate pulmonary function. Right-to-left shunting may occur across the interatrial septum via unrecognized patent foramen ovale (PFO) or even atrial septal defects. Shunting may be insignificant before LVAD placement, whereas device implantation may decrease left atrial pressure sufficiently to cause considerable conduction of venous blood into the left atrium [42].

LVAD, however, presents a dangerous context for interatrial septal shunts. With the existing devices, the inflow cannula is placed within the left atrium or left ventricle and fills the device by gravity. In this way, left atrial pressure is reduced, creating a gradient that may result in considerable shunting and hypoxemia when interatrial communications are present. Factors that increase right atrium pressure may compound this effect. The degree of shunting across interatrial septal shunts may be aggravated by chest closure or pleural suction. Commonly, hypoxemia after orthotopic heart transplantation is due to pulmonary hypertension, pulmonary complications, and acute allograft rejection; rarely, it can be caused by structural defects either in the donor or recipient heart. In such case, similarly to post LVAD implantation period, hypoxemia is caused by an increased right-to-left shunt produced by volume overload of the donor right ventricle during the period of early postoperative myocardial depression [43].

Preimplantation transcranial Doppler thanks to its high sensitivity was able to correctly detect a right-to-left shunt in all patients scheduled for LVAD, whereas transesophageal echocardiography with bubble test was used to assess the type of shunt in those patients with positive transcranial Doppler (PFO versus an extracardiac fistula) [44].

20.5 Practical Keys for Patient Selection

For all we discussed above, the selection of patients for device-based closure should necessarily still be driven by a meticulous study of the clinical patients' profile and the evaluation of different biochemistry assays, together with a complete neurological work-up aimed in excluding acquired or genetic neurological syndromes eventually responsible of the clinical symptoms.

20.5.1 Patients' Clinical Profile

Patients should be evaluated not only for history and site of previous stroke or the other PFO-related conditions but also for classical risk factors, previous history of deep vein thrombosis, hematologic conditions contraindicating antiplatelet agents

to be taken after the device-closure procedure, neoplastic disease limiting the life expectance despite the young age, active systemic infectious disease that enables the patients to undergo an invasive procedure, and, finally, any dental pathologies that may act as infectious foci after device implantation.

20.5.2 RoPE Score

Recently, in order to help the clinicians to manage patients with symptomatic PFO, a clinical score has been implemented. The RoPE score [45] calculator is based on some clinical characteristics combined with age classes accounting for a score (Table 20.4).

The RoPE score has been shown to successfully disaggregate stroke patients into a stratum with a PFO prevalence that matches the background population (23 % RoPE score 0–3), which increases linearly to the highest RoPE scores with a very high prevalence of PFO (73 % RoPE score 9–10). This helps to stratify the patients in whom the PFO may be considered not a confounding factor but presumably a causing factor.

By the way, this score is a clinical score and it doesn't account for anatomical or functional characteristics, which have been suggested to be important for the patient selection and clinical decision-making process, such as the permanent shunt, the large shunt, the presence of atrial septal aneurysm, etc. Nevertheless, it can be used for an initial stratification of patients with PFO and stroke who should be subsequently checked for biochemistry data and obviously shunt grade.

20.5.3 Biochemistry Assay

Complete hematologic assay with platelet count and a complete assessment of coagulation protein abnormalities including protein C and S, antithrombin III, factor V Leiden, factor VII, factor IX, and factor X should be added to the normal biohumoral assay which is active in any center, before the device-based procedure.

20.5.4 Shunt Severity

The proper quantification of the right-to-left shunt remains necessary for any therapeutic decision about management of PFO patients. The TCD with bubble test identifies three shunt patterns under Valsalva maneuver:

- Mild (<10 bubbles within three cardiac cycles)
- Moderate (>10 bubbles within three cardiac cycles) with shower effect (many bubbles but still countable)
- Severe (>10 bubbles within three cardiac cycles) with curtain effect (many bubbles but not countable)

A distinct pattern of shunt occurs when bubbles are identifiable before the Valsalva maneuver (basal or permanent shunt) [46, 47]. In PFO patients, TEE identifies the shunt under Valsalva maneuver in trivial, small, moderate, and severe following current classification. Usually shower or curtain pattern of shunt correlates with moderate to severe shunt on TEE [48]. Severe and permanent shunt seems to correlate to an increased risk of paradoxical embolism [49].

20.5.5 Accepted Indications

Generally most national consensus and in particular the Italian consensus [50], despite some differences, accept as indications:

1. Cryptogenic event in medical treatment – naïve patients with >1 risk factor (patients should be informed that the mechanical closure is alternative to medical therapy). Risk factors include atrial septal aneurysm, large PFO, basal right-to-left shunt, Eustachian valve >10 mm, Chiari network, long PFO tunnel, multiple ischemic lesions on neuroimaging, Valsalva-associated clinical event, ischemic event on arousal, long travel/immobilization event, and simultaneous systemic or pulmonary embolism.
2. Any cryptogenic event (first or recurrent) on antiplatelet or anticoagulant therapy.

Other PFO-related syndromes such as platypnea-orthodeoxia, unexplained hypoxemia, peripheral or coronary paradoxical embolism, and refractory migraine with aura deserve a specific multidisciplinary work-up in order to identify patients who can benefit from PFO device-based closure.

20.6   Preoperative Evaluation

Preoperative cardiovascular assessment (Table 20.5) of patients with PFO is usually aimed to two main reasons:

1. To evaluate the clinical, anatomical, and functional characteristics of patients with PFO in order to confirm the clinical indication to mechanical closure
2. To evaluate the anatomical characteristics of patients with PFO in order to establish the suitability to device-based closure respective to the different device to be used and prevent eventual intraoperative technical complications or challenges

20.6.1 TTE and TEE

TTE and TEE are fundamental for a first screening of patients with suspected PFO as primary cause of their paradoxical embolism (cerebral or extra-cerebral): when

Table 20.5 Anatomical-functional characteristics of patients with ASD/PFO

Characteristic	Diagnostic tool	Significance
Left-to-right shunt >2	TEE, MRI	Therapeutic decision-making
Severe right-to-left shunt	TDC, TEE	Therapeutic decision-making
Permanent right-to-left shunt	TDC, TEE	Therapeutic decision-making
ASA	TEE	Management/device selection
Eustachian valve/Chiari network	TEE	Management/technical challenge
Long tunnel	TEE	Management/technical challenge
Left atrial dysfunction	TTE	Therapeutic decision-making
Associated anomalies	TEE, MRI	Management/technical challenge
Hypertrophy of the rims	TEE, MRi	Technical challenge

MRI magnetic resonance imaging, *TDC* transcranial Doppler, *TEE* transesophageal echocardiography

associated with the bubble test, preferably with the aid of second harmonic, TTE allows for a first diagnosis of PFO and atrial septal aneurysm (ASA) and a gross quantification of the shunt also in case of secundum ASD. The TEE is considered the principal imaging tool in defining PFO with or without ASA [51] and of suspected complex ASD, such as cribrosus ASD. It allows for confirming the first diagnosis of PFO and offers a precise quantification of the shunt, it visualizes properly the ASA, and it can evaluate the presence of an eventual basal shunt and its direction. It is important for defining presence of eventual embryonal remnants such as an incomplete floor of the fossa ovalis, which is not infrequent in ASD patients also presenting with ASA, and residuals of caval vein valves such as the Eustachian valve and the Chiari network. It allows for measuring the diameter of the fossa ovalis and of the defect, the length of the rims, the rim thickness, and eventual enlargement and dysfunction of left atrium and the left ventricle in PFO patients, important elements in deciding the management in particular of PFO patients >50 years old.

20.6.2 Transcranial Doppler Ultrasound

The TDC is the most sensitive imaging tool in detecting right-to-left shunt and remains the most preferred technique in quantifying the presence of basal shunt and Valsalva-induced shunt in PFO patients. Usually the study protocol includes monitoring of both MCAs through the temporal window by the use of 2-MHz probes. The contrast is obtained by mixing 100 cc of saline solution with 2–3 cc of Emagel and loading a 10-cc syringe with this mixture. The solution, agitated between two 10-mL syringes, connected by a three-way stopcock, is immediately injected with a 20-gauge/32-mm catheter placed in the antecubital vein to obtain a bolus of air microbubbles. This procedure is performed three times during normal breathing and the same number of times during a Valsalva maneuver. The bolus of microbubbles is injected in 1–2 s when this 7-s period ended. The importance of RLSh is evaluated by counting the number of signals in 1 MCA within 7 s of the injection, as previously reported [46].

20.6.3 Cardiac MRI

Magnetic resonance imaging can give us almost the same information as echocardiography as regards right chamber size, fossa ovalis and defect size, and shunt ratio but seems superior in depicting structure and relative rapports of eventual associated pulmonary venous return [52].

With the aid of these imaging tools, every patient with PFO scheduled for device-based closure should be evaluated in respect of ASA extension, Eustachian valve or Chiari network presence and extension, interatrial septal thickness, and tunnel presence and length in order to plan the proper device and technique to be used.

20.6.4 Atrial Septal Aneurysm (ASA)

Atrial septal aneurysm (ASA) has a prevalence in the general population between 0.22 and 4 %, but it rises to 8–15 % in patients with stroke [53]. It is a congenital malformation of the atrial septum characterized by bulging of at least 15 mm of the septum overlying the fossa ovalis region into either atrium.

After the first suggestion by Homma et al. [54], more recently, some studies suggested that PFO and ASA patients have multiple lesions on magnetic resonance imaging more frequently than PFO patients; Santamarina et al. observed that an embolic pattern was more frequent in PFO/ASA patients (44 %) compared with PFO patients (26.2 %) [55].

The coexistence of PFO and ASA is strongly associated to cerebral ischemic events through a supposed paradoxical embolism mechanism, but other new hypotheses are matter of investigation as the one proposed by our study group, consistent with an "atrial fibrillation-like" mechanism based on left atrial dysfunction [39].

It can have different degree of amplitude or severity (1–5), and it can be fixed or mobile toward the right (R) or left (L) atrium following the Olivares classification [56]. From a technical point of view, TEE is mandatory in properly identifying the severity of ASA. The presence of moderate to large ASA associated with a PFO usually induces the operator to select a stiff metallic device to stabilize the interatrial septum increasing the risk of misalignment and residual shunt after closure.

20.6.5 Eustachian Valve and Chiari Network

From an embryological point of view, the EV is a derivative of the right sinus venosus valve; it has a semicircular shape and is facing the anterior-inferior aspect of the inferior vena cava. The CN represents a very huge multi-perforated Eustachian valve with a network-like appearance, and it has been found in 1.3–4 % of autopsies. The EV and CN guarding the anterior-inferior aspect of the inferior vena cava

have a crucial role in deflecting the blood flow through the foramen ovale during the fetal life predisposing to paradoxical embolism [57]. Large PFO and prominent EV or right atrial filamentous strands were found more frequently in patients with septal aneurysm compared with those without (37.7 % vs. 10.9 %, $p < 0.001$ and 59.4 % vs. 43.1 %, $p = 0.02$) [58]. As previously reported by TEE and intracardiac echocardiographic studies, an EV is present in 48 % of patients with cryptogenic stroke, and a large CN is associated with PFO in 83 % of cases [59]. From a technical point of view, the presence of such structures should be taken into account during transcatheter closure, representing potential technical difficulties.

20.6.6 Interatrial Septal Thickness and Lipomatosis

Interatrial septal thickness in the general population is about 6 mm, and usually it increases to about 7 mm in aged population [60]. Interatrial septal hypertrophy (IASH) and lipomatosis have been defined when thickness is >8 mm and >15 mm, respectively. IASH is common in elderly people and is related with hypertension and smoke but not with vascular disease. Lipomatosis of the interatrial septum is a benign tumoral process characterized by fat accumulation in the interatrial septum [61]. Both conditions may have a deep impact on transcatheter closure because a stiff device such as those of the Amplatzer family should be contraindicated, due to the inability of such device to stretch the waist zone more of 7–8 mm.

20.6.7 Tunnelized PFO

Not infrequently, PFO appears as a tunnellike opening between the right and left atrium, and this feature can be associated with a variety of other anatomical variants, such as hypertrophy of the rims, different degree of ASA, etc. Recently this kind of anatomy has been correlated with an increased risk of paradoxical embolism [62], for its potential role in causing thrombosis in situ within the channel, in particular if long >10–12 mm. From a technical point of view, TEE and in particular intraoperative ICE can be useful in determining the length of the tunnel and in selecting the proper device, which should be an asymmetrical opening device which could adapt to this anatomy theoretically better than stiffer metallic symmetrically opening double-disk device.

Conclusion

Patient selection and preoperative evaluation remain of paramount importance for ensuring appropriateness and efficacy of PFO transcatheter closure. The interventional cardiologist plays only as the protagonist during the interventional procedure itself, but he cannot act as a bystander in the decision-making process regarding clinical indication and anatomo-functional characterization.

References

1. Marelli AJ, Mackie AS, Msc RI, Rahme E, Pilote L. Congenital heart disease in the general population. Changing prevalence and age distribution. Circulation. 2007;115:163–72.
2. Kilner PJ, Yang GZ, Wilkes AJ, Mohiaddin RH, Firmin DN, Yacoub MH. Asymmetric redirection of flow through the heart. Nature. 2000;404:759–61.
3. Rigatelli G. Patent foramen ovale: the evident paradox between the apparently simple treatment and the really complex pathophysiology. J Cardiovasc Med (Hagerstown). 2007;8:300–4.
4. Langholz D, Louie EK, Konstadt SN, Rao TL, Scanlon PJ. Transesophageal echocardiographic demonstration of distinct mechanisms for right to left shunting across a patent foramen ovale in the absence of pulmonary hypertension. J Am Coll Cardiol. 1991;18:1112–7.
5. Nootens MT, Berarducci LA, Kaufmann E, Devries S, Rich S. The prevalence and significance of a patent foramen ovale in pulmonary hypertension. Chest. 1993;104:1673–5.
6. Konstantinides S, Geibel A, Kasper W, Olschewski M, Blumel L, Just H. Patent foramen ovale is an important predictor of adverse outcome in patients with mayor pulmonary embolism. Circulation. 1998;97:1946–51.
7. Shanoudy H, Soliman A, Raggi P, Liu JW, Russell DC, Jarmukli NF. Prevalence of patent foramen ovale and its contribution to hypoxemia in patients with obstructive sleep apnea. Chest. 1998;113:91–6.
8. Soliman A, Shanoudy H, Liu J, Russell DC, Jarmukli NF. Increased prevalence of patent foramen ovale in patient with severe chronic obstructive pulmonary disease. J Am Soc Echocardiogr. 1999;12:99–105.
9. Rietvel AP, Merrman L, Essed CD, Trimbos JB, Hagemiejer F. Right-to-left shunt, with severe hypoxemia, at the atrial level in a patient with hemodynamically important right ventricular infarction. JACC. 1982;2:776–9.
10. Giebler R, Kollenberg B, Pohlen G, Peters J. Effect of positive end-expiratory pressure on the incidence of venous air embolism and on the cardiovascular response to the sitting position during neurosurgery. Br J Anaesth. 1998;80:30–5.
11. Gallaher ME, Sperling DR, Gwinn JL, Meyer BW, Fyler DC. Functional drainage of the inferior vena cava into the left atrium-three cases. Am J Cardiol. 1963;12:561–6.
12. Schoevvaerdts D, Gonzalez M, Evrard P, Buche M, Installe E. Patent foramen ovale: a cause of significant post-coronary and bypass grafting morbidity. Cardiovasc Surg. 2002;10:615–7.
13. Laybourn KA, Martin ET, Cooper RAS, Holman WL. Platypnea and orthodeoxia: shunting associated with an aortic aneurysm. J Thorac Cardiovasc Surg. 1977;113:955–6.
14. Smeenk FWJM, Postmus PE. Interatrial right-to-left shunting developing after pulmonary resection in the absence of elevated right-sided pressure. Chest. 1993;103:528–31.
15. Klepper JI, Seifer F, Lawson WF, et al. Intracardiac right-to-left shunting following cardiac surgery. Am Heart J. 1988;116:189–92.
16. Sievert H, Ruygrok P, Salkeld M, Baumgartner H, Meier B, Windecker S, Juliard JM, Aubry P, Tiefenbacher C, Krumsdorf U, Vermeersch P, Ewert P, Piéchaud JF. Transcatheter closure of patent foramen ovale with radiofrequency: acute and intermediate term results in 144 patients. Catheter Cardiovasc Interv. 2009;73(3):368–73. doi:10.1002/ccd.21809.
17. Aral M, Mullen M. The Flatstent versus the conventional umbrella devices in the percutaneous closure of patent foramen ovale. Catheter Cardiovasc Interv. 2015;85(6):1058–65.
18. Sievert H, Wunderlich N, Reiffenstein I, Ruygrok P, Grube E, Buellesfeld L, Meier B, Schofer J, Muller D, Jones RK, Gillam L. Initial clinical experience with the Coherex FlatStent™ and FlatStent™ EF PFO closure system for in-tunnel PFO closure: results of the Coherex-EU study. Catheter Cardiovasc Interv. 2014;83(7):1135–43. doi:10.1002/ccd.24565. Epub 2013 Nov 27.
19. Mügge A, Daniel WG, Angermann C, Spes C, Khandheria BK, Kronzon I, Freedberg RS, Keren A, Denning K, Engberding R, et al. Atrial septal aneurysm in adult patients. A multicenter study using transthoracic and transesophageal echocardiography. Circulation. 1995;91(11):2785–92.

20. Bogousslavsky J, Garazi S, Jeanrenaud X, Aebischer N, Van Melle G. Stroke recurrence in patients with patent foramen ovale: the Lausanne Study. Lausanne Stroke with Paradoxical Embolism Study Group. Neurology. 1996;46(5):1301–5.

21. Cujec B, Mainra R, Johnson DH. Prevention of recurrent cerebral ischemic events in patients with patent foramen ovale and cryptogenic strokes or transient ischemic attacks. Can J Cardiol. 1999;15(1):57–64.

22. Mas JL, Arquizan C, Lamy C, Zuber M, Cabanes L, Derumeaux G, Coste J, Patent Foramen Ovale and Atrial Septal Aneurysm Study Group. Recurrent cerebrovascular events associated with patent foramen ovale, atrial septal aneurysm, or both. N Engl J Med. 2001;345(24): 1740–6.

23. Mattioli AV, Aquilina M, Oldani A, Longhini C, Mattioli G. Atrial septal aneurysm as a cardioembolic source in adult patients with stroke and normal carotid arteries. A multicentre study. Eur Heart J. 2001;22(3):261–8.

24. Lamy C, Giannesini C, Zuber M, Arquizan C, Meder JF, Trystram D, Coste J, Mas JL. Clinical and imaging findings in cryptogenic stroke patients with and without patent foramen ovale: the PFO-ASA study. Atrial Septal Aneurysm. Stroke. 2002;33(3):706–11.

25. Furlan AJ, CLOSURE I Investigators. PFO closure: CLOSURE. Stroke. 2013;44(6 Suppl 1):S45–7.

26. Furlan AJ, Reisman M, Massaro J, Mauri L, Adams H, Albers GW, Felberg R, Herrmann H, Kar S, Landzberg M, Raizner A, Wechsler L, CLOSURE I Investigators. Closure or medical therapy for cryptogenic stroke with patent foramen ovale. N Engl J Med. 2012;366(11):991–9.

27. Serena J, Marti-Fàbregas J, Santamarina E, Rodríguez JJ, Perez-Ayuso MJ, Masjuan J, Segura T, Gállego J, Dávalos A, CODICIA, Right-to-Left Shunt in Cryptogenic Stroke Study, Stroke Project of the Cerebrovascular Diseases Study Group, Spanish Society of Neurology. Recurrent stroke and massive right-to-left shunt: results from the prospective Spanish multicenter (CODICIA) study. Stroke. 2008;39(12):3131–6.

28. Horner S, Niederkorn K, Gattringer T, Furtner M, Topakian R, Lang W, Maier R, Gamillscheg A, Fazekas F. Management of right-to-left shunt in cryptogenic cerebrovascular disease: results from the observational Austrian paradoxical cerebral embolism trial (TACET) registry. J Neurol. 2013;260(1):260–7.

29. Khattab AA, Windecker S, Jüni P, Hildick-Smith D, Dudek D, Andersen HR, Ibrahim R, Schuler G, Walton AS, Wahl A, Mattle HP, Meier B. Randomized clinical trial comparing percutaneous closure of patent foramen ovale (PFO) using the Amplatzer PFO Occluder with medical treatment in patients with cryptogenic embolism (PC-Trial): rationale and design. Trials. 2011;12:56.

30. Carroll JD, Saver JL, Thaler DE, for the RESPECT Investigators, et al. Closure of patent foramen ovale versus medical therapy after cryptogenic stroke. N Engl J Med. 2013;368:1092–100.

31. Ma B, Liu G, Chen X, Zhang J, Liu Y, Shi J. Risk of stroke in patients with patent foramen ovale: an updated meta-analysis of observational studies. J Stroke Cerebrovasc Dis. 2014;23(5):1207–15.

32. Capodanno D, Milazzo G, Vitale L, Di Stefano D, Di Salvo M, Grasso C, Tamburino C. Updating the evidence on patent foramen ovale closure versus medical therapy in patients with cryptogenic stroke: a systematic review and comprehensive meta-analysis of 2,303 patients from three randomised trials and 2,231 patients from 11 observational studies. EuroIntervention. 2014;9(11):1342–9.

33. Khan AR, Bin Abdulhak AA, Sheikh MA, Khan S, Erwin PJ, Tleyjeh I, Khuder S, Eltahawy EA. Device closure of patent foramen ovale versus medical therapy in cryptogenic stroke: a systematic review and meta-analysis. JACC Cardiovasc Interv. 2013;6(12):1316–23.

34. Pickett CA, Villines TC, Ferguson MA, Hulten EA. Percutaneous closure versus medical therapy alone for cryptogenic stroke patients with a patent foramen ovale: meta-analysis of randomized controlled trials. Tex Heart Inst J. 2014;41(4):357–67.

35. Stortecky S, da Costa BR, Mattle HP, Carroll J, Hornung M, Sievert H, Trelle S, Windecker S, Meier B, Jüni P. Percutaneous closure of patent foramen ovale in patients with cryptogenic embolism: a network meta-analysis. Eur Heart J. 2015;36(2):120–8.

36. Patti G, Pelliccia F, Gaudio C, Greco C. Meta-analysis of net long-term benefit of different therapeutic strategies in patients with cryptogenic stroke and patent foramen ovale. Am J Cardiol. 2015;115(6):837–43.

37. Wilmshurst P, Nightingale S. The role of cardiac and pulmonary pathology in migraine: a hypothesis. Headache. 2006;46:429–34.

38. Kaaro J, Partonene T, Naik P, Hadjikhani N. Is migraine a lateralization defect? Neuroreport. 2008;19:1351–3.

39. Rigatelli G, Aggio S, Cardaioli P, et al. Left atrial dysfunction in patients with patent foramen ovale and atrial septal aneurysm: an alternative concurrent mechanism for arterial embolism? JACC Cardiovasc Interv. 2009;2:655–62.

40. Nozari A, Dilekoz E, Sukhotinsky I, et al. Microemboli may link spreading depression, migraine aura, and patent foramen ovale. Ann Neurol. 2010;67:221–9.

41. Tarantini G, D'Amico G, Bettella N, Mojoli M, Rigatelli G. Patent foramen ovale closure and migraine time course: clues for positive interaction. Int J Cardiol. 2015;195:235–6.

42. Baker JE, Stratmann G, Hoopes C, Donateillo R, Tseng E, Russell IA. Profound hypoxemia resulting from shunting across an inadvertent atrial septal tear after left ventricular assist device placement. Anesth Analg. 2004;98:937–40.

43. Schulman LL, Smith CR, Drusin R, Rose EA, Enson Y, Reemtsma K. Patent foramen ovale complicating heart transplantation. A window on posttransplantation hemodynamics. Chest. 1987;92:569–72.

44. Rigatelli G, Faggian G, Cardaioli P, Mazzucco A. Contemporary management of patent foramen ovale in patients undergoing ventricular assisting devices or heart transplantation. J Cardiovasc Med (Hagerstown). 2009;10(1):9–12.

45. Thaler DE, Di Angelantonio E, Di Tullio MR, et al. The risk of paradoxical embolism (RoPE) study: initial description of the complete database. Int J Stroke. 2013;8:612–9.

46. Lang RM, Bierig M, Devereux RB, Flachskampf FA, Foster E, Pellikka PA, et al; American Society of Echocardiography's Nomenclature and Standards Committee, Task Force on Chamber Quantification, American College of Cardiology Echocardiography Committee, American Heart Association; European Association of Echocardiography, European Society of Cardiology. Recommendations for chamber quantification. Eur J Echocardiogr. 2006;7:79–108.

47. Anzola GP, Morandi E, Casilli F, Onorato E. Different degrees of right-to left shunting predict migraine and stroke: data from 420 patients. Neurology. 2006;66:765–7.

48. Anzola GP, Morandi E, Casilli F, Onorato E. Does transcatheter closure of patent foramen ovale really "shut the door?"A prospective study with transcranial doppler. Stroke. 2004;35:2140–4.

49. Rigatelli G, Dell'Avvocata F, Cardaioli P, Giordan M, Braggion G, Aggio S, Chinaglia M, Mandapaka S, Kuruvilla J, Chen JP, Nanjundappa A. Permanent right-to-left shunt is the key factor in managing patent foramen ovale. J Am Coll Cardiol. 2011;58(21):2257–61.

50. Pristipino C, Anzola GP, Ballerini L, Bartorelli A, Cecconi M, Chessa M, Donti A, Gaspardone A, Neri G, Onorato E, Palareti G, Rakar S, Rigatelli G, Santoro G, Toni D, Ussia GP, Violini R, Italian Society of Invasive Cardiology (SICI-GISE), Italian Stroke Association (ISA-AIS), Italian Association of Hospital Neurologists, Neuroradiologists, Neurosurgeons (SNO), Congenital Heart Disease Study Group of Italian Society Of Cardiology, Italian Association Of Hospital Cardiologists (ANMCO), Italian Society Of Pediatric Cardiology (SICP), Italian Society of Cardiovascular Echography (SIEC), Italian Society of Hemostasis and Thrombosis (SISET). Management of patients with patent foramen ovale and cryptogenic stroke: a collaborative, multidisciplinary, position paper: executive summary. Catheter Cardiovasc Interv. 2013;82(1):122–9.

51. Messe SR, Silverman IE, Kizer JR, Homma S, Zahn C, Gronseth G, et al.; Quality Standards Subcommittee of the American Academy of Neurology. Practice parameter: recurrent stroke with patent foramen ovale and atrial septal aneurysm: report of the Quality Standards Subcommittee of the American Academy of Neurology. Neurology. 2004;62:1042–50.

52. Marcu CB, Beek AM, van Rossum AC. Clinical applications of cardiovascular magnetic resonance imaging. CMAJ. 2006;175:911–7.

53. Homma S, Sacco RL, Di Tullio MR, Sciacca RR, Mohr JP, PFO in Cryptogenic Stroke Study (PICSS) Investigators. Effect of medical treatment in stroke patients with patent foramen ovale: patent foramen ovale in Cryptogenic Stroke Study. Circulation. 2002;105:2625–31.
54. Agmon Y, Khandheria BK, Meissner I, et al. Frequency of atrial septal aneurysm in patients with cerebral ischemic events. Circulation. 1999;99:1942–4.
55. Santamarina E, Gonzalez-Alujas MT, Munoz V, Rovira A, Rubiera M, Ribo M, et al. Stroke patients with cardiac atrial septal abnormalities: differential infarct patterns on DWI. J Neuroimaging. 2006;16:334–40.17.
56. Olivares-Reyes A, Chan S, Lazar EJ, Bandlamudi K, Narla V, Ong K. Atrial septal aneurysm: a new classification in two hundred five adults. J Am Soc Echocardiogr. 1997;10:644–56.
57. Schuchlenz HW, Saurer G, Weihs W, Rehak P. Persisting eustachian valve in adults: relation to patent foramen ovale and cerebrovascular events. J Am Soc Echocardiogr. 2004;17:231–3.
58. Schneider B, Hofmann T, Justen MH, Meinertz T. Chiari's network: normal anatomic variant or risk factor for arterial embolic events? J Am Coll Cardiol. 1995;26:203–10.
59. Rigatelli G, Dell'Avvocata F, Braggion G, Giordan M, Chinaglia M, Cardatoli P. Persistent venous valves correlate with increased shunt and multiple preceding cryptogenic embolic events in patients with patent foramen ovale: an intracardiac echocardiographic study. Catheter Cardiovasc Interv. 2008;72:973–6.
60. Agmon Y, Meissner I, Tajik AJ, Seward JB, Petterson TM, Christianson TJ, O'Fallon WM, Wiebers DO, Khandheria BK. Clinical, laboratory, and transesophageal echocardiographic correlates of interatrial septal thickness: a population-based transesophageal echocardiographic study. J Am Soc Echocardiogr. 2005;18:175–82.
61. Christoph MH, Thomas K, Stefan PL, Torsten TB, Volkmar N. Lipomatous hypertrophy of the interatrial septum: a prospective study of incidence, imaging findings, and clinical symptoms. Chest. 2003;124:2068–73.
62. Goel SS, Tuzcu EM, Shishehbor MH, de Oliveira EI, Borek PP, Krasuski RA, Rodriguez LL, Kapadia SR. Morphology of the patent foramen ovale in asymptomatic versus symptomatic (stroke or transient ischemic attack) patients. Am J Cardiol. 2009;103:124–9.

PFO Closure: Techniques and Devices

21

Dennis Zavalloni

21.1 Historical Perspectives

The description of a possible persistent communication between the left and right atrium, in the absence of a clear congenital septal defect at the level of the foramen of Botallo (patent foramen ovale, PFO), dates back to Leonardo da Vinci's studies on human anatomy. Nevertheless, the first reported paradoxical embolism through a congenital atrial septal defect (ASD) was first described in the nineteenth century [1]. Since that time, several other cases of paradoxical embolism through an inter-atrial septum communication (either ASD or PFO) have been reported in the literature, making them of medical interest, in particular in regard to treatment. The first attempts of ASD closure were restricted to surgery, with the first successful operation occurring in the late 1940s [2, 3]. In 1952, Lewis and Taufic reported the first successful open heart repair of ASD in a 5-year-old girl. This marked the onset of the open heart surgical era, and ASD surgical repair became the gold standard for treatment [4]. It was only in the 1970s that the initial experimental transcatheter closure of ASDs was performed [5]. The results of canine research were very encouraging and led to a first device prototype: the King-Mills Cardiac Umbrella (Fig. 21.1). This prosthesis consisted of six stainless steel struts covered with Dacron in a double-umbrella configuration, with a snap lock mechanism to fix them together. Eventually, in 1975 a 17-year-old girl, refusing surgery because of scarring issues on her chest, was successfully treated with the transcatheter device [6]. Over time, several devices have been introduced into the medical market in order to

D. Zavalloni, MD, FESC
Invasive Cardiology Department, Humanitas Research Hospital, IRCCS,
Rozzano, Milano, Italy
e-mail: dennis.zavalloni_parenti@hunimed.eu
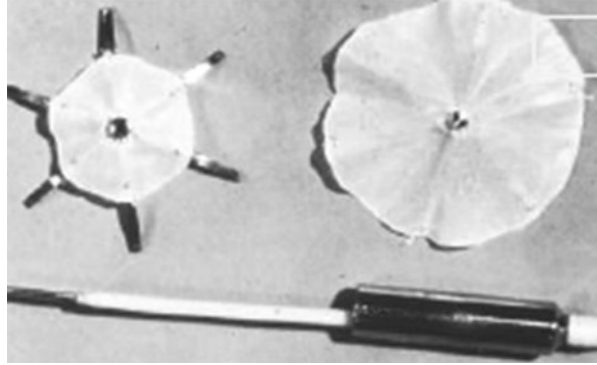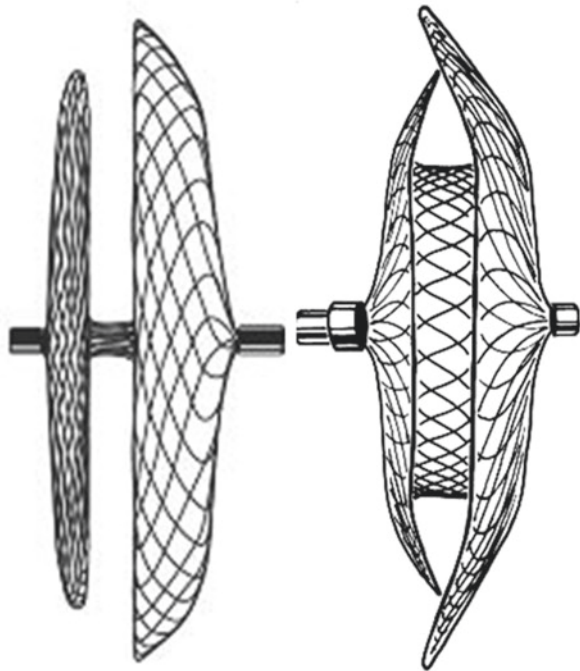
255

Fig. 21.1 The King-Mills device

Fig. 21.2 PFO (*left*) and ASD (*right*) devices (Courtesy of St. Jude Medical)

improve acute and long-term results of ASD transcatheter closure. Improvements have been performed to increase their usability, primarily to ameliorate the rates of acute closure of the defect, the possibility to retrieve and reposition the device, and the delivery. In a few years, the rapid evolution of technologies and clinical researches enabled transcatheter closure to be considered the first choice of treatment in ostium secundum ASDs [7]. Based on this experience, PFO-dedicated prostheses were then developed for patients with recurrent cryptogenic stroke. The main difference between the two prostheses consists in the central waist (Fig. 21.2) being reel shaped in the ASD and thin in the PFO ones. At present, several different types

of devices have been developed and tested in a clinical setting, remaining the double-disk prostheses those with the best performances in terms of procedural and clinical results [8].

21.2 Procedural Approach

Transcatheter closure of PFO has been established as a safe and effective treatment for patients with PFO-related diseases. However, the procedure should not be thought as a mere technical issue. The skill of the physician should include several aspects other than percutaneous intervention. They should be knowledgeable in atrial embryology and anatomy, in the use of the diverse imaging modalities, and in the management of periprocedural drug therapy.

21.2.1 Background: Atrial Embryology and Anatomy

A proper echocardiographic assessment of PFO requires an adequate knowledge of anatomy and embryology of the heart [9, 10].

In embryonic life, the primitive atrium is a single cavity. The primary septum grows down from the supero-posterior wall of the atrium toward the endocardial cushions (Fig. 21.3(1), at the level of atrioventricular canal, thus limiting an area known as the primary foramen (ostium primum) (Fig. 21.3(2)). Meanwhile, the ostium primum progressively closes owing to the fusion of septum primum with endocardial cushions; multiple small perforations begin to develop and coalesce at the superior portion of the primary septum (Fig. 21.3(3)) to form a secondary communication between the two atria, known as the secondary foramen (ostium secundum). In the 12th week, an infolding of tissue, known as the secondary septum (septum secundum) (Fig. 21.3(4)), grows down along the right atrial side of the primary septum, progressively covering the ostium secundum (Fig. 21.3(5)), but leaving a free area inferiorly. As a result, a sort of canal (tunnel) guarantees a passage between the two atria, as required by the fetal circulation (Fig. 21.3(6)). After postnatal changes in pulmonary and systemic circulation, septum secundum forms a support against which the septum primum may press and fuse. This occurs in about 70 % of subjects, whereas in the remaining 30 %, the tunnel converts into a "flap-like" valve between the two atria that may open every time the right atrial pressure overcomes the left one.

The area where this "flap-like" valve is located is called the fossa ovalis, and the individual variability in morphology of all the structures participating in the formation of the fossa and of the PFO may result in several different anatomic variants: the fusion between the two septa may be irregular and more than one orifice may be detected; the degree of overlapping between the two septa (defined as tunnel, Fig. 21.4) is variable, and as a result, it is possible to have either very long or very short tunnel of the PFO; when septum primum is thin and redundant, it may be excessively mobile and creates a aneurysmal fossa ovalis (Fig. 21.5); the presence of abundant adipose tissue within the infolding septum secundum may result in a
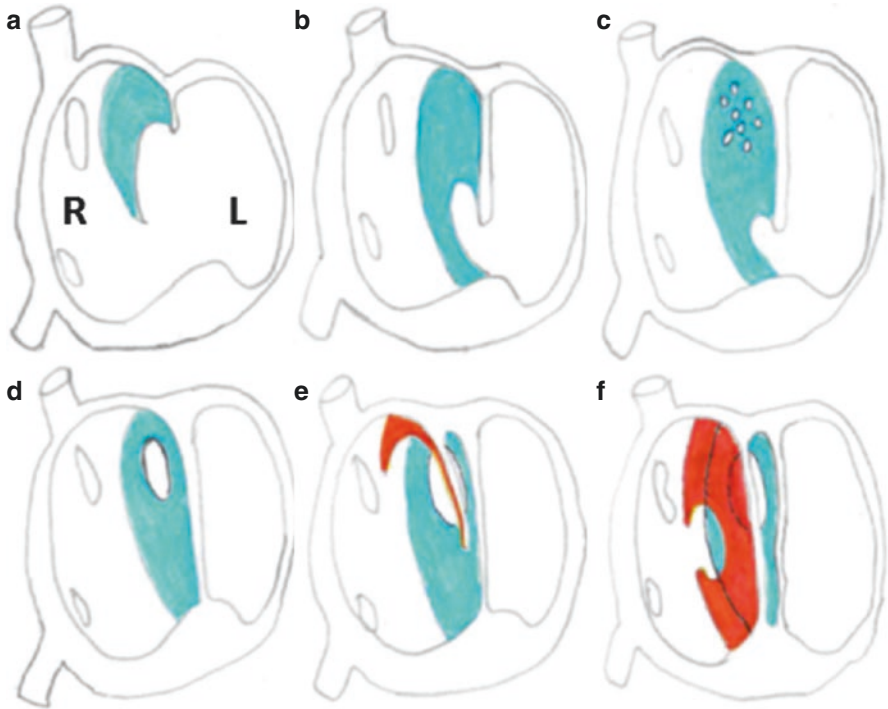
Fig. 21.3 The embryonic development of atrial septum. *Light blue* = septum primum. *Red* = septum secundum. *R* right atrium, *L* left atrium
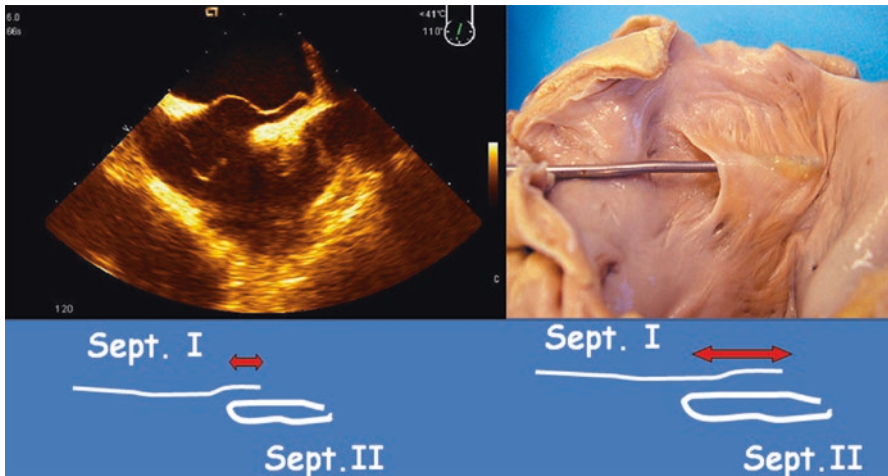

Fig. 21.4 The PFO tunnel is created by the overlapping of the septum primum and secundum. On the *left* the echo image, on the *right* the anatomic pathology
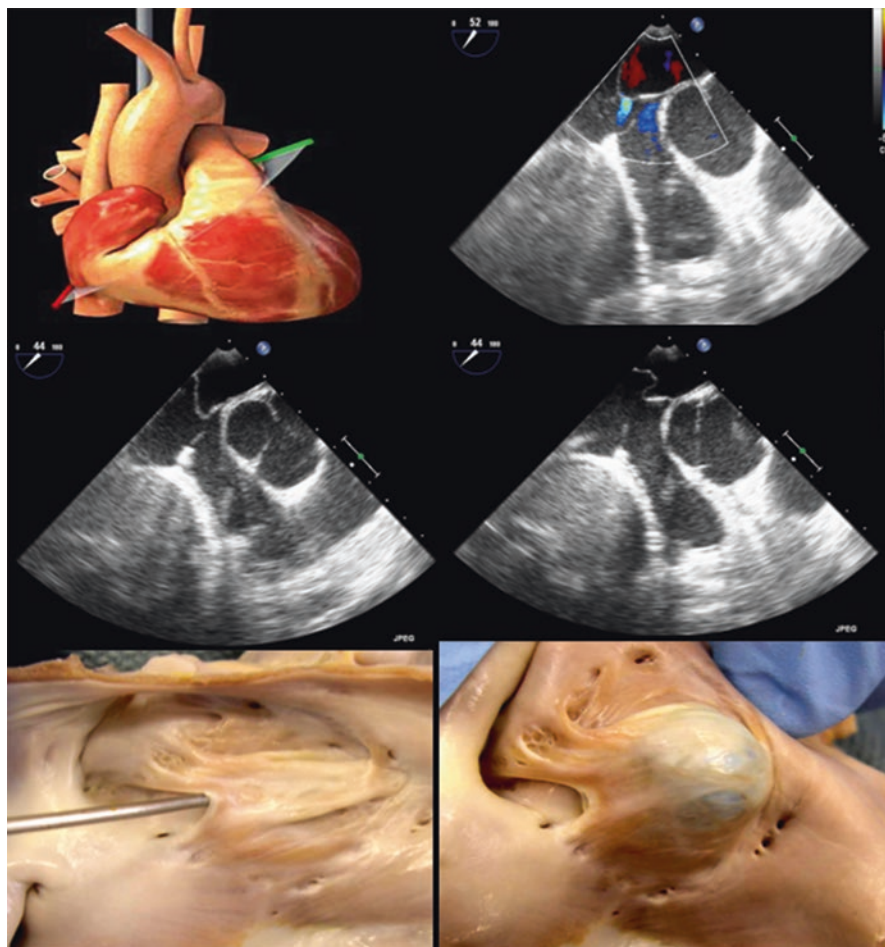
Fig. 21.5 The echocardiographic projection and the echocardiographic image of an aneurysmal septum primum. The floppy septum waves in the atrial cavities. At the color Doppler, a septal cribrosity is visible in addition to the PFO. At the *bottom* the anatomic pathology

very thick and bulky septum (Fig. 21.6). Other important structures that may pose issues with the device delivery and placement are redundant Eustachian valve and the Chiari network, two embryonic remnants. Based on the anatomic features, we may therefore differentiate a simple from a complex PFO, where one or more of these characteristics are present (Table 21.1).

21.2.2 Patient Preparation

Preparation of patients for the intervention should start with a complete counseling to make them aware that PFO is thought to be the cause of their clinical event and
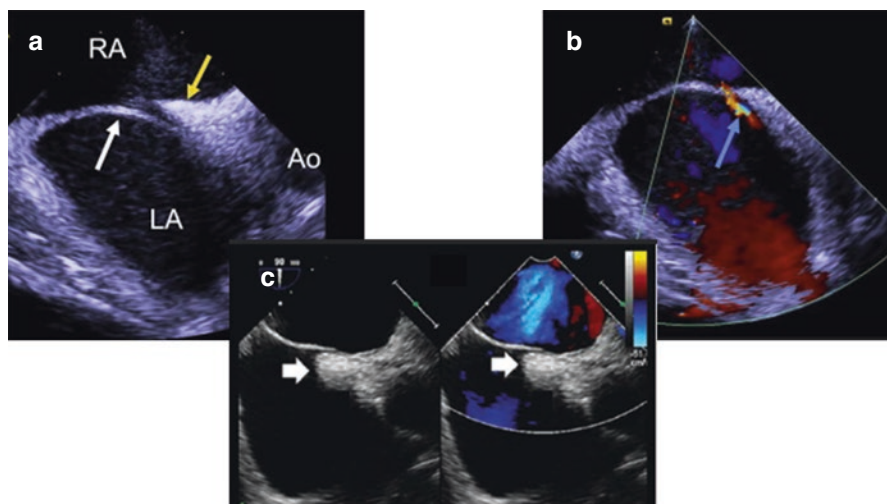
Fig. 21.6 (**a**) Simple PFO (*white arrow* septum primum, *yellow arrow* septum secundum). (**b**) At the color Doppler *right* to *left* shunt across the PFO. (**c**) Lipomatosis of the septum secundum (*thick white arrow*)

Table 21.1 Anatomic characteristics of simple and complex PFO

PFO category	Anatomical characteristics
Simple	Bare standard anatomy
Complex (≥1 anatomical characteristics)	Long tunnel (>10 mm)
	Atrial septum aneurysm
	Thick septum secundum (>10 mm)
	Multiple orifices in the left atrium
	Eustachian valve or Chiari network

that similar events may occur also in patients without PFO. Even though the closure of PFO removes a cause for cryptogenic stroke, the possible role of misdiagnosed atrial fibrillation should be mentioned. This aspect is particularly important because of the inconclusive results of the main randomized trials comparing percutaneous closure and medical treatment [11–13].

Other important aspects concern the exclusion of inherited or acquired thrombophilia, in order to give proper peri- and postprocedural antithrombotic therapy, and allergy to nickel (a very frequent issue in the general population) that is contained in most of the available prostheses [14].

Prior to the procedure, patients are usually treated with aspirin 100 mg and clopidogrel (loading dose 300 mg). An anticoagulant may be required tailored to the thrombotic risk in case of coagulation disorders, depending on the type of thrombophilia. Patients should also receive a single intravenous antibiotic dose within 1 h of percutaneous access, typically with cefazolin 2 g (or vancomycin in the presence of

allergy to penicillin). Patients should receive intravenous normal saline at 1 mL/kg/h before and during the procedure to avoid left atrial hypovolemia, possibly with an air-eliminating filter in position. During procedure heparin 70 mg/kg is administered, soon after sheet insertion, to maintain ACT >250 s. Nasal cannula oxygen at 6 L/min is administered for hyperoxygenation, in case of an air embolus while catheterizing the left atrium.

21.2.3 Implantation Technique

The technique for percutaneous closure of PFO borrowed that used for ASD, but skills in the use of different devices are also required, because several different prostheses have been over the years. The two main approaches currently favored by the operators consist of an echo-guided or a fluoroscopy-guided procedures [15]. Debate continues about whether echocardiographic guidance is required for PFO closure, as opposed to fluoroscopic guidance alone. The former is carried out using either transesophageal echocardiography (TEE) or intracardiac echocardiography (ICE), and when TEE is performed, the presence of both the echocardiographer and the anesthetist (to reduce patient discomfort during the procedure) is required. Conversely, the latter approach has the advantage of completely avoiding the need for the anesthetist during the procedure even though a complete study of PFO morphology with TEE is mandatory before the intervention. However, it cannot be excluded that, during the procedure, the operator may need TEE to perform a transseptal puncture rather than manage possible prosthetic mismatches or misunderstood complications. So, this kind of approach should be limited to expert operators and is advisable in the treatment of simple PFO.

   The procedure is carried out through a systemic venous approach. The femoral site is the more suitable because it allows to trace the direction of blood flow as it is in the fetal circulation that is also at the basis of pathophysiology of PFO-related diseases. For this reason, it is usually preferred over all other attempted approaches: internal jugular [16], axillary [17], or hepatic vein [18]. After local anesthesia of the groin, a regular 0.035-in. J-tip guidewire is introduced through a puncture needle, followed by a 6-Fr sheath insertion. Owing to the anatomy of PFO (with a vertically angled tunnel directed from the inferior border of the fossa ovalis in the right atrium to the superior left atrium), the simple advancement of the 0.035-in. J-tipped guidewire will readily pass through the PFO into the left atrium in about half of the cases. If not, a curved catheter (multipurpose shape, curve 1 or 2) placed at the level of the diaphragm will direct the wire medially toward the PFO. If the PFO still cannot be passed, it may be negotiated with the catheter alone or, if that fails, with a straight wire or a PCI guidewire. A typical situation for this would be a PFO that consists only of a small hole in one of the corners of the initial foramen (Fig. 21.7). In this case, it would be necessary to guide the wire to a sharp turn once it has entered the PFO tunnel. Occasionally, it may be necessary to learn more about anatomy before passing the PFO displaying the fossa ovalis injecting contrast medium, withdrawing a MP catheter previously positioned in the superior vena cava toward the interatrial

Fig. 21.7 Lateral view of the interatrial septum. The area between *dotted* and *solid line* is the zone of fusion of the two septa. * = different possible positions of PFO (they may also coexist)

Superior vena cava

Area of fusion of the two septa

Inferior vena cava
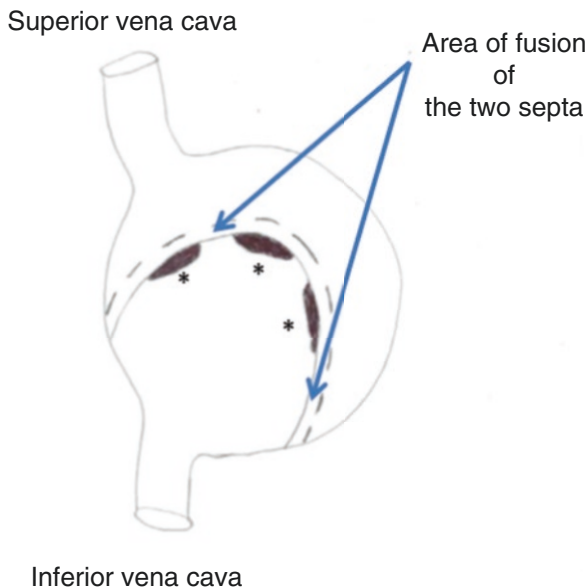
septum in the direction where the PFO is suspected to be (in the left anterior oblique projection). In other cases, especially when the procedure is performed with fluoroscopic guidance, right atrial angiography may be performed with a pigtail catheter in the left anterior/oblique (40/40°) projection, to see the PFO and potential atrial septal aneurysm. In small PFOs, hand injection contrast angiography through the catheter can help identify the entry point. In cases with difficult advancement of the guidewire into the left atrium, a JR4, hockey stick, or XB 3.5 guide catheters may be used. Should there be fenestrations within the PFO that prohibit advancement of the catheter, a 4- or 5-F catheter may be used. When PFO is located in a very eccentric position and delivery of a large size prosthesis is required (as in cases with wide septal aneurysm), a transseptal puncture may be performed in the middle of the fossa ovalis to allow central positioning of the prosthesis. When the assessment of tunnel length or foramen width is important in the choice of device, gentle balloon sizing of the PFO may be performed. The sizing balloon catheters are usually mounted on a shaft in an "over-the-wire" system and advanced across the PFO, inflated gently until they assume a "dog bone" configuration. Radiopaque markers on the shaft may help in the measurement of the foramen/tunnel size. Another technique to assess compressible tunnel is to inflate a balloon-tipped pulmonary capillary wedge catheter within the left atrium, withdrawing the balloon against the septum, and perform a hand injection of contrast medium through the guiding catheter in the right atrium. Once the catheter is in the left atrium, the guidewire is advanced into one of the pulmonary veins (usually the left superior one). It is mandatory to exclude that the guidewire is into the left appendage to prevent atrial perforation. So the proper position may be confirmed by hemodynamic measurement of left atrial pressure, by fluoroscopy (the catheter is typically "outside" of the heart shadow), or by echocardiography. The
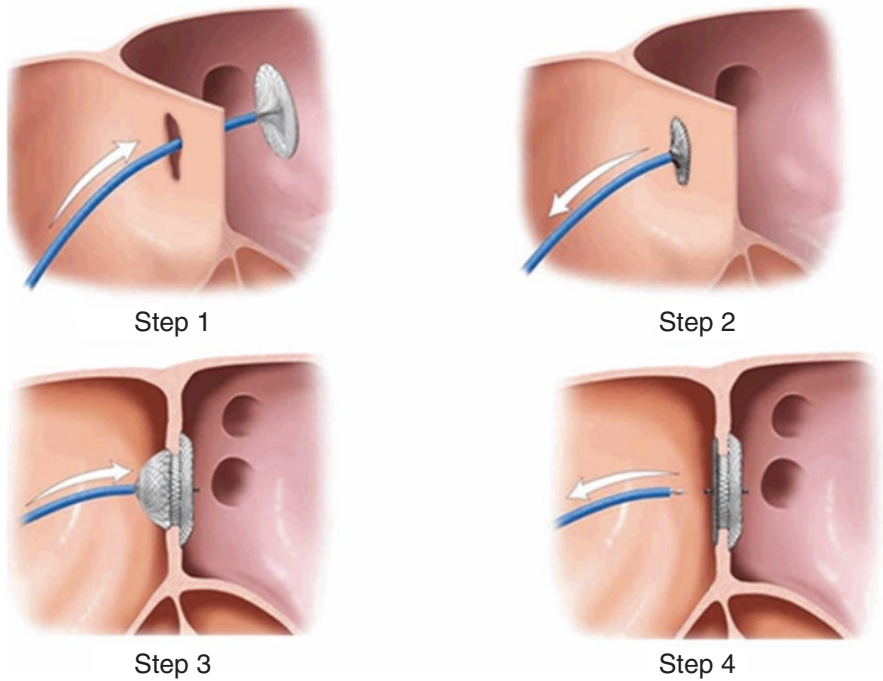
Step 1

Step 2

Step 3

Step 4

Fig. 21.8 The main steps of percutaneous transcatheter closure of PFO (Courtesy of St Jude Medical)

catheter is then advanced into the correspondent pulmonary vein and exchanged over a 260-cm, 0.035-in. extra-stiff guidewire to support the positioning of the guide catheter through the PFO. After choosing the proper device (type and size), the delivery system is advanced in the left atrium. Each device has its own preparation and delivery technique, but a common mandatory step during the preparation is to check for the complete elimination of air bubbles from the system. After which the device is advanced, through the guide catheter, to the left atrium and pushed out of the sheath up to the middle waist so that the left disk can fully form. The sheath and the pusher are then pulled back, as a single unit, until the left disk gets stopped at the septum. From there on, only the sheath will be pulled back while gently advancing on the pusher cable. The entire set is pushed against the septum to put the right disk into its proper place (Fig. 21.8). Device stability was controlled by means of the Minnesota maneuver, pushing and pulling the device toward both atria before deployment. Depending on which approach is chosen, echo or contrast hand injection through the sheath next to the right atrial disk is used to confirm that the device is positioned correctly. At fluoroscopy, in the left anterior oblique projection, the two disks are seen in profile. The distance between the two disks superiorly reflects the thickness of the septum secundum. After device delivery, the guide catheter may be retrieved, and 10-min manual compression of the femoral vein is enough to achieve a complete hemostasis at the puncture site.

21.2.4 Imaging to Guide PFO Closure: TEE and ICE

Accurate and precise knowledge of the anatomy of the atrial septum and the nearby structures is essential for the effectiveness and safe performance of PFO closure. Therefore, irrespective of the planned procedural approach, a systematic and comprehensive approach to TEE should be performed in all patients before undergoing percutaneous closure of PFO [19]. The goal of this examination is the meaningful understanding of atrial anatomy, of all the atrial structures that may be relevant for device selection and deployment. A proper checklist for evaluation should be carried out on all patients, as follows:

- General assessment of atrial dimension (size in different projections, length of the septum)
- Definition of simple or complex PFO morphology (Table 21.1)
- Exclusion of concomitant defects (including anomalous pulmonary venous return)
- Measurement of the rims (defined as the atrial septal tissue between the fossa ovalis and the structures adjacent to it)
- Measurements of PFO features that may be used for the selection of the device (size of opening of PFO, tunnel length, septum secundum thickness, presence of Eustachian valve or Chiari network (Fig. 21.9))
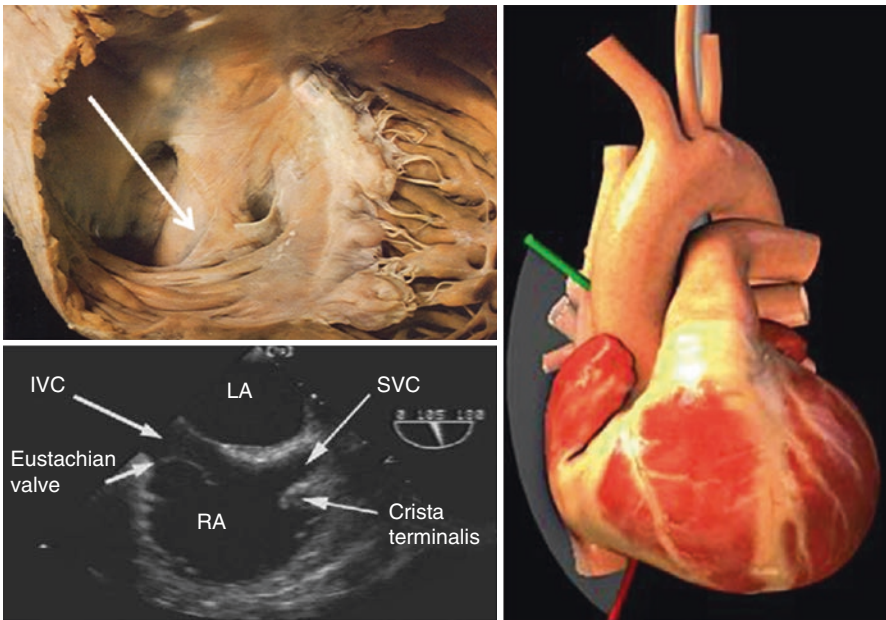
Fig. 21.9 The anatomic pathology (*white arrow*) and the echocardiographic appearance of Eustachian valve. On the *right* the correspondent echocardiographic projection

Table 21.2   Technical characteristics of ICE devices

	Shaft size	US technology	Field depth	Image	Steerable	Doppler
AcuNav	8 F	64-element phased array transducer	16 cm	90°	All directions	Yes
		5.5–10.0 MHz				
ViewFlex Plus	9 F	64-element phased array transducer	12 cm	90°	Axial rotation	Yes
		4.5–8.5 MHz			Anterior and posterior bending	
Ultra ICE	9 F	Single transducer	5 cm	360° radial	No	No
		9 MHz				

When TEE is used along with fluoroscopy during the procedure, it may be useful to guide the crossing of PFO (especially when transseptal puncture is required), the positioning of the device, the post-closure monitoring of the relationship between the prosthesis and the adjacent structures, and the monitoring for possible complications [20]. The recent introduction of 3D echo technology allowed a better understanding of PFO morphology [21]. In particular, by using real-time 3D TEE imaging, it is possible to measure the size the of left and right atrial PFO opening and of tunnel length included in between the two openings [22]. 3D TTE is a promising modality to provide comprehensible en face imaging of ASD because of its noninvasiveness, low cost, portability, and wide availability [23].

A valid alternative to TEE is the use of intracardiac echocardiography (ICE) that allows to perform the procedure without sedation and without the need for an expert echocardiographer during the intervention [24, 25]. Currently available ICE systems are the AcuNav catheter (Siemens Medical Systems), the ViewFlex catheter (St Jude Medical), and the Ultra ICE (Boston Scientific). Table 21.2 shows the main technical characteristics of each system. Each catheter requires a specific ultrasound console for the visualization of the images, which is generally compatible with other devices from the same manufacturer. When using ICE, femoral, jugular, or subclavian accesses are possible. However, the femoral is the preferred access for most of the physicians because of its strategic position on the table. To avoid vascular complications, the catheter should be carefully advanced from the groin toward the heart under continuous fluoroscopic guidance because of its stiffness. The use of a long sheath (30 cm) is strongly recommended to protect vessels until below the heart. In the phased array technology devices, once the catheter is positioned in the right atrium, its manual advancement, clockwise rotation, and posterior flexion allow a complete visualization of all the main structures of the heart, thus enabling performance of all steps necessary for PFO closure, including possible transseptal puncture. The main disadvantages of ICE when compared to TEE are that it requires a second femoral vein puncture and adds significant odds and costs to the procedure [26].

21.2.5 Device Selection

In the majority of cases, device selection is based on TEE images. Although some operators only perform transthoracic echocardiography and/or transcranial Doppler studies before bringing the patient to the cardiac catheterization laboratory, a transesophageal echocardiogram should be considered critical in selecting devices and technical strategies likely for success in advance of the procedure [27].

For simple PFOs, the use of the smallest available device size properly fitting the atrial septum (as an average, the 20–25-mm diameter prostheses are the most commonly used) is generally enough to obtain complete occlusion of the communication. The size of the device should be decided according to the dimension of interatrial septum seen in the short axis passing through the aortic root.

In patients with wide atrial septal aneurysm and/or large tunnel diameter, the use of larger prostheses is suggested, mainly depending on the anatomical characteristics of the septum primum and secundum. When septum primum has a floppy morphology, the adaptability of the prosthesis is higher than in cases with rigid septum, where larger devices with higher tractive forces are required. In these cases, devices with the two disks of the same size are preferred to overcome possible atrial/prosthesis mismatch.

If septum primum is widely aneurysmatic but is thick enough to bear the encumbrance of the device, an ASD prosthesis may be deployed after balloon sizing the width of the tunnel. The advantage lies in the total obliteration of the tunnel with the central waist of the device.

In case of thickness of septum secundum, softer devices may be required to increase the adaptability of the prosthesis to the atrial anatomy. In particular, when a thick septum secundum is coupled with a thin and highly movable septum primum, the use of rigid devices may cause pinching of the septum primum with risk over time of laceration of the thin tissue.

When choosing a device, the possible nickel allergy should be taken into account, even if it is a poorly defined syndrome. There have been several case reports of severe nickel allergy after implantation of an Amplatzer Occluder device that required surgical removal. The newer prostheses have been designed to overcome this limitation (see Sect. 21.3).

21.2.6 Postprocedural Care and Follow-Up

The postprocedural care is mainly aimed to check for early procedural complications (device displacement, peripheral vascular complication, early arrhythmias), whereas after hospital discharge, the major clinical issues are the antithrombotic regimen, the detection of residual shunts, atrial fibrillation, and the prevention of endocarditis.

For these reasons, patients should stay in bed for 8 h with telemetry and with saline infusion to maintain a proper atrial volume. A 24-h transthoracic echocardiography or transcranial Doppler with bubble study should be planned. Until endothelialization of

the device has not been completed, a certain degree of early residual shunting is expected, but this evaluation may be useful to make proper comparisons with follow-up controls. The rates of endothelialization depend on the type and size of devices so a persistent relevant residual shunt should not be diagnosed until after at least 18 months of follow-up. In the postoperative period, patients are usually treated with a double antiplatelet therapy. The duration of DAPT has not been well defined in the main clinical trials, but a period between 3 and 6 months of treatment is strongly suggested [11–13]. Routine echo control should be planned after 6 months, and if the PFO has been successfully closed, the patients do not need any further instrumental follow-up unless clinically driven. In case of significant residual shunt, reintervention depends on the clinical status of the patient and on the shunting mechanism. In fact, the presence of the device across the PFO may guarantee a mechanical barrier to recurrent paradoxical embolism despite a moderate shunt; on the other hand, a peri-prosthetic residual shunt (due, e.g., to the device causing a laceration of the septum primum) may be a different issue because the possible paradoxical emboli carried by the shunt may not be entrapped by the presence of the device itself. In these cases, the deployment of another device is feasible and effective in abolishing the residual shunt.

Elective dental work should be deferred for 6 months, but, if necessary, an antibiotic prophylaxis to prevent device endocarditis should be administered.

If patients note occasional palpitations persisting for more than 10 min, cardiac evaluation with a 12-lead electrocardiogram is indicated. Premature supraventricular beats are most commonly diagnosed but, in some cases, a paroxysmal atrial fibrillation may onset because of the mechanical irritation by the device that can lead to an inflammatory response of the atrial myocardium favoring new macro-reentry circuits [28]. Arrhythmias should be treated according to standard clinical practice. Atrial fibrillation usually requires antiarrhythmic drugs for a period of 3–6 months without further recurrence after treatment withdrawal.

No restrictions are asked for and even sports are permitted immediately, with the exception of contact sports until DAPT has been administered.

21.3 Device

Several technologies have been developed for PFO percutaneous procedures, and the majority of these involve devices made of metallic framework and polymeric tissue scaffold. But different attempts have included the use of radiofrequency [29], percutaneous septal suturing [30], in-the-tunnel designs [31], and bioabsorbable prostheses [32].

Such a wide variety of different technologies reflects the complexity of atrial anatomy and the lack of a unique prosthesis that fits properly with all the possible morphologies. Beyond the technical consideration about the need to travel within a small sheath, the ideal PFO device should be easily deliverable, retrievable and repositionable, conformable, biocompatible, atraumatic, able to guarantee an immediate and complete closure, and with low rates of procedure related complications, in particular with low thrombogenicity.

Over time, the double-disk prostheses proved to be characterized by the majority of these technically acclaimed properties. Furthermore, innovation is moving toward an increase in biocompatibility of prostheses with a reduction of the rates of nickel release in the blood stream (to face the higher rates of hypersensitivity reactions) and to guarantee MRI compatibility over time. The most important devices currently available in the market are listed below.

21.3.1 Amplatzer PFO Occluder (St. Jude Medical, Minnesota, USA)

The Amplatzer Occluder is a self-centering device composed of a unique weave of 0.004–0.00.8 nitinol wires forming two circular disks joined at the center by a 3-mm-long narrow and flexible connecting waist, attached slightly eccentrically to the two disks. Its function is mainly to keep each disk well tight to the septal wall. A polyester mesh is incorporated inside the disk to enhance elimination of flow across the metallic stitches. Depending on prosthesis size, the right atrial disk may be larger than the left one. In the center of both disks is visible a small pin that holds together the nitinol wires on the left disk and contains a microscrew for the attachment of the delivery cable.

The delivery system is composed of a delivery cable with a plastic vise for the attachment/release of the device, a Teflon loader combined with a hemostasis valve, and a sheath with a dilator. Before being mounted, the device is soaked in a saline solution for few minutes. The delivery cable is advanced through the Teflon loader+ hemostasis valve, and then, the device is screwed onto the distal tip of the delivery cable and pulled into the loader, during continuous flushing with saline solution. Once the sheath is in the left atrium, the device is introduced and advanced into the delivery sheath. The device can be easily recaptured and redeployed for optimal placement. After proper deployment, the device is released from the delivery cable unscrewing plastic vise. In some cases, the Cribriform Septal Occluder (with double-matched disk diameters) may be used for PFO closure, when multiple fenestrations are present or in case of wide septal aneurysm [33] (Table 21.3 and Fig. 21.10).

Table 21.3 Technical characteristics of Amplatzer devices

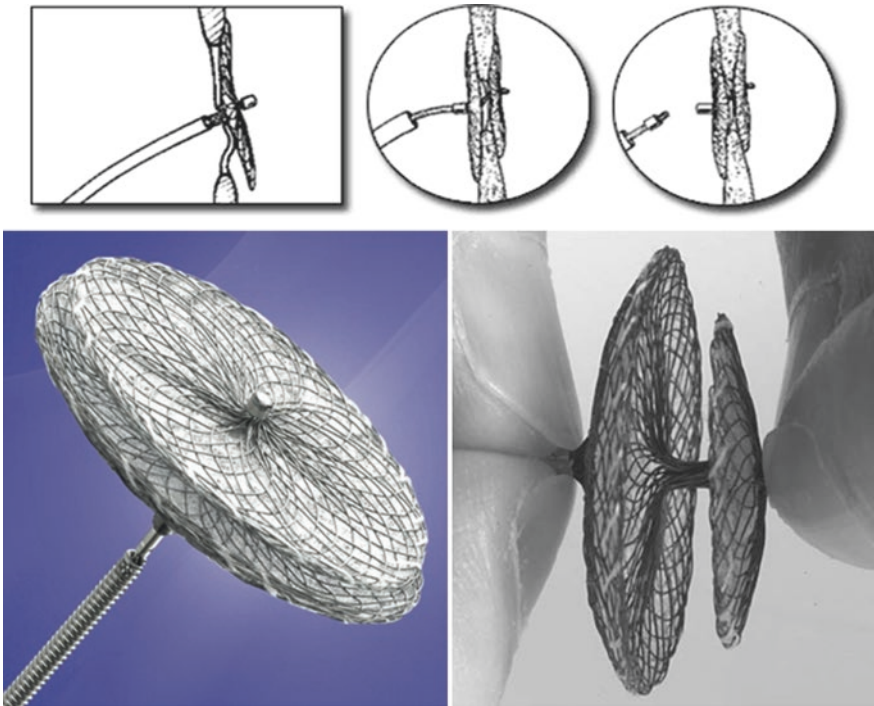| Device, size (mm)	Right atrial disk diameter (mm)	Left atrial disk diameter (mm)	Min. recommended sheath size (F)
PFO 18	18	18	8 F, 45° curve
PFO 25	25	18	8 F, 45° curve
PFO 30	30	30	8 F, 45° curve
PFO 35	35	25	9 F, 45° curve
Cribriform 18	18	18	8 F, 45° curve
Cribriform 25	25	25	8 F, 45° curve
Cribriform 30	30	30	8 F, 45° curve
Cribriform 35	35	35	9 F, 45° curve
Cribriform 40	40	40	10 F, 45° curve

Fig. 21.10 The Amplatzer PFO device and the main steps of prosthesis delivery (Courtesy of St Jude Medical)

21.3.2 GORE Cardioform Septal Occluder (W.L. Gore & Associates, USA)

The occluder is composed of five platinum-filled nitinol wire frames that are covered with an expanded polytetrafluoroethylene (ePTFE) film. The occluder has right and left atrial disks that form on either side of the atrial septum, act to close the defect, and hold the occluder in place. It uses a framework of minimal metal mass to hold a biocompatible ePTFE patch in close apposition to the septum. This design creates a right and left atrial disk with a low profile that can closely approximate the contours of the native septum. The device is delivered using conventional catheter delivery techniques. The delivery system consists of a 75-cm working length 10-Fr outer diameter delivery catheter coupled to a handle. The handle facilitates loading, deployment, and locking of the occluder. It also allows repositioning and retrieval of the occluder via a retrieval cord if necessary. The presence of the retrieval cord gives the physician the ability to view the occluder placement in a tension-free configuration before it is fully released. Thus, each implant can be fully evaluated for optimal positioning. If desired positioning is not achieved, the device can be removed and replaced quickly. The functionality provided by the handle delivery system is unique to GORE Septal Occluder [34] (Table 21.4 and Fig. 21.11).

Table 21.4 Technical characteristics of GORE Cardioform devices

Device, size (mm)	Right atrial disk diameter (mm)	Left atrial disk diameter (mm)	Min. recommended sheath size (F)
PFO 15	15	15	10 F
PFO 20	20	20	10 F
PFO 25	25	25	11 F
PFO 30	30	30	10 F
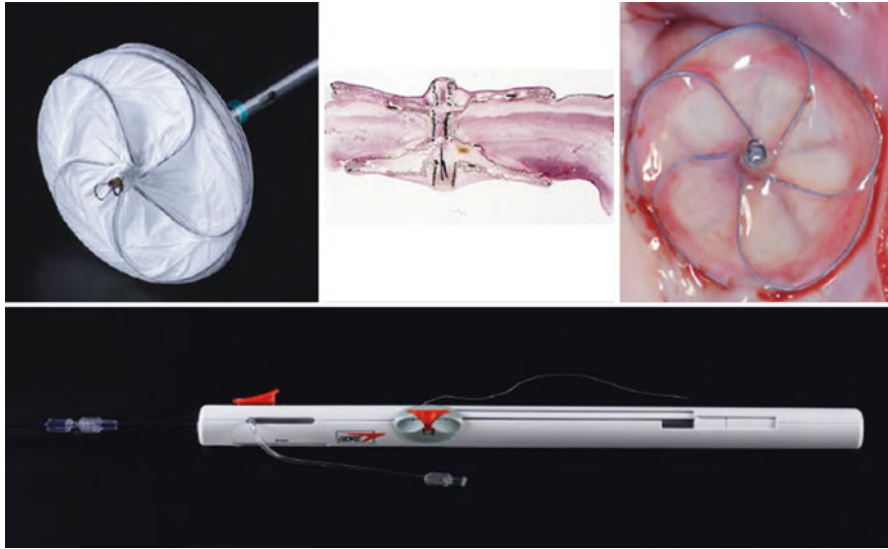
Fig. 21.11 The GORE Cardioform device and delivery system. *Upper right*: the anatomic pathology (Courtesy of Gore Medical)

21.3.3 Figulla Flex II PFO (Occlutech, Germany)

The device is made of braided nitinol threads and it is quite similar to the Amplatzer. The device consists of two disks with a small intermediate waist. Inside each of the disks, there is a polyethylene (PET) patch to support the immediate closure. This helps stop the blood going through the meshwork of the device. The ceramic titanium oxide surface gives the "golden" aspect of the nitinol wires. The device will be pushed through the delivery catheter across the defect, then both disks will fix the device at the septum wall, and the device will then be released when placed in the correct position to close the defect. The delivery system is an angled bioptome-type delivery system which allows a full circular movement of the device [35] (Tables 21.4 and 21.5, Fig. 21.12).

Table 21.5 Technical characteristics of Figulla Flex devices

Device, size (mm)	Right atrial disk diameter (mm)	Left atrial disk diameter (mm)	Min. recommended sheath size (F)
PFO 18	18	16	9 F
PFO 25	25	23	9 F
PFO 30	30	27	9 F
PFO 35	35	31	9 F
Uniform 17	17	17	7 F
Uniform 24	24	24	9 F
Uniform 28,5	28,5	28,5	9 F
Uniform 33	33	33	11 F
Uniform 40	40	40	12 F
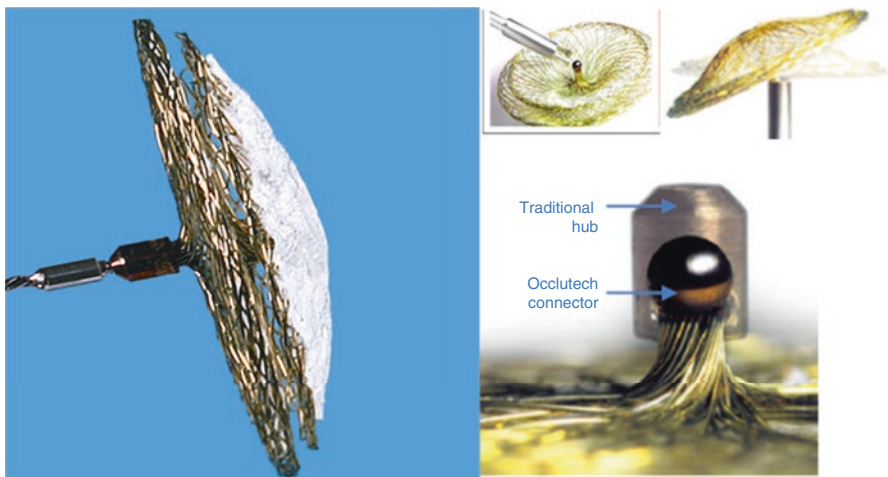
Fig. 21.12 The Figulla Flex device and the flexibility of the delivery system (Courtesy of Occlutech Medical)

21.3.4 Ultrasept PFO (Cardia Eagan, Minnesota, USA)

This is the last generation of CARDIA PFO double-umbrella closure devices. Each disk frame is made of 19 nitinol wires bended to form six petals entirely covered by a polyvinyl alcohol (PVA) sail. The waist is a 3-mm-long structure made of a multi-joined titanium strut, covered by PVA, permitting each disk to articulate independently. The delivery system consists in a long sheath available in two lengths (60–80 cm), 45° angled, and a bioptome mechanism to fix the prosthesis during positioning and delivery. The device is completely retrievable and repositionable. PVA allows a very low nickel exposure to patients [36] (Table 21.6 and Fig. 21.13).

Table 21.6 Technical characteristics of Ultrasept devices

Device, size (mm)	Right atrial disk diameter (mm)	Left atrial disk diameter (mm)	Min. recommended sheath size (F)
PFO 20	20	16	9/10 F
PFO 25	25	20	10 F
PFO 30	30	25	11 F
PFO 35	35	30	11/12 F

Positive locking ring
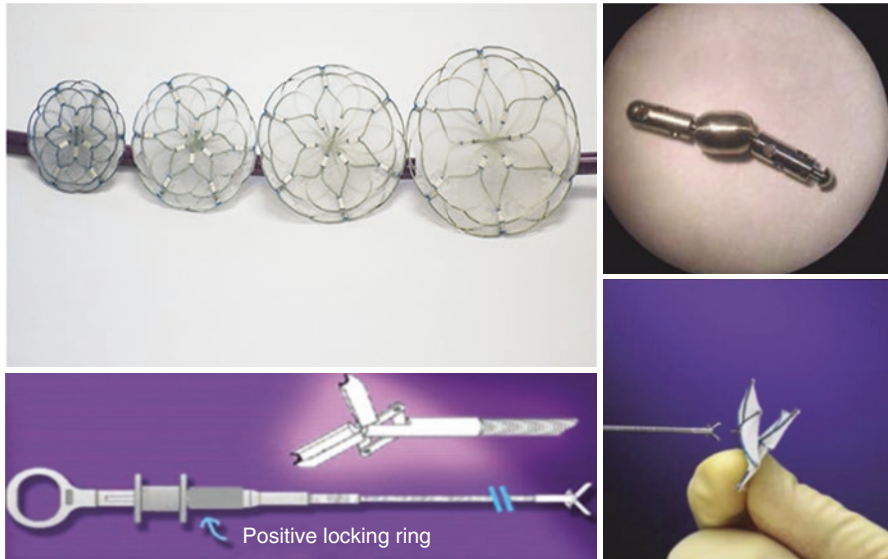
Fig. 21.13 The Cardia Ultrasept devices and their delivery system. *Upper right* the multi-joined waist strut that articulates the two disks (Courtesy of Cardia Inc.)

21.3.5 Nit-Occlud PFO (PFM Medical, Koln, Germany)

The occluder consists of a double-disk prosthesis made of a single nitinol wire. The left atrial part of Nit-Occlud PFO is designed as a concave single-layer disk, thus reducing the amount of metal by half in the left atrium. Moreover, a polyester membrane sewed facing the LA promotes accelerated endothelialization. The right disk is designed as a double-layer disk including another polyester membrane. The implant is connected to the pusher via retaining wires. A locking wire fixes this connection. To release the implant, the locking wire has to be pulled through the loop of the retaining wires. This eliminates any bulky connectors over the disks [37] (Table 21.7 and Fig. 21.14).

Table 21.7 Technical characteristics of Nit-Occlud devices

Device, size (mm)	Right atrial disk diameter (mm)	Left atrial disk diameter (mm)	Min. recommended sheath size (F)
PFO 20	20	20	9 F
PFO 26	26	26	9 F
PFO 30	30	30	10 F
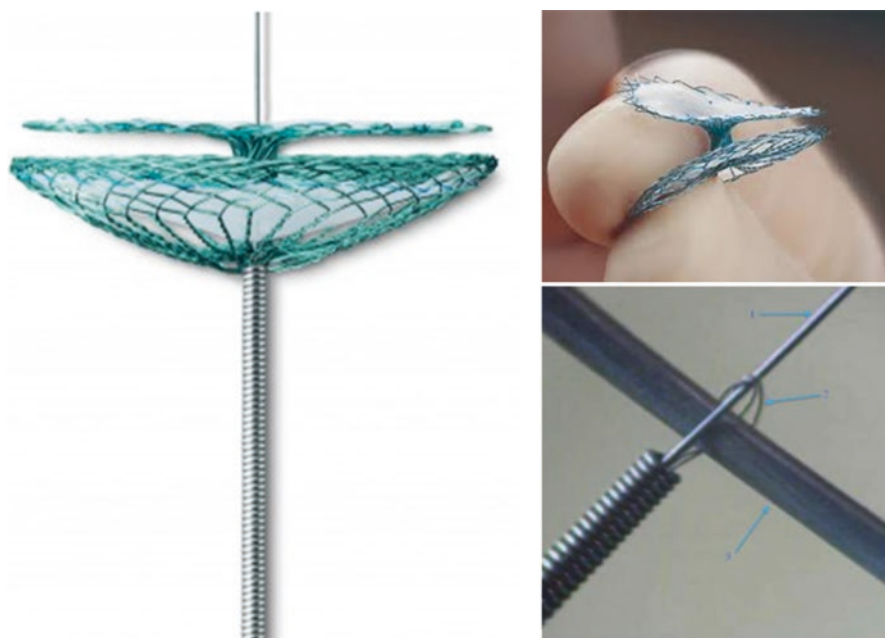
Fig. 21.14 The Nit-Occlud device and the locking wire connecting the device to the delivery system (Courtesy of pfm medical ag, Germany)

21.3.6 CeraFlex PFO Occluder (LifeTech Scientific Corporation, Shenzhen, China)

The device consists of self-expandable double-disk prosthesis made of a nitinol wire mesh shaped into two flat disks and of a polyethylene terephthalate (PET) membrane sewed into each disk, to increase sealing and tissue growth over the prosthesis soon after delivery. A special characteristic of this device is the ceramic coating (titanium nitride) on the wire mesh that reduces the risk of thrombosis and provides fast endothelialization, thus improving biocompatibility. Furthermore, it provides a 90 % reduction of nickel release in the blood stream. Differently from other devices, the prosthesis comprises only one stainless steel hub at the right atrial disk for cable connection and a connection system to the delivery cable. The delivery system allows a maximum range of Pivot 360° for accurate positioning during the procedure [38] (Table 21.8 and Fig. 21.15).

Table 21.8 Technical characteristics of CeraFlex devices

Device, size (mm)	Right atrial disk diameter (mm)	Left atrial disk diameter (mm)	Min. recommended sheath size (F)
PFO 18 18	18	18	9 F
PFO 25 18	25	18	10 F
PFO 25 25	25	25	10 F
PFO 30 25	30	25	12 F
PFO 30 30	30	30	12 F
PFO 35 25	35	25	14 F
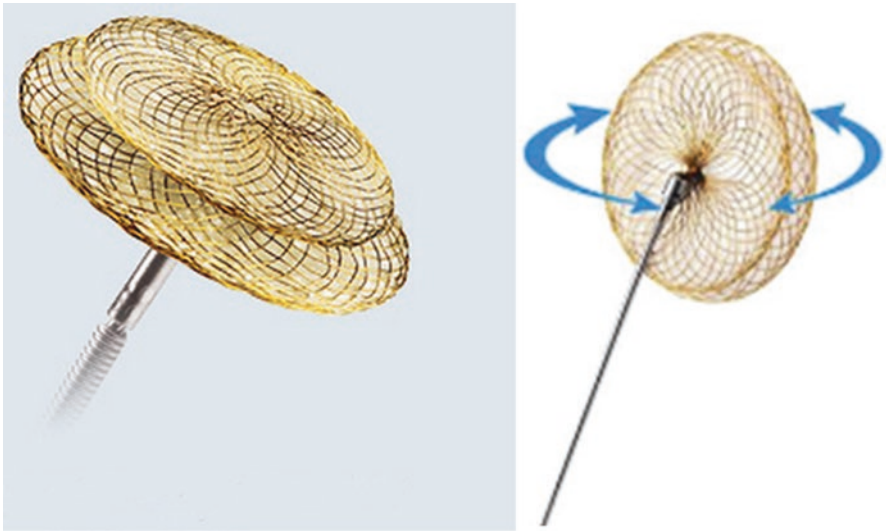
Fig. 21.15 The CeraFlex device and the flexibility of the delivery system (Courtesy of Lifetech Scientific)

References

1. Kapadia S. Patent foramen ovale closure: historical perspective. Cardiol Clin. 2005;23: 73–83.
2. Murray G. Closure of defects in cardiac septa. Ann Surg. 1948;128:843–52.
3. Alexi-Meskishvili V, Konstantinov I. Surgery for atrial septal defect: from the first experiments to clinical practice. Ann Thorac Surg. 2003;76:322–7.
4. Lewis FJ, Taufic M. Closure of atrial septal defects with the aid of hypothermia; experimental accomplishments and the report of one successful case. Surgery. 1953;33:52–9.
5. King TD, Mills NL. Nonoperative closure of atrial septal defects. Surgery. 1974;75:383–8.
6. King TD, Thompson SL, Steiner C, Mills NL, et al. Secundum atrial septal defect: nonoperative closure during cardiac catheterization. JAMA. 1976;235:2506–9.
7. The Task Force on the Management of Grown-up Congenital Heart Disease of the European Society of Cardiology (ESC) Endorsed by the Association for European Paediatric Cardiology (AEPC) European Heart Journal. ESC guidelines for the management of grown-up congenital heart disease. Eur Heart J. 2010;31:2915–57.

8. Kent DM, Dahabreh IJ, Ruthazer R. Device closure of patent foramen ovale after stroke: pooled analysis of completed randomized trials. J Am Coll Cardiol. 2016;67(8):907–17.

9. Harms V, Reisman M, Fuller CJ, et al. Outcomes after transcatheter closure of patent foramen ovale in patients with paradoxical embolism. Am J Cardiol. 2007;99:1312–5.

10. Braun MU, Fassbender D, Schoen SP, et al. Transcatheter closure of patent foramen ovale in patients with cerebral ischemia. J Am Coll Cardiol. 2002;39:2019–25.

11. Furlan AJ, Reisman M, Massaro J. Closure or medical therapy for cryptogenic stroke with patent foramen ovale. N Engl J Med. 2012;366(11):991–9.

12. John D, Carroll MD, Jeffrey L, Saver MD, et al. Closure of patent foramen ovale versus medical therapy after cryptogenic stroke. N Engl J Med. 2013;368(12):1082–100.

13. Meier B, Kalesan B, Mattle HP, et al. Percutaneous closure of patent foramen ovale in cryptogenic embolism. N Engl J Med. 2013;368(12):1083–91.

14. Dasika UK, Kanter KR, Vincent R. Nickel allergy to the percutaneous patent foramen ovale occluder and subsequent systemic nickel allergy. J Thorac Cardiovasc Surg. 2003;126:2112.

15. Mangieri A, Godino C, Montorfano M, et al. PFO closure with only fluoroscopic guidance: 7 years real-world single centre experience. Catheter Cardiovasc Interv. 2015;86(1):105–12.

16. Sader MA, De Moor M, Pomerantsev E, et al. Percutaneous transcatheter patent foramen ovale closure using the right internal jugular venous approach. Catheter Cardiovasc Interv. 2003;60:536–9.

17. Carter LI, Cavendish JJ. Percutaneous closure of a patent foramen ovale via left axillary vein approach with the Amplatzer Cribriform septal occluder. J Interv Cardiol. 2008;21:28–31.

18. Ebeid MR, Joransen JA, Gaymes CH. Transhepatic closure of atrial septal defect and assisted closure of modified Blalock/Taussig shunt. Catheter Cardiovasc Interv. 2006;67:674–8.

19. Rana BS, Thomas MR, Calvert PA, et al. Echocardiographic evaluation of patent foramen ovale prior to device closure. JACC Cardiovasc Imaging. 2010;3(7):749–60.

20. Singh V, Badheka AO, Patel NJ, et al. Influence of hospital volume on outcomes of percutaneous atrial septal defect and patent foramen ovale closure: a 10-years US perspective. Catheter Cardiovasc Interv. 2015;85(6):1073–81.

21. Balzer J, Kelm M, Kühl HP. Real-time three-dimensional transoesophageal echocardiography for guidance of non-coronary interventions in the catheter laboratory. Eur J Echocardiogr. 2009;10(3):341–9.

22. Rana BS, Shapiro LM, McCarthy KP, Ho SY. Three-dimensional imaging of the atrial septum and patent foramen ovale anatomy: defining the morphological phenotypes of patent foramen ovale. Eur J Echocardiogr. 2010;11(10):i19–25.

23. Watanabe N, Taniguchi M, Akagi T, et al. Usefulness of the right parasternal approach to evaluate the morphology of atrial septal defect for transcatheter closure using two-dimensional and three-dimensional transthoracic echocardiography. J Am Soc Echocardiogr. 2012;25:376–82.

24. Vigna C, Marchese N, Zanchetta, et al. Echocardiographic guidance of percutaneous patent foramen ovale closure: head-to-head comparison of transesophageal versus rotational intracardiac echocardiography. Echocardiography. 2012;9:1103–10.

25. Mitchell-Heggs L, Lim P, Bensaid A, et al. Usefulness of trans-oesophageal echocardiography using intracardiac echography probe in guiding patent foramen ovale percutaneous closure. Eur J Echocardiogr. 2010;11(5):394–400.

26. Budts W, Troost E, Voigt JU, et al. Intra-cardiac echocardiography in atrial septal interventions: impact on hospitalization costs. Acta Cardiol. 2010;65(2):147–52.

27. Bayar N, Arslan Ş, Çağırcı G, et al. Assessment of morphology of patent foramen ovale with transesophageal echocardiography in symptomatic and asymptomatic patients. J Stroke Cerebrovasc Dis. 2015;6:1282–6.

28. Wagdi P. Incidence and predictors of atrial fibrillation following transcatheter closure of interatrial septal communications using contemporary devices. Clin Res Cardiol. 2010;99(8):507–10.

29. Sievert H, Ruygrok P, Salkeld M, et al. Transcatheter closure of patent foramen ovale with radiofrequency: acute and intermediate term results in 144 patients. Catheter Cardiovasc Interv. 2009;73(3):368–73.

30. Majunke N, Baranowski A, Zimmermann W, et al. A suture not always the ideal solution: problems encountered in developing a suture-based PFO closure technique. Catheter Cardiovasc Interv. 2009;73(3):376–82.
31. Reiffenstein I, Majunke N, Wunderlich N, et al. Percutaneous closure of patent foramen ovale with a novel FlatStent. Expert Rev Med Devices. 2008;5(4):419–25.
32. Mullen MJ, Hildick-Smith D, De Giovanni JV, et al. BioSTAR Evaluation STudy (BEST): a prospective, multicenter, phase I clinical trial to evaluate the feasibility, efficacy, and safety of the BioSTAR bioabsorbable septal repair implant for the closure of atrial-level shunts. Circulation. 2006;114(18):1962–7.
33. Pandit A, Aryal MR, Pandit AA, et al. Amplatzer PFO occluder device may prevent recurrent stroke in patients with patent foramen ovale and cryptogenic stroke: a meta-analysis of randomised trials. Heart Lung Circ. 2014;23(4):303–8.
34. Geis NA, Pleger ST, Katus HA, et al. Using the GORE® Septal Occluder (GSO) in challenging patent foramen ovale (PFO) anatomies. J Interv Cardiol. 2015;28(2):190–7.
35. Saguner AM, Wahl A, Praz F, et al. Figulla PFO occluder versus Amplatzer PFO occluder for percutaneous closure of patent foramen ovale. Catheter Cardiovasc Interv. 2011;77(5):709–14.
36. Puricel S, Arroyo D, Goy JJ, et al. A propensity score-matched comparison between Cardia and Amplatzer PFO closure devices – insights from the SOLUTION registry (Swiss percutaneOus patent foramen ovale cLosUre in recurrent clinical events prevenTION). EuroIntervention. 2015;11(2):230–7.
37. Steinberg DH, Bertog SC, Momberger J, et al. Initial experience with the novel patent foramen ovale occlusion device Nit-Occlud® in patients with stroke or transient ischemic attack. Catheter Cardiovasc Interv. 2015;85(7):1262–7.
38. Fiszer R, Szkutnik M, Chodor B, et al. Preliminary experience in the use of CERA occluders for closure of different intracardiac and extracardiac shunts. J Invasive Cardiol. 2014;26(8):385–8.

Difficult Cases and Complications from the Catheterization Laboratory: PFO Device Embolization and Settling in the Distal Aorta

22

Niels Thue Olsen and Lars Sondergaard

22.1 Case Presentation

A 40-year-old female patient without clinical risk factors for stroke experienced a short episode of hemiparesis. CT and MR imaging revealed multiple small ischemic lesions of both cerebral hemispheres. Neurological testing showed decreased short-term memory and attention. Coagulopathy screen and cardiac rhythm monitoring were negative. A persistent foramen ovale (PFO) was evident on transesophageal echocardiography and a spontaneous right-to-left shunting was demonstrated using agitated saline contrast. The atrial septum was found to be aneurysmal with a maximum excursion of 12 mm. No other structural abnormalities were noted. Paradoxical embolism was considered a probable cause for the multiple cerebral lesions. The patient was offered device closure of the PFO, which she accepted.

The procedure was performed under local anesthesia using bilateral femoral venous access. An intracardiac echocardiography (ICE) catheter (AcuNav, Biosense Webster, Diamond Bar, CA) was advanced through the left femoral vein to the right atrium. From the right femoral vein, a multipurpose catheter and hydrophilic guidewire were advanced through the PFO into the left upper pulmonary vein. The wire was exchanged for a 0.035″ Amplatz Super Stiff wire. A 25-mm PTS sizing balloon (B. Braun Interventional Systems, Bethlehem, PA)

N.T. Olsen, MD, PhD
Department of Cardiology, Gentofte Hospital, Copenhagen, Denmark

L. Sondergaard, MD, DMSc (✉)
Department of Cardiology, Rigshospitalet,
Copenhagen, Denmark
e-mail: lars.sondergaard@rh.dk
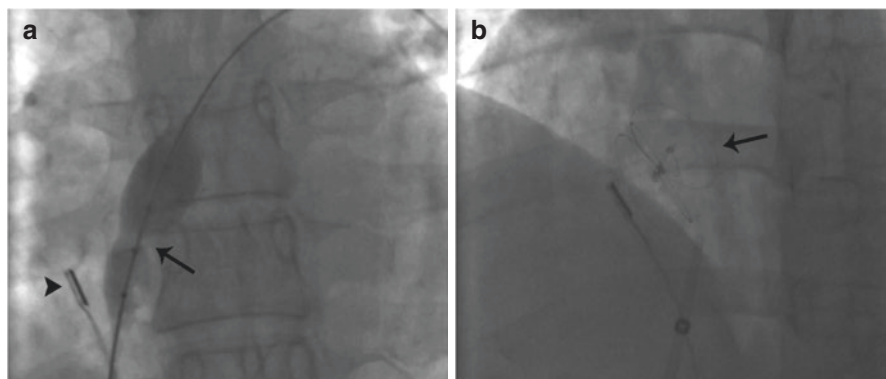
Fig. 22.1 Panel (**a**) balloon sizing the persistent foramen ovale (PFO) at the first procedure. The waist on the balloon (*arrow*) is situated at the defect and was used to measure the length and diameter of the PFO tunnel. The ICE catheter is seen in the right atrium (*arrowhead*). Panel (**b**) The Helex Septal Occluder after release. Note the mobile aneurysmal intra-atrial septum. Online video

was advanced over the guidewire and expanded within the PFO under fluoroscopy and ICE monitoring to measure the size of the defect (see Fig. 22.1a). The PFO was found to measure 5 mm in diameter and 4 mm in length. A Helex Septum Occluder 25 mm (WL Gore and Ass., Flagstaff, AZ) was advanced over the wire and deployed. A tug test was performed and revealed stable position before the device was released (Fig. 22.1b). Subsequently, fluoroscopy showed that the released device was very mobile during the cardiac cycle, probably due to the aneurysmal septum (Video 22.1). However, ICE confirmed a well-placed device with no residual shunt.

Transthoracic echocardiography (TTE) on the next day was interpreted as successful device closure with small residual shunt. The patient was discharged but after a few days was readmitted for leg pain and numbness, especially in the left leg. Clinical examination was noted as normal, and she was discharged without additional imaging.

At follow-up visit after 1 year, TTE and fluoroscopy showed that the device had embolized, and contrast computer tomography (CT) scan revealed the device positioned in the iliac bifurcation. Catheterization was performed with venous and arterial access. There was evidence of local dissection of the distal aorta extending from the renal arteries to the bifurcation, where an organized thrombus was located with reduced flow into the left common iliac artery, but with good collateral flow (Figs. 22.2a, b and 22.3a, b). The invasive blood pressure difference from the distal aorta to the common iliac artery was 35 mmHg. An attempt was made to retrieve the device with a snare from the right femoral artery, but the device could not be mobilized probably due to endothelialization. The PFO was crossed from the right femoral vein using a 25-mm PTS sizing balloon resized to a stretched diameter of
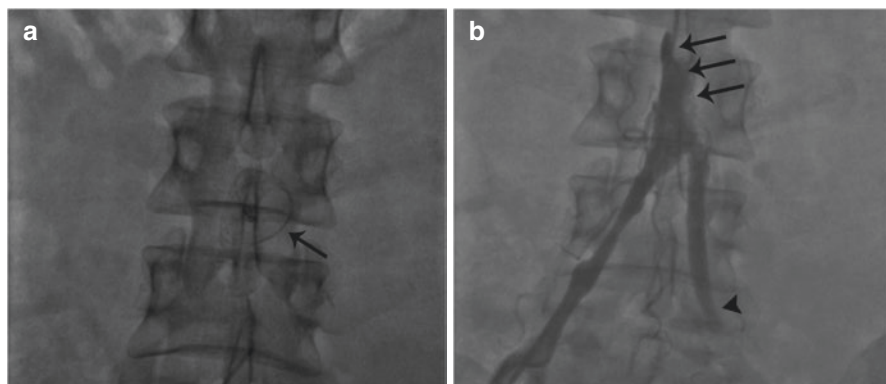
Fig. 22.2 Panel (**a**) fluoroscopy showing device (*arrow*) at iliac bifurcation. Panel (**b**) Angiography showing dissection in the distal abdominal aorta (*arrows*) and reduced flow to particularly the left common iliac artery (*arrowhead*)
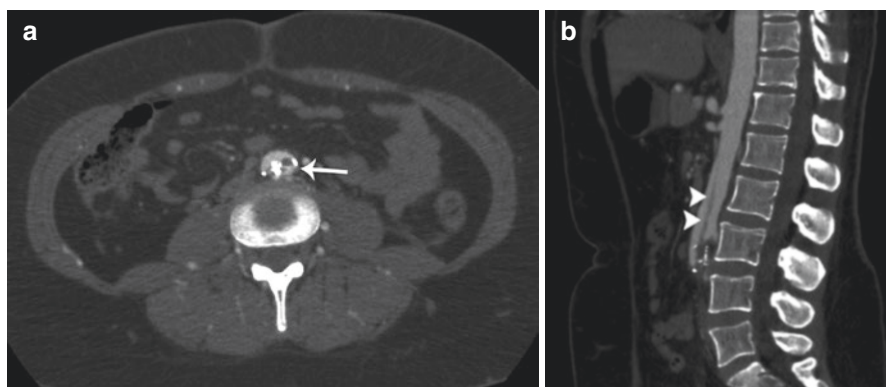

Fig. 22.3 Contrast computer tomography images. Panel (**a**) axial image. Device (*arrow*) at aortic bifurcation. Panel (**b**) sagittal reconstruction showing dissection (*arrowheads*) of the distal abdominal aorta

18 mm (Fig. 22.4a). A 21-mm Occlutech Figulla ASD Occluder (Occlutech International, Helsingborg, Sweden) was implanted without complications (Fig. 22.4b).

In collaboration with the vascular surgery team, initial conservative treatment was recommended with the option for open surgical repair of the distal aorta and proximal iliac arteries in case of symptom progression. During the following 4 years, CT findings have been unchanged, and the patient has reported low degree of claudication and declined open surgery due to the low intensity of symptoms.
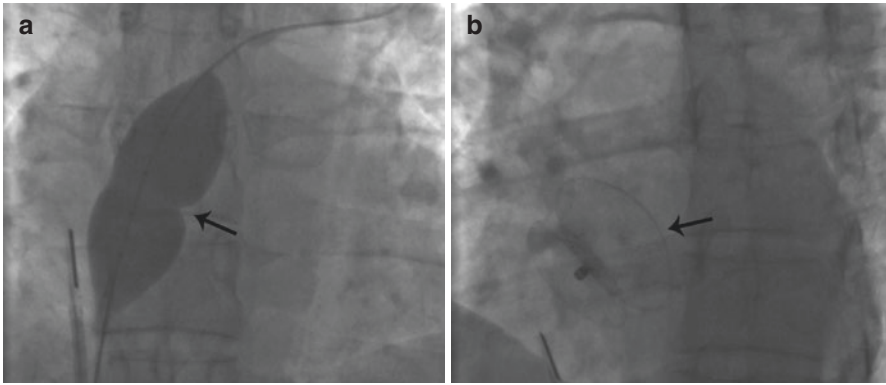
Fig. 22.4 Panel (**a**) balloon sizing the persistent foramen ovale at the second procedure. The waist on the balloon (*arrow*) is situated at the defect. Panel (**b**) Occlutech Figulla ASD occluder in position (*arrow*)

22.2 Discussion

This case demonstrates the occurrence of device embolization after PFO occlusion, which was diagnosed late and resulted in the permanent settling of the device in the distal aorta. The reason for the embolization was probably undersizing of the device. Furthermore, the late diagnosis prevented easy catheter-based retrieval presumably due to tissue overgrowth and the development of chronic dissection.

Embolization itself is a rare event, reported to occur in approximately 0.3–0.6 % of PFO closure cases [1, 2], which is a slightly lower incidence than after ASD closure [2, 3]. Devices preferably tend to embolize to the left circulation after PFO closure and to the right circulation after ASD closure. In cases of device embolization, retrieval is recommended. Several important learning points can be extracted from the case:

22.2.1 Correct Device Sizing and Device Selection Is Essential for Safe Device Deployment in PFO Closure

The echocardiography-visualized PFO channel is deceptively narrow, which can lead to the misconception that choice of disk size does not matter. However, the visualized defect is only the narrow slit revealing incomplete fixation of the entire flap-like septum primum to the rim. The extension of incomplete fixation is difficult to ascertain with imaging, also because the higher left-sided atrial pressure will tend to keep the flap closed. Only balloon dilation within the defect can reveal the full size of the potential orifice.

For non-self-centering devices with small diameter central connectors between the left and right atrial disks, such as the Helex Septal Occluder, the usual recommendation is to achieve at least a 2:1 ratio between disk size and dilated defect

diameter. For a circular defect, this will result in the disk always covering the defect, even when the central connector is positioned at the margin. However, for eccentric and slit-like defects like a PFO, the long-axis diameter of the defect can be up to 1.6 (π/2) times larger than the dilated diameter where the defect is forced by the balloon to assume a circular shape [4]. Thus, to ensure coverage, a 3:1 ratio would then theoretically be needed for such slit-like lesions.

In this example, it seems the balloon was inadequately dilated at the first procedure, resulting in an underestimation of the defect size. This may have been due to a tissue string across the PFO, which was ruptured during device deployment. Thus, the "true" size of 18 mm was determined at the second procedure. The majority of PFOs have diameters below 10 mm, but particularly in cases of an aneurysmal septum, larger defects are occasionally encountered [5]. A defect of 18-mm diameter was outside the recommended range for the Helex Septal Occluder, as a 2:1 ratio is recommended for the largest available 35-mm device. The use at the first procedure of an undersized non-self-centering device in an exceptionally large defect was probably the main reason for embolization.

The patient in the current report had an aneurysmal septum primum, which may be defined as a mobile membranous septum with a protrusion >10 mm from the midline of the atrial septum on echocardiography. An aneurysmal septum often coincides with a PFO and may in itself be a risk factor for thromboembolic events [6]. It is probably also associated with a higher risk for device embolization [1], and it is recommended to use a larger device in these cases to ensure coverage and immobilization of the septum. In the present case, the aneurysmal septum probably aggravated the problem of undersizing the device.

22.2.2 A High Index of Suspicion for Complications Is Needed After Interventional Procedures

Although the risk for complications is low in PFO closure, it is not negligible. And as exemplified in this case, there was a time constraint on handling complications. Malpositioned devices will eventually get stuck due to vascular tissue overgrowth, and late percutaneous retrieval may then be impossible.

In this case, both imaging and clinical symptoms should have suggested the diagnosis of device embolization in the days after the procedure. A possible explanation for the lack of response to imaging findings suggestive of device embolization is the fact that visualization of a correctly deployed device may be difficult. The frame of the Helex Septal Occluder is composed of a thin nitinol wire, and it is not well visualized on fluoroscopy and echocardiography. In the current version, the GORE Septal Occluder (WL Gore and Ass., Flagstaff, AZ), a platinum core, has been added in the nitinol wires to offer better echocardiographic and fluoroscopic visualization [7].

It is imperative for clinicians involved in handling interventional cases to always explore unexplained symptoms and to carefully review routine imaging, even after low-risk procedures such as PFO closure.

References

1. Goel SS, Aksoy O, Tuzcu EM, Krasuski RA, Kapadia SR. Embolization of patent foramen ovale closure devices: incidence, role of imaging in identification, potential causes, and management. Tex Heart Inst J. 2013;40:439–44.
2. Abaci A, Unlu S, Alsancak Y, Kaya U, Sezenoz B. Short and long term complications of device closure of atrial septal defect and patent foramen ovale: meta-analysis of 28,142 patients from 203 studies. Catheter Cardiovasc Interv. 2013;82:1123–38.
3. Chessa M, Carminati M, Butera G, Bini RM, Drago M, Rosti L, Giamberti A, Pome G, Bossone E, Frigiola A. Early and late complications associated with transcatheter occlusion of secundum atrial septal defect. J Am Coll Cardiol. 2002;39:1061–5.
4. Alibegovic J, Bonvini R, Sigwart U, Dorsaz P, Camenzind E, Verin V. The role of the sizing balloon in selection of the patent foramen ovale closure device size. Exp Clin Cardiol. 2008;13:42–6.
5. Hagen PT, Scholz DG, Edwards WD. Incidence and size of patent foramen ovale during the first 10 decades of life: an autopsy study of 965 normal hearts. Mayo Clin Proc. 1984;59:17–20.
6. Mugge A, Daniel WG, Angermann C, Spes C, Khandheria BK, Kronzon I, Freedberg RS, Keren A, Denning K, Engberding R, Sutherland GR, Vered Z, Erbel R, Visser CA, Lindert O, Hausmann D, Wenzlaff P. Atrial septal aneurysm in adult patients. A multicenter study using transthoracic and transesophageal echocardiography. Circulation. 1995;91:2785–92.
7. Sondergaard L, Loh PH, Franzen O, Ihlemann N, Vejlstrup N. The first clinical experience with the new GORE(R) septal occluder (GSO). EuroIntervention. 2013;9:959–63.

Difficult Cases and Complications from the Catheterization Laboratory: A Case of Platypnea-Orthodeoxia Syndrome

Dennis Zavalloni

23.1 Case

A 59-year-old woman with a clinical history of thyroidectomy due to a multinodular goiter, obesity, and recent removal of a cervical ganglioneuroma extending from intervertebral foramina at C5–C7 level to the proximal insertion of the anterior scalene muscle was evaluated for progressive onset of resting dyspnea. Oxygen arterial saturation was 85 % in clinostatism with further decrease to 71 % in orthostatism.

CT scan excluded major lung diseases, in particular pulmonary embolism, and revealed right diaphragm elevation. The cardiac origin of the problem was also investigated with transthoracic and transesophageal echocardiography. Both the exams were normal except for a significant spontaneous right-to-left shunt through patent foramen ovale (PFO):

The presence of PFO does not elicit spontaneously a significant right-to-left shunt and its pathologic relevance usually concerns cryptogenic stroke due to paradoxical embolism [1, 2]. However, in particular conditions such as right diaphragmatic elevation [3], ascending aorta tortuosity or aneurism [4] and right lung inferior pneumonectomy [5], the deformation of atrial septum due to the extrinsic stretching (or compression) induces an opening of PFO with development of significant right-to-left shunt, regardless of normal pulmonary pressure. Under the same pathogenic mechanisms right atrial pressure increases and right ventricular compliance decreases, causing a preferential flow direction from the inferior vena cava to the left atrium sustaining the right-to left shunt, as happens during foetal circulation. Further

D. Zavalloni, MD, FESC
Invasive Cardiology Department, Humanitas Research Hospital, IRCCS,
Rozzano, Milano, Italy
e-mail: dennis.zavalloni_parenti@hunimed.eu

283

Fig 23.1 AP projection. Two prostheses are delivered across PFO. The second is positioned behind the first one and acts as a "staple" of the two disks of the first prosthesis
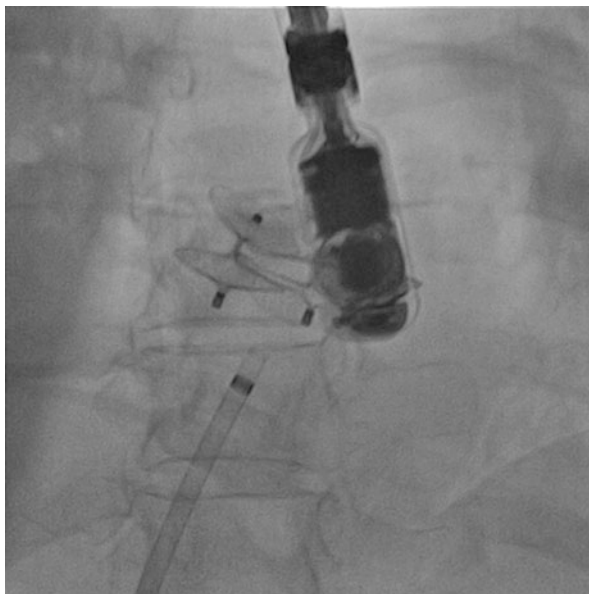
decrease in oxygen arterial saturation is exacerbated by the orthostatic position, when preload decreases and atrial deformation is amplified with a worsening of the right-to-left shunt (the reduction of preload together with the right-to-left shunt translate also into a reduction of pulmonary output that further amplifies arterial desaturation) [6]. From a clinical point of view, patients are characterized by dyspnoea and arterial desaturation exacerbated by the upright position and relieved by recumbency, a condition known as Platypnea-orthodeoxia Syndrome (P-OS) [7].

This syndrome may be also caused by primary pulmonary or hepatic diseases but, when PFO is responsible, the first choice treatment consists in the abolition of the right-to-left shunting with percutaneous closure of the inter-atrial communication [8].

The patient was therefore treated with percutaneous closure of PFO with delivery of an Amplatzer PFO Occluder 30-mm device (AGA Medical, Golden Valley, MN, USA) according to the standard procedural technique, under 2D echo monitoring. Soon after the intervention, a significant reduction of the shunt was observed, but a moderate residual right-to-left shunt persisted in the posterior part of the atrial communication, behind the implanted prosthesis. Arterial saturation improved up to 90 %, without orthodeoxia recurrence, and the patient was then referred to the rehabilitation unit where a progressive relief of symptoms was observed. After 18 days the patient suffered a transient ischemic attack with left hemiparesis. MRI revealed a lesion typical for cardioembolism. In the absence of other potential causes for stroke, we decided to treat residual interatrial shunt with a second device delivery (Amplatzer PFO Occluder 18 mm, AGA Medical, Golden Valley, MN, USA) that was deployed behind the previous one, with a complete abolition of the shunt through a compression of the two disks of the first prosthesis by the two disks of the second one (Fig. 23.1). After the intervention, arterial saturation further improved up to 98 %, and 6 months later, the patient remained uneventful and echo showed persistent closure of PFO.
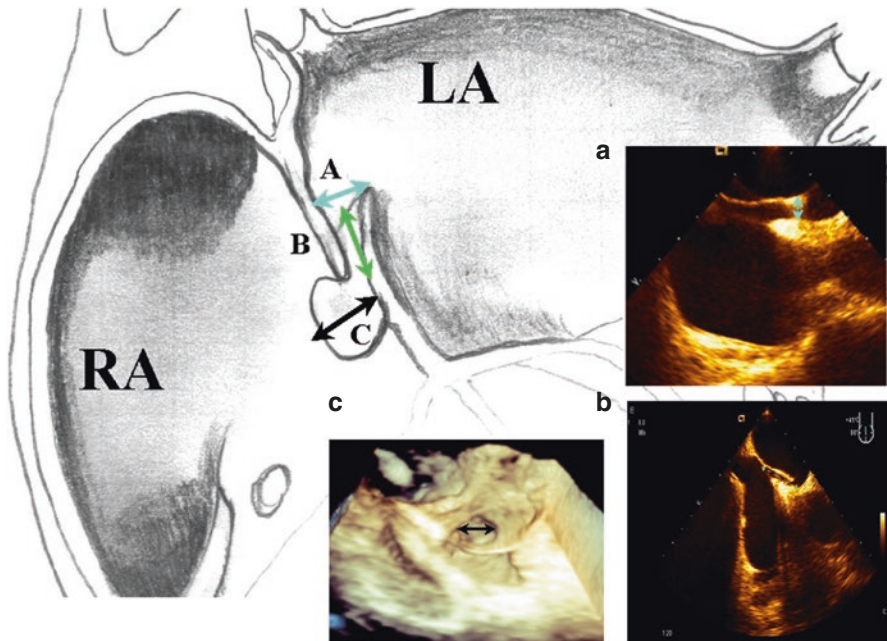
Fig 23.2 *LA* left atrium; *RA* right atrium. *PFO* patent foramen ovale. (**A**) (*light blue arrow*) represents the degree of PFO opening (separation between septum primum and septum secundum) and the corresponding echographic projection 30–60°(**a**). (**B**) (*green arrow*) represents the degree of overlapping between septum primum and septum secundum and the corresponding echographic projection 30–60° (**b**). (**C**) represents the width of the slit between septum primum and septum secundum in 3D-Echo view(**c**)

23.1.1 Procedural and Technical Issues

The peculiar anatomic modifications of atrial septum in the context of P-O syndrome make percutaneous treatment challenging for either diagnostic or procedural aspects. For this reason, PFO closure should be considered more complex in the course of P-O syndrome than in other clinical settings. In particular two major issues should be considered:

1. Anatomic definition of the defect
2. The choice of the right prosthesis

1. The stretching of the right atrium observed with P-O syndrome leads to a very difficult echocardiographic evaluation of the anatomy, in particular, of the real shape of defect and of septum primum characteristics. This is a major tool because a faulty intraprocedural echocardiographic evaluation may lead to a mismatch between the delivered prosthesis and the atrial septum, and a significant residual shunt may persist. Figure 23.2 shows how 2D imaging techniques may properly provide either the degree of PFO opening evaluated by the distance between the two septa or the degree of overlapping between septum primum and septum secundum but do not provide a correct estimation of the width of the PFO

slit that, on the contrary, can be assessed by 3D technology. Rana et al. [9] high-lighted how 3D rather than 2D echocardiography allowed a detailed understanding of the different PFO anatomies and of its neighboring structures and how these knowledge can be considered the main determinant for the choice of device and procedural success during percutaneous closure.

In this case, the residual shunt persisting behind the first implanted prosthesis suggests that the width of the slit between septum primum and septum secundum had been underestimated. So additional information obtained by 3D echo might have been helpful in guiding the procedure. When 3D echo is not available, a possible effective alternative is to perform a balloon sizing of the PFO to select the device to deploy, based on the dimension of the waist of the inflated balloon across the PFO, measured at fluoroscopy [10].

2. In this particular clinical context, the choice of the proper device to implant is mandatory to obtain symptom relief and to reduce the risk of paradoxical embolism that is higher in case of persistent rather than transient right-to-left shunt.

In the treatment of large PFO, the deployment of an atrial septal defect (ASD) device rather than a PFO one should be considered: when the foramen is wide and the atrial septum is stretched, the persistent overlapping of the two atrial septa, usually obtained with a PFO prosthesis, is not always achievable. The ASD device has a central waist, larger than that of PFO, which may work as a plug to the fossa ovale, facilitating the complete obliteration of the defect.

When residual shunt persists, a double-device deployment is required with the second one stapling the disks of the first one (Fig. 23.1). From a technical point of view, it is important to release the right-sided disk under a proper traction in order to include both the disks of the first device within the disks of the second one.

When this kind of procedure is carried out, the risk of device embolization should be taken into account. Our advice is to use a second percutaneous access for the second device positioning, in order to release both the prostheses only after the second one has been positioned.

As a general rule in treating PFO-related P-O syndrome, left venous femoral access should be the first choice because the manipulation of the catheter may be more difficult if it is used as a second access.

In conclusion, percutaneous closure of PFO in cases of P-O syndrome is feasible but some technical issues should be considered. All currently available few series and case reports on P-O syndrome address the importance of a detailed comprehension of PFO morphology before performing percutaneous closure to obtain acute procedural success. However, in case of postprocedural residual shunt, they may be successfully treated with a second device delivery.

References

1. Altman M, Robin ED. Platypnea (diffuse zone I phenomenon?). N Engl J Med. 1969;281:1347–8.
2. Robin ED, Altman M. By a waterfall: zone I and zone II. phenomena in obstructive lung disease. Am J Med Sci. 1969;258:219–23.

3. Ghamande S, Ramsey R, Rhodes JF, Stoller JK. Right hemidiaphragmatic elevation with a right-to-left interatrial shunt through a patent foramen ovale: a case report and literature review. Chest. 2001;120(6):2094–6.
4. Faller M, Kessler R, Chaouat A, Ehrhart M, Petit H, Weitzenblum E. Platypnea-orthodeoxia syndrome related to an aortic aneurysm combined with an aneurysm of the atrial septum. Chest. 2000;118(2):553–7.
5. Bhattacharya K, Birla R, Northridge D, Zamvar V. Platypnea-orthodeoxia syndrome: a rare complication after right pneumonectomy. Ann Thorac Surg. 2009;88(6):2018–9.
6. Toffart AC, Bouvaist H, Feral V, Blin D, Pison C. Hypoxemia-orthodeoxia related to patent foramen ovale without pulmonary hypertension. Heart Lung. 2008;37(5):385–9.
7. Sanikommu V, Lasorda D, Poornima I. Anatomical factors triggering platypnea-orthodeoxia in adults. Clin Cardiol. 2009;32(11):E55–7.
8. Calvert PA, Rana BS, Kydd AC, Shapiro LM. Patent foramen ovale: anatomy, outcomes, and closure. Nat Rev Cardiol. 2011;8(3):148–60.
9. Rana BS, Shapiro LM, McCarthy KP, Ho SY. Three-dimensional imaging of the atrial septum and patent foramen ovale anatomy: defining the morphological phenotypes of patent foramen ovale. Eur J Echocardiogr. 2010;11(10):i19–25.
10. Alibegovic J, Bonvini R, Sigwart U, Dorsaz P, Camenzind E, Verin V. The role of the sizing balloon in selection of the patent foramen ovale closure device size. Exp Clin Cardiol. 2008;13(1):42–6.

Difficult Cases and Complications from the Catheterization Laboratory: A Case of Nitinol Intolerance

24

Jonathan M. Tobis and Amir B. Rabbani

24.1 Introduction

Patent foramen ovale (PFO) affects up to 20 % of the adult population and has been linked with several clinical conditions including migraines, obstructive sleep apnea, and recurrent transient neurologic deficits [1]. PFOs have been observed in up to 40 % of patients presenting with cryptogenic stroke, which represents a particular clinical challenge [2]. To date, three randomized clinical trials have been published evaluating the efficacy of percutaneous PFO closure [3–5]. As ongoing trials continue to define the role of percutaneous PFO closure, an estimated 8000 closure procedures are performed annually in the United States. The overall safety of PFO closure has been demonstrated in several observational studies; however, complications do arise. A retrospective analysis involving 13,736 device implantations over 18 institutions showed a 0.28 % rate of device explantation [6]. While the overall rate of explantation is low, the necessity for open heart surgery makes this a particularly worrisome outcome.

The following case example illustrates a scenario that led to device explantation.

J.M. Tobis, MD, MSCAI • A.B. Rabbani, MD, FACC
David Geffen School of Medicine at UCLA, University of California,
Los Angeles, CA 90095, USA
e-mail: jtobis@mednet.ucla.edu

24.2 Case Example

A 54-year-old woman presented with a history of migraine headaches with aura since age 12 and subsequently was found to have a patent foramen ovale. Due to the frequency of her migraine headaches, the patient underwent PFO closure with an 18-mm cribriform Amplatzer ASD device 9 years prior to the current admission. Within days after implantation, the patient experienced an increase in the number of migraines with aura, chest pain, and episodic atrial fibrillation. She was treated with steroids and antiplatelet therapy with minimal symptom improvement. A TRUE skin patch test for nickel allergy was negative. She was referred to a tertiary medical center where surgical device explantation was recommended; however she chose continued observation and medical therapy. Nine years later, the patient experienced sudden onset of ataxia, weakness, and left hemianopsia and was found to have an embolic stroke on MRI in the absence of atrial fibrillation (Fig. 24.1). The patient underwent a transesophageal echocardiogram that revealed an atrial septal aneurysm without residual shunt or thrombus on the device on the left atrial appendage (Fig. 24.2). The patient underwent robotic-assisted surgery to remove the device. The explanted device showed severe fibrosis and scarring predominantly over the left atrial disk (Fig. 24.3). The patient underwent robotic-assisted surgery to remove the device. The explanted device showed severe fibrosis and scarring predominantly over the left atrial disk. After explantation, the patient had resolution of her chest pain, migraines, and palpitations but continued to experience a visual field defect and left-sided weakness from the prior stroke.
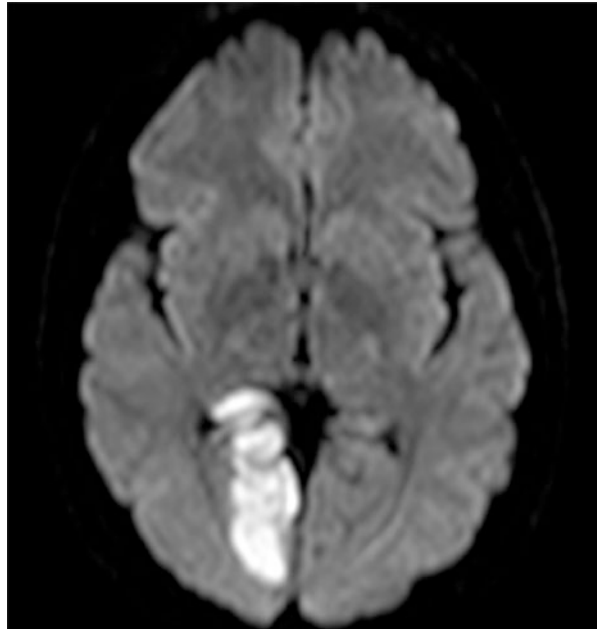
Fig. 24.1 MRI showing right posterior stroke
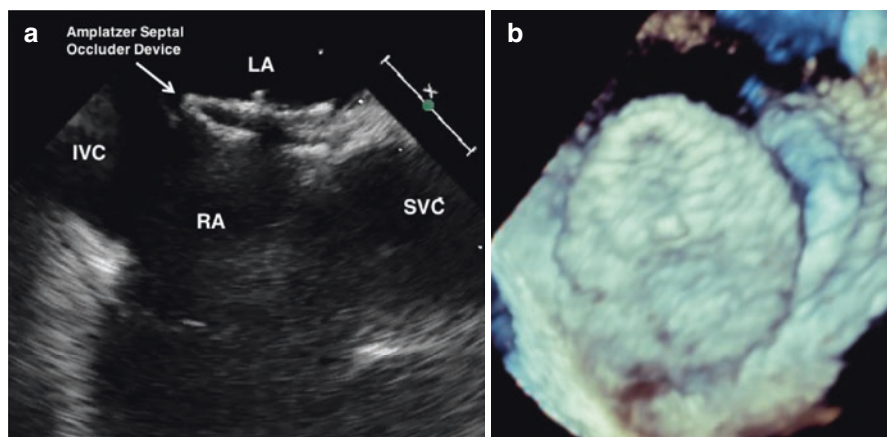
Fig. 24.2 Transesophageal echocardiogram showing no evidence of residual shunt and no evidence of thrombus on the left atrial side of the septal occluder device (**a**). View from the left atrium showing well-seated septal occluder without thrombus on the device or in the left atrium (**b**)
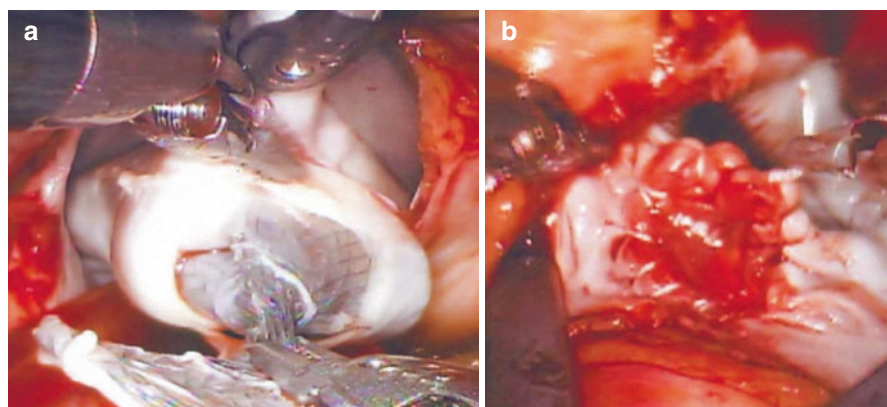
Fig. 24.3 Robotic surgical excision of the Amplatzer device showing severe scarring over the left atrial disk (**a**). Final patch closure of the ASD after device explantation (**b**)

24.3   Discussion

While the majority of PFO closures are performed safely with minimal complications, a small percentage of percutaneous closures do result in the need for surgical explantation of the device. Verma and Tobis showed that up to 0.28 % of patients undergoing PFO closure across 18 institutions required surgical explantation. While several reasons were cited for device removal, chest pain (often secondary to nickel allergy when tested) was the most common. Of the patients that had removal secondary to chest pain, over half tested positive for nickel allergy based on the TRUE skin patch test. Other indications for removal included persistence of residual shunt,

Table 24.1 Complications associated with PFO closure by device

Type of device				
	CardioSEAL	Amplatzer	Helex	Other
Implants	2023	9109	1201	1403
Explants	16	19	2	1
% Explanted	0.79 %*	0.21 %*	0.16 %	0.07 %

Verma and Tobis [6]

*$p < 0.0003$

thrombus on the device, or, much less frequently, perforation or pericardial effusion. The type of device implanted also appeared to have an impact on the rate of explantation, with the CardioSEAL (NMT Medical) and Amplatzer (St. Jude Medical) devices comprising the majority of explantations (Table 24.1).

PFO has a high prevalence in the general population affecting up to 20 % of people. A higher incidence of PFO (50 %) is seen in patients presenting with cryptogenic stroke. While studies are ongoing to assess the efficacy of PFO closure in patients presenting with cryptogenic stroke or migraine with transient neurologic events, a large number of procedures continue to be performed. While the newer PFO closure devices are safe and effective, a small percentage of patients may require device explantation, which necessitates an open heart operation. At the present time, it is not possible to identify at-risk patients and prevent this complication from occurring, although patients who are allergic to nickel may do better with a device made from e-PTFE.

References

1. Johansson MC, Eriksson P, Dellborg M. The significance of patent foramen ovale: a current review of associated conditions and treatment. Int J Card. 2009;134:17–24.
2. Homma S, Sacco RL. Patent foramen ovale and stroke. Circulation. 2005;112:1063–72.
3. Carroll JD, Saver JL, Thaler DE, et al. Closure of patent foramen ovale versus medical therapy after cryptogenic stroke. N Eng J Med. 2013;368:1092–100.
4. Meier B. Closure of the patent foramen ovale, who says a must say B. Cath Cardiovasc Interv Off J Soc Cardiac Angiography Interv. 2013;82:959–60.
5. Furlan AJ, Reisman M, Massaro J, et al. Closure or medical therapy for cryptogenic stroke with patent foramen ovale. N Eng J Med. 2012;366:991–9.
6. Verma SK, Tobis JM. Explantation of patent foramen ovale closure devices: a multicenter survey. J Am Coll Card Cardiovasc Interv. 2011;4:579–85.

Part V

Interventricular Defect Closure

Percutaneous Repair of Post-myocardial Infarction Ventricular Septal Rupture

25

Francesco Versaci, Antonio Trivisonno, Francesco Prati,
Anna De Fazio, Carlo Olivieri, Giampiero Vizzari,
and Francesco Romeo

Postinfarction ventricular septum rupture (VSR) is a rare fatal complication of an acute myocardial infarction (AMI). Risk factors associated to VSR include hypertension, advanced age, female gender, diabetes mellitus, severe coronary stenosis, or total occlusion without compensatory collateral circulation [1–3]. Absence of history of angina has been associated with increased incidence of VSR [4], possibly because angina leads to myocardial preconditioning and collateral formation, which protect the myocardium from the rupture [5, 6].

After the use of more aggressive and efficient revascularization therapy using antithrombotic medication or by primary angioplasty, the incidence of postinfarction VSR decreases from 1–3 % to 0.25–0.31 % [7]. However, the nature of presentation has changed. VSR generally occurs during the first week after AMI [8].

F. Versaci, MD, FACC (✉)
Department of Cardiovascular Medicine, Tor Vergata University of Rome, Rome, Italy
e-mail: francescoversaci@yahoo.it

A. Trivisonno • G. Vizzari
Department of Cardiovascular Disease, Ospedale "Antonio Cardarelli",
Contrada Tappino, 86100 Campobasso, Italy

F. Prati
Department of Cardiovascular Disease, Ospedale "San Giovanni-Addolorata", Rome, Italy

A. De Fazio
Department of Cardiovascular Disease, Ospedale "Giovan Battista Grassi", Rome, Italy

C. Olivieri
Department of Cardiovascular Disease, Ospedale "Ferdinando Veneziale", Isernia, Italy

F. Romeo
Department of Cardiovascular Medicine, Tor Vergata University of Rome, Rome, Italy

Whereas the average time interval between infarction and rupture used to be 5–6 days, it is now closer to 1 day. The surgical mortality rate increased at the same time [9]. It is likely that the nature of patients coming to surgery has changed. The thrombolytic treatment may increase the proportion of ruptures that are complex and therefore more difficult to repair. Furthermore, patients in the first 24–48 h after AMI are probably less able to sustain the surgery stress than they would be after more days necessary for anatomic and hemodynamic stabilization.

To date, postinfarction VSR still carries a poor prognosis [10, 11]. Over 80 % of untreated patients die within the first month and >90 % within the first year after VSR following AMI [12, 13]. The mortality of patients with cardiogenic shock due to VSR is as high as 67 % within 48 h and 100 % within 30 days [14]. It is well documented that surgical closure of postinfarction VSR is the treatment of choice for this serious complication [15]. After the first surgical description in 1957 [16], mortality rates of surgical closure remain high at 20–87 % in current series [12, 13, 17]. The incidence of a large residual shunt and re-rupture after surgery is between 10 % and 20 % [10, 18], and, among patients who survived in the perioperative period, the 5-year survival rate reported is 50 % [17]. Such high mortality rates are not unexpected given the advanced patient age and comorbidities. Norell and colleagues [19] in a univariate analysis found hypotension, oliguria, elevated creatinine, and cardiogenic shock to be associated with non-survivors. Moreover, a consistent finding is that rupture following inferior infarction carries a considerably higher operative mortality than following anterior infarction [20]. Current guidelines recommend immediate surgical VSR closure irrespective of patient's clinical status to avoid further hemodynamic deterioration [21, 22]. However, many surgeons recommend surgical VSR closure after a 3–4 weeks delay to allow scarring of the surrounding tissue, which allows for firmer anchoring of suture and patch material.

Transcatheter VSR closure has become a treatment option for patients with postinfarction VSR [12, 23], even in the acute setting [24]. Immediate reduction of the left-to-right shunt, even if the VSR is not completely closed, may stabilize the patient enough to function to bridge to surgery [24].

25.1 Indication to Transcatheter Closure and Timing

Despite ACC/AHA guidelines, there is a tendency to defer surgical treatment by 2–4 weeks. In this time, the necrotic process will stabilize, and scaring of the surrounding tissue will occur, which will form a better fundamental for a fixation of the patch. Moreover, the VSR diameter will often increase over time until stabilization, due to fragility of the necrotic tissue.

The decision if deferring is feasible or not should be based on the hemodynamic stability of the patient. Patients will typically be treated with supportive medication, an intra-aortic balloon or mechanical circulatory support [25–27]. Patients suffering from a VSR will frequently present with cardiogenic shock due to left-to-right shunt complicating the initial AMI with tremendous increase in mortality rate. Recently, Thiele et al. [24] in a prospective study where all postinfarction VSR was treated
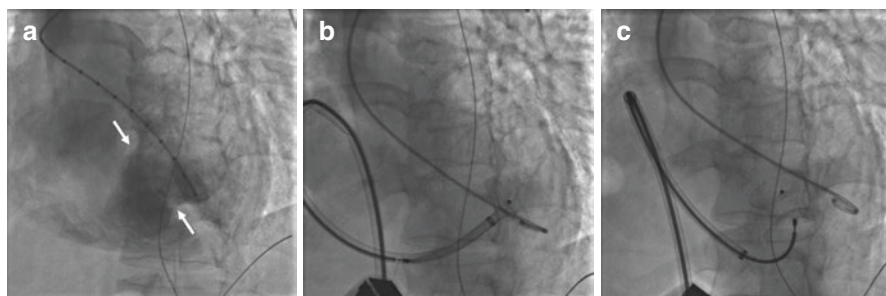
Fig. 25.1 Panel (**a**) Left ventricular angiography showing a large ventricular septal defect (*white arrows*) in the middle portion of the ventricular septum. Panel (**b**) Ventricular septal defect closure attempt, by using the largest size of the Amplatzer Septal Occluder device. The distal disk of the device appears to be deployed and well positioned against the left side of the ventricular septum. Panel (**c**) Unsuccessful placement of the Amplatzer Septal Occluder device, due to intraprocedural dislodgment of the device through the defect into the right ventricle

directly after VSR diagnosis independently of the hemodynamic status demonstrated that percutaneous VSR treatment is feasible also in acute phase and might lead to stabilization or prevention of further deterioration.

Maltias et al. suggest a new treatment algorithm where acute small or medium VSR are initially treated with transcatheter closure device allowing myocardial fibrosis, facilitating delayed surgical correction if significant residual VSR persists. Large ($\geq$15 mm) VSR should undergo immediate surgical correction for the high rate of unsuccessful to percutaneous repair. In fact, these patients are likely to experience dislodgment of the device through the defect into the right ventricle (Fig. 25.1), embolization in pulmonary artery, or residual VSR with high mortality rate [28].

Another important aspect concerns the timing of percutaneous coronary revascularization (PTCA). Usually VSR closure is prior to PTCA except in case of recurrent angina. In patients who undergo VSR first, no antiplatelet drugs are used before the procedure, and aspirin is prescribed after VSR closure if there is no residual shunt. In case of clinical stabilization, PTCA should be deferred to allow the device re-endothelialization. In case of clinical stabilization, a myocardial perfusion scintigraphy should be performed to decide the therapeutic approach (Fig. 25.2).

25.2   Occluder Devices

Based on the existing literature, a variety of devices for percutaneous closure of postinfarction VSR have been used. These devices are the atrial septal defect occluder, muscular ventricular septal defect occluder, and recently a dedicated postinfarction muscular ventricular septal defect occluder device developed by Amplatz (Fig. 25.3). The diameters of the applied devices are, on purpose, significantly larger than the diameter of the VSR measured using different imaging techniques. The strategy to "oversizing" is particularly important when closures are attempted in the acute phase. In this situation the optimal diameter should be twice
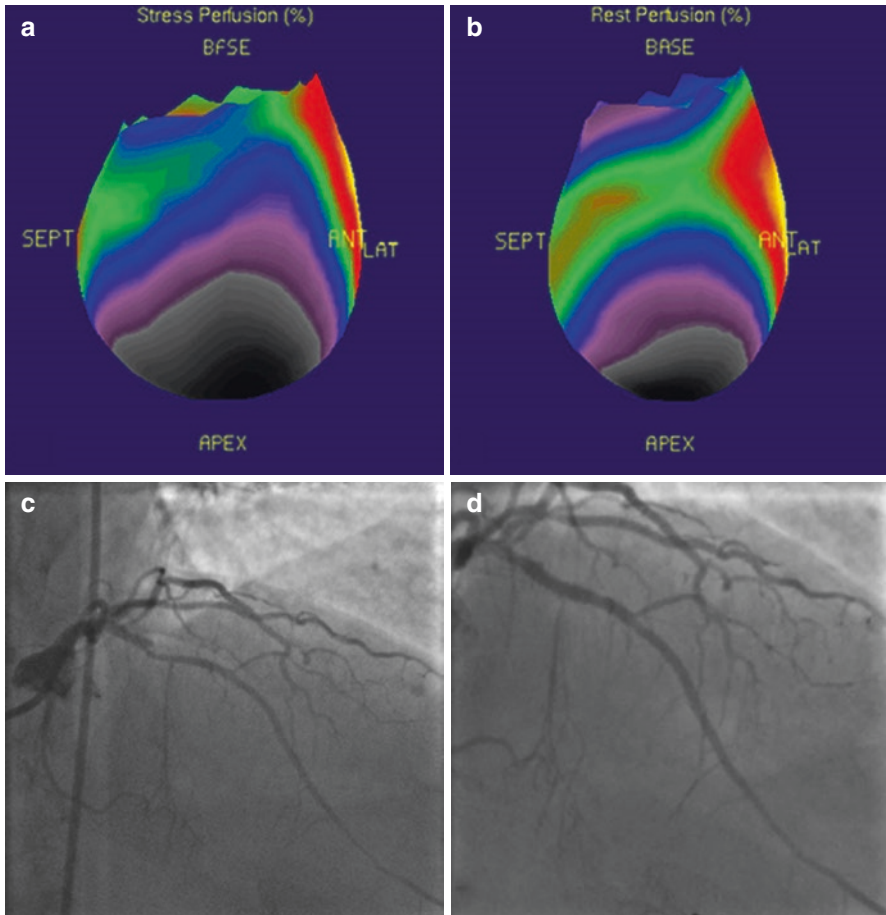
Fig. 25.2 Panel (**a**, **b**) Thallium myocardial scintigraphy performed 3 months after percutaneous closure of postinfarction VSR shows the presence of a significant amount of transitory perfusion defect in the territory supplied by the left anterior coronary artery (LAD). Panel (**c**) Coronary angiography demonstrated the presence of a significant stenosis on the proximal portion of LAD. According to clinical and scintigraphic results, this lesion was successfully treated with PTCA and stent implantation. Panel (**d**)

the size of the measured VSR diameter or at least 10-mm larger [28, 29]. This prevents incomplete closure or dislodging and subsequent embolization of the device due to continued septal necrosis. Instead, occlusion in the chronic phase requires occluding devices sized only 4–7-mm larger than the VSR [30]. The choice of the most suitable device is not certain and varies from case to case: generally the specific postinfarction muscular ventricular septal defect occluder device developed by Amplatz is considered by many authors the most suitable. This device has a wider waist, larger disks, and a denser construction, which should lead to a faster occlusion over a wider septal region. Therefore, larger disks are likely to cover any

Fig. 25.3 Amplatzer postinfarction muscular ventricular septal defect occluder (St. Jude Medical, St. Paul, Minnesota, USA)

accessory VSR that often accompanies the main VSR [30–32]. The use of atrial septal defect occluder should be utilized only in particular cases: the combination of a high-pressure gradient between the two ventricles and the high permeability makes this device unable to provide a complete occlusion of the VSR.

25.3   Procedure

The technique of percutaneous closure of a postinfarction VSR is based upon the well-proven and widely used percutaneous technique for closing a congenital ventricular septal defect. Color Doppler echocardiography is used to determine the size and the anatomy of the VSR. Other imaging methods, such as computed tomography, could be utilized to obtain more detailed informations.

The procedure is performed under fluoroscopic and echocardiographic guidance. All patients receive antibiotic prophylaxis as well as aspirin (500 mg) and heparin (60 UI/Kg) intravenously maintaining the activating clotting time over 300 s.

Cannulation of the femoral artery and femoral vein or jugular vein is performed using Seldinger technique. A guidewire is introduced into the artery, through the aortic valve. The injection of contrast medium in left ventricle (oblique lateral view) is utilized to visualize the position of VSR (Fig. 25.4). The use of catheters with radiopaque markers is useful for making measurements of VSR during the procedure.

The VSR is generally crossed from the left ventricle using a diagnostic right Judkins or a multipurpose catheter, and a soft or hydrophilic long wire is advanced into the pulmonary artery or in superior vena cava (Fig. 25.5a). The wire is then

Fig. 25.4 The injection of the contrast medium in the left ventricle simultaneously displays also the right ventricle due to the rupture of the interventricular septum (*white arrow*). The use of a pigtail catheter with radiopaque markers is useful for making measurements of VSR during the procedure
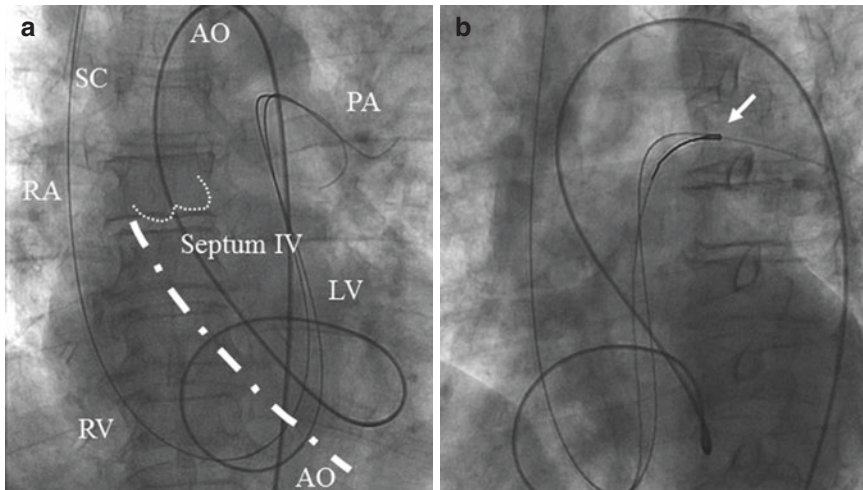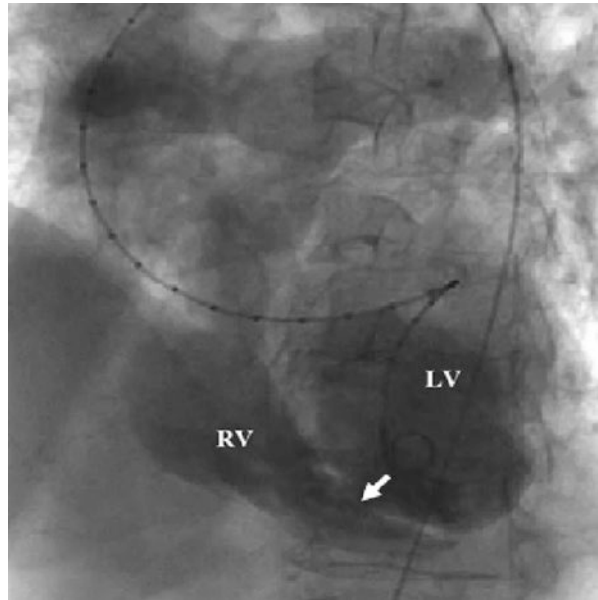
Fig. 25.5 Panel (**a**) The VSR is generally crossed from the left ventricle using a diagnostic right Judkins or a multipurpose catheter, and a soft or hydrophilic long wire is advanced into the pulmonary artery or in superior vena cava. Panel (**b**) The wire is then snared using a GooseNeck snare device and exteriorized out of the vein, thereby establishing an arterial-venous circuit

snared using a Gooseneck snare device and exteriorized out of the vein, thereby establishing an arterial-venous circuit (Fig. 25.5b). The delivery sheath is advanced from the venous side loop over the guidewire through the VSR into the left ventricle (Fig. 25.6). Using fluoroscopy and echocardiography, correct positioning of the

Fig. 25.6 The delivery sheath is advanced from the venous side loop over the guidewire through the VSR into the left ventricle
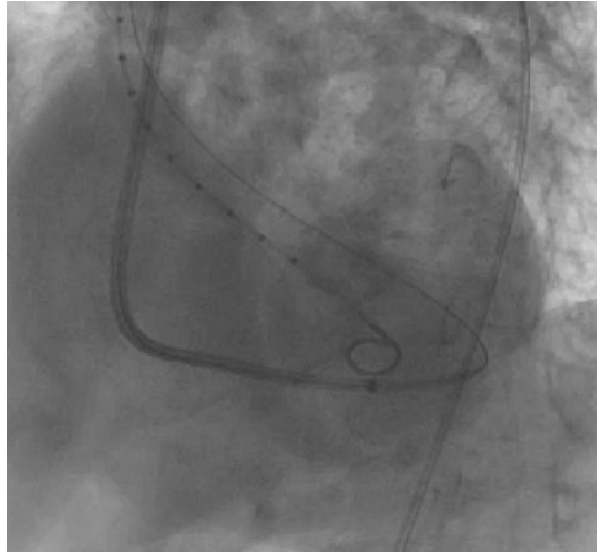
Fig. 25.7 Using fluoroscopy and echocardiography, correct positioning of the delivery sheath is confirmed. The guidewire is then retracted leaving the delivery sheath in position (*white arrow*)
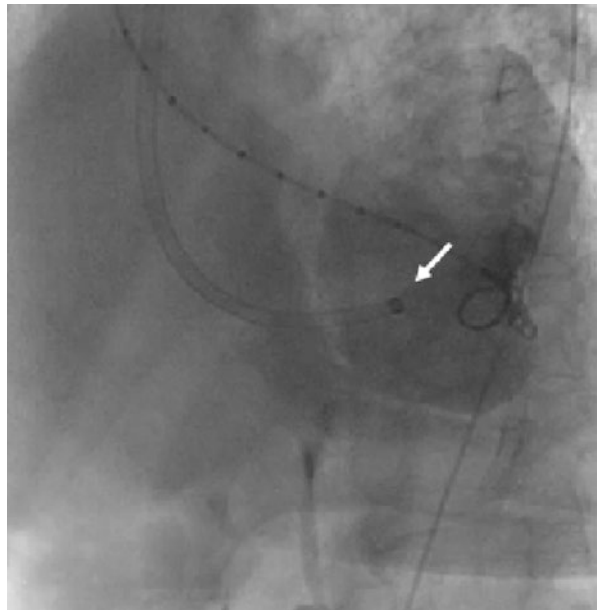
delivery sheath is confirmed. The guidewire is then retracted leaving the delivery sheath in position (Fig. 25.7). Once echocardiography confirmation of the necessary device size has been achieved, the device is placed inside its catheter and advanced through the VSR using the delivery sheath. The distal disk is opened (Fig. 25.8) and then the device is retracted, so that it will be secured against the septal tissue at the side of the left ventricle. Then the proximal disk is opened by further retracting the

Fig. 25.8 The device is placed inside its catheter and advanced though the VSR using the delivery sheath. The distal disk is opened and then the device is retracted, so that it will be secured against the septal tissue at the side of the left ventricle. Then the proximal disk is opened by further retracting the delivery sheath. Correct positioning of the device and closure are confirmed by echocardiography and by fluoroscopy
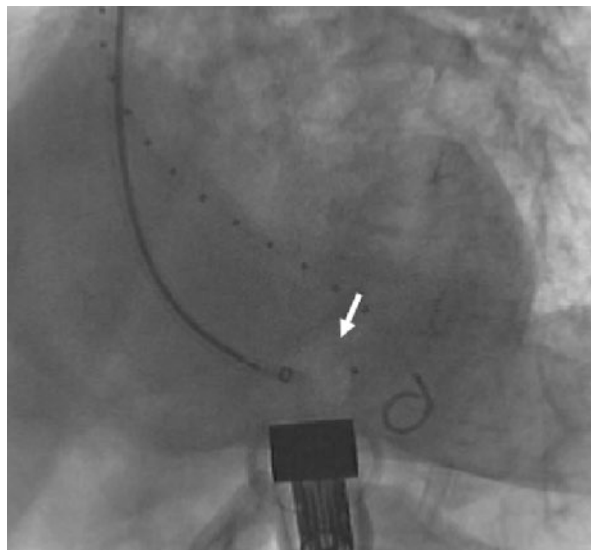
Fig. 25.9 An injection of dye is useful to confirm the right position; then if placement is satisfactory, the device is released. The *white arrow* shows the detachment of the device from the delivery system
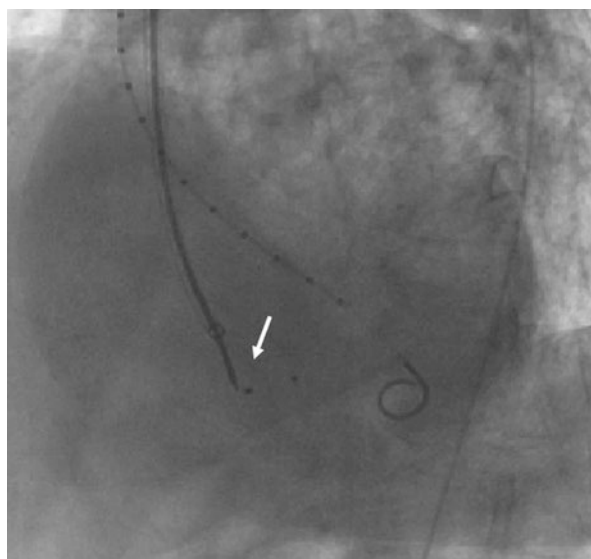
delivery sheath. Correct positioning of the device and closure are confirmed by echocardiography and by fluoroscopy. An injection of dye is useful to confirm the right position; then if placement is satisfactory, the device is released (Figs. 25.9 and 25.10). Computed tomography (CT) scan and ventricular angiography can be performed in follow-up to confirm the correct position of the device and the complete repair of septal rupture without any passage of contrast medium in the right ventricle (Figs. 25.11 and 25.12).

Fig. 25.10 The device (*white arrows*) is completely detached and closes the ventricular septal rupture
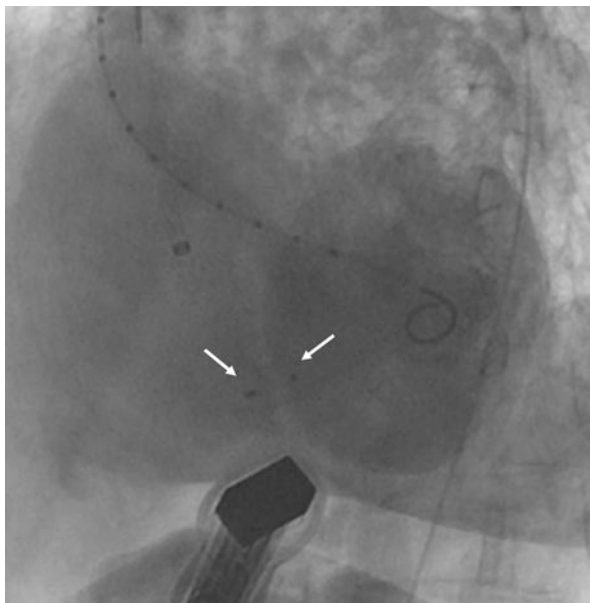
Fig. 25.11 Computed tomography scan shows the correct position of the device
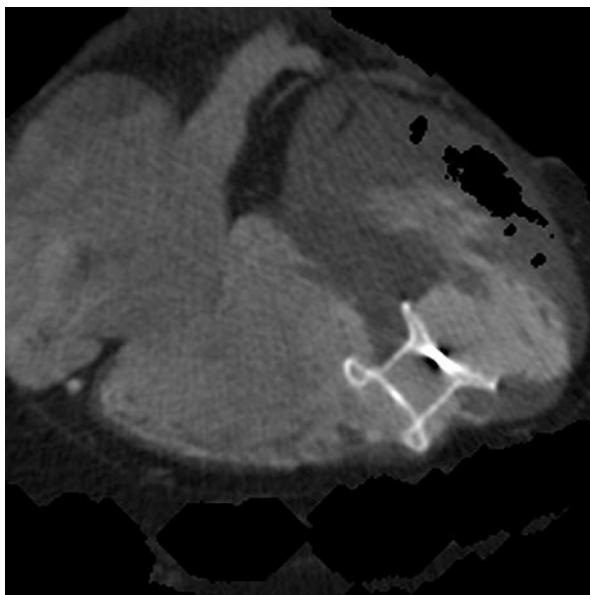
When percutaneous treatment is performed, a variety of procedure-related complications may occur. In particular, the device has to be placed in fragile necrotic tissue where every manipulation can lead to an increase of the VSR diameter and device displacement. Persistent left-to-right shunt can be caused by progressive septal necrosis or complication in relation to device placement. The presence of such

Fig. 25.12 Left ventricular angiography performed 6 months later shows the complete repair of septal rupture without any passage of contrast medium to the right ventricle

residual shunt differs greatly among the different authors (12.5–100 %) [29–34]. Other possible complications are left ventricle free wall rupture, arrhythmia, hematoma at the puncture side, and hemolysis. Complications not related to the procedure are multiple organ failure [29], hemolytic anemia [33], and sepsis. Mortality occurring in the long-term period following intervention is often the result of one of these complications.

Conclusions

Although the gold standard for the treatment of postinfarction VSR is still surgical repair, the application of this strategy to all patients might not be reasonable, especially when patients are critically ill or have multiple comorbidities. Transcatheter device closure of postinfarction VSR can be an alternative or a bridge to surgical repair, such as in patients with uncertain neurologic status or multiple organ failure at presentation. Moreover, this strategy has a role in selected patients with simple defects that are <15 mm, in the subacute or chronic (>3–4 weeks post-AMI) setting where an occluder device may provide a definitive treatment.

It should be emphasized that the mortality rate after percutaneous closure remains high, especially in the setting of cardiogenic shock or large VSR. New combined techniques are currently evolving using hybrid approach. At the present, a team of interventional cardiologists and surgeons should carefully discuss the most convenient strategy for each individual patient. It is feasible that the combined use of ventricular support and the development of new techniques and devices will improve future outcomes.

References

1. Lopez-Sedon J, et al. Global Registry of Acute Coronary Events (GRACE) investigators. Factors related to heart rupture in acute coronary syndromes in the Global Registry of Acute Coronary Events. Eur Heart J. 2010;31:1449–56.
2. Crenshauw BS, et al. Risk factors, angiographic patterns, and outcomes in patients with ventricular septal defect complicating acute myocardial infarction. GUSTO-I (Global Utilization of Streptokinase and TPA for Occluded Coronary Arteries) Trial Investigators. Circulation. 2000;101:27–32.
3. Slatter J, et al. Cardiogenic shock due to cardiac free-wall rupture or tamponade after acute myocardial infarction: a report from the SHOCK Trial Registry. Should we emergently revascularize occluded coronaries for cardiogenic shock? J Am Coll Cardiol. 2000;36:1117–22.
4. Menon V, et al. Outcome and profile of ventricular septal rupture with cardiogenic shock after myocardial infarction: a report from the SHOCK Trial Registry. Should we emergently revascularize occluded coronaries for cardiogenic shock? J Am Coll Cardiol. 2000;36:1110–6.
5. Park JY, et al. Delayed ventricular septal rupture after percutaneous coronary intervention in acute myocardial infarction. Korean J Intern Med. 2005;20:243–6.
6. Serpytis P, et al. Post-infarction ventricular septal defect: risk factors and early outcomes. Hellenic J Cardiol. 2015;56:66–71.
7. Moreya AE, et al. Trends in incidence and mortality rates of ventricular septal rupture during acute myocardial infarction. Am J Cardiol. 2010;106(8):1095–100.
8. Crenshaw BS, et al. Risk factors, angiographic patterns, and outcomes in patients with ventricular septal defect complicating acute myocardial infarction. Circulation. 2000;100:27.
9. Rhydwen GR, et al. Influence of thrombolytic therapy on the patterns of ventricular septal rupture after acute myocardial infarction. Postgrad Med J. 2002;78:408–12.
10. Deja MA, et al. Post infarction septal defect: can we do better? Eur J Cardiothorac Surg. 2000;18:194–201.
11. Morillon-Lutun S, et al. Therapeutic management changes and mortality rates over 30 years in ventricular septal rupture complicating acute myocardial infarction. Am J Cardiol. 2013;112(9):1273–8.
12. Lowe HC, et al. Compassionate use of Amplatzer ASD closure device for residual postinfarction ventricular septal rupture following surgical repair. Catheter Cardiovasc Interv. 2003;59:230–3.
13. Zhu X, et al. Long-term efficacy of transcatheter closure of ventricular septal defect in combination with percutaneous coronary intervention in patients with ventricular septal defect complicating acute myocardial infarction: a multicentre study. Euro Interv. 2013;8(11):1270–6.
14. Lemery R, et al. Prognosis in rupture of the ventricular septum after acute myocardial infarction and role of early surgical intervention. Am J Cardiol. 1992;70:147–51.
15. Nishimura RA, et al. Early repair of mechanical complications after acute myocardial infarction. JAMA. 1986;256:47–50.
16. Cooley DA, et al. Surgical repair of ruptured interventricular septum following acute myocardial infarction. Surgery. 1957;41:930–7.
17. Jeppsson A, et al. Surgical repair of post infarction ventricular septal defects: a rational experience. Eur J Cardiothorac Surg. 2005;27:216–21.
18. Madsen JC, Daggett WM. Repair of postinfarction ventricular septal defects. Semin Thorac Cardiovasc Surg. 1998;10:117–27.
19. Norell MS, et al. Ventricular septal rupture complicating myocardial infarction: is earlier surgery justified? Eur Heart J. 1987;8:1281–6.
20. Dalrymple-Hay MJR, et al. Postinfarction ventricular septal rupture: the Wessex experience. Semin Thorac Cardiovasc Surg. 1998;10:111–6.
21. Antman EM, et al. ACC/AHA guidelines for the management of patients with ST-elevation myocardial infarction – executive summary. Circulation. 2004;110:588–636.
22. Van de Werf F, et al. Management of acute myocardial infarction in patients presenting with ST-segment elevation. Eur Heart J. 2003;24:28–66.

23. Holzer R, et al. Transcatheter closure of postinfarction ventricular septal defects using the new Amplatzer muscular VSD occlude: results of a U.S. Registry. Catheter Cardiovasc Interv. 2004;61:196–201.
24. Thiele H, et al. Immediate primary transcatheter closure of postinfarction ventricular septal defects. Eur Heart J. 2009;30:81–8.
25. Thiele H, et al. Short and long-term hemodynamic effects of intra-aortic balloon support in ventricular septal defects complicating acute myocardial infarction. Am J Cardiol. 2003;92:450–4.
26. Thiele H, et al. Reversal of cardiogenic shock by percutaneous left-atrial-to-femoral arterial bypass assistance. Circulation. 2001;104:2917–22.
27. Thiele H, et al. Randomized comparison of intraaortic balloon support versus a percutaneous left ventricular assist device in patients with revascularized acute myocardial infarction complicated by cardiogenic shock. Eur Heart J. 2005;26:1276–83.
28. Maltais S, et al. Postinfarction ventricular septal defects: towards a new treatment algorithm? Ann Thorac Surg. 2009;87(3):687–92.
29. Martinez MW, et al. Transcatheter closure of ischemic and post-traumatic ventricular septal ruptures. Cather Cardiovasc Interv. 2007;69(3):403–7.
30. Szkutnik M, et al. Postinfarction ventricular septal defect closure with Amplatzer occluders. Eur J Cardiothorac Surg. 2003;23(3):323–7.
31. Wacinski P, et al. Successful early percutaneous closure of acute ventricular septal rupture complicating acute myocardial infarction with Amplatzer ventricular septal occlude. Cardiology. 2007;14(4):411–4.
32. Bjornstad PG, et al. Catheter based closure of ventricular septal defects. Scand Cardiovasc J. 2010;44(1):9–14.
33. Ahmed J, et al. Percutaneous closure of post-myocardial infarction ventricular septal defects: a single centre experience. Heart Lung Circ. 2008;17(2):119–23.
34. Goldstein JA, et al. Transcatheter closure of recurrent postmyocardial infarction ventricular septal defects utilizing the Amplatzer postinfarction VSD device: a case series. Cather Cardiovasc Intv. 2003;59(2):238–43.

Sameer Gafoor, Predrag Matic, Fawad Kazemi,
Luisa Heuer, Jennifer Franke, Stefan Bertog,
Laura Vaskelyte, Ilona Hofmann, and Horst Sievert

26.1 Case

26.1.1 Case Summary

An 85-year-old female presented with acute ST elevation myocardial infarction. She went to the cardiac catheterization laboratory 3 days after presentation of symptoms. She received a bare metal stent to the LAD with restoration of flow. Her symptoms improved in terms of chest pain but her shortness of breath persisted. She was found to have a murmur on examination that was a holosystolic murmur.

She soon decompensated with worsening hemodynamics and development of cardiogenic shock. Lactate had climbed to 15 and mean arterial pressure was 45 mmHg. An intra-aortic balloon pump (IABP) was placed and she was transferred

S. Gafoor
Swedish Heart and Vascular, Seattle, WA, USA

Cardiovascular Center Frankfurt CVC,
Seckbacher Landstrasse 65, 60389 Frankfurt am Main, Germany

P. Matic • F. Kazemi • L. Heuer • L. Vaskelyte • I. Hofmann • H. Sievert (✉)
Cardiovascular Center Frankfurt CVC,
Seckbacher Landstrasse 65, 60389 Frankfurt am Main, Germany
e-mail: info@cvcfrankfurt.de

J. Franke
Cardiovascular Center Frankfurt CVC,
Seckbacher Landstrasse 65, 60389 Frankfurt am Main, Germany

University of Heidelberg, Heidelberg, Germany

S. Bertog
Minneapolis Veterans Affairs Hospital, Minneapolis, MN, USA

Cardiovascular Center Frankfurt CVC,
Seckbacher Landstrasse 65, 60389 Frankfurt am Main, Germany
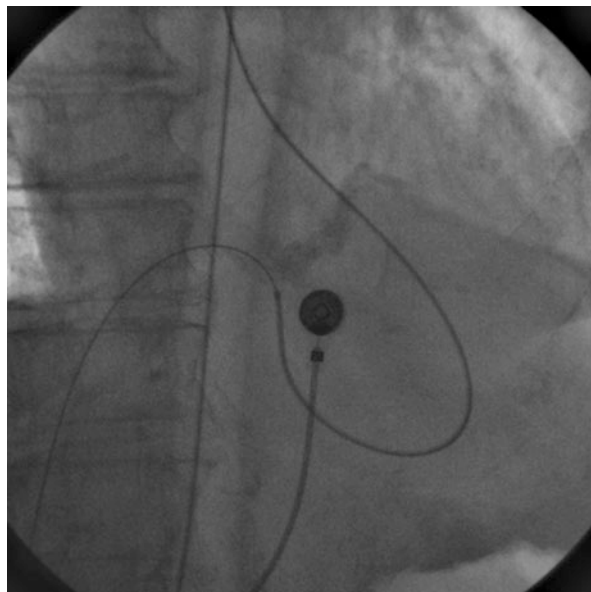
emergently for ventricular septal defect closure. The patient was intubated and supported with high doses of catecholamines.

A 5-Fr sheath was placed in the right femoral artery. A JR4 catheter and a curved long stiff hydrophilic wire were used to cross the aortic valve and then the ventricular septal defect. This was brought to the pulmonary artery. A 5-Fr sheath was placed in the right femoral vein. This was upsized to an 8-Fr sheath, and a snare was brought to the level of the pulmonary artery to snare the Terumo wire. The Terumo wire was then externalized through the venous access. This then created an arteriovenous rail (Fig. 26.1).

A 10-Fr sheath was brought over the Terumo wire to the level of the aortic valve (Fig. 26.2). This was used to advance the device. Device measurements were made based on echocardiographic measurements showing the largest diameter was 19 mm. This was then used to advance an Amplatzer 24-mm ASD device (Fig. 26.3). This was deployed (Fig. 26.4); however, it was found to be fully on the left ventricular side of the defect (Fig. 26.5).

It was recaptured and repositioned (Fig. 26.6). Original injection was unsatisfactory for assessment (Fig. 26.7). Therefore a pigtail catheter was placed in the left ventricle to assess flow across the defect (Fig. 26.8). The key finding was flow through the defect but no flow around the neck of the device, showing good filling of the interventricular septum. Transthoracic echocardiography showed no flow. The device was then released (Fig. 26.9).

Learning Points: The learning points from this case are the advantages and disadvantages of fluoroscopy to show positioning and adequacy of closure. The defect is not easily seen but can be assessed by device conformation and injection. Post-MI

Fig. 26.2 10-Fr sheath coming in from venous approach, with sheath and dilator sitting across aortic valve
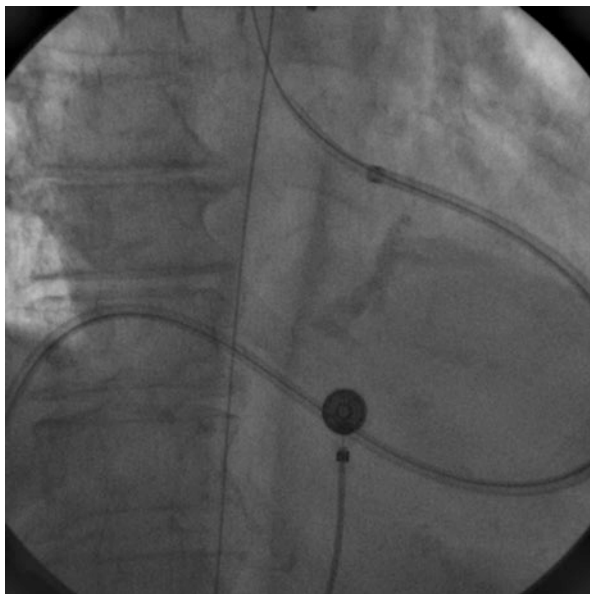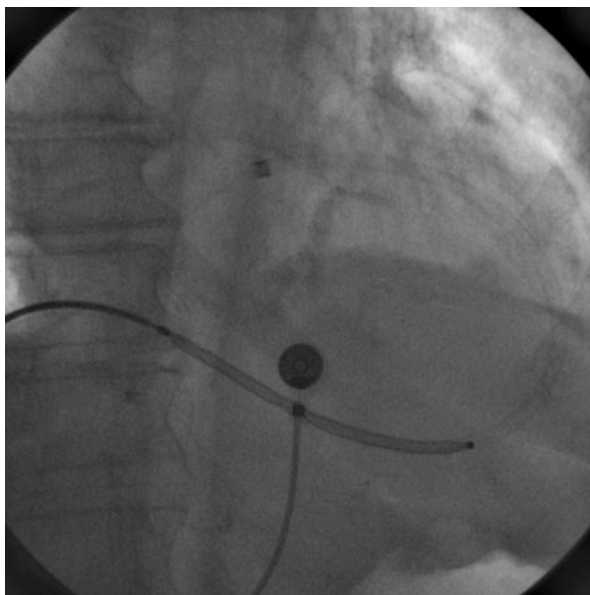

Fig. 26.3 Device being advanced through sheath from venous approach. Notice the absence of wire in the aorta as this had to be sacrificed to advance the device

VSD can be closed with atrial septal defect devices. As in congenital ventricular septal defect devices, it is easier to cross the defect from the left ventricular side, whereas the device should be introduced from the venous side. Recapture may be necessary to ensure adequate positioning. A dedicated left ventricular pigtail injection may be helpful in ensuring adequate seal.

Fig. 26.4 Deployment of the 24-mm Amplatzer ASD device
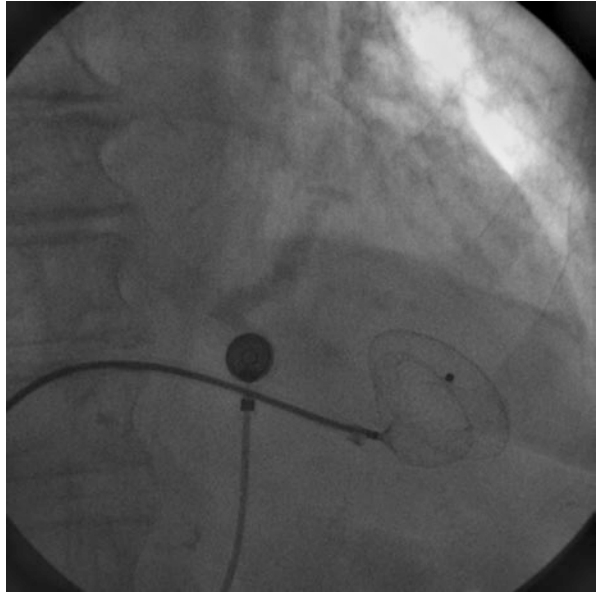
Fig. 26.5 Injection of contrast through the venous sheath to check for crossing. The image intensifier is in the LAO cranial view. Transthoracic echocardiogram is performed to evaluate for shunting or leak. As seen by fluoroscopy, the whole device is on the left ventricular side of the defect; there is no compression of the disks or device
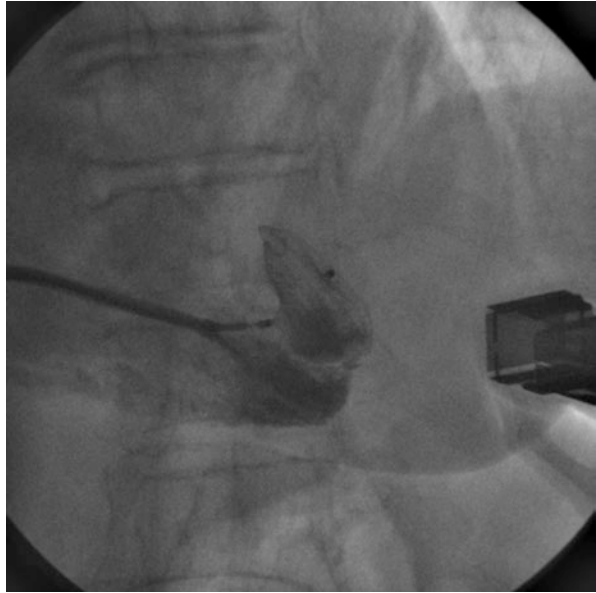
Fig. 26.6 Recapture and repositioning of 24-mm Amplatzer device. Notice how the device is being stretched across the defect
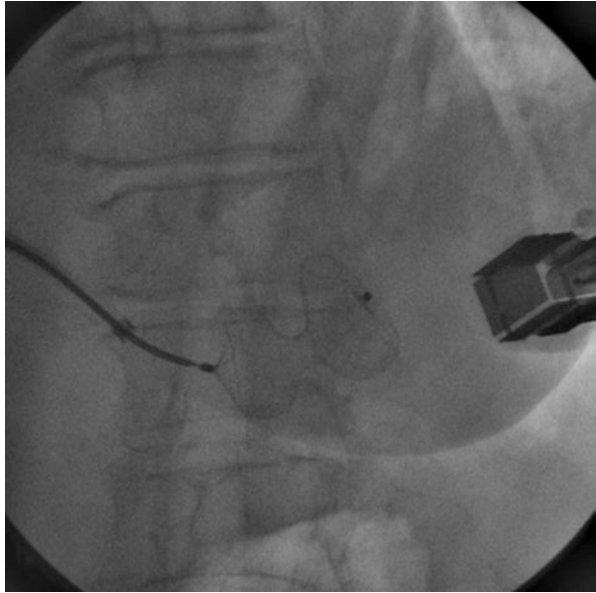
Fig. 26.7 Injection after recapture and reposition. Note how the injection shows no flow across the defect; this is most likely due to the catheter being too far away
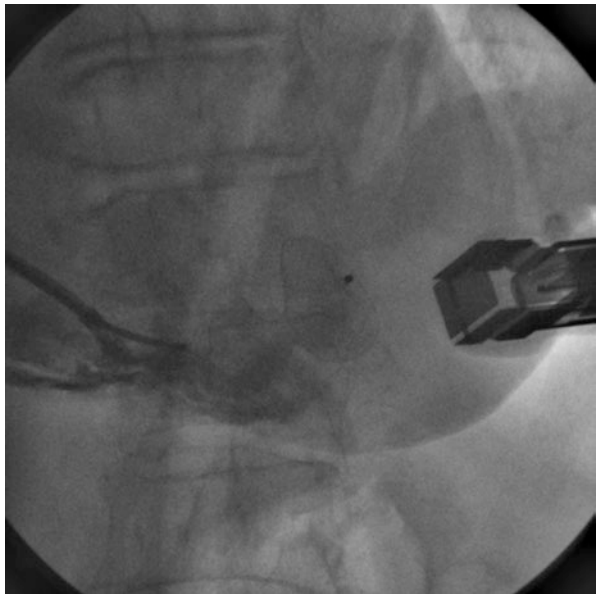
Fig. 26.8 Placement of a pigtail catheter in the LV to evaluate flow from the left ventricle to the right ventricle. This shows small significant residual flow through the device by presence of contrast in both ventricles; however there is no accessory flow across the defect next to the neck of the device
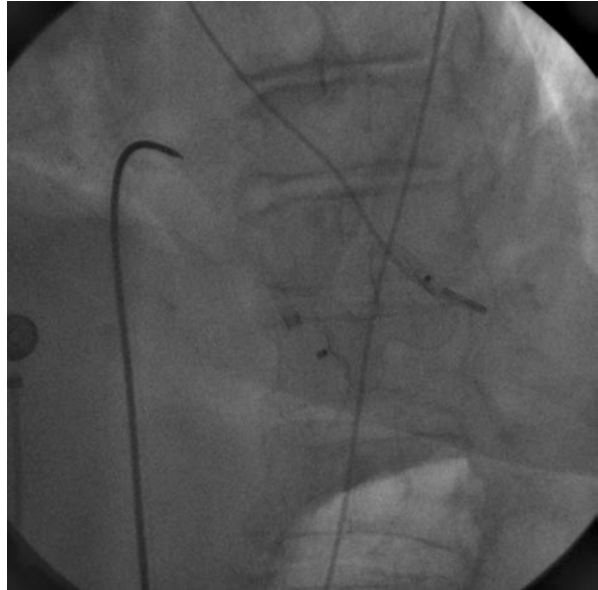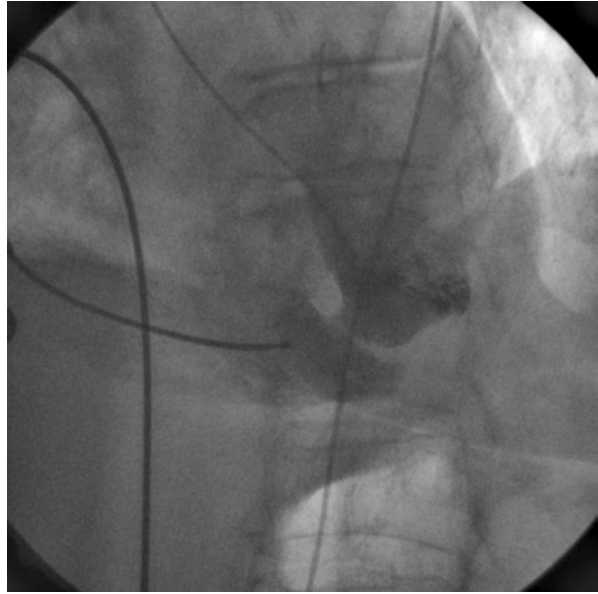
Fig. 26.9 Release of device and final position

Difficult Cases and Complications from the Catheterization Laboratory: Postinfarction Ventricular Septal Defect Closure

Michele Pighi and Anita W. Asgar

27.1 Introduction

Ventricular septal defects (VSDs) are the most common congenital heart disease, accounting for 25 % of all congenital heart defects [1]. Alternatively, a VSD can be acquired during adulthood either after a myocardial infarction (MI), as a complication of cardiac surgery, or rarely after trauma to the chest. VSDs secondary to MI are much less common in the post-reperfusion therapy era, occurring in only 0.2–0.34 % of patients receiving thrombolysis for acute MI in the Global Utilization of Streptokinase and Tissue Plasminogen Activator for Occluded Coronary Arteries (GUSTO-I) trial [2].

27.2 Background

An 88-year-old male with a history of prolonged chest pain was admitted to a community hospital and diagnosed with a late presentation anteroseptal myocardial infarction. The patient underwent urgent coronary angiography, which demonstrated the presence of in-stent restenosis in the left anterior descending coronary artery and antero-apical akinesia.

Transthoracic echocardiography (TTE) demonstrated the following:

- Severe left ventricular dysfunction with an ejection fraction of 30 %
- Basal anterior and mid-circumferential akinesia anterior, inferior, basal, and mid-septal akinesia

M. Pighi, MD (✉) • A.W. Asgar, MD
Montreal Heart Institute, Montreal, Quebec, Canada
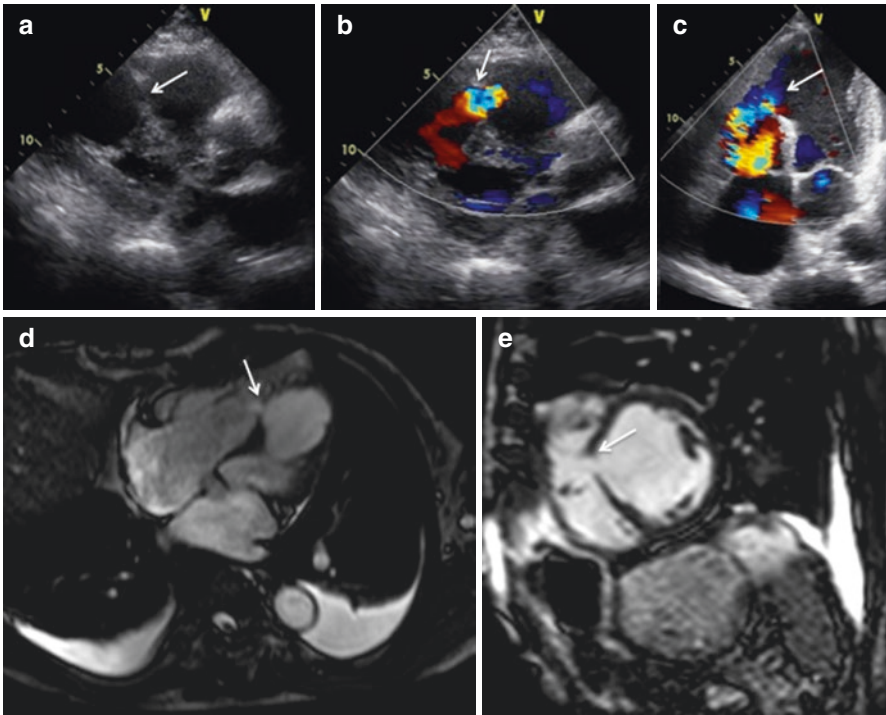e-mail: Michele.pighi@hotmail.it

Fig. 27.1 Transthoracic echocardiography (TTE) images (**a**) 2D parasternal short axis, (**b**) Doppler parasternal short axis, and (**c**) Doppler four chamber depicting the ventricular septal defect (VSD) (*white arrows*). Magnetic resonance imaging (**d**) long axis and (**e**) short axis magnifying the ventricular communication (*white arrows*)

- Ventricular septal defect (measuring 6–8 mm), placed at the lower third of the interventricular septum at the junction of the anterior and inferior segments, characterized by a left-to-right shunt and an interventricular gradient equal to 45 mmHg (Fig. 27.1a–c; Video 27.1)
- Tricuspid valve regurgitation 2/4

The patient had recurrent episodes of heart failure and was subsequently referred to our institution for further investigation and treatment. Cardiac magnetic resonance imaging (MRI) was performed and confirmed the presence of a 9-mm ventricular septal defect at the junction of the mid- and inferior septum and a transmural infarct on late enhancement imaging (Fig. 27.1d, e). There was a significant, left-to-right shunt with a pulmonary-to-systemic blood flow ratio (Qp/Qs) equal to 2.

Given the clinical presentation of the patient, as well as the echo and MRI findings, the decision was made for percutaneous VSD closure.

27.3   Percutaneous VSD Closure

Following patient consent, percutaneous VSD closure was planned using the following strategy: general anesthesia and intraprocedural transesophageal echo to guide device closure using an Amplatzer Post-MI VSD Occluder. The preferred strategy was to cross the ventricular septal defect anterogradely following transseptal puncture and then close the defect with the appropriately sized device.

The steps of the procedure were as follows:

1. Vascular access and vessel pre-closure using Perclose ProGlide (Abbott Vascular).
2. The VSD was measured by TEE color Doppler imaging to determine the largest diameter. Given the friable nature of post-MI VSDs, balloon sizing was not done, and device choice was made on the basis of the echo and MRI measurements, 8–9 mm (Fig. 27.2). TEE guided transseptal puncture using 8-French (Fr) Mullins sheath and Brockenbrough needle with placement of the Mullins catheter in the left atrium (Fig. 27.3a–c). Intravenous heparin was given following transseptal puncture to maintain an activated clotting time (ACT) >250 s.
3. A 7-Fr balloon-tipped catheter (arrow) was advanced on a 0.35-mm wire into the left atrium (Fig. 27.4a). The balloon was inflated, and the catheter was then guided across the mitral valve into the left ventricle (Fig. 27.4b) and then across the ventricular septal defect into the right ventricle (Fig. 27.4c). Once on the right side, the balloon-tipped catheter was then advanced into the pulmonary artery (Figs. 27.3d and 27.4d).
4. Once safely in the distal pulmonary artery, a 0.35-mm Amplatz Super Stiff (ST1) wire was advanced through the balloon-tipped catheter into the pulmonary artery. The balloon-tipped catheter and Mullins were then removed, and a 10-Fr 180° Amplatzer TorqueVue delivery catheter was advanced over the ST1 wire into the right ventricle.
5. The dilator and the wire were removed, and the sheath was allowed to bleed back and then flushed with saline.
6. The appropriately sized closure device (**Amplatzer 16 mm Post-MI VSD Occluder**) was then screwed onto the delivery cable and brought inside a loader.
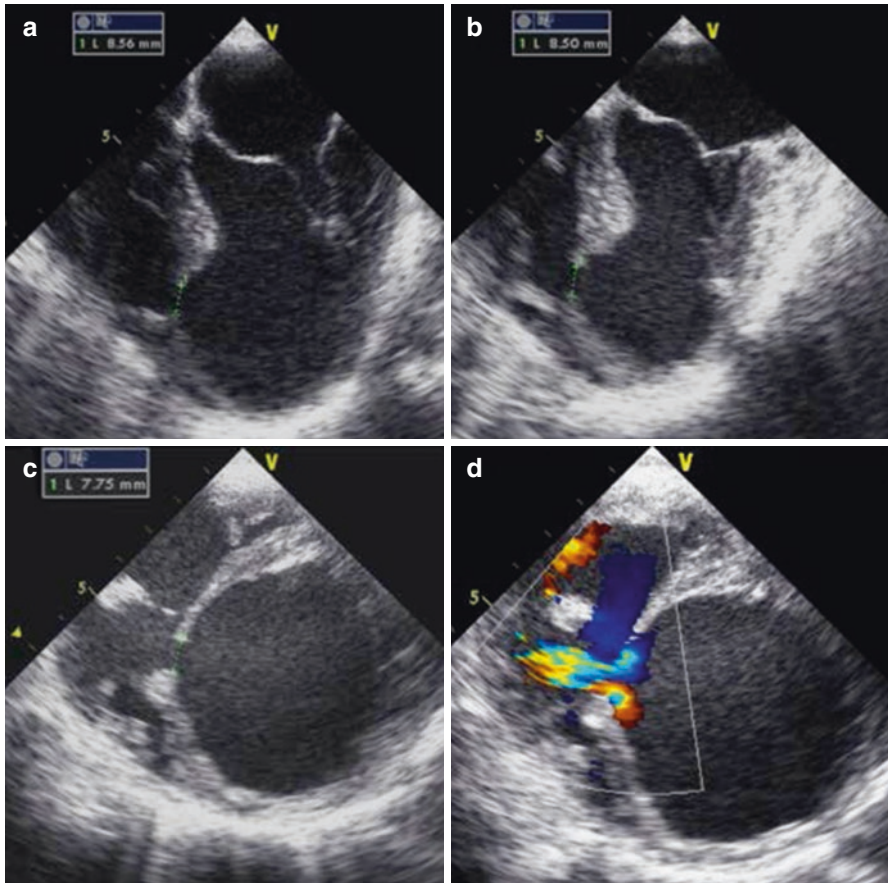
Fig. 27.2 Transesophageal echocardiography (TEE) images showing intraprocedural measurements (**a**–**c**) and Doppler evaluation (**d**) of septal defect for the sizing of the VSD occluder

7. The loader was then flushed with saline, and the device introduced through the delivery sheath with the help of the loader and slowly advanced by pushing the cable (Fig. 27.5a).
8. Once the device reached the tip of the sheath in the right ventricle, the right-sided disk was opened slowly under direct fluoroscopic and echocardiographic guidance (Figs. 27.3b,and 27.4a; Video 27.2).
9. Once the right-sided disk was fully deployed, the device and sheath were pulled back to approximate the right-sided disk to the ventricular septum guided by echo imaging (Figs. 27.3c and 27.4b; Video 27.3).
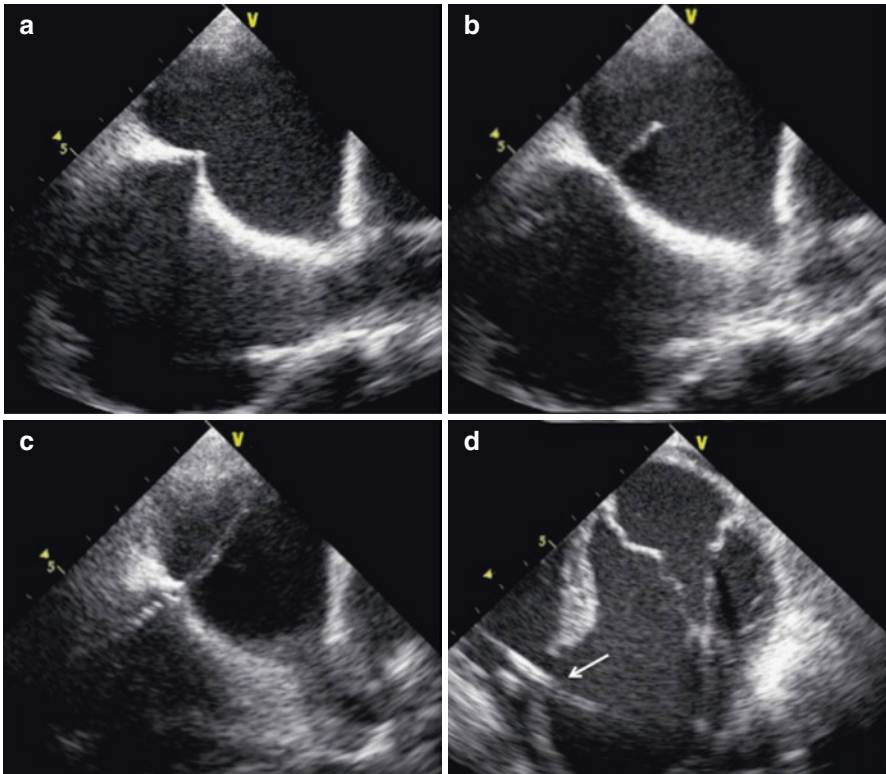
Fig. 27.3 TEE images showing (**a–c**) the transseptal puncture technique and (**d**) the advancing of the Mulling sheath through the VSD from the left-to-the right ventricle (*white arrow*)

10. When the right-sided disk was in good position, the remainder of the waist and the left-sided disk was deployed by retracting the delivery sheath over the delivery cable (Figs. 27.3d and 27.4c; Video 27.4).
11. Final check of adequate device positioning was performed by TEE, and the device was released (Fig. 27.4d; Videos 27.5 and 27.6).
12. The cable was then withdrawn into the sheath, and the sheath was pulled back gently into the right atrium.

Final TEE evaluation at the end of the procedure showed a complete closure of the VSD with no evidence of residual shunting (Figs. 27.5, 27.6, and 27.7).
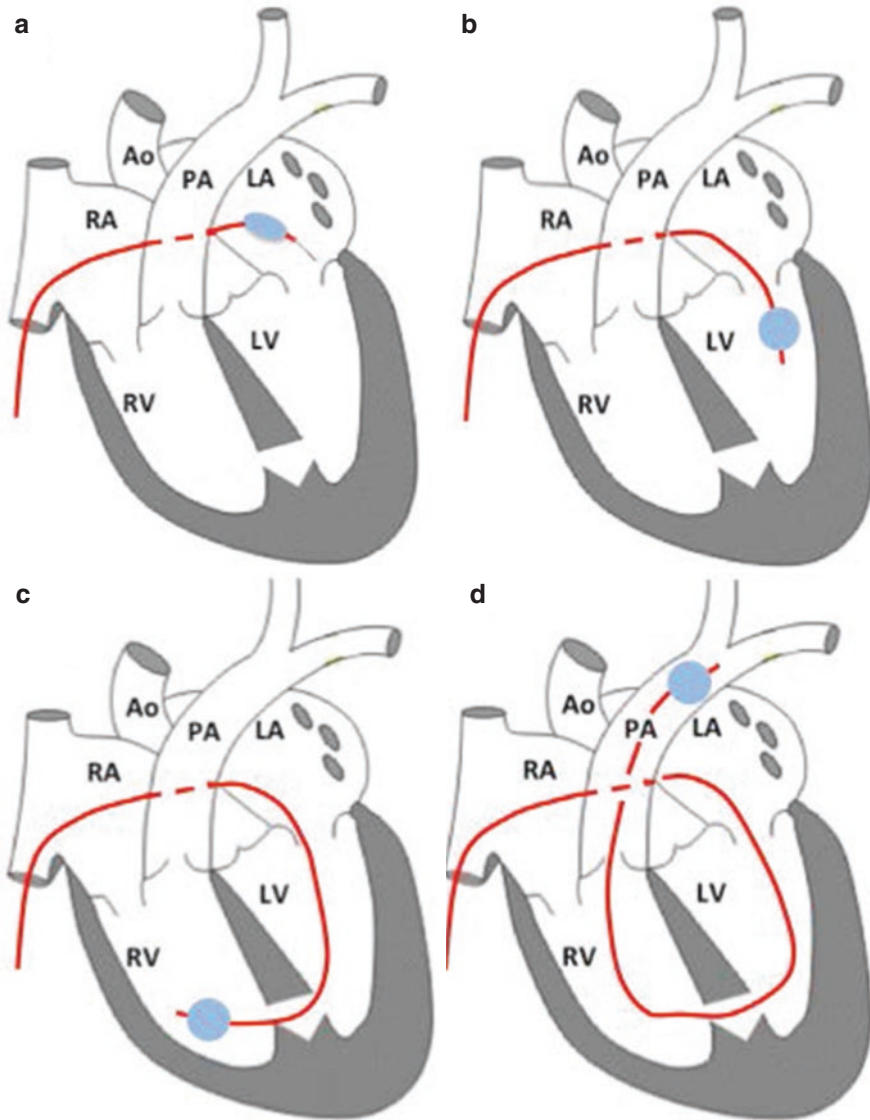
Fig. 27.4 Schematic representation of the advancement of the balloon-tipped catheter: into left atrium through the transseptal puncture (**a**), left ventricle through the mitral valve (**b**), right ventricle through the VSD (**c**), and finally into the pulmonary artery (**d**), *RA* right atrium, *LA* left atrium, *LV* left ventricle, *RV* right ventricle, *Ao* aorta, *PA* pulmonary artery
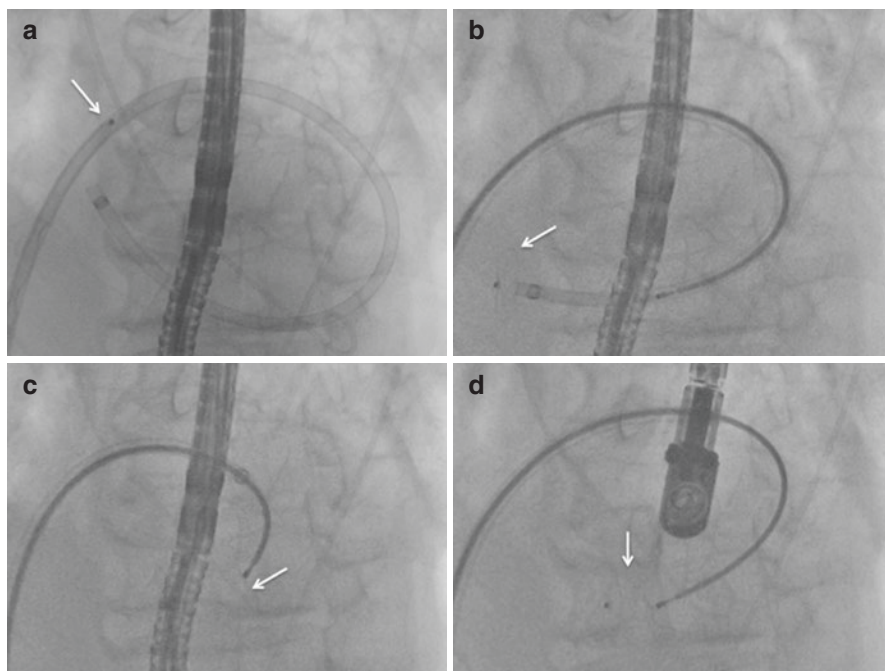
Fig. 27.5 Angiographic images showing (**a**) the advancing of the Amplatzer 16-mm Post-MI VSD Occluder through the delivery sheath; (**b**) the release of the right-sided disk in the right ventricle; (**c**) the approximation of the right-sided disk to the septum, and finally (**d**) the release of the waist through the defect and the left-sided disk in the left ventricle

27.4   Discussion

Post-myocardial infarction VSD is characterized by a poor prognosis. Indeed, survival to 1 month without intervention is 6 % [3]. Although surgical repair represents the cornerstone for this condition, this approach often requires an initial healing period of at least 2 weeks before proceeding.

The Amplatzer™ family of VSD closure devices represents an alternative to surgical repair allowing earliest intervention. Calvert PA et al. [4] published a large series of postinfarction VSD closure experience in the United Kingdom, presenting data about 53 patients from 11 centers between 1997 and 2012. Procedural success was reported in 89 % of patients, with a median time from myocardial infarction and closure procedure of 13 [Q1–Q3 5–54] days. Major periprocedural complications included procedural death and need for emergency cardiac surgery. Immediate shunt
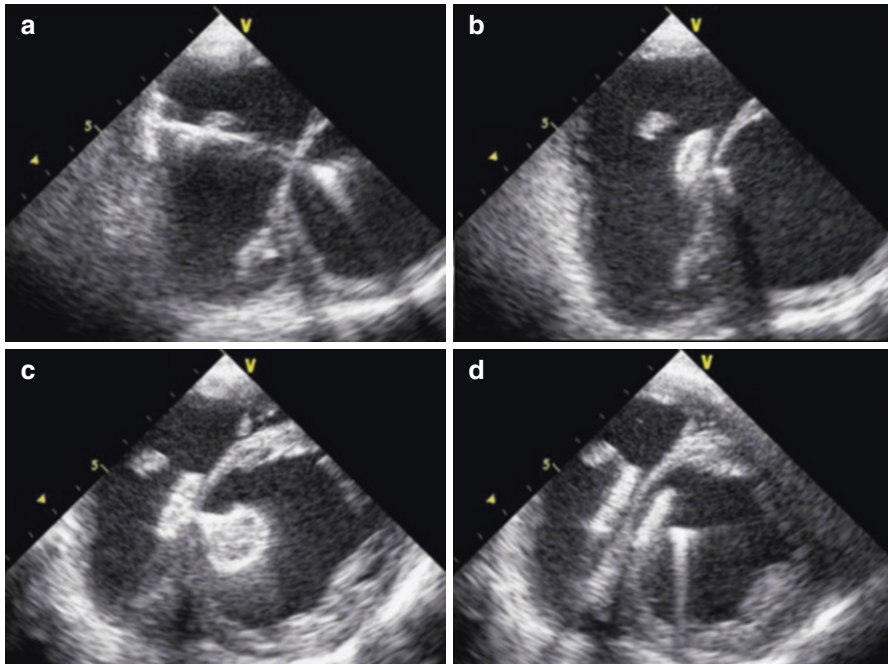
Fig. 27.6 TEE images showing (**a**) the advancing and initial release of the Amplatzer 16-mm Post-MI VSD Occluder through defect; (**b**) the release of the right-sided disk in the right ventricle; (**c**) the approximation of the right-sided disk to the septum with initial waist and left-sided disk release, and finally (**d**) the full release of the waist through the defect and the left-sided disk in the left ventricle with the device in place

reduction was achieved in 22 % of patients and partially in 63 %. The authors found that factors associated with death after postinfarction VSD closure were age, female sex, NYHA class IV, cardiogenic shock, defects size, creatinine levels, and absence of revascularization therapy, confirming data from previous surgical data [5]. Conversely, prior surgical closure and immediate shunt reduction were associated with survival.

From a technical perspective, it is necessary to stress that postinfarction VSD closure is a demanding procedure, whose success requires significant operator experience and close collaboration among interventionalist, imaging specialist, and anesthetist. The challenging setting of post-myocardial infarction (i.e., presence of serpiginous, multiple defects or friable rims) makes effective device closure difficult. As a result, as illustrated by the case, the use of multimodality imaging (TTE, TEE, and MRI) for device sizing, in addition to careful device selection and procedural preparation, is the cornerstone of a successful procedure.
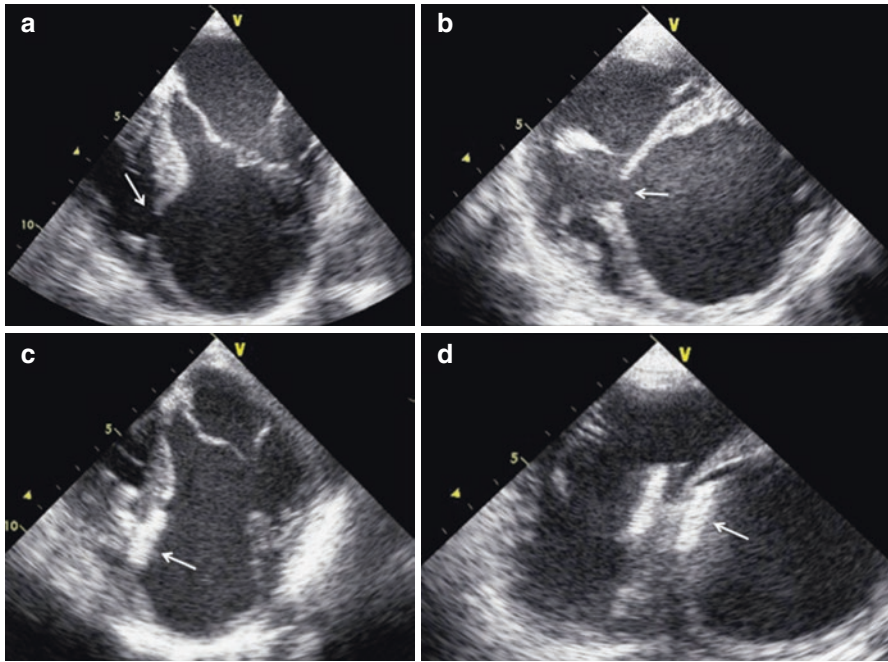
Fig. 27.7 TEE images showing long-axis view of the VSD (**a**) pre- and (**c**) post-closure and short-axis view of the VSD (**b**) pre- and (**d**) post-closure

References

1. Warnes CA, Williams RG, Bashore TM, Child JS, Connolly HM, Dearani JA, ACC/AHA, et al. Guidelines for the management of adults with congenital heart disease: executive summary: a report of the American College of Cardiology/American Heart Association Task Force on Practice Guidelines (Writing Committee to Develop Guidelines for the Management of Adults with Congenital Heart Disease): developed in collaboration with the American Society of Echocardiography, Heart Rhythm Society, International Society for Adult Congenital Heart Disease, Society for Cardiovascular Angiography and Interventions, and Society of Thoracic Surgeons. Circulation. 2008;118(23):2395–451.
2. Birnbaum Y, Fishbein MC, Blanche C. Ventricular septal rupture after acute myocardial infarction. N Engl J Med. 2002;347(18):1426–32.
3. Crenshaw BS, Granger CB, Birnbaum Y, Pieper KS, Morris DC, Kleiman NS, et al. Risk factors, angiographic patterns, and outcomes in patients with ventricular septal defect complicating acute myocardial infarction. GUSTO-I (Global Utilization of Streptokinase and TPA for Occluded Coronary Arteries) Trial Investigators. Circulation. 2000;101(1):27–32.
4. Calvert PA, Cockburn J, Wynne D, Ludman P, Rana BS, Northridge D, et al. Percutaneous closure of postinfarction ventricular septal defect: in-hospital outcomes and long-term follow-up of UK experience. Circulation. 2014;129(23):2395–402.
5. Arnaoutakis GJ, Zhao Y, George TJ, Sciortino CM, McCarthy PM, Conte JV. Surgical repair of ventricular septal defect after myocardial infarction: outcomes from the Society of Thoracic Surgeons National Database. ATS. 2012;94(2):436–44. Elsevier Inc.